

UNIVERSIDADE DE LISBOA
Faculdade de Medicina Veterinária



**The role of Jagged1 in adult angiogenesis and in solid tumor
development**

Ana Rita Ponce Álvares de Águeda Pedrosa

Orientador: Doutor António Freitas Duarte

Co-Orientador: Doutor Alexandre Neto Trindade

Tese especialmente elaborada para obtenção do grau de Doutor em Ciências Veterinárias, especialidade de Ciências Biológicas e Biomédicas

UNIVERSIDADE DE LISBOA

Faculdade de Medicina Veterinária



UNIVERSIDADE
DE LISBOA



The role of Jagged1 in adult angiogenesis and solid tumor development

Ana Rita Ponce Álvares de Águeda Pedrosa

Orientador: Doutor António Freitas Duarte

Co-Orientador: Doutor Alexandre Neto Trindade

Tese especialmente elaborada para obtenção do grau de Doutor em Ciências Veterinárias, especialidade de Ciências Biológicas e Biomédicas

Júri:

Presidente: Doutor Rui Manuel de Vasconcelos e Horta Caldeira

Vogais:

- Doutora Carmen de Lurdes Fonseca Jerónimo
- Doutor António Freitas Duarte
- Doutora Maria da Conceição da Cunha e Vasconcelos Peleteiro
- Doutora Maria de Fátima Rodrigues Moutinho Gartner
- Doutora Susana Constantino Rosa Santos

2015

“The journey of a thousand miles begins with one step.”

Lao Tzu (601-531 BC)

“Do not go where the path may lead, go instead where there is no path and leave a trail.”

Ralph Waldo Emerson (1803-1882)

“Look deep in to Nature, and then you will understand everything better.”

Albert Einstein (1879-1955)

To my beloved father, António Vasco Pedrosa and grandfather, António Rosa Pedrosa. May we meet again. In the meanwhile may my path on this earth contribute to the understanding of the complex process that is cancer. May your lives and deaths serve as an inspiration to never loose courage or determination in this mission.

ACKNOWLEDGMENTS

This thesis is the result of six years of scientific work. Much has been accomplished, but also much was left behind, either being failed experiences, dead-ends, mistakes, wrong directions, etc... However, even what was left out of this thesis was essential for gaining new ideas and even to try different ways or paths. Similarly to all things achieved in life, in order to succeed one must constantly rise from unsuccessful attempts. Gladly, I arrive at the end of this stage, one I am hoping will allow me to enter a new and exciting phase, full of new challenges and new attempts. This long journey was possible due to many people's contributions which I want to acknowledge here.

The first contact I made when I realized that I wanted to follow an academic career was with Prof. Doctor Luís Costa, who I wish to thank for the wise advice and for directing me to Prof. Doctor António Duarte. Prof. António Duarte, my supervisor, has been a leader along these years helping me to build up my career as well as allowing me a certain level of independence which helped me to fight my own battles and to also grow as a confident, creative scientist. Through his vital established collaborations, I was allowed to have experiences abroad in a different scientific environment and to use equipment from other institutions, which I also consider to have been critical for achieved skills and knowledge. For welcoming me and for all the passed knowledge, trust and for believing in my potential I am most grateful.

I would also like to acknowledge Doctor Alexandre Trindade who has been a strong support throughout my PhD. More than a co-supervisor he has become a trusty teacher and friend with whom I am able to freely discuss my ideas, results and engage in very enriching scientific discussions. There are no sufficient words to demonstrate my gratitude and recognition of his contribution to this work and to my life.

I also had the opportunity to receive some guidance from other post-docs in the lab, especially Doctor Ana Teresa Tavares and Doctor Elisabete Silva. Both helped and advised me in critical times sharing their experience and knowledge.

I could not pass this opportunity without acknowledging my dear bench colleagues and friends, Joana Carinhas, Carina Fernandes, Sofia Henriques, Margarida Simões, Liliana Mendonça, Marta Baptista, Catarina Carvalho, Marina Badenes and Daniel Murta. To José Graça who performed and helped more closely with the final part of my work my many thanks.

To Prof. Doctor Maria da Conceição Peleteiro and Sandra Carvalho from the Pathology Lab who were precious contributors for the work presented here.

To Doctor Ralf H. Adams who welcomed me in his lab in Muenster, Germany, and always demonstrated a great availability and willingness to help, discuss and advise me relative to my work. I am most thankful for the opportunities. To Rodrigo Diéguez Hurtado, a post-doc in R. Adams lab who kindly and patiently accompanied me during my visits and helped me with his wise suggestions and advice.

Being a part of the FMV family since 2002 and of the CIISA group since 2009 has been a great opportunity and both have become my second home and have gained a special place in my hearth, which I will always remember with immense joy and gratefulness. To Prof. Doctor Luís Tavares, president of this faculty, I thank for the opportunities that both these institutions gave me to attend lectures, courses and congresses and not only to become a Veterinarian but also, now to become a biomedical investigator.

To FCT for the funding given to my PhD studies and to projects in the lab.

To my family, especially, to Maria João Álvares, my mother, who always believed, taught and encouraged me to follow my objectives and dreams and raised me to her image as a strong, independent, determined and courageous woman. She has been an example and a heroin for me and I am truly proud to be her daughter. To my grandmother Isabel Pedrosa, who has also taught me so much about life and the meaning of learning to let go while having the strength to wake each day with a renewed smile. To my grandmother Lurdes Álvares, a great matriarch, who has taught me the true meaning of family and its importance in each one's life. To the rest of my family, my brothers, Diogo and Gonçalo, my stepfather, João Pinheiro, and my aunts, uncles and cousins, who have always been there to support me in every moment of my life my many thanks and love.

To my dear friend and colleague Ricardo Assunção who has witnessed and accompanied me since my faculty years my deep appreciation, love and gratefulness for his unlimited friendship, support and love. To Ana Margarida Almeida, my dearest friend since childhood, I want to acknowledge her contribution to my life and to my inner sense of belonging. We have grown and become adults always in the cherished presence, support and love from one another.

Finally, to my beloved Bruno Seixas who has been a major pillar since the day we met. His love, dedication and presence have made me who I am today. He has been a superman supporting me in both my personal and professional life, even when I doubt myself, he always believes in me. I am truly blessed for having him in my life.

To all who have contributed to this work I am truly grateful and honored.

FUNDING

I thank the Portuguese Foundation for Science and Technology (FCT) for the financial support of my individual PhD grant SFRH /BD/ 44964 /2008. And for the financial support of the following projects: SAU-ONC/116164/2009; SAU-ONC/121742/2010; PTDC/SAU-OSM/102468/2008; PTDC/CVT/115703/2009; and PEst-OE/ AGR/U10276/2014.



CIISA
Centro de Investigação Interdisciplinar
em Sanidade Animal

Título- Avaliação do papel do ligando Jagged1 na regulação da angiogénese do adulto e no desenvolvimento de tumores sólidos.

Resumo- A via Notch é uma via de sinalização intercelular altamente conservada que está envolvida na determinação do destino, e na regulação da proliferação e diferenciação celulares. Jagged1 é um ligando desta via, que tem sido descrito como essencial ao processo de angiogénese durante o desenvolvimento embrinário e que desempenha um papel crucial em diversos aspectos de biologia tumoral. No processo do desenvolvimento angiogénico da retina, Jagged1 foi descrito como tendo um efeito contrário ao de outro ligando da via, o Dll4, mas esta interacção continua por demonstrar noutros contextos angiogénicos. Além de ser expresso na vasculatura, Jagged1 também é detectado em células epiteliais de vários órgãos. Em tumores já foi descrito que a expressão epitelial de Jagged1 aumenta ao longo do desenvolvimento tumoral. Jagged1 é desta forma considerado um marcador de mau prognóstico e de elevado potencial metastático em diversos tipos de cancro, nomeadamente da mama e da próstata. No entanto, o mecanismo intrínseco de sinalização Jagged1/Notch nos contextos acima referidos ainda permanece pouco compreendido.

Como tal, o trabalho apresentado nesta tese descreve o papel do ligando Jagged1 na regulação da angiogénese fisiológica e sua interacção com o ligando Dll4. Descreve ainda o seu papel na angiogénese tumoral do adulto, no desenvolvimento de tumores da próstata e finalmente o potencial terapêutico do bloqueio dos ligandos Jagged no tratamento do cancro da próstata.

Para investigar o papel do ligando Jagged1 no processo angiogénico do adulto recorreu-se ao uso de mutantes endoteliais específicos de ganho e perda-de-função de *Jag1* (*eJag1OE* e *eJag1cKO*, respectivamente) num modelo de cicatrização de feridas cutâneas. Ainda neste contexto, para investigar as interacções entre os dois ligandos Notch, Jagged1 and Dll4, os mesmos modelos genéticos foram combinados com inibição farmacológica de Dll4 ou Jagged1, respectivamente.

Além disso, os mesmos mutantes endoteliais específicos foram ainda utilizados na investigação do papel do ligando Jagged1 na angiogénese tumoral. Para este fim recorreu-se a dois modelos diferentes de tumores no ratinho: o modelo de tumores transplantados subcutaneamente de células Lewis Lung Carcinoma (LLC) e o modelo autóctone de tumor da próstata murino- Transgenic Adenocarcinoma of the Mouse Prostate (TRAMP). Em relação aos processos angiogénicos foram avaliados nos diferentes mutantes, e combinações, diversos parâmetros tais como: densidade, maturidade, funcionalidade e permeabilidade vasculares. Simultaneamente, as populações endoteliais e perivasculares dos diferentes mutantes foram isoladas e efectuada uma análise específica de transcrição de genes envolvidos na regulação da angiogénese nestes tipos celulares. Na avaliação do contributo do ligando Jagged1 expresso no endotélio para o desenvolvimento de tumores da próstata foram ainda analisados os pesos da próstata nos términos das experiências, as lesões

classificadas histologicamente bem como outros aspectos de biologia tumoral, tais como proliferação, apoptose e diferenciação celulares e transição epitélio-mesenquimal.

Foi também efectuada uma análise da transcrição e expressão dos membros da via de sinalização Notch, incluindo ligandos (Dll1, 3, 4 e Jagged1 e 2), receptores (Notch1-4) e efectores (Hes1, 2, 5 e Hey1, 2, L), em próstatas de ratinhos saudáveis e de ratinhos TRAMP. Esta análise foi efectuada para descrever a dinâmica dos membros da via de sinalização Notch na tumorigénese da próstata de forma a poder identificar membros ectopicamente expressos na próstata tumoral quando comparados com a próstata normal. Foram ainda isoladas as diferentes subpopulações celulares da próstata, basal, luminal e do estroma e os seus perfis transcripcionais comparados entre próstatas normais e com lesões tumorais (TRAMP).

Por fim, avaliou-se o potencial terapêutico de um anticorpo anti-Jagged1/2 no tratamento do cancro da próstata, administrando um anticorpo bloqueador anti-Jagged1/2 aos ratinhos TRAMP. Estes ensaios terapêuticos foram realizados em duas janelas temporais distintas: numa fase precoce do desenvolvimento de tumores da próstata, das 12 às 18 semanas de idade e numa fase mais tardia, das 18 às 24 semanas de idade, simulando uma detecção precoce e tardia da doença nos humanos. A eficácia terapêutica foi avaliada pelos pesos da próstata no término da experiência, classificação histopatológica das lesões, análise da vasculatura, proliferação, apoptose e diferenciação celulares, alterações nos compartimentos celulares da próstata, transição epitélio-mesenquimal, e alterações da população de células cancerosas estaminais (CSCs).

Nestes trabalhos foram utilizadas técnicas de imunofluorescência, imunohistoquímica, “fluorescent associated cell sorting” (FACS), e “quantitative real time PCR” (qRT-PCR).

Colectivamente, os resultados aqui apresentados demonstram que Jagged1 é um ligando pró-angiogénico em contextos de angiogénese do adulto, tanto fisiológica como tumoral.

No modelo de cicatrização de feridas foi demonstrado que os mutantes de ganho-de-função (*eJag1OE*) exibiam um processo de cicatrização de feridas cutâneas e de desenvolvimento de tumores sólidos acelerado, relativamente aos respectivos controlos, enquanto os mutantes de perda-de-função exibiam o fenótipo oposto. Estas diferenças fenotípicas entre os mutantes deveram-se aos primeiros exibirem uma vasculatura mais densa, com maior número de células de suporte, e portanto mais funcional e menos permeável, enquanto que os segundos exactamente o oposto.

O papel pró-angiogénico do ligando Jagged1 foi também demonstrado ser exercido através de complexas interações com diferentes receptores Notch. Utilizando o modelo de cicatrização de feridas foi demonstrado que Jagged1 presente no endotélio regula negativamente a transcrição e activação de Notch1, e portanto bloqueia a activação de Notch1 mediada por Dll4. Ao contrário do que acontece com Notch1, foi também demonstrado que Jagged1 regula positivamente a transcrição e activação de Notch4. Esta observação foi

averiguada tanto no contexto angiogénico fisiológico como tumoral. Adicionalmente, a sinalização por Jagged1/Notch4 foi implicada na maturação vascular, uma vez que quer as feridas e tumores dos mutantes *eJag1OE* quer as feridas de ratinhos administrados com um anticorpo Notch4 agonista exibiram aumento da maturação vascular. Também foi demonstrado que Jagged1 endotelial é capaz de activar Notch3/HeyL expresso nas células perivasculares e assim também contribuir para a regulação do recrutamento dessas mesmas células de suporte, tornando a vasculatura mais funcional e menos permeável, contribuindo para a cicatrização e desenvolvimento tumorais.

Adicionalmente, foi demonstrado que o ligando endotelial Jagged1 contribui para a displasia tumoral não só pela sua função pró-angiogénica, limitando o aporte de nutrientes e oxigénio às células tumorais, mas também por uma função angiócrina mediada pela activação de Notch3 e expressão de Hey1 nas células tumorais. Desta forma, este ligando regula ainda a proliferação, apoptose e diferenciação das células tumorais prostáticas, assim como o processo de transição epitélio-mesenquimal.

Inclusivamente, através do estudo da expressão dos diferentes componentes Notch na próstata tumoral versus próstata normal, o eixo Jagged1/2/Notch3/Hey1 foi identificado como estando ectopicamente expresso no tecido prostático tumoral. Esta observação sugere então que para a regulação dos processos tumorigénicos referidos anteriormente, não só é importante o papel pró-angiogénico e angiócrino do ligando Jagged1 endotelial, mas também o seu papel directo decorrente da expressão aumentada ao nível das células tumorais.

Por último, foi demonstrado que o bloqueio da sinalização Notch mediada pelos ligandos Jagged inibe o desenvolvimento e progressão de tumores da próstata do ratinho e que como tal, pode constituir uma nova potencial abordagem terapêutica no tratamento do cancro da próstata. O bloqueio de Jagged1/2 mimetizou o fenótipo vascular decorrente da perda-de-função endotelial específica de Jagged1, produzindo uma neo-vascularização menos densa, imatura e conseqüentemente menos funcional e mais permeável, inibindo fortemente o desenvolvimento de tumores da próstata murinos. De forma semelhante ao verificado nos mutantes de perda-de-função, o bloqueio de ambos os ligandos Jagged levou à inibição do crescimento celular prostático, restringindo a proliferação e promovendo a apoptose celular e inibindo a transição epitélio-mesenquimal. Adicionalmente, o tratamento com o anticorpo bloqueador também teve um efeito protector relativamente às alterações nos compartimentos celulares decorrentes da displasia prostática. O tratamento minimizou a perda da identidade celular luminal, inibiu a proliferação do compartimento basal e a des-diferenciação de um fenótipo luminal para um mais basal. O bloqueio de Jagged1/2 também apresentou um efeito benéfico ao nível da regulação do “pool” de células cancerosas estaminais da próstata, apresentado um efeito inibitório sobre a sua proliferação e sobrevivência. Adicionalmente, as amostras tratadas com anti-Jagged1/2 apresentaram uma significativa sub-expressão de *Notch3* e *Hey1* nesta subpopulação celular.

Em conclusão, os resultados aqui apresentados contribuem para uma compreensão mais abrangente do papel do ligando Jagged1 no organismo adulto, fora do sistema nervoso central, inclusivamente em cenários tumorais, como o caso do cancro da próstata. De forma mais específica, a sinalização mediada por Jagged1, foi demonstrada ser uma rede complexa envolvendo múltiplos aspectos em diferentes tipos celulares e dependente do receptor envolvido. No endotélio Jagged1 actua como um ligando pró-angiogénico através de um efeito antagonístico a Dll4/Notch1 e mediado quer pela activação de Notch4/Hey1 no endotélio quer pela activação de Notch3/HeyL nas células perivasculares. Também foi importante verificar que ambas estas funções da sinalização por Jagged1/Notch são altamente conservadas em diferentes contextos no adulto, incluindo nos processos angiogénicos fisiológicos e patológicos. O ligando Jagged1 expresso por células endoteliais exerce ainda um papel angiocrino mediado pela activação de Notch3 e expressão de Hey1 na regulação do desenvolvimento tumoral da próstata. Esta função angiocrina juntamente com a expressão ectópica dos ligandos Jagged nos tecidos tumorais da próstata do ratinho constituem importantes fontes de regulação dos diversos aspectos da biologia tumoral. O bloqueio de Jagged1 pode desta forma vir a constituir um nova e promissora forma terapêutica no tratamento do cancro da próstata.

Palavras-chave: Jagged1, Notch, angiogénese, desenvolvimento tumoral, cancro da próstata.

Title- The role of Jagged1 in adult angiogenesis and in solid tumor development.

Abstract- Jagged1 (*Jag1*) is a Notch signaling ligand, which has been described as essential for developmental angiogenesis and to play an important role in several aspects of tumor biology. However the underlying mechanism related to Jagged1/Notch signaling still remain incompletely understood.

Therefore this thesis analyzed Jagged1 driven Notch signaling enrolment in adult angiogenesis settings, and in tumor development. To address the role of endothelial *Jag1* in physiological and tumoral angiogenesis, endothelial-specific *Jag1* mutants driven angiogenic phenotypes were assessed in skin wound healing and in transplanted tumors and prostatic autochthonous tumor growth, respectively. An extensive transcription and expression analysis of Notch signaling members in the tumorigenic development of the mouse prostate was also performed to identify ectopically expressed Notch members. Lastly, the therapeutic potential of an Anti-Jagged1/2 antibody in mouse prostate cancer was evaluated.

Altogether, results presented here demonstrate that Jagged1 is a pro-angiogenic ligand due to its ability to antagonize Dll4/Notch1 mediated signaling. It also has a pro-maturation function by both endothelial Notch4 and perivascular Notch3 mediated signaling. Both these functions contribute to accelerated wound healing and tumor growth, by inducing a more functional vasculature. Moreover, we have identified a new angiocrine function for endothelial Jagged1, mediated through Notch3/Hey1 activation in tumor cells. Finally, we have demonstrated that either by mediated endothelial-specific angiocrine function or by tumor cells mediated Jagged1 ectopic expression, this ligand regulated tumor cell proliferation, apoptosis, de-differentiation, epithelial-to-mesenchymal transition and cancer stem-like cells proliferation and survival. Ultimately, we have demonstrated that blocking Jagged-mediated Notch signaling inhibited development and progression of mouse prostate cancer and therefore constitutes a promising therapeutic approach in prostate cancer treatment.

Keywords: Jagged1, Notch, angiogenesis, tumor development, prostate cancer.

TABLE OF CONTENTS

INTRODUCTION	1
LITERATURE REVIEW	5
1. Notch signaling pathway	6
1.1 Notch receptors	7
1.2 Notch ligands	8
1.2.1 Delta-like ligands	8
1.2.2 Jagged ligands (Jagged1 and Jagged2)	9
1.3 Notch signaling pathway activation	9
1.4 Notch effectors.....	11
2. Blood vessel formation	13
2.1 Angiogenesis	14
2.2 Angiogenesis regulation.....	15
2.2.1 VEGF signaling	15
2.2.2 Angiopoietins signaling.....	18
2.2.3 PDGF signaling	19
2.2.4 Notch signaling.....	20
2.2.4.1 Notch signaling in sprouting angiogenesis	20
2.2.4.2 Notch signaling in vessel maturation.....	24
3. Notch signaling regulation of physiological angiogenesis	26
4. Notch signaling regulation of tumor angiogenesis	28
5. Notch signaling regulation of tumor cell biology.....	32
5.1 Mechanisms of Notch activation in solid tumors.....	32
5.2 Notch signaling function in solid tumors	33
6. Prostate.....	34
6.1 Histology of the prostate	34
6.2 Prostate Cancer.....	35
6.2.1 Mouse models of prostate cancer- TRAMP model.....	36
6.3 Effects of Notch signaling in prostate tumor development.....	37
6.3.1 Notch signaling regulation of prostatic tumor cell proliferation and apoptosis ...	39
6.3.2 Notch signaling regulation of Cancer Stem Cells (CSCs)	40
6.3.3 Notch signaling regulation of epithelial-to-mesenchymal transition (EMT), invasion and metastasis	41
7. Targeting the Notch signaling pathway as a therapeutic approach to cancer	43
7.1 Gamma- and alfa-secretase inhibitors (GSIs and ASIs)	43
7.1.1 Therapeutic Notch inhibition in prostate cancer	44
7.2 Specific targeting of Notch pathway components.....	44
7.3 Notch decoys.....	45
EXPERIMENTAL WORK	46

Chapter I – Endothelial Jagged1 Antagonizes Dll4 Regulation of Endothelial Branching and Promotes Vascular Maturation Downstream of Dll4/Notch1.	47
1. Abstract	48
2. Introduction	49
3. Materials and Methods.....	50
3.1 Experimental animals	50
3.2 Wounding procedures	50
3.3 Tissue preparation and immunofluorescence	51
3.4 Quantitative transcriptional analysis	53
3.5 Flow cytometry	53
3.6 Statistical analysis	53
4. Results.....	54
4.1 Endothelial Jagged1 accelerates wound healing by promoting angiogenesis and vessel maturation	54
4.2 Regulation of angiogenic gene expression by Jagged1/Notch Signaling	58
4.3 Blocking Dll4 in endothelial <i>Jag1</i> knockout mice rescues angiogenesis but not mural cell coverage	61
4.4 Vascular maturation in endothelial-specific Dll4 gain-of-function or conditional overexpression mice is impaired by Jagged1 blockade	65
4.5 Endothelial Jagged1 activates Notch3 receptor in perivascular cells and Notch4 in ECs	67
4.6 Administration of a Notch4 agonist to wild-type mice accelerates wound healing by promoting vessel maturation without affecting angiogenic growth	75
5. Discussion	79
6. Conclusions	82
Chapter II - Endothelial Jagged1 promotes solid tumor growth through both pro angiogenic and angiocrine functions.	83
1. Abstract	84
2. Introduction	85
3. Materials and Methods.....	86
3.1 Experimental animals	86
3.2 LLC subcutaneous tumor model.....	87
3.3 Tissue preparation and immunohistochemistry.....	87
3.4 Quantitative transcriptional analysis	89
3.5 Flow cytometry	89
3.6 Statistical analysis	90
4. Results.....	90
4.1 Modulation of endothelial <i>Jag1</i> interferes with the growth of LLC subcutaneous tumor transplants.....	90
4.2 Endothelial Jagged1 contributes to prostate cancer development and progression	91
4.3 Endothelial Jagged1 has a pro-angiogenic function in tumor development.....	96
4.4 Endothelial Jagged1 elicits changes in the transcription profile of angiocrine factors of endothelial and perivascular tumor associated cells.....	103

4.5 Modulation of neo-vasculature of prostatic tumors leads to alterations in local hypoxic levels.....	106
4.6 Endothelial Jagged1 induces proliferation and inhibits apoptosis in the surrounding tumor tissues.....	106
4.7 Modulation of endothelial <i>Jag1</i> leads to alterations in epithelial-to-mesenchymal transition (EMT).....	108
4.8 Endothelial Jagged1 exerts its angiogenic function through Notch4/Hey1 and its angiocrine function through Notch3/Hey1 influencing tumor cell proliferation and de-differentiation.....	111
5. Discussion	112
6. Conclusions	117
Chapter III - Notch signaling dynamics in the adult healthy prostate and in prostatic tumor development.	118
1. Abstract	119
2. Introduction.....	120
3. Materials and Methods.....	121
3.1 Experimental animals	121
3.2 Tissue preparation, immunohistochemistry and immunofluorescence	121
3.3 Quantitative transcriptional analysis	123
3.4 Flow cytometry	123
3.5 Statistical analysis	124
4. Results.....	124
4. 1 Notch ligands and receptors are transcribed in the adult prostate	124
4.2 Notch components and effectors are expressed in all lobes of the adult prostate	125
4.3 Prostatic tumor development is accompanied by up-regulation of Notch signaling pathway.....	127
4.4 Early and late stages of prostatic tumor development are accompanied by significant changes in the expression of Notch components.....	130
4.5 Early and late stages of prostatic tumor development are accompanied by significant changes in the expression of Notch effectors	138
4.6 Very late stages of prostatic tumor development also presented changes in Notch signaling expression.....	138
4.7 Notch signaling components are differentially transcribed and expressed in specific cell populations of the healthy and tumoral prostates.	145
4.8 The axis Jagged1/Notch3/Hey1 is highly activated in prostate tumor development	149
5. Discussion	151
6. Conclusions	154
Chapter IV - Targeting Jagged1/2 is a new promising therapeutic approach for prostate cancer.	156
1. Abstract	157
2. Introduction.....	158
3. Materials and Methods.....	159
3.1 Experimental animals	159

3.2 Therapeutic Intervention Trials	159
3.3 Tissue preparation and immunohistochemistry	160
3.4 Instrument details	161
3.5 Quantitative transcriptional analysis	161
3.6 Flow cytometry	162
3.7 Statistical analysis	162
4. Results.....	163
4.1 Administration of a blocking antibody against Jagged1 and Jagged2 inhibited prostate tumor development and progression.....	163
4.2 Blocking Jagged1/2 had an anti-angiogenic effect in tumor vasculature	164
4.3 Blocking Jagged1/2 led to alterations in local hypoxia levels	167
4.4 Blocking Jagged1/2 promoted apoptosis and inhibited proliferation of prostatic tumor cells.....	168
4.5 Treatment of prostatic tumor lesions with Anti-Jagged1/2 antibody inhibited the loss of the luminal identity and the proliferation of the basal compartment.....	170
4.6 Anti-Jagged1/2 antibody inhibited epithelial-to-mesenchymal transition (EMT) in prostatic tumor lesions.....	172
4.7 Jagged1 and Jagged2 signal through Notch3/Hey1	174
4.8 Blocking Jagged1/2 rescued the loss of Androgen receptor expression in TRAMP prostates	174
4.9 Jagged1/2 also regulated the proliferation of prostate cancer stem-like cells.....	176
4.10 Therapeutic intervention trials using Anti-Jagged1/2 antibody had no toxic side effects other than in the skin.....	179
5. Discussion	180
6. Conclusions	185
GENERAL DISCUSSION, CONCLUSIONS AND FUTURE DIRECTIONS.....	186
GENERAL DISCUSSION	187
CONCLUSIONS.....	195
FUTURE DIRECTIONS.....	197
REFERENCES	198
ANNEX I primers pair sequence list	198

TABLE OF FIGURES

Figure 1- Notch receptors and ligands structure.....	6
Figure 2- Notch signaling pathway.	11
Figure 3- Modes of vessel formation.	13
Figure 4- The angiogenic process.....	15
Figure 5- Vegf family members.	16
Figure 6- Ang/Tie2 signaling.	19
Figure 7- PDGFB/PDGFR β signaling in regulation of mural cell recruitment.	20
Figure 8- Retina development as a model system for investigation of angiogenic sprouting.	21
Figure 9- Model of Notch-driven lateral inhibition.	22
Figure 10- Proposed model for the modulation of Dll4-Notch signaling by Jagged1.	23
Figure 11- Jag1/Notch3 signaling in a model of lateral induction of vessel maturation.	26
Figure 12- Wound repair phases.....	27
Figure 13- The angiogenic switch in tumor growth.	29
Figure 14- Paradoxical effect of Anti-Dll4 based therapies.....	31
Figure 15- Prostate cell populations.....	34
Figure 16- Progression pathway for human prostate cancer.	35
Figure 17- Prostate cancer development in the TRAMP model.....	36
Figure 18- Comparison of the human and mouse prostates anatomy.	37
Figure 19- Notch signaling in prostate cancer hallmarks.	38
Figure 20- Potential cancer therapeutics that target Notch signaling.	43
Figure I.1- Effect of endothelial <i>Jag1</i> overexpression in wound healing.	55
Figure I.2- Effect of endothelial <i>Jag1</i> loss of function in wound healing.....	56
Supplemental Figure I.1- Immunostaining for Pdgfr- β in <i>eJag1OE</i> and <i>eJag1cKO</i> mutants.	57
Figure I.3- Gene expression analysis in <i>eJag1OE</i> and <i>eJag1cKO</i> mutants.....	59
Figure I.4- Immunostaining for Hey1 and Hey2 in <i>eJag1OE</i> and <i>eJag1cKO</i> mutants.....	60
Figure I.5- Endothelial <i>Jag1</i> loss of function combined with administration of anti-Dll4 antibody in wound healing assay.	62
Supplemental Figure I.2- Pericyte vascular coverage, vascular perfusion and extravasation analyses in wound samples from endothelial <i>Jag1</i> loss-of-function mice treated with Anti-Dll4 antibody.	63
Supplemental Figure I.3- Gene expression analyses in <i>eJag1cKO</i> treated with Anti-Dll4 antibody.	64
Figure I.6- Endothelial-specific Dll4 overexpression combined with administration of anti-Jagged1 antibody in wound healing assay.....	66
Supplemental Figure I.4- Pericyte vascular coverage, vascular perfusion and extravasation analyses in wound samples from endothelial-specific <i>Dll4</i> over-expression mutant mice treated with Anti-Jagged1 antibody.	68
Supplemental Figure I.5- Gene expression analyses in <i>eDll4OE</i> treated with Anti-Dll4 antibody.	69

Supplemental Figure I.6- Immunostaining for Notch3 intra-cellular domain (N3ICD) in wound tissues of <i>eJag1OE</i> and Anti-Jag1-treated <i>eDII4OE</i> mutants.	71
Figure I.7- Immunostaining of Notch1 and Notch4 intracellular domains (N1ICD and N4ICD) in <i>eJag1OE</i> and <i>eJag1cKO</i> mutants.	72
Supplemental Figure I.7- Immunostaining of Notch1 and Notch4 intra-cellular domains (N1ICD and N4ICD) in wound tissues of Anti-DII4-treated <i>eJag1cKO</i> and Anti-Jag1-treated <i>eDII4OE</i> mutants.	73
Supplemental Figure I.8- Immunostaining for Notch4 and Notch1 intra-cellular domains (N4ICD and N1ICD) in wound tissues of Anti-DII4 treated <i>eJag1cKO</i> and Anti-Jag1-treated <i>eDII4OE</i> mutants, respectively.	74
Supplemental Figure I.9- Notch4 Agonist treated WT mice in wound healing assay.	76
Supplemental Figure I.10- Pericyte vascular coverage in WT mice treated with a Notch4 agonist.	77
Supplemental Figure I.11- Gene expression analysis and immunostaining for Hey1 and Hey2 in Notch4 agonist treated WT mice.	78
Figure I.8- Proposed model for Jagged1/Notch signaling in wound angiogenesis.	81
Figure II.1- LLC transplant tumor volume in endothelial specific Jag1 mutants.	91
Figure II.2- Modulation of endothelial Jag1 in TRAMP mice.	94
Supplemental Figure II.1- Modulation of endothelial <i>Jag1</i> in TRAMP mice.	95
Supplemental Figure II.2- Jag1 expression and transcription in endothelial-specific <i>Jag1</i> mutants.	96
Supplemental Figure II.3- LLC xenograft tumor vascular phenotype in endothelial specific <i>Jag1</i> mutants.	98
Figure II.3- Prostate tumor vascular phenotype in TRAMP endothelial-specific Jag1 mutants.	99
Supplemental Figure II.4- Prostate tumor endothelial pericyte coverage in TRAMP endothelial-specific <i>Jag1</i> mutants.	100
Supplemental Figure II.5- LLC xenograft tumor endothelial pericyte coverage in endothelial-specific <i>Jag1</i> mutants.	101
Figure II.4- Prostate tumor vascular perfusion and extravasation in TRAMP endothelial-specific Jag1 mutants.	102
Supplemental Figure II.6- LLC xenograft tumor vascular perfusion and extravasation in endothelial specific <i>Jag1</i> mutants.	103
Figure II.5- Transcription profile of angiocrine factors by endothelial and perivascular tumor associated cells in TRAMP endothelial-specific <i>Jag1</i> mutants.	104
Supplemental Figure II.7- Transcription profile of angiocrine factors by endothelial and perivascular tumor associated cells in TRAMP endothelial-specific <i>Jag1</i> mutants at 18 weeks of age.	105
Figure II.6- Prostate tumor hypoxic levels in TRAMP endothelial-specific <i>Jag1</i> mutants. ...	107
Figure II.7- Prostate cellular apoptosis and proliferation in TRAMP endothelial-specific Jag1 mutants.	109
Figure II.8- Epithelial-to-mesenchymal transition in prostate lesions of TRAMP endothelial-specific Jag1 mutants.	110
Supplemental Figure II.8- Immunostaining for Notch4 intra-cellular domains (N4ICD) in TRAMP. <i>eJag1OE</i> and <i>eJag1cKO</i> mutants.	112
Figure II.9- Hey1 transcription and expression and Notch3 intracellular domain (N3ICD) expression in prostate lesions of TRAMP endothelial-specific <i>Jag1</i> mutants.	113

Figure III.1- Transcription of Notch components in the healthy adult prostate tissue.	125
Figure III.2- Immunohistochemistry of Notch components in the four lobes (Dorsal, Lateral, Ventral and Anterior) of the healthy adult prostate.	125
Figure III.3- Immunohistochemistry of Notch effectors in the four lobes (Dorsal, Lateral, Ventral and Anterior) of the healthy adult prostate.	128
Figure III.4- Transcription analysis of whole prostate in TRAMP mice at three stages of tumor development (18, 24 and 30 wks of age).	129
Figure III.5- Immunohistochemistry of Notch components in the dorsal prostate of TRAMP mice at early (18 wks) and late (24 wks) stages of tumor development.	131
Supplemental Figure III.1- Immunohistochemistry of Notch ligands in the lateral prostate of TRAMP mice at early (18 wks) and late (24 wks) stages of tumor development.	132
Supplemental Figure III.2- Immunohistochemistry of Notch ligands in the ventral prostate of TRAMP mice at early (18 wks) and late (24 wks) stages of tumor development.	133
Supplemental Figure III.3- Immunohistochemistry of Notch ligands in the anterior prostate of TRAMP mice at early (18 wks) and late (24 wks) stages of tumor development.	134
Supplemental Figure III.4- Immunohistochemistry of Notch receptors in the lateral prostate of TRAMP mice at early (18 wks) and late (24 wks) stages of tumor development.	135
Supplemental Figure III.5- Immunohistochemistry of Notch receptors in the ventral prostate of TRAMP mice at early (18 wks) and late (24 wks) stages of tumor development.	136
Supplemental Figure III.6- Immunohistochemistry of Notch receptors in the anterior prostate of TRAMP mice at early (18 wks) and late (24 wks) stages of tumor development.	137
Figure III.6- Immunohistochemistry of Notch effectors in the dorsal prostate of TRAMP mice at early (18 wks) and late (24 wks) stages of tumor development.	139
Supplemental Figure III.7- Immunohistochemistry of Notch effectors in the lateral prostate of TRAMP mice at early (18 wks) and late (24 wks) stages of tumor development.	140
Supplemental Figure III.8- Immunohistochemistry of Notch effectors in the ventral prostate of TRAMP mice at early (18 wks) and late (24 wks) stages of tumor development.	141
Supplemental Figure III.9- Immunohistochemistry of Notch effectors in the anterior prostate of TRAMP mice at early (18 wks) and late (24 wks) stages of tumor development.	142
Figure III.7- Immunohistochemistry of Notch ligands and receptors in phylloides (PHY) and poorly differentiated adenocarcinoma (PDA) lesions of prostate cancer at 30 weeks of age.	143
Supplemental Figure III.10- Immunohistochemistry of Notch effectors in phylloides (PHY) and poorly differentiated adenocarcinoma (PDA) lesions of prostate cancer at 30 weeks of age.	144
Supplemental Figure III.11- Immunohistochemistry of Synaptophysin in poorly differentiated adenocarcinoma (PDA) lesions of prostate cancer at 30 weeks of age.	145
Figure III.8- Cell population specific transcription and expression analysis in prostate tumor development.	147
Supplemental Figure III.12- Immunofluorescence of Jagged1/2 and CK5 in healthy and tumorigenic prostates at 24 weeks of age.	148
Supplemental Figure III.13- Immunofluorescence of Jagged1, N3ICD and Hey1 in healthy and tumorigenic prostates.	150
Figure III.9- Models of Notch expression in healthy and cancerous murine prostate.	153
Figure IV.1- Administration of a blocking antibody against Jagged1 and Jagged2 inhibited prostate tumor development.	165
Figure IV.2- Prostate tumor vascular phenotype in TRAMP mice treated with Anti-Jagged1/2 antibody.	166

Supplemental Figure IV.1- Prostate tumor vascular perfusion and extravasation in Anti-Jagged1/2 treated samples.	167
Figure IV.3- Prostate tumor hypoxic levels in TRAMP mice treated with Anti-Jagged1/2 antibody.	168
Figure IV.4- Prostate cellular apoptosis and proliferation in TRAMP mice administered with blocking Jagged1/2 antibody.	169
Figure IV.5- Treatment of TRAMP mice with Anti-Jagged1/2 antibody inhibited the loss of the luminal identity and the proliferation of the basal cell compartment of the prostate.	171
Supplemental Figure IV.2- Basal cell proliferation in Anti-Jagged1/2 treated samples.	172
Figure IV.6- Epithelial-to-mesenchymal transition in prostate lesions of TRAMP mice treated with Anti-Jagged1/2 antibody.	173
Figure IV.7- Notch3 intracellular domain (N3ICD) expression and Hey1 transcription and expression in prostate lesions of TRAMP mice treated with Anti-Jagged1/2 antibody.	175
Supplemental Figure IV.3- Androgen receptor (AR) expression in prostate samples from Anti-Jagged1/2 treated TRAMP mice.	176
Figure IV.8- Cancer-stem like phenotype in prostatic lesions from TRAMP mice treated with Anti-Jagged1/2 antibody.	178
Supplemental Figure IV.4- Side effects of Anti-Jagged1/2 administration to TRAMP mice.	180
Figure 21- Vascular phenotype comparison between eJag1cKO and anti-Jagged1/2 treated prostate samples.	190
Figure 22- Prostate cell proliferation and apoptosis comparison between eJag1cKO and anti-Jagged1/2 treated prostate tumor samples.	192
Figure 23- EMT phenotype comparison between eJag1cKO and anti-Jagged1/2 treated prostate tumor samples.	192
Figure 24- Cell population changes comparison between eJag1cKO and anti-Jagged1/2 treated prostate tumor samples.	193
Figure 25- Prostate weights comparison between eJag1cKO and anti-Jagged1/2 treated prostate tumor samples.	194
Figure 26- Jagged1 functions in the regulation of prostatic tumor growth.	196

LIST OF ABBREVIATIONS

ADAM - A Disintegrin And Metalloproteinase

ADT - Androgen deprivation therapy

Ag. - Agonist

Akt - Thymoma viral proto-oncogene

Ang - Angiopoietin

ANK - Ankyrin

Anti-Dll4 - Antibody directed against Dll4

Anti-Jag1 - Antibody directed against Jagged1

Anti-Jag1/2 - Antibody directed against both Jagged ligands (Jagged1 and Jagged2)

AR - Androgen Receptor

ASI - Alfa secretase Inhibitors

bHLH - Basic Helix-loop-helix domain

BSA - Bovine Serum Albumine

CADASIL - Cerebral Autosomal Dominant Arteriopathy with Subcortical Infarcts and Leukoencephalopathy

Casp - Caspase

CBF - Cp-binding factor

Ccn - Cyclin

cDNA - complementary DNA

Cdk - Cyclin dependent kinase

Cdkn - Cyclin dependent kinase inhibitor

CIISA - "Centro Interdisciplinar de Investigação em Sanidade Animal"

CK - Cytokeratin

CRPC - Castrate resistance prostate cancer

CSC - Cancer Stem-like cell

CSL - Protein domain present in CBF1, supressor of hairless and LAG-1

CT - Cycle threshold

CTRL - Control

DAPI - 4,6-diamino-2-fenil indol

DAPT - N-S-phenyl-glycine-t-butyl ester

Dll - Delta like

DMEM - Dulbeccos's Modified Eagles's Medium"

DMSO - Dimetil sulfóxido

dNTPs - Deoxyribonucleotides
dpc - Days post-coitum
DSL - Homologous of *delta/serrate/lag-2*
DNA - Deoxyribonucleic acid
E - Embryonic day
EC - Endothelial cell
E-cad - E-cadherin
EGF - Epidermal growth factor
EMT - Epithelial-to-mesenchymal transition
ERT2 - Estrogen receptor T2
*eJag1*OE - Endothelial *Jag1* over-expression
*eJag1*CKO - Endothelial *Jag1* conditional Knock-out
*eDII4*OE - Endothelial *DII4* over-expression
FACS - Fluorescent-Activated Cell Sorting
FCT - Portuguese Foundation for Science and Technology
FDA - Food and drug administration
FELASA - Federation for Laboratory Animal Science Associations
FGF - Fibroblast growth factor
FITC - Fluorescein isothiocyanate
FMV - “Faculdade de Medicina Veterinária”
GSI - Gamma secretase Inhibitors
Hes - Hairy/enhancer of split
Hey - Hairy/enhancer-of-split related with YRPW motif
HERP - Homocysteine-induced endoplasmic reticulum protein
HIF - Hypoxia inducible factor
HNSCC - Head and Neck squamous cell carcinoma
HRP - Horseradish peroxidase
H&E - Hematoxylin and Eosin
H₂O₂ - Hydrogen Peroxide
IgG - Immunoglobulin G
IHC - Immunohistochemistry
IP - Intraperitoneal
LIN - Lineage
LLC - Lewis Lung Carcinoma
LSC - Lin⁻Sca-1⁺CD49f⁺

KO - Knock-out
MAML - Mastermind like
MAPK - Mitogen activated protein kinase
MDA – Moderately differentiated adenocarcinoma
MMP - Matrix metalloproteinase
MMTV - Mouse mammary tumor viruses
mRNA - Messenger ribonucleic acid
mTOR - Mammalian target of Rapamycin
N - Number
NE - Neuroendocrine
NECD - Notch extracellular domain
NED - Neuroendocrine differentiation
NF- κ B - Nuclear factor Kappa Beta
NGP - Neuroblastoma
NICD - Notch intracellular domain
NIH - National Institutes of Health
NLS - Nuclear localization signals
Nrarp - Notch-regulated ankyrin repeat protein
NRR - Negative regulatory regions
NRP - Neuropilin
N1 - Notch1
N3 - Notch3
N4 - Notch4
OE - Over-expression
PBS-W - Phosphate buffered saline-Tween-20
PBS - Phosphate buffered saline
PCR - Polymerase chain reaction
PDA - Poorly differentiated adenocarcinoma
PDGF - Platelet derived growth factor
PE - Phycoerithrin
PECAM - Platelet-endothelial cell adhesion molecule
PEST - Proline, glutamate, serine, threonine rich sequence
PFA - Paraformaldehyde
pH - Hydrogen Potential
PHY - Phylloides

PIN - Prostatic Intraepithelial Neoplasia
PI3K - Phosphatidylinositol-4,5-bisphosphate 3-kinase
PTEN - Phosphatase and tensin homolog
PSMA - Prostate specific membrane antigen
qRT-PCR - Quantitative real-time PCR
RAM - RBPJ-associated molecule
Rb - Retinoblastoma
RBP-jk - Recombination signal binding protein for immunoglobulin kappa J region
RGB - Red, Green and Blue
RNA - Ribonucleic acid
rtTA - Reverse tetracycline-controlled transactivator
sDII4-Fc - Soluble DII4 fusion protein
SEM - Standard error mean
SMA - Smooth muscle actin
SV - Simian Virus
TACE - TNF-alpha converting enzyme
TAD - Transactivation domain
Tet-O - Tetracycline-Controlled Transcriptional Activation
Tie - Tyrosine kinase receptor
TGF β - Transforming growth factor beta
Tris - Tris(Hidroximetil)aminometano
Tween - polyoxyethylene (20) sorbitan monolaurate
uPAR - Urokinase receptor
v - Vascular
VE- Cadherin - Vascular endothelial cadherin
VEGF - Vascular endothelial growth factor
VEGFR - Vascular endothelial growth factor receptor
vSMA- Vascular smooth muscle actin
WDA - Well differentiated adenocarcinoma
wks - Weeks
WT - Wild-type



INTRODUCTION



During normal body growth and in many disease processes, blood vessels proliferate by angiogenesis, where new vessels sprout from existing ones and remodel into complex new vascular networks. Angiogenesis is essential for embryonic development, reproduction, and repair or regeneration of tissues during wound healing. Changes in the fine balance between angiogenic stimulators and inhibitors, which regulate this process, are associated with a broad range of angiogenesis-dependent diseases such as atherosclerosis, age-related macular degeneration, rheumatoid arthritis and neoplastic disturbances. Angiogenesis is now recognized as one critical hallmark required for tumor progression, in which continuous growth is dependent on vascular induction and the development of a neovascular network (Hanahan, Weinberg, & Francisco, 2000).

The experimental study of new blood vessels formation, i.e. angiogenesis began in the late 1930s and early 1940s, when several investigators studied the events of neovascularization in experimental tumors (Algire, 1943; Ide & Warren, 1939). In these experiments tumors were separated from host tissue by a micropore filter and demonstrated that an unknown diffusible substance was released from the tumor and could stimulate new blood vessel growth. However, prior to 1970, the prevailing belief was that tumor angiogenesis was a side-effect of dying tumor cells. It was only in 1969 that Judah Folkman raised the possibility of tumor growth being angiogenesis-dependent by observing a retinoblastoma in a child, which consisted of a large tumor that protruded from the retina into the vitreous and it was highly vascularized. Moreover he observed tiny metastasis shed in the vitreous that were all avascular and had a necrotic center. Therefore, he developed the concept that tumors could not grow beyond approximately 1-2 millimeters without recruiting new blood vessels. These findings were published in 1971 (Folkman, 1971) and since then a revolution in the field of angiogenesis allowed for the investigation and discovery of several molecular mechanisms that contribute to the process of angiogenesis.

Many signaling pathways have been identified as key contributors to the neo-angiogenic process. Among them is the Notch signaling pathway, an evolutionary conserved signaling system that regulates proliferation, differentiation, cell-fate determination, progenitor and stem-cell self-renewal, in both embryonic and adult tissues (Artavanis-Tsakonas, Rand, & Lake, 1999; Schweisguth, 2004). The Notch pathway is composed of 5 ligands (Jagged1, Jagged2, and Delta-like 1, 3, and 4) and 4 receptors (Notch 1–4). Among the ligands, Dll4 is the most broadly studied in vascular biology and shown to be essential for developmental (Duarte et al., 2004; Krebs et al., 2004; Gale et al., 2004; Lobov et al., 2007; Suchting et al., 2007; Hellström et al., 2007) and tumor angiogenesis (Noguera-Troise et al., 2006; Ridgway et al., 2006; Sclafani et al., 2007), and known to be expressed specifically in the endothelial layer (Shutter et al., 2000). Jagged1 is a Notch ligand with a broader expression pattern, present in both the endothelium as in vascular smooth muscle support cells (Doi et al., 2006) and also found to be essential for developmental angiogenesis of the embryo (Xue et al., 1999) and of the post-

natal retina (Benedito et al., 2009). In the growing retinal vascular plexus, Jagged1 was shown to be a critical positive regulator of sprouting angiogenesis due to its ability to modulate Dll4-Notch signaling in the endothelium. However the underlying cellular mechanisms regulated by Jagged1/Notch signaling still remain incompletely understood, especially in an adult setting. Therefore the research work presented in this thesis aimed to analyze Jagged1 driven Notch signaling enrolment in physiological and tumor angiogenesis, in prostate tumorigenesis, and finally the potential therapeutic application of blocking Jagged ligands in prostate cancer management. Firstly, the role of endothelial Jagged1 in wound healing kinetics and angiogenesis was investigated with endothelial-specific *Jag1* gain-of-function and loss-of-function mouse mutants (*eJag1OE* and *eJag1cKO*). Moreover, to study the interactions between the 2 Notch ligands (Jagged1 and Dll4), the genetic mouse models were combined with pharmacological inhibition of Dll4 or Jagged1, respectively. Secondly, with the same endothelial-specific *Jag1* mutants the role of endothelial Jagged1-mediated Notch signaling in the context of tumor angiogenesis was investigated using two different mouse tumor models: subcutaneous Lewis Lung Carcinoma (LLC) tumor transplants and the autochthonous Transgenic Adenocarcinoma of the Mouse Prostate (TRAMP). Thirdly, we analyzed Notch family members transcription and expression, including ligands (Dll1, 3, 4 and Jagged1 and 2), receptors (Notch1-4) and effectors (Hes1, 2, 5 and Hey1, 2, L), in both normal and tumor bearing mouse prostate to better understand the dynamics of Notch signaling in prostate tumorigenesis. And finally, to investigate the potential therapeutic application of blocking Jagged ligands in prostate tumor management we administered blocking anti-Jagged1/2 antibody to transgenic adenocarcinoma of the mouse prostate model (TRAMP) mice. The above studies were converted into four articles, submitted for publication in international journals, and constitute the four chapters of the experimental work included in this thesis, as follows:

1. Endothelial Jagged1 antagonizes Dll4 regulation of endothelial branching and promotes vascular maturation downstream of Dll4/Notch1.

Pedrosa A-R., Trindade A., Fernandes A-C., Carvalho C., Gigante J., Tavares A-T., Diéguez-Hurtado R., Yagita H., Adams R-H. And Duarte A.. *Arterioscler Thromb Vasc Biol.* 2015;35(5):1134-1146. DOI: 10.1161/ATVBAHA.114.

2. Endothelial Jagged1 promotes solid tumor growth through both pro-angiogenic and angiocrine functions.

Pedrosa A-R., Trindade A., Carvalho C., Graça J., Carvalho S., Peleteiro M-C., Adams R-H. and Duarte A.. *Oncotarget* 2015; 6(27). DOI:10.18632/oncotarget.4380.

3. Notch signaling dynamics in the adult healthy prostate and in prostatic tumor development.

Pedrosa A-R., Graça J-L., Carvalho S., Peleteiro M-C., Duarte A. and Trindade A.. *The Prostate*, 2016; 76(1); 80-96. DOI:10.1002/pros.2310.

4. Targeting Jagged1/2 as a new promising therapeutic approach for prostate cancer.

Pedrosa A-R., Trindade A., Carvalho C., Peleteiro M-C., Gigante J., West J. and Duarte A. Manuscript in preparation.



**LITERATURE
REVIEW**

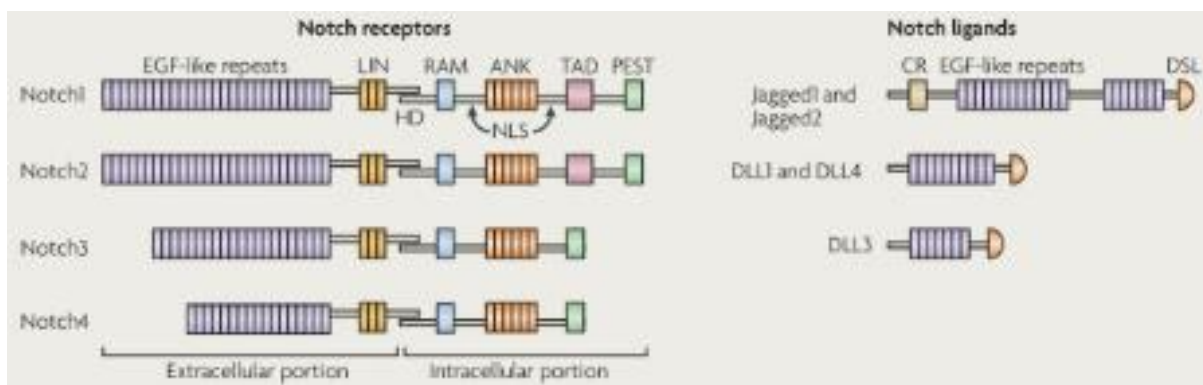


1. Notch signaling pathway

The Notch signaling pathway was first discovered about 100 years ago when John Dexter, in 1904, described *Drosophila melanogaster* variants displaying wing phenotypes now associated with Notch pathway mutations (Dexter, 1914). Three years later Thomas Morgan was able to identify the mutant alleles (Morgan, 1917), but it was only after the molecular biology revolution, that Spyros Artavanis-Tsakonas and Michael Young were able to clone the Notch receptor and thus attribute the wing-notching phenotype to gene haplo-insufficiency (Wharton, Johansen, Xu, & Artavanis-Tsakonas, 1985; Kidd, Kelley, & Young, 1986). These initial studies created the basis foundation for a new era in various fields, including developmental and stem cell biology, neuroscience, and cancer biology (Fortini, Rebay, Caron, & Artavanis-Tsakonas, 1993). Since then, the Notch signaling pathway has been extensively characterized in its role in cell-fate determination, differentiation, proliferation, progenitor and stem-cell self-renewal, in a diversity of embryonic and adult tissues (Artavanis-Tsakonas et al., 1999; Schweisguth, 2004).

The Notch signaling pathway is a highly conserved pathway among metazoan species. In mammals, four transmembrane Notch receptors (Notch 1-4) and five distinct ligands (Jagged1-2, Delta-like 1, 3, and 4) are synthesized (Fig.1).

Figure 1- Notch receptors and ligands structure. In (Osborne & Minter, 2007).



Notch protein receptors reside on the cell surface as non-covalently linked heterodimers that are comprised of the extracellular and transmembrane (intracellular) Notch polypeptides. Extracellular portions are characterized by numerous epidermal growth factor (EGF)-like repeats. Transmembrane portions include the membrane-proximal RBP-J-associated molecule (RAM) domain, which mediates interaction with several cytosolic and nuclear proteins; the Ankyrin (ANK) domain, which is also important for protein-protein interactions; two nuclear-localization sequences (NLSs); a carboxy-terminal transactivation domain (TAD), which is important for activating transcription; and a PEST (proline-, glutamate-, serine- and threonine-rich) domain, which is important for regulating Notch degradation. Transmembrane Notch3 and Notch4 are shorter and lack the TAD. The heterodimerization domain (HD) spans the region of interaction between the extracellular and transmembrane portions.

The Notch ligands contain an EGF-like repeat region and a conserved sequence also known as Delta/Serrate/Lag (DSL). Jagged1 and Jagged2 each have a conserved cysteine-rich (CR) domain.

1.1 Notch receptors

Notch receptors are transmembrane molecules containing EGF-like repeats, that consist of an N-terminal extracellular (NECD) domain and a C-terminal transmembrane-intracellular subunit (Blaumueller, Qi, Zagouras, & Artavanis-Tsakonas, 1997). Additionally, the receptor contains a negative regulatory region (NRR) comprised of three cysteine-rich Lin12/Notch repeats (Aster et al., 1999) (Fig.1). Notch receptors expression varies significantly in adult and embryonic tissues with overlapping expression patterns, but they do have specific roles during hematopoietic stem cells generation, immune cell fate and lineage development, and vascular morphogenesis (Ntziachristos, Lim, Sage, & Aifantis, 2014).

Notch 1 is the most broadly studied Notch receptor and the main receptor responsible for Notch signaling associated phenotypes. Genetic deletion of Notch1 in mice results in embryonic lethality by severe vascular and cardiovascular defects (Swiatek, Lindsell, del Amo, Weinmaster, & Gridley, 1994). Moreover, Notch1 has also been reported to be essential for proper somitogenesis (Conlon, Reaume, & Rossant, 1995). Besides its classical inhibitory angiogenic function, Notch1 has also been associated with several other cell functions, namely in adult tissue homeostasis and tumor development (Ntziachristos et al., 2014).

The Notch2 gene was the second of the mammalian Notch family receptors to be cloned (Weinmaster, Roberts, & Lemke, 1992). Later, mice homozygous for a hypomorphic Notch2 mutation were reported to present defects in development of the kidney, heart and eye vasculature (McCright et al., 2001). Notch2 was also shown to be expressed in vascular smooth muscle cells and to play a critical role in vascular maturation (Hamada et al., 1999; Varadkar et al., 2008; Wang, Zhao, Kennard, & Lilly, 2012).

The Notch3 gene was the third mammalian Notch homologue to be identified and initially described as being expressed in proliferating neuroepithelium (Lardelli, Dahlstrand, & Lendahl, 1994). Even though it was demonstrated that the Notch3 gene is not essential for embryonic development or fertility in mice (Krebs et al., 2003), Notch3 loss-of-function in mice resulted in profound structural and functional defects in arteries, due to impaired vascular maturation indicating a potential role in smooth muscle cell differentiation (Domenga et al., 2004). In smooth muscle cells, Notch3 is the predominant Notch receptor and is the causal gene for the neurovascular disorder CADASIL (cerebral autosomal dominant arteriopathy with subcortical infarcts and leukoencephalopathy) (A. Joutel et al., 2000; A. Joutel et al., 1996). CADASIL consists of a type of stroke and dementia whose key features include recurrent subcortical ischaemic events, vascular dementia, leukoencephalopathy, and a non-atherosclerotic, non-amyloid angiopathy involving mainly the small cerebral arteries (Joutel et al., 1996).

Notch4, the fourth and last mammalian Notch homologue to be discovered, was cloned from mice and humans (Uyttendaele et al., 1996; Li et al., 1998). Notch4 is primarily expressed on

the endothelium and the endocardium (Uyttendaele et al., 1996; Shirayoshi et al., 1997; Li et al., 1998) and genetic deletion of Notch4 in mice, even though it did not produce a detectable phenotype on its own, exacerbated the embryonic lethal vascular defects associated with Notch1 when the two mutations were combined (Krebs et al., 2000; Gridley, 2001), suggestive of an important role in vascular development.

1.2 Notch ligands

The DSL ligands have also been conserved throughout metazoan evolution (D'Souza, Miyamoto, & Weinmaster, 2008). On the basis of structural homology to the two *Drosophila* ligands, Delta and Serrate, the mammalian canonical ligands are designated as either Delta-like (DII1, DII3 and DII4) or Jagged (Jagged1 and Jagged2) (Bray, 2006). DSL ligands are also transmembrane proteins, similarly to the Notch receptors, with an extracellular domain that contains a characteristic number of EGF-like repeats and a cysteine-rich N-terminal DSL domain. The DSL domain is a conserved motif that is found in all DSL ligands and is required for their interaction with Notch (Fig.1).

1.2.1 Delta-like ligands

The murine Delta-like 1 gene was first isolated in 1995 (Bettenhausen, Hrabě de Angelis, Simon, Guénet, & Gossler, 1995) and described to be essential for normal somitogenesis and neuronal differentiation (Hrabě de Angelis, McIntyre, & Gossler, 1997). Later its expression was found in several organs epithelia, skeletal and smooth muscles, central nervous system and in some sensory epithelia (Beckers, Clark, Wünsch, Hrabé De Angelis, & Gossler, 1999). In more recent years, DII1 was shown to be essential for post-natal arteriogenesis (Limbourg et al., 2007) and established as a critical endothelial Notch ligand required for maintaining arterial identity during mouse fetal development (Sørensen, Adams, & Gossler, 2009).

DII3 is a structurally divergent DSL family member that is expressed in the developing brain, thymus and paraxial mesoderm (Dunwoodie, Henrique, Harrison, & Beddington, 1997). Unlike DII1, DII3 lacks structural characteristics important for DSL ligands to bind to Notch in trans and thereby activate Notch signaling (Ladi et al., 2005). Overexpression of DII3 in mammalian cells blocks Notch signaling supporting the notion that DII3 is a Notch antagonist (Ladi et al., 2005).

The DII4 ligand was first described as a vascular endothelium specific ligand (Shutter et al., 2000). In the developing embryo, expression of DII4 is initially restricted to large arteries, whereas in adult mice its expression is limited to small arteries and microvessels (Duarte et al., 2004). Haplo-insufficiency of DII4 in mice results in embryonic lethality at approximately 10.5 dpc due to defective vascular development, including abnormal stenosis and atresia of the aorta, defective arterial branching from the aorta, arterial regression, gross enlargement of

the pericardial sac and failure to remodel the yolk sac vasculature. This studies revealed Dll4 to be essential for the normal arterial patterning and vascular remodeling during embryonic development (Duarte et al., 2004; Krebs et al., 2004; Gale et al., 2004). Another study in developing mouse embryos has revealed Dll4 expression not only in the vascular system but also in the nervous, gastrointestinal and urinary systems (Benedito & Duarte, 2005). Dll4 is also considered to be an essential regulator of physiological and tumoral angiogenesis, by its ability to inhibit proliferating angiogenesis, normalizing the vasculature (Noguera-Troise et al., 2006; Ridgway et al., 2006; Trindade et al., 2012).

1.2.2 Jagged ligands (Jagged1 and Jagged2)

Jag1-null mouse mutants die at 11.5 dpc because of heart defects and abnormal development of the yolk sac and head vasculature (Xue et al., 1999). Moreover, mutations in the human *JAG1* gene cause Alagille syndrome, which comprises complex cardiac defects and vascular anomalies (Spinner et al., 2001). Unlike Dll4, whose expression is restricted to the arterial and capillary endothelium (Shutter et al., 2000), Jagged1 is also expressed in vascular smooth muscle cells (Doi et al., 2006). This fact led to several studies in which Jagged1 was shown to be essential for perivascular cell recruitment and vascular maturation (High et al., 2008; Liu, Kennard, & Lilly, 2009). Moreover, Jagged1 is also expressed in a variety of other tissues, like the skin (Aho, 2004), liver (Louis et al., 1999), nervous tissue (Nyfeler et al., 2005) and cells of the immune system (Beverly, Ascano, & Capobianco, 2006), among others. Increased Jagged1 expression has also been described in several types of tumors, including: pulmonary (Jiang et al., 2007), mammary (Dickson et al., 2007) and prostatic (Santagata et al., 2004). Jagged-2 (*Jag2*) was first identified in 1996 (Shawber, Boulter, Lindsell, & Weinmaster, 1996) and found to be required for craniofacial, limb and T cell development (Jiang et al., 1998). It was also found to be expressed in endothelial cells and hematopoietic progenitors (Tsai, Fero, & Bartelmez, 2000).

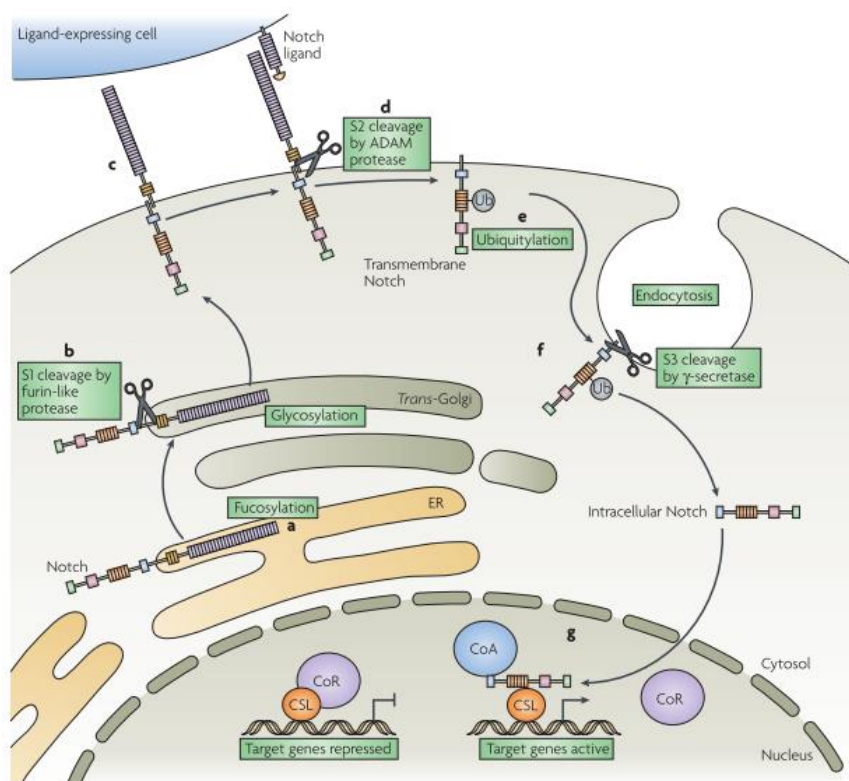
1.3 Notch signaling pathway activation

The functional Notch receptors are translocated to the cell surface as processed heterodimers. The final heterodimeric form of the receptors is preceded by a series of transformations which include: a Furin-dependent cleavage (S1 cleavage) in the NECD, that occurs during trafficking through the Golgi complex (Logeat et al., 1998); and a glycosylation by O-fucosyltransferase and Fringe family N-acetylglucosaminidyl transferases that is crucial for proper folding of the Notch receptor and the interaction with ligand-specific DSL domains (Delta, Serrate, Lag-2) (Rana & Haltiwanger, 2011) (Fig.2).

Distinct ligand affinities exist for the various receptors, altered by glycosylation, which influences downstream transcriptional activation (Ntziachristos et al., 2014). Notch pathway

activation requires ligand-receptor binding in close proximity cells because the ligands remain immobilized as transmembrane proteins. After Notch receptor binding, the ligand undergoes endocytosis within the ligand-emitting cell, which causes a mechanical disruption of the Notch receptor by changing the conformation of the negative regulatory region of the receptor. This conformational change in the Notch receptors, allows for a second cleavage (S2) of the ectodomain by an ADAM17 metalloprotease/TNF- α converting enzyme (TACE) (Brou et al., 2000) followed by a third cleavage (S3) mediated by the presenilin- γ -secretase complex (De Strooper et al., 1999). These series of cleavages lead to the release of the intracellular portion of the Notch receptor (NICD). The NICD contains nuclear localization signals (NLSs) within the RAM domain (Fig.1) which allows for the translocation to the nucleus where it forms a complex with the inactive DNA-binding factor CSL/RBPjk (CBF1/Suppressor of Hairless/Lag1) and recruits other co-activator proteins from the Mastermind-like family of proteins such as MAML1 (Nam, Sliz, Song, Aster, & Blacklow, 2006; Wilson & Kovall, 2006). In the absence of NICD, RBP-Jk associates with a corepressor complex and acts as a transcriptional repressor of Notch target genes (Kao et al., 1998). In turn, the NICD/RBP-Jk complex leads to the transcription of Notch downstream target genes, such as several helix–loop–helix transcription factors (*Hey* and *Hes* gene families among others) (Schweisguth, 2004) (Fig.2). Notch signaling activation in more distant cells, without direct cell contact, has also been reported. A soluble JAGGED1 extracellular domain, generated by ADAM proteolytic cleavage, has been implicated in mediating paracrine Notch signaling between endothelial cells and tumor cells (Lu et al., 2013). Moreover, Dll4 has also been described to be incorporated into exosomes that can transfer the Dll4 protein from one cell type to another and incorporate it into the plasma membrane (Sheldon et al., 2010).

Figure 2- Notch signaling pathway. *In* (Osborne & Minter, 2007).



A. In the endoplasmic reticulum (ER), the Notch polypeptide is fucosylated by the fucosyltransferase FUT1. **B.** Shuttling of the Notch protein to the trans-Golgi, where it is cleaved by a furin-like protease at the S1-cleavage site to generate the non-covalently linked Notch heterodimer, comprised of the extracellular portion and the intracellular portion. The heterodimer then undergoes glycosylation by several specific glycosylases, including Manic fringe, Radical fringe and Lunatic fringe, which are all members of the Fringe glycosyltransferase family. **C.** The Notch heterodimer associates with the plasma membrane, where it becomes available to interact with Notch ligand on a ligand-expressing cell. **D.** Interaction with a Notch ligand induces proteolytic cleavage of the Notch receptor by the ADAM (a disintegrin and metalloproteinase) protease TACE (tumour-necrosis-factor- α -converting enzyme). **E.** Mono-ubiquitylation of the intracellular portion of the transmembrane Notch fragment. **F.** Endocytosis of the transmembrane fragment of the Notch protein, facilitating cleavage by γ -secretase in an early endosome, resulting in the release of the intracellular Notch fragment. **G.** Intracellular Notch then travels to the nucleus, where it associates with the transcriptional repressor CSL (CBF1-suppressor of hairless–Lag1), resulting in the expression of genes that are regulated by CSL. CoA, co-activator; CoR, co-repressor.

1.4 Notch effectors

The main Notch signaling transducers are Hairy and Enhancer-of-split-related basic helix-loop-helix (bHLH) transcription factors, such as Hey and Hes in mammals (Iso, Kedes, & Hamamori, 2003). This bHLH family of transcriptional regulators plays determinant roles in the development of various organs and cell types (Murre et al., 1994). To date, seven Hes

members (1-7) (Akazawa, Sasai, Nakanishi, & Kageyama, 1992; Sasai, Kageyama, Tagawa, Shigemoto, & Nakanishi, 1992; Ishibashi, Sasai, Nakanishi, & Kageyama, 1993; Hirata, Ohtsuka, Bessho, & Kageyama, 2000; Bae, Bessho, Hojo, & Kageyama, 2000; Pissarra, Henrique, & Duarte, 2000; Koyano-Nakagawa, Kim, Anderson, & Kintner, 2000; Bessho, Miyoshi, Sakata, & Kageyama, 2001), and three HERP/Hey members (Hey1, 2 and L) (Kokubo, Lun, & Johnson, 1999; Leimeister, Externbrink, Klamt, & Gessler, 1999; Chin et al., 2000; Zhong, Rosenberg, Mohideen, Weinstein, & Fishman, 2000; Iso et al., 2001) have been isolated in mammals. Both Hes and Hey factors were described to act as transcriptional repressors with the exception of Hes6, which antagonizes the function of Hes1, resulting in de-repression (Bae et al., 2000; Koyano-Nakagawa et al., 2000).

Hes1 mRNA was found to be expressed in various tissues of both embryos and adults, and present at a high level in epithelial cells (Sasai et al., 1992), whereas *Hes2* mRNA was found to be present as early as embryonic day 9.5 and detected in a variety of tissues of both embryos and adults (Ishibashi et al., 1993). Initially, *Hes5* mRNA was found to be specifically expressed in the nervous system (Akazawa et al., 1992) and later found to be transcribed also in vascular smooth muscle cells (Joutel et al., 2000).

Regarding Hey effectors, all three genes (*Hey1*, *Hey2*, and *HeyL*) are expressed in dynamic patterns in multiple tissues of the mouse embryo (Leimeister et al., 1999; Nakagawa, Nakagawa, Richardson, Olson, & Srivastava, 1999). Both *Hey1* and *Hey2* mRNAs were shown to be highly expressed in the aorta (Chin et al., 2000) and the other HERP member *HeyL* mRNA was also detected in the aortic smooth muscle layer of the mouse embryo (Leimeister, Schumacher, Steidl, & Gessler, 2000). The knock-out of *Hey2*, also known as *Hesr2/CHF1/Hrt2/Herp1*, revealed a critical function during heart development with most of the affected mice dying during the first week of life with severe heart defects (Donovan, Kordylewska, Jan, & Utset, 2002; Gessler et al., 2002). Moreover, its expression has been associated with the arterial identity in assignment of vessel-specific cell fate (Zhong et al., 2000). *Hey1* knock-out mice did not show a discernible phenotypic defect, however, the combined loss of *Hey1* and *Hey2*, led to a lethal vascular defect that affected the placenta, the yolk sac, and the embryo itself, due to impaired arterial fate determination and maturation (Fischer, Schumacher, Maier, Sendtner, & Gessler, 2004). The Hey family of transcription factors, due to its involvement in multiple aspects of vascular development, are considered the main Notch effectors in the vascular system.

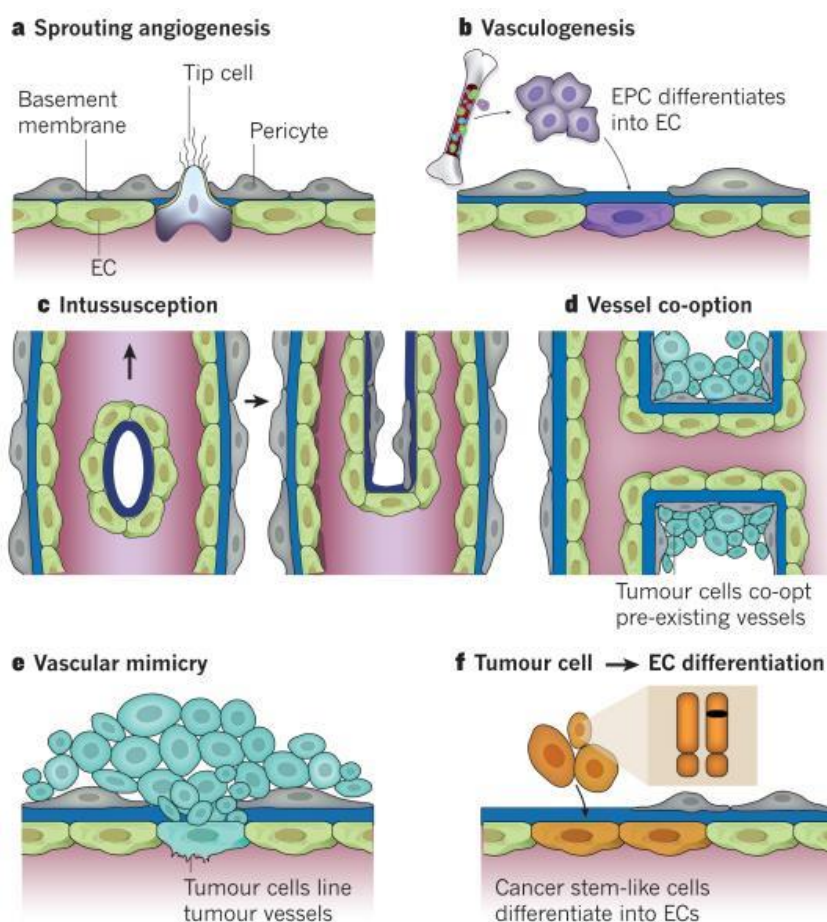
More recently another Notch downstream target was identified, *Nrarp*, encoding a small protein containing two ankyrin repeats, which expression is activated in *Xenopus* embryos by the CSL-dependent Notch pathway (Lamar et al., 2001). During mouse embryogenesis, the *Nrarp* gene was shown to be expressed in several tissues in which cellular differentiation is Notch regulated and *Nrarp* transcript levels were shown to be regulated by the level of Notch1

signaling in both cultured cell lines and mouse embryos (Krebs, Deftos, Bevan, & Gridley, 2001).

2. Blood vessel formation

Tissues can become vascularized by several mechanisms (Fig. 3) beyond sprouting angiogenesis (Fig. 3a), which is the formation of new blood vessels from existing ones. In the developing mammalian embryo, angioblasts differentiate into endothelial cells, which assemble into a new vascular bed, a process known as vasculogenesis (Fig. 3b). Post-natal vasculogenesis, even though less well understood, can also occur, during which bone-marrow-derived cells (BMDCs) and/or endothelial progenitor cells are recruited and become incorporated into the endothelium (Ribatti, Vacca, Nico, Roncali, & Dammacco, 2001). Pre-existing vessels can split by a process known as intussusception, giving rise to daughter vessels (Fig. 3c). In other cases, tumor cells can hijack the existing vasculature leading to vessel co-option (Fig. 3d), or they can line the vessels leading to vascular mimicry (Fig. 3e). Cancer stem-like cells can also generate tumor endothelium (Wang et al., 2010) (Fig. 3f).

Figure 3- Modes of vessel formation. *In* (Carmeliet & Jain, 2011).



There are several known methods of blood vessel formation in normal tissues and tumours. Vessel formation can occur by sprouting angiogenesis (a), by the recruitment of bone-marrow-derived and/or vascular-wall-resident endothelial progenitor cells (EPCs) that differentiate into endothelial cells (ECs; b), or by a process of vessel splitting known as intussusception (c). Tumour cells can co-opt pre-existing vessels (d), or tumour vessels can be lined by tumour cells (vascular mimicry) (e) or by endothelial cells, with cytogenetic

abnormalities in their chromosomes, derived from putative cancer stem cells (f). Unlike normal tissues,

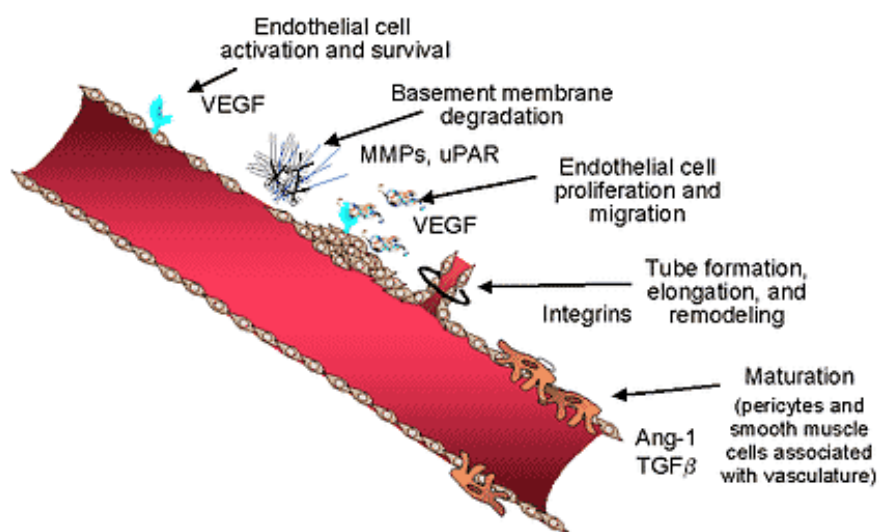
which use sprouting angiogenesis, vasculogenesis and intussusception (a–c), tumours can use all six modes of vessel formation (a–f).

2.1 Angiogenesis

The first description of the process of angiogenesis was made in 1794 by a British surgeon and anatomist, John Hunter (Hunter, 1794). Angiogenesis refers to the formation of new blood vessels from pre-existing ones (Risau, 1997) and requires a series of complex remodeling processes such as: vasodilation, cellular permeability, peri-endothelial support, proliferation, migration, lumenization, survival, differentiation and remodeling (Carmeliet, 2000). Triggering angiogenesis requires a disruption between the fine balance of pro-angiogenic and anti-angiogenic molecules (Karamysheva, 2008). It is initiated through endothelial basal membrane and extracellular matrix degradation of the pre-existing vessels, which is mediated by metalloproteases (Moses, 1997) (Fig. 4). A new matrix is then synthesized by stromal cells and laid down, which together with soluble growth factors, enables the migration and proliferation of endothelial cells (Papetti & Herman, 2002). The vascular endothelial growth factor A (VEGFA) determines the migration direction, which is performed by specialized endothelial cells named tip-cells (Gerhardt et al., 2003). After sufficient endothelial cell division and migration has occurred, endothelial cells arrest in a monolayer and form a tube-like structure. Mural cells (pericytes and smooth muscle cells) are then recruited (Papetti & Herman, 2002) for maturation of the newly formed vessel. Finally, if proper angiogenesis took place, blood flow is then established in the new vasculature.

Figure 4- The angiogenic process. *Adapted from (www.medscape.org).*

The Angiogenic Process



The angiogenic process occurs during embryonic development (Carmeliet, 2005) and in the adult it can occur in physiological situations, like the oestrus cycle in the females (Fraser & Lunn, 2000) or in wound healing situations (Arbiser, 1996), whereas in adult pathological scenarios it occurs in tumor growth (Folkman, 1971), among others (Carmeliet, 2003).

2.2 Angiogenesis regulation

There are several signaling pathways involved in angiogenesis regulation, such as VEGF, Angiopoietin, PDGF and Notch (Rossant & Howard, 2002; Karamysheva, 2008).

2.2.1 VEGF signaling

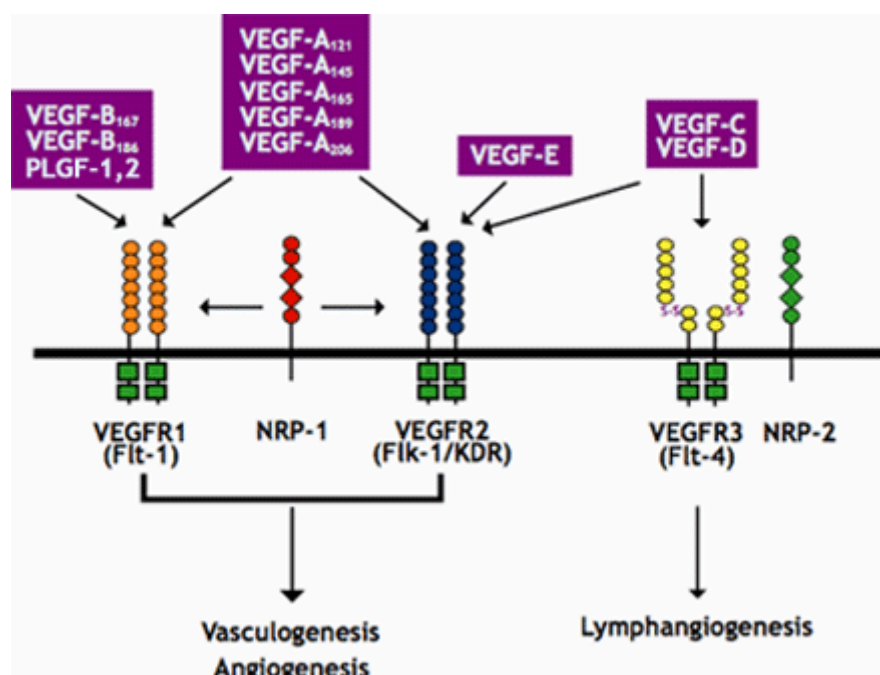
Vascular endothelial growth factor (VEGF) signaling cascade is considered to be the main pathway in the regulation of angiogenesis. In 1983, Senger and Dvorak first identified a vascular permeability factor (VPF) (Senger et al., 1983) and later in 1989, Ferrara and collaborators independently purified a protein with growth-promoting activity for ECs and named it VEGF (Ferrara & Henzel, 1989). In the same year, VEGF was cloned and suggested the existence of several molecular species of this factor (Leung, Cachianes, Kuang, Goeddel, & Ferrara, 1989). To date, extensive studies on VEGF family revealed the existence of more than seven members (Fig. 5). There are 4 *Vegf* genes known in the mouse, *Vegf-A*, *B*, *C* and *D* and one growth factor associated, *placental growth factor (PlGF)* (Neufeld, Cohen, Gengrinovitch, & Poltorak, 1999) (Fig.5). *Vegf-A* is the family gene more relevant for embryonic development being a powerful inducer of angiogenesis (Shweiki, Itin, Soffer, & Keshet, 1992; Hanahan & Folkman, 1996), and also an important factor regulating vascular permeability (Senger et al., 1983). Homozygous loss-of-function mouse embryos die between embryonic

days 8,5 and 9,5 (Carmeliet et al., 1996) and loss of a single *Vegf* allele is also lethal between 11 and 12 dpc and angiogenesis and blood-island formation are impaired, resulting in several developmental anomalies (Carmeliet et al., 1996; Ferrara et al., 1996).

The *Vegf-A* gene is transcribed in different mRNA forms. The three more common are translated into different isoform proteins with specific molecular weights: 120 amino acid (aa) residues, 164 and 188 (Ferrara & Davis-Smyth, 1997). An important biological property that distinguishes the different VEGF isoforms is their heparin and heparan-sulfate binding ability. For example, VEGF₁₂₁ lacks the amino acids encoded by exons 6 and 7 of the *Vegf* gene (Tischer et al., 1991) and does not bind to heparin or extracellular matrix (Park, Keller, & Ferrara, 1993), being a completely soluble ligand. The ability of becoming soluble secreted ligands is important because it creates a gradient of VEGF that ultimately is responsible for inducing proliferation of endothelial cells and *in vivo* angiogenesis, which is the case with the isoforms 121, 145 and 165 (Park et al., 1993; Zhang et al., 1995; Poltorak et al., 1997).

Hypoxia is one of the most important inducers of VEGF expression (Dor & Keshet, 1997). For example, many human solid tumor cells express increased amounts of VEGF in response to hypoxia, thus stimulating development of new vessels in the growing tumor tissue.

Figure 5- Vegf family members. In (Hicklin & Ellis, 2005).



Binding specificity of various vascular endothelial growth factor (VEGF) family members and their receptors. The VEGF family consists of seven ligands derived from distinct genes (VEGF-A, -B, -C, -D, and -E, placenta growth factor [PlGF] -1 and -2). VEGF family members have specific binding affinities to VEGF receptor (VEGFR) -1, VEGFR-2 and VEGFR-3 tyrosine kinase receptors as shown. In addition, neuropilin (NRP)-1 and NRP-2 are co-receptors for specific isoforms of VEGF family members and increase binding affinity of these ligands to their respective receptors.

Growth factors of the VEGF family exert their biological effect via interaction with receptors located on endothelial cell membranes (Fig. 5). Three receptors have been identified that bind different VEGF growth factors: VEGFR1 (Flt1), VEGFR2 (Flk1/KDR), and VEGFR3 (Flt4) (Steinle et al., 2002; Karamysheva, 2008). These receptors are transmembrane proteins that belong to the superfamily of receptor tyrosine kinases (RTK). Beyond VEGFR there are also accessory receptors, Neuropilin-1 (NRP-1) and Neuropilin-2 (NRP-2), known transmembrane glycoproteins, receptors for class-3 semaphorins, which are mainly responsible for axon guidance during the development of the nervous system in vertebrates (Neufeld, Kessler, & Herzog, 2002; Byrne, Bouchier-Hayes, & Harmey, 2005). Unlike the VEGFRs, these receptors do not have a tyrosine kinase domain and therefore are unable to transduce VEGF signals on their own, unless in conjunction with a VEGF receptor (Byrne et al., 2005).

Similarly to what was seen with *Vegf-a* mouse mutants, disruption of the genes encoding the VEGF tyrosine-kinase receptors VEGFR-2 (Shalaby et al., 1995) and VEGFR-1 (Fong, Rossant, Gertsenstein, & Breitman, 1995) results in severe abnormalities of blood vessel formation in homozygous animals. Mouse embryos homozygous for a targeted mutation in the *flt1* locus, died in utero at 8,5 dpc with an increase in the number of endothelial cells in the embryonic and extra-embryonic areas which assembled into abnormal vascular channels (Fong et al., 1995). Mice deficient in *Flk1* died in utero between 8.5 and 9.5 dpc, as a result of an early defect in the development of haematopoietic and endothelial cells, demonstrating that this gene is essential for yolk-sac blood-island formation, vasculogenesis and for the migration and differentiation of endothelial cells to the appropriate sites in the embryo (Shalaby et al., 1995; Veikkola, Karkkainen, Claesson-Welsh, & Alitalo, 2000). VEGFR3 is also required for developmental angiogenesis and mouse embryos with *Vegfr-3* loss-of-function die in utero at 9,5 dps with cardiovascular failure and fluid accumulation in the pericardial cavity due to defective large blood vessel development with defective lumens (Dumont et al., 1998). Even though in adults VEGFR3 becomes mainly expressed on the endothelium of lymphatic vessels, therefore selectively affecting lymphangiogenesis (Kaipainen et al., 1995; Alitalo & Carmeliet, 2002) it has also been detected in endothelial venules and fenestrated capillaries (Partanen et al., 2000).

VEGFA has been shown to interact with VEGFR1 and VEGFR2. Following ligand-receptor activation occurs receptor dimerization followed by trans/auto-phosphorylation of tyrosine residues in the cytoplasmic kinase domain. However, even though VEGFR1 was firstly identified (Shibuya et al., 1990), it was shown that VEGFA stimulates only very weak auto-phosphorylation of VEGFR1 (Waltenberger, Claesson-Welsh, Siegbahn, Shibuya, & Heldin, 1994), and mouse embryos that had just the tyrosine kinase of the *Vegfr-1* deleted formed normal vascular structures and survived with defects in macrophage migration (Hiratsuka, Minowa, Kuno, Noda, & Shibuya, 1998). These observations suggest this receptor functions as a decoy for VEGFA, or negative regulator, limiting its availability for VEGFR2 and not as a

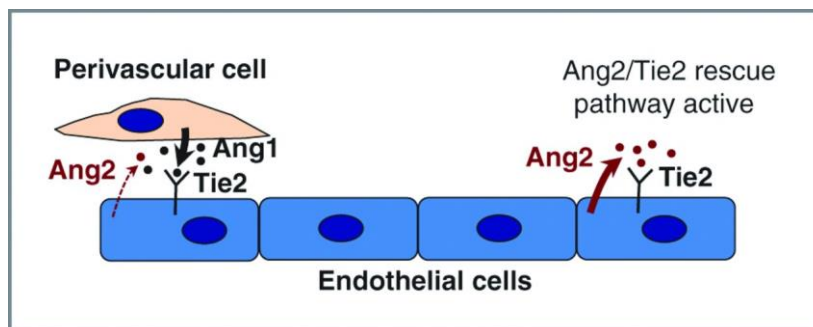
VEGF signal transducer (Hiratsuka et al., 1998; Hiratsuka, Nakao, Nakamura, Katsuki, & Maru, 2005; Veikkola et al., 2000). In opposition, activation of VEGFR2 by VEGFA stimulates a number of signal transduction pathways that later drive mitogenesis, migration, and survival of endothelial cells (Karamysheva, 2008). Furthermore, VEGFA does not interact with receptor VEGFR3, its ligands being two other members of this family, VEGFC and VEGFD (Lee et al., 1996; Achen et al., 1998).

2.2.2 Angiopoietins signaling

Another signaling system that is involved in the regulation of angiogenesis and most specifically in the regulation of interactions between endothelium and surrounding support cells is the Angiopoietin pathway. This pathway is composed of two tyrosine kinase receptors Tie1 and Tie2 (*Tek*) and four ligands—angiopoietins 1-4 (Ang1-4) (Ward & Dumont, 2002). The Tie/Ang signaling system is necessary for vascular system development during embryogenesis, since transgenic mice with inactive *Tie2* gene die between 9,5 and 10,5 days of embryonic development (Dumont et al., 1994). These transgenic mice did not present any defects at the vasculogenesis stage and primary vascular plexus formation. Defects were found only at the developmental processes of capillary maturation and stabilization, and the primary capillary plexus was unable to evolve to a complex branched vascular network (Dumont et al., 1994; Sato et al., 1995; Suri et al., 1996).

Knock-out mice for the gene encoding the Tie2 ligand angiopoietin Ang1 or mice over-expressing another ligand of the same receptor, Ang2, presented a similar phenotype (Davis et al., 1996; Maisonpierre et al., 1997). These studies demonstrate that Ang1 and Ang2, despite both binding to Tie2, exert different effects in the Tie2- signaling cascade. While Ang1 is able to stimulate Tie2 phosphorylation, interaction with Ang2 does not result in activation of the receptor. Therefore, similarly to what was described to Vegfr1, Ang2 is a competitive inhibitor, or antagonist, of Ang1 (Maisonpierre et al., 1997).

Angiopoietin 1 was shown to be expressed by mesenchymal cells, including pericytes and smooth muscle cells, while Tie2 is expressed on the surface of endothelial cells (Ramsauer & D'Amore, 2002). Consequently, Ang1/Tie2 signaling promotes the association between endothelial cells and perivascular support cells, contributing to stabilization of the maturing vascular system and decreased vascular permeability (Armulik, Abramsson, & Betsholtz, 2005) (Fig. 6).

Figure 6- Ang/Tie2 signaling. *In* (Daly et al., 2012).

The angiopoietins Ang1 (*ANGPT1*) and Ang2 (*ANGPT2*) are secreted factors that bind to the endothelial cell-specific receptor tyrosine kinase Tie2 (*TEK*) and regulate angiogenesis. Ang1 activates Tie2 to promote blood vessel maturation and stabilization. In contrast, Ang2, which is highly expressed by tumor endothelial cells, is thought to inhibit Tie2 activity and destabilize blood vessels.

2.2.3 PDGF signaling

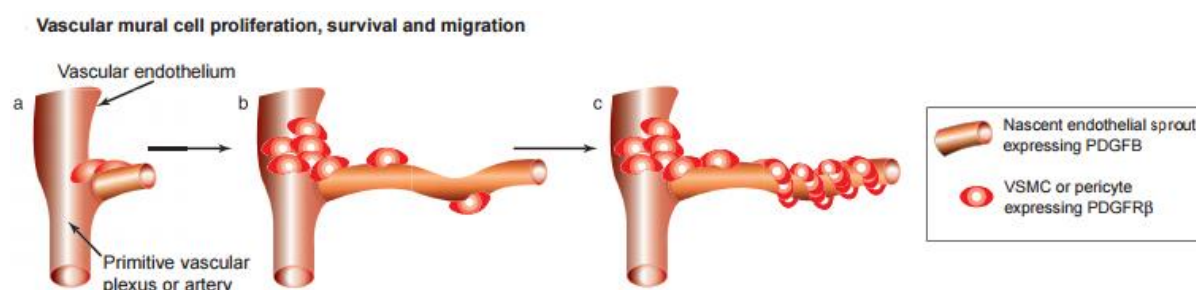
PDGF signaling is another pathway involved in recruitment of pericytes to form the walls of newly formed vessels (Betsholtz, 2004). The PDGF family consists of four different PDGF isoforms (A-D) establishing functional homodimers (PDGF-AA, PDGF-BB, PDGF-CC, and PDGF-DD) or a heterodimer PDGF-AB (Fredriksson, Li, & Eriksson, 2004) (Fig. 7). PDGF receptors (PDGFR α and PDGFR β) like VEGF receptors belong to the superfamily of receptor tyrosine kinases and are transmembrane proteins whose intracellular region contains the tyrosine kinase domain (Betsholtz, 2004). Upon interaction with their ligands, PDGFR receptors form homo- or heterodimers (Betsholtz, 2004; Fredriksson et al., 2004). PDGF-AA binds only PDGFR α , while PDGF-BB exhibits higher affinity for receptor PDGFR β but is also able to bind PDGFR α and PDGFR heterodimers (Betsholtz, 2004).

Mice deficient for receptor *Pdgfr- β* or its ligand *Pdgf-b* presented decreased number of pericytes. Moreover, their blood vessels were characterized by enhanced dilatation, due to edemas which emerged during embryonic development and resulted in embryonic death (Lindahl, 1997).

During angiogenesis, endothelial cells were shown to express PDGF-B, and tip-cells transcribed high levels of *Pdgf-b* mRNA (Fig. 7a). This generates a gradient of the concentration of this factor that stimulates recruitment of pericytes which express PDGFR β on their surface and thus creation of the newly formed capillary wall (Gerhardt et al., 2003; Bergers & Song, 2005)(Fig. 7b and c). Endothelial cells do not express PDGFR- β (Lindahl, 1997; Westermarck & Heldin, 2009), therefore, PDGF-B provides for paracrine regulation between endothelial cells secreting this factor and the PDGFR- β -expressing cells- pericytes and vascular smooth muscle cells (vSMCs) (Hirschi, Rohovsky, Beck, Smith, & D'Amore, 1999). PDGF-B exhibits a mitogenic effect on pericytes/vSMCs, directs migration and incorporation into the vessel wall (Armulik et al., 2005) (Fig. 7). Upon reaching endothelial cells, vSMCs and

pericytes tightly encircle and associate with the endothelium producing survival and anti-proliferative factors that stabilize nascent vessels (Hoch & Soriano, 2003).

Figure 7- PDGFB/PDGFR β signaling in regulation of mural cell recruitment. *In* (Hoch & Soriano, 2003).



During remodeling angiogenesis PDGFB is expressed in nascent vascular endothelial sprouts (a) and drives the proliferation of PDGFR β -expressing pericytes and VSMCs near arterial walls and primitive vascular plexi (b). PDGFB also directs the migration and/or survival of these mural cells along endothelial sprouts (b,c). Upon reaching their destination, VSMCs and pericytes encircle and associate tightly with the endothelium (c); survival and anti-proliferative factors produced by mural cells stabilize nascent vessels.

2.2.4 Notch signaling

Notch signaling regulation of angiogenic processes can be divided in two major steps: sprouting angiogenesis and maturation of newly formed vessels.

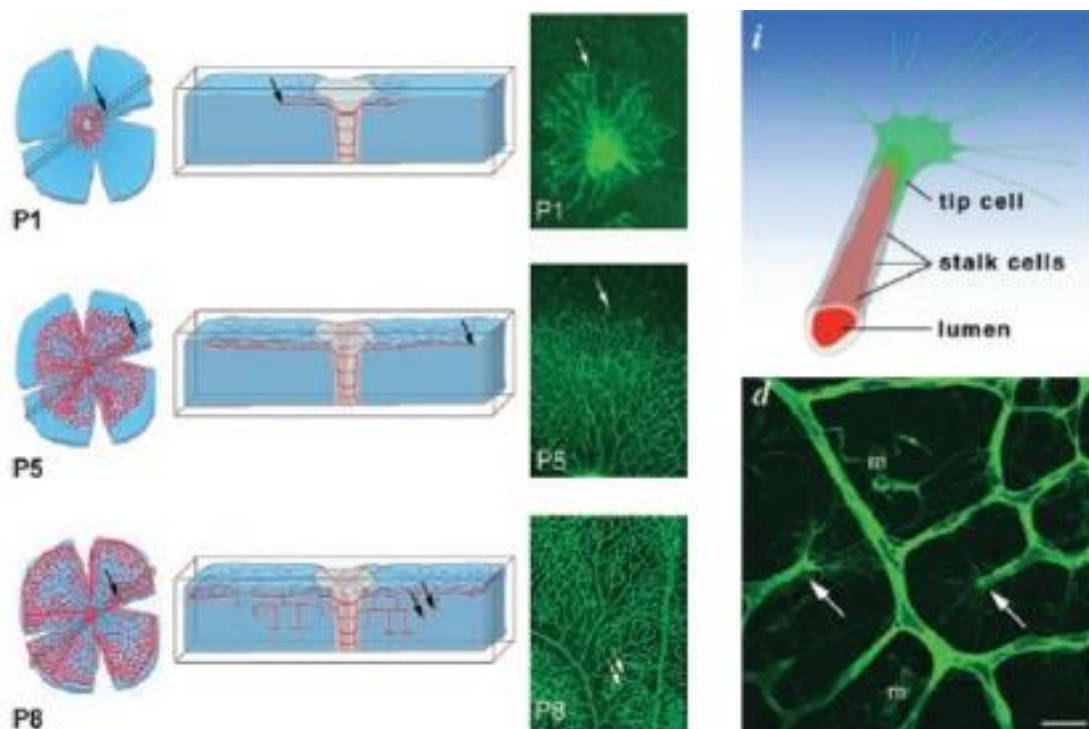
2.2.4.1 Notch signaling in sprouting angiogenesis

Sprouting angiogenesis is strictly regulated by the interplay between VEGF and Dll4/Notch signaling. This interplay is the basis for the lateral induction model, currently accepted as the prevailed mechanistic model explaining sprouting angiogenesis, and tip- and stalk cell selection. The supporting evidence for this was established in the post-natal retina developing vascular plexus. The murine retinal vasculature starts its development just after birth by planar radial growth and during a two-week period it evolves to a complex tridimensional vascular system. Retinal vessels start to grow from the center to the periphery developing a defined pattern of arterial and venous vessels. In the angiogenic periphery specialized tip-cells are responsible for extending phyllopodii that allow for the contact between neighbor ECs, which is essential for the continuous formation of the vascular network (Gerhardt et al., 2003) (Fig. 8).

In response to spatial gradients of VEGFA, secreted by neuroglia cells migrating radially ahead of the vascular front, tip-cells sprout phyllopodii towards this gradient (Gerhardt et al., 2003) (Fig. 9ab). This effect is mediated by the interaction of VEGFA with VEGFR2 receptor, the

concentration of which is especially high in tip-cells. Once tip-cells are selected and begin to move forward, formation of new capillaries begin because of the proliferation and migration of adjacent stalk ECs.

Figure 8- Retina development as a model system for investigation of angiogenic sprouting. *In* (Gerhardt et al., 2003).

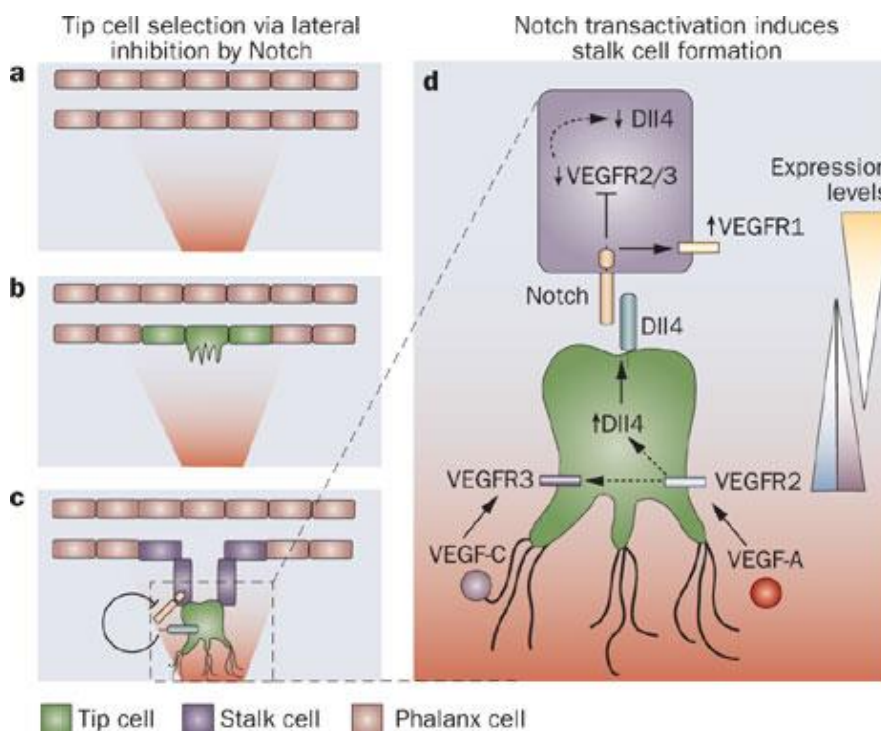


On the left, top view displays the primary plexus in the fiber layer of the retina. Sprouting occurs toward the periphery in the primary plexus (P1 and P5, arrows) and subsequently into deeper layers (P8, arrows), where branching and fusion leads to plexus formation. On the top right graphic illustration of tip cell and stalk cell. On the bottom right arrows point to sprouting tips at remodeling sites (arrows) in the primary plexus.

When VEGFA gradients activate endothelial cells they induce expression of Dll4 and Notch1 (Liu et al., 2003) (Fig. 9cd). The tip-cell specific characteristics are preferably acquired by endothelial cells devoid of Notch1 and with high Dll4 expression. Dll4/Notch-associated transduction causes inhibition of sprouting by lowering ECs sensitivity to VEGFA. It was shown that in Dll4-hyperexpressing endothelial cells, expression of VEGFR2 was significantly inhibited (Williams, Li, Murga, Harris, & Tosato, 2006). Therefore, endothelial cells expressing Notch1 receptor which was activated by adjacent Dll4 ligand, are prevented from transitioning to an active state, by lowering VEGFR2 levels, and thus Dll4/Notch signaling restricts the emergence of an excessive number of tip-cells, restricting excessive sprouting (Siekmann & Lawson, 2007; Suchting et al., 2007; Hellström et al., 2007). Additionally, VEGFR3 is expressed in active endothelium (Kubo et al., 2000) and is mainly confined to filopodial

extensions on tip cells at the sprouting front (Tammela et al., 2008). Blocking VEGFR3 was shown to reduce the number of sprouts and branch points and EC proliferation. VEGFR2 signaling induces VEGFR3 expression in tip cells, whereas Notch1 activation downregulates its expression in stalk cells (Tammela et al., 2008). Recently, Notch-dependent VEGFR3 upregulation was shown to allow angiogenesis without VEGF-VEGFR2 signalling (Benedito et al., 2012). However, these results were counteracted by Zarkada and colleagues demonstrating that VEGFR2 is absolutely required for the sprouting of new vessels and that VEGFR3 activity cannot rescue the angiogenic sprouting even when the Notch pathway signaling activity is inhibited (Zarkada, Heinolainen, Makinen, Kubota, & Alitalo, 2015). Furthermore, both endothelial tip and stalk cells express VEGFR1 during retinal vascular development (Gerhardt et al., 2003), which is up-regulated by Dll4-Notch activation in stalk cells (Harrington et al., 2008) (Fig. 9d). The overall effect on VEGF receptors, in turn, downregulates Dll4 specifically in stalk cells, while high expression levels are maintained on tip cells. Consequently, the Dll4 and Notch1 expression becomes tessellated among endothelial cells in the vessel area, creating a “salt-and-pepper” effect. As a result, decreased levels of Dll4 expression or blocking Notch signaling enhances tip-cell formation, leading to significant increased formation, branching, and fusion of new endothelial tubules (Sainson et al., 2005; Noguera-Troise et al., 2006; Ridgway et al., 2006; Suchting et al., 2007; Hellström et al., 2007).

Figure 9- Model of Notch-driven lateral inhibition. *In* (Carmeliet, De Smet, Loges, & Mazzone, 2009).



(a) VEGFA forms a gradient. (b) ECs exposed to the highest amount of VEGF are activated by VEGFR2 and migrate, but only one cell (the future tip cell) should take the lead in order to prevent ECs from moving at the same time and being able to form a correct branch. (c) The tip cell acquires a competitive advantage amongst the others, by inhibiting its neighbors.

(d) ECs fate specification is accomplished by several mechanisms: VEGFR2 activation in the tip cell leads to up-regulation of VEGFR3 and Dll4 ligand in the tip cell; In its turn Dll4 activates Notch in adjacent

Fringe modification of Notch1 receptor in stalk ECs enhanced Notch signaling by Dll4-presenting tip cells, which reduced VEGF receptor expression and maintained the stalk phenotype, accordingly to the lateral inhibition model described previously. Additionally, Dll4 was antagonized by Jagged1, which promoted angiogenesis and increased tip cell numbers by lowering Notch activation levels, while VEGF signaling was enhanced. Therefore, angiogenic sprouting can be positively or negatively modulated by differential regulation of Jagged1 and Dll4 in endothelial cells. Moreover, Jagged1 in stalk cells prevented that co-expressed Dll4 would be able to activate Notch in neighboring (stalk or tip) ECs. This activity of Jagged1 depended on Notch1 receptor Fringe modulation, which reduced the ability of Jagged1 to activate Notch1 thereby leading to effective competition between a strong agonist (Dll4) and antagonistically Jagged1 action.

2.2.4.2 Notch signaling in vessel maturation

An important step of vessel maturation is the recruitment of mural cells - pericytes and vascular smooth muscle cells (vSMCs) (Jain, 2003). Pericytes are in direct intercellular contact with endothelial cells and line capillaries and immature blood vessels, whereas the walls of mature blood vessels and large diameter blood vessels, like arteries and veins, are formed by several layers of smooth muscle cells separated from the endothelium by a layer of basement membrane.

In the last decade a wealth of evidence has emerged, supporting a pivotal role for Notch receptors/ligands in mediating endothelial cell to pericyte and smooth muscle cell communication (Campos, 2002; Doi et al., 2006; Anderson & Gibbons, 2007; Tang, Urs, & Liaw, 2008; High et al., 2008; Boucher, Peterson, Urs, Zhang, & Liaw, 2011). Distinguishing pericytes from vSMCs is not an easy task, since they can share several markers, have overlapping origins and even differentiate in to one another (Armulik, Genové, & Betsholtz, 2011).

PDGFR has been identified as a downstream gene target of Notch signaling in vSMC following over expression of Notch1ICD or Notch3ICD (Jin et al., 2008). Moreover, Notch1 and Notch3 were shown to regulate the *PDGFR* promoter through distinct CBF1 binding sites (Jin et al., 2008), raising the possibility of distinct regulatory functions downstream of Notch receptors, and highlighting the importance of changes in receptors expression during diseased and normal basal vascular states.

Additionally, as mentioned previously, *NOTCH3* is mutated in the human stroke and dementia syndrome CADASIL (cerebral autosomal-dominant arteriopathy with subcortical infarcts and leukoence-phalopathy), which involves degeneration of vSMCs (Joutel et al., 1996). *Notch3* knockout mice have revealed an abnormal maturation of arterial vSMCs, which has been connected to reduced expression of a number of arterial vSMC markers, including PDGFR- β (Domenga et al., 2004; Jin et al., 2008). Moreover, increased expression of Notch3 in mural cells has also been shown to increase expression of certain vSMC markers (Liu et al., 2009).

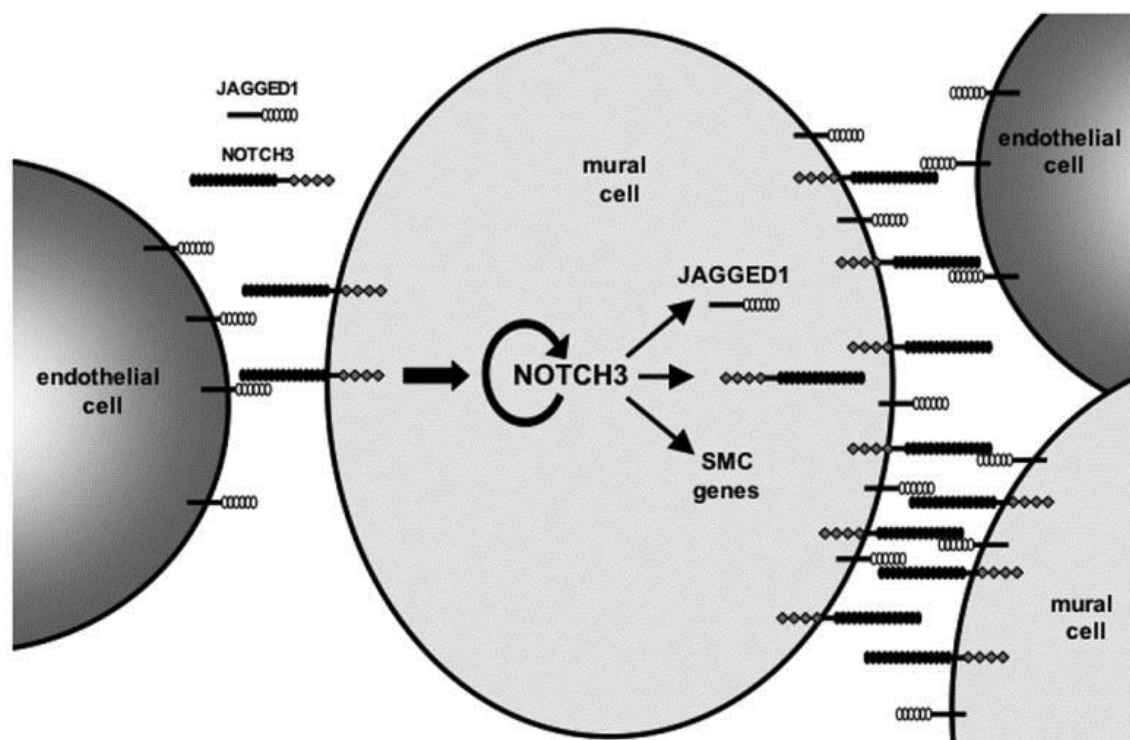
Furthermore, Notch2 has been reported as required for promoting the expansion of cardiac neural crest-derived vSMC around the developing outflow tracks (Varadkar et al., 2008). Also, combinatory effects of Notch2 and Notch3 were shown to have a critical role in vascular smooth muscle development: Notch2 being essential to activate not only smooth muscle genes but also Notch3 transcription, synergistically driving the differentiation program (Wang et al., 2012).

The Delta-like 4 ligand has been shown to increase vessel maturation (Scehnet et al., 2007; Trindade et al., 2008) and to be able to convert myogenic cells to pericytes, acting together with PDGF-B (Cappellari et al., 2013).

However, the critical Notch ligand in the context of mural cell recruitment appears to be Jagged1. Evidence for a role of Jagged1 in endothelial contact-dependent recruitment of smooth muscle progenitor cells in vivo was provided by the deletion of Notch signaling activity in neural crest-derived smooth muscle progenitors (High et al., 2007) and in experiments where *Jag1* was deleted specifically in ECs (F. A High et al., 2008). Later, endothelial Jagged1 was shown to be able to bind Notch3 on neural crest-derived smooth muscle progenitors, leading to the lateral induction of Jagged1/Notch signaling and directing the expression of *HeyL* and other signals laterally into the circumferentially growing wall (Liu et al., 2009) (Fig. 11). Another report showed that expression of soluble Jagged1, which acted as an inhibitor of Notch signaling, attenuating Notch/Hey1 signaling, was able to reduce vSMC proliferation and migration after balloon injury of rat carotid arteries, resulting in reduced neo-intimal lesion formation (Caolo et al., 2011). More recently, mouse retinal vasculature models were used to show that Jagged1/Notch signaling can increase vSMC maturation by regulating their adhesion properties during vessel development and maturation (Scheppke et al., 2012).

Figure 11- Jag1/Notch3 signaling in a model of lateral induction of vessel maturation.

In (Liu et al., 2009).



Endothelial cells, through the JAGGED1 ligand induce NOTCH3 expression, which auto-regulates itself by a positive feedback loop that in turn activates smooth muscle-specific gene expression and maintains vascular support cells in a differentiated phenotype.

3. Notch signaling regulation of physiological angiogenesis

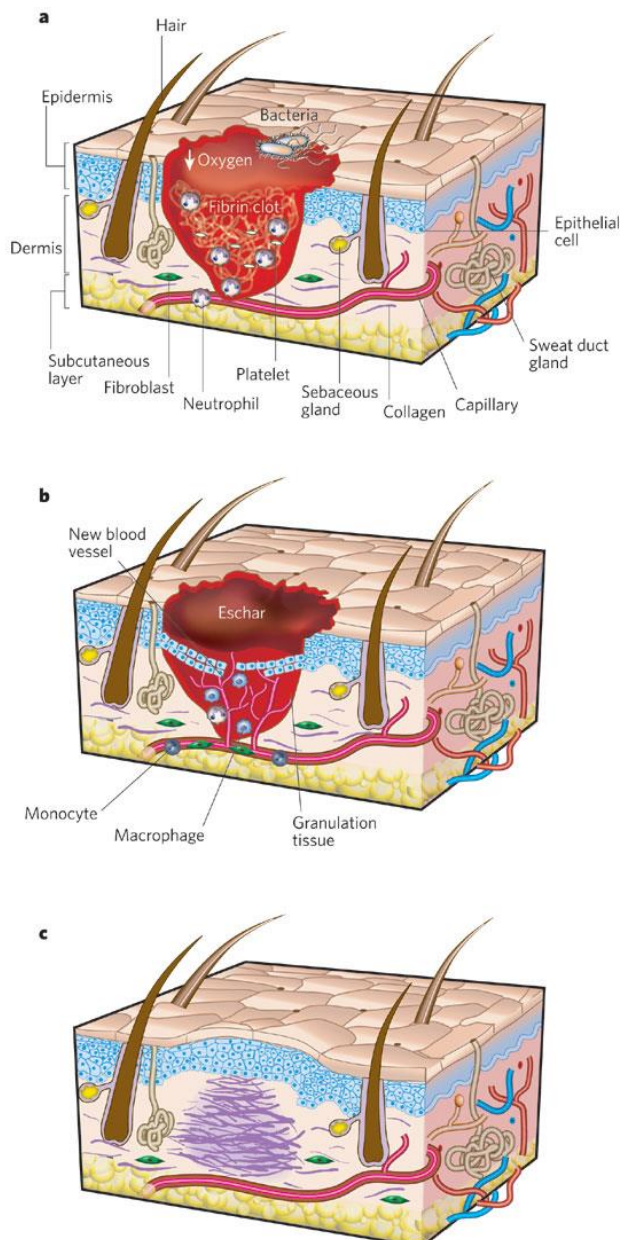
In mammals, physiological angiogenesis occurs mainly during tissue regeneration, such as in healing wounds, and in the female reproductive cycle. In particular, the wound healing assay constitutes a fast, easy, and reliable *in vivo* model of physiological angiogenesis for studying the molecular mechanisms involved in the formation and remodeling of vascular structures (Eming, Brachvogel, Odoriso, & Koch, 2007).

Wound healing is a dynamic process involving complex interactions of extracellular matrix (ECM) molecules, soluble mediators, resident and infiltrating inflammatory cells. The healing process is comprised of three phases that overlap in time and space: inflammation, tissue formation, and tissue remodeling (Fig. 12).

The second stage of wound repair — new tissue formation — comprises neovascularization of the wound's granulation tissue, which has increased oxygen and nutrient demands, that occurs by the process of angiogenesis. In wound angiogenesis, the resident endothelial cells of the wound's adjacent mature vascular network proliferate, migrate, sprout and remodel into neo-vessels that grow into the initially avascular wound tissue aided by differentiated stromal cells such as fibroblasts. In the later part of this stage, fibroblasts, which are attracted from the

edge of the wound or from the bone marrow are stimulated by macrophages, and some differentiate into myofibroblasts. Myofibroblasts are contractile cells that in time, are responsible for bringing the edges of a wound together and that can also contribute to blood vessel maturation. Fibroblasts and myofibroblasts interact and produce extracellular matrix, mainly in the form of collagen, which ultimately forms the bulk of the mature scar (Eming et al., 2007; Gurtner, Werner, Barrandon, & Longaker, 2008).

Figure 12- Wound repair phases. *In* (Gurtner et al., 2008).



There are three classic stages of wound repair: inflammation (a), new tissue formation (b) and remodelling (c). (a) Inflammation: this stage lasts about 48 h after injury, in which the wound is characterized by a hypoxic (ischaemic) environment in which a fibrin clot has formed. Bacteria, neutrophils and platelets are abundant in the wound. Normal skin appendages (such as hair follicles and sweat duct glands) are still present in the skin outside the wound. (b) New tissue formation: this stage occurs about 2–10 days after injury. An eschar (scab) has formed on the surface of the wound. Most cells from the previous stage of repair have migrated from the wound, and new blood vessels now populate the area. (c) Remodelling: this stage lasts for a year or longer, in which disorganized collagen has been laid down by fibroblasts that have migrated into the wound.

As a critical regulator of angiogenesis, inflammation and cell-fate determination, Notch signaling contribution to wound healing responses has been investigated in the past. Healing of full-thickness dermal wounds was shown to be significantly delayed in Notch antisense transgenic mice and in normal mice treated with gamma-secretase inhibitors that block proteolytic cleavage and activation of Notch (Chigurupati et al., 2007). Contrastingly, mice treated with a Notch ligand Jagged1 peptide displayed enhanced wound healing (Chigurupati et al., 2007). Moreover, in the same study it was demonstrated, using an *in vitro* scratch wound healing model that activation or inhibition of Notch signaling altered the behaviors of cultured vascular endothelial cells, consistently with Notch signaling function. In another study, wounds in *Notch1*^{+/-} mice were shown to have increased vascularization and collagen deposition (Outz, Wu, Wang, & Kitajewski, 2010). Moreover, *in vitro*, they have found that macrophage upregulation of vascular endothelial growth factor receptor-1 (VEGFR-1) was Notch signaling dependent (Outz et al., 2010), providing a mechanistic explanation for the *Notch1*^{+/-} wound angiogenesis phenotype.

In a more recent report from our lab, it was shown that both endothelial specific *Dll4* overexpression and endothelial specific *Dll4* loss-of-function led to delayed wound healing. The first, was related to decreased vascular density with increased maturation, and the latter to increased vascular density with reduced maturation, both phenotypes leading to reduced tissue perfusion. Contrastingly, *Dll4* heterozygote mice presented accelerated wound regeneration with associated improved vascular density as well as near-normal percentage of perfused blood vessels. The latest result led to testing low dosage inhibition of Dll4/Notch signaling, using a soluble Dll4 fused protein (sDll4-Fc), which proved to be effective in accelerating the healing response by improving overall vessel functionality (Trindade et al., 2012).

4. Notch signaling regulation of tumor angiogenesis

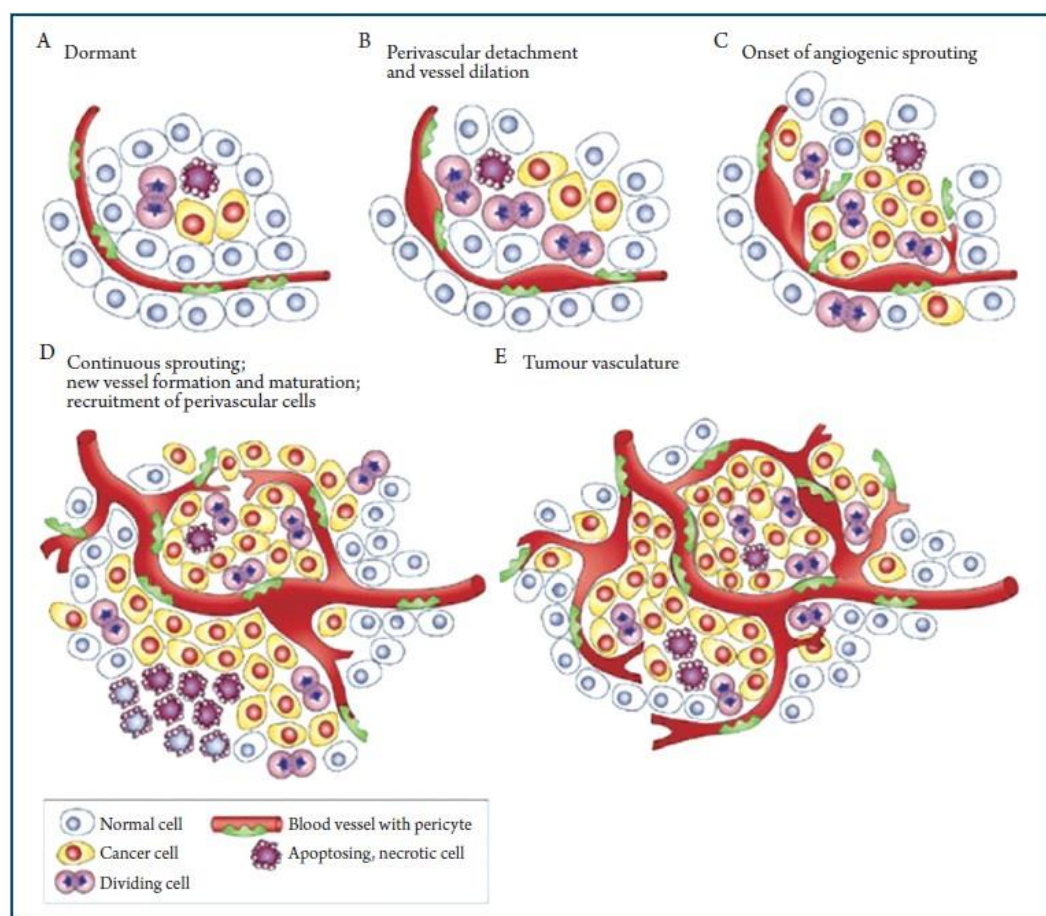
The concept of tumor growth being angiogenesis dependent was created by the observations of Judah Folkman in 1969 of a retinoblastoma in a child (Folkman, 1971). Tumor growth is restricted in an early avascular phase and to be able to progress and develop it requires the so-called angiogenic switch (Hanahan & Folkman, 1996). Tumor angiogenesis is initiated when endothelial cells respond to local stimuli and migrate towards the growing mass, which results in the formation of tubular structures that ultimately recruit perivascular support cells in order to create a well-established neo-vasculature allowing tumor development and eventual metastasis (Hanahan & Folkman, 1996) (Fig. 13).

Since Folkman's seminal discovery, many signaling pathways have been identified as key contributors to the neo-angiogenic process, leading to the creation and application of anti-angiogenic drugs in cancer treatment, such as the anti-VEGF antibody bevacizumab and the

tyrosine kinase inhibitors like sunitinib or sorafenib, among others (Hurwitz et al., 2004; Kerbel, 2006; Meadows & Hurwitz, 2012).

The vasculature of a growing tumour normally contains actively growing and abnormal blood vessels. When treated with vascular endothelial growth factor (VEGF) inhibitors, the tumour vasculature becomes pruned and “normalized”, which results in overall decreased tumour perfusion and decreased tumour growth, although the perfusion of the remaining vessels may be very good (Fig. 14).

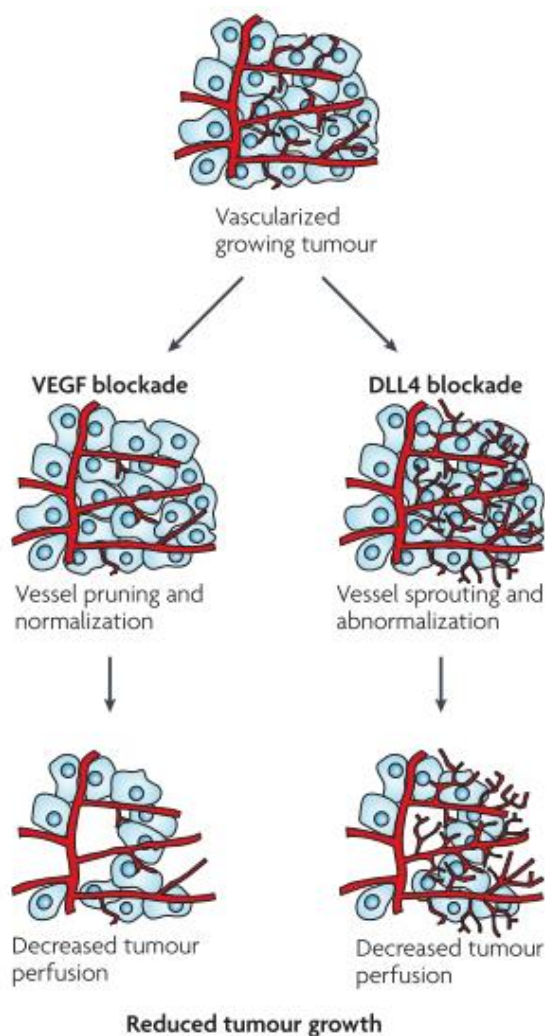
Figure 13- The angiogenic switch in tumor growth. In (Georgiou, Namdarian, Corcoran, Costello, & Hovens, 2008)



A. Most tumors start as dormant avascular nodules that grow until reaching a steady state, in which proliferation is balanced by apoptosis. The initiation of angiogenesis- angiogenic switch, must occur to trigger exponential tumor growth. **B.** The switch begins with perivascular detachment and vessel dilation. **C.** This step is followed by angiogenic sprouting. **D.** Finally, new vessel formation, maturation and recruitment of perivascular cells occurs. Blood-vessel formation will continue as long as the tumor grows. **E.** These newly formed blood vessels feed hypoxic and necrotic areas of the tumor and provide it with essential nutrients and oxygen for their continued growth and invasion.

The Notch signaling pathway has also been implicated in the regulation of tumor angiogenesis. Dll4 is an anti-angiogenic molecule, since endothelial loss-of-function of this gene caused a vascular phenotype characterized by increased vessel density. However, in 2006, two reports were published in Nature revealing the paradoxical phenotype of inhibiting Dll4 in restricting tumor growth (Noguera-Troise et al., 2006; Ridgway et al., 2006). In one report the authors used soluble forms of Dll4, as well as antibodies to Dll4 that block the binding of mouse Dll4 to Notch1 receptor (Noguera-Troise et al., 2006). In the other report a humanized phage antibody that binds with high affinity to Dll4, blocking the binding of mouse and human Dll4 to Notch1, was used (Ridgway et al., 2006). Remarkably, the reduced tumor growth was associated with an increase in vessel density but an overall decreased perfusion (Fig. 14). These two reports provided the first evidence that for tumor development the amount of vessels present is of less importance than the ability of the neo-vasculature to effectively deliver nutrients and oxygen to the actively dividing tumor cells (Thurston, Noguera-Troise, & Yancopoulos, 2007). This ability is provided in part by the maturation status of the newly formed vessels, and given that *Dll4* loss-of-function mutants presented decreased mural cell recruitment, the vessel walls become leaky, and thus less perfused and functional (Scehnet et al., 2007; Trindade et al., 2012). By contrast with the VEGF blockade, Delta-like ligand 4 (Dll4) inhibitors resulted in increased tumour vessel density, characterized by sprouting and proliferating small vessel branches. However, these vessels were poorly functional, also resulting in decreased tumour perfusion overall and decreased tumour growth. Thus came the new concept that one could reduce tumor growth by “abnormalization” of tumor vasculature (Thurston et al., 2007).

Figure 14- Paradoxical effect of Anti-Dll4 based therapies. *In* (Thurston et al., 2007).



Comparison of VEGF and Dll4 blockade in tumor angiogenesis and growth. While VEGF blockade restricts tumor growth by inhibiting vessel growth, leading to vessel normalization, Dll4 blockade causes excessive enhancement of angiogenesis resulting in the disturbance of correct vascularization. However, in the last case, such vessels appear to be of low functionality—resulting in increased hypoxia, insufficient tissue perfusion, and finally, in tumor growth inhibition.

Jagged1 has also been studied in tumor development by its ability to regulate tumor angiogenesis. Two reports have suggested that Jagged1 expressed in tumor cells can stimulate angiogenesis. Firstly, Jagged1 expressed by cancer cells was dependent on activation of the mitogen-activated protein kinase (MAPK) signaling pathway. Thus, MAPK activation led to expression of Jagged1 which in turn influenced tumor neovascularization (Zeng et al., 2005). In this report, knockdown of Jagged1 expression significantly inhibited the pro-angiogenic effects of squamous carcinoma cells, when assessed *in vitro*. Moreover, analysis of Jagged1 expression in human head and neck squamous cell carcinoma (HNSCC) samples suggested that Jagged1 was associated with the level of vascularization in tumors (Zeng et al., 2005). Secondly, Jagged1 expressed in breast tumor cells was shown to influence tumor angiogenesis (Funahashi et al., 2008). This report utilized a soluble form of the Notch1 receptor (Notch1 decoy), which functions as a ligand-dependent Notch antagonist, and assessed its effect on angiogenesis. The Notch1 decoy could reduce Notch1 signaling stimulated by the action of at least three distinct Notch ligands; Dll1, Dll4 and Jagged1. Notch1 decoy was also shown to block the activity of Notch4 expressed by endothelial cells. Thus, the

Notch1 decoy functioned as an antagonist of ligand-dependent Notch signaling. In the latest report this Jag1-angiogenesis dependent phenotype was efficiently attenuated by expression of a NOTCH1 decoy in those cells. Moreover, using neuroblastoma (NGP) cells and a mouse mammary Mm5MT cells overexpressing fibroblast growth factor (FGF) 4 (Mm5MT-FGF4) as xenografts, they have demonstrated that expression of the NOTCH1 decoy by tumor cells resulted in a marked reduction in xenograft viability and angiogenesis, accompanied by an increase in tumour cell apoptosis and intratumoural haemorrhage (Funahashi et al., 2008). These results point to the fact that contact- dependent Notch ligand signals provided by tumor cells may be important in endothelial cell differentiation.

Furthermore, a recent report using a Notch1 decoy, that specifically blocks both Jagged ligands mediated interactions, was shown to decrease xenograft growth by an anti-angiogenic effect and by the ability to destabilize pericyte-ECs interactions (Kangsamaksin et al., 2014). Moreover, the anti-angiogenic effect observed was likely due to increased secretion of the soluble form of Vegf-r1, and thus to decreased Vegf/Vegfr-2 signaling, suggesting that Jag1/Notch signaling is also able to positively regulate the VEGF pathway (Kangsamaksin et al., 2014).

5. Notch signaling regulation of tumor cell biology

Beyond the role of Notch signaling in tumor angiogenesis, a major hallmark of cancer development, it has also been implicated in the regulation of tumor cell proliferation and survival, in epithelial-to-mesenchymal transition, invasion and metastasis and in the regulation of cancer stem cells, in a variety of hematologic and solid malignancies (Ntziachristos et al., 2014). Depending on expression patterns, the Notch pathway can be either oncogenic or tumor suppressive, even though the mechanisms are not fully understood. These mechanisms may include tissue and cell dependent specific target genes, and varying cytokines and growth factors present in distinct microenvironments. Generally, it seems to be activating in hematological malignancies and adenocarcinomas, reflecting its normal functions in those tissues.

5.1 Mechanisms of Notch activation in solid tumors

Abnormal regulation of the Notch pathway may occur by a variety of mechanisms including mutational activation or inactivation, overexpression, post-translational modifications, and epigenetic regulation (South, Cho, & Aster, 2012). For example, in ovary and breast cancers, somatic mutations, copy number alterations (The Cancer Genome Atlas Research Network, 2011), amplifications (Park et al., 2006), and gene rearrangements (Robinson et al., 2011) have implicated Notch pathway members in tumor pathophysiology. Moreover, Notch pathway regulation of tumor development can be closely related to other signaling cues involved in

tumorigenesis, such as Akt, PTEN and NF- κ B, as demonstrated in prostate cancer (Bin Hafeez et al., 2009; Whelan, Kellogg, Shewchuk, Hewan-Lowe, & Bertrand, 2009; Wang et al., 2010; Kwon et al., 2014). Lastly, Notch activation can also be directly potentiated by other transcription factors. For example, in mouse cell lines, hypoxia-inducible transcriptional factor 1 alpha (Hif1 α) was shown to be able to directly bind to cleaved Notch receptors, modulating activation of Notch-responsive promoters, and increasing the expression of Notch downstream targets (Gustafsson et al., 2005).

5.2 Notch signaling function in solid tumors

Notch signaling activation can promote cell growth in a variety of human solid tumors (Ntziachristos et al., 2014). Of these, breast (mammary gland) cancer, as a highly studied endocrine-dependent type of tumor, serves as a paradigm for understanding the effects of Notch signaling in solid tumors. One of the first clues that Notch signaling may play a role in solid tumors came from experiments with mouse mammary tumor viruses (MMTVs). Integration of the MMTV genome next to the “Int-3” locus resulted in a Notch4 activating mutation, which led to the constitutive activation of the receptor and breast cancer development (Gallahan & Callahan, 1997). Since this discovery, a number of studies have confirmed that activation of Notch signaling plays an oncogenic role in breast cancer. Inclusive, Notch1 and Notch3 oncogenic activity has been demonstrated in the mouse mammary gland (Hu et al., 2006), as well as, in humans, high levels of JAGGED1 and NOTCH1 proteins have been associated with particularly aggressive breast cancer cases (Reedijk et al., 2005).

Breast cancer shares the first place of the list of the most common invasive cancers with prostate cancer, the first in women and the second in men. Even though these cancers arise in organs that are different in terms of anatomy and physiological function both require glandular endocrine stimulus for their development. Both tumor types are typically hormone-dependent and have remarkable underlying biological similarities. Moreover, an increasingly number of advances made in the pathophysiological understanding of breast and prostate cancers have opened the way for new treatment strategies (Risbridger, Davis, Birrell, & Tilley, 2010).

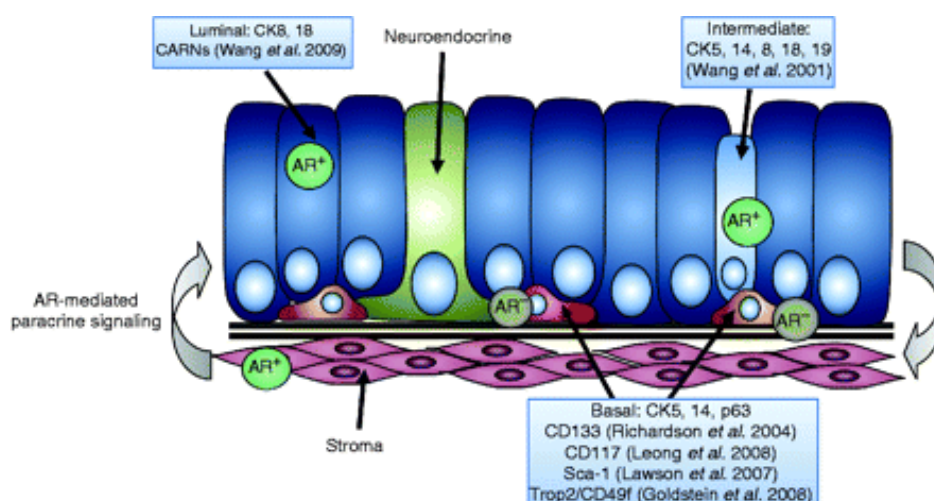
In the following chapter, prostate cancer will be the main focus, since it was the cancer model used for the study of Jag1/Notch signaling in the context of tumor cell biology regulation.

6. Prostate

6.1 Histology of the prostate

The prostate is an exocrine gland of the male mammalian reproductive system, the primary function of which is to produce seminal fluids and it is also required for bladder control and normal sexual functioning. The prostate consists of a glandular epithelium surrounded by a fibromuscular stroma (Fig. 15). Prostatic epithelium is composed of several different cell types, that include basal, luminal (secretory), and neuroendocrine cells (Taylor, Toivanen, & Risbridger, 2010) (Fig.15). Additionally there is an intermediate cell type that shares properties of both luminal and basal cells (Wang, Hayward, Cao, Thayer, & Cunha, 2001). Luminal cells compose the majority of the epithelial layer and exert secretory functions by responding directly to androgens, since they express androgen receptors (ARs) (Hudson, 2004; Heer, Robson, Shenton, & Leung, 2007). Luminal cells also express specific markers such as CK8 and CK18 (Wang et al., 2001). On the other hand, basal cells exist as one or two layers of cells attached to the basement membrane below the luminal layer (Kurita, Medina, Mills, & Cunha, 2004). In the human prostate basal cells form a continuous layer whereas in other species, like the mouse, they have a more scattered appearance (Taylor et al., 2010). They also can be readily distinguishable from the other prostatic cells by their morphology, ranging from small, flattened cells with condensed chromatin and small amounts of cytoplasm to triangular-like cells with an increased cytoplasm and more open-appearing chromatin. Basal cells also express specific markers such as CK5, CK14 and p63 and have low AR expression, whereas intermediate cells can express both luminal (CK8 and CK18) and basal cell markers (CK5 and CK14) (Wang et al., 2001). Lastly, neuroendocrine cells are rare cells located in the luminal layer of the epithelium and the least studied epithelial cell population (Taylor et al., 2010). They are believed to regulate prostate growth and development through endocrine–paracrine actions (Taylor et al., 2010).

Figure 15- Prostate cell populations. *In* (Taylor et al., 2010).



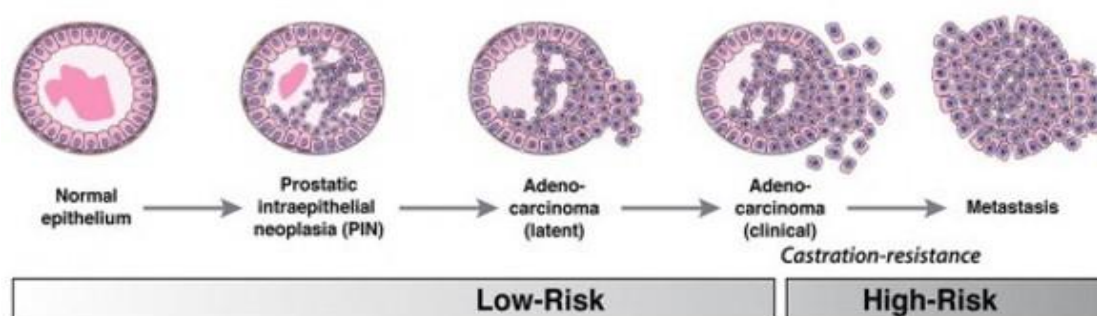
The prostate is composed of stromal and epithelial compartments that communicate through reciprocal communication. The epithelium consists of different cell types, including basal, intermediate, luminal,

and neuroendocrine cells that have specific cytokeratin (CK) profiles and androgen receptor (AR) expression.

6.2 Prostate Cancer

Since 2010 prostate cancer is the second most frequently diagnosed cancer (at 15% of all male cancers) (“World Cancer Report 2014,” 2014) and the sixth leading cause of cancer death in males worldwide (Jemal et al., 2011). Prostate cancer is treated by surgery or radiation when is localized at time of diagnosis, and because it is an androgen-dependent malignancy, if disease relapse occurs androgen deprivation therapy (ADT) is also used (Taylor et al., 2010). However, prostatic cancer cells can adapt to androgen-depleted conditions and patients inevitably progress from hormone sensitive to develop castration-resistant prostate cancer (CRPC). Over 90% of prostate tumors arise within the glandular epithelial cell compartment (Hayward, Rosen, & Cunha, 1997). Prostate cancer in men usually arises in the peripheral zone of the prostate and metastatic spread can be both lymphatic and hematogenous, spreading primarily to the bones, but also to the lungs and liver. On a histological level, early lesions consist of epithelial crowding and stratification with hyperchromatism and disruption of the basal cell layer and are classified as prostatic intraepithelial neoplasia (PIN). Lesions of PIN rapidly can progress by invading the surrounding stroma leading to development of adenocarcinoma progressively less-differentiated and eventually to metastatic spread (Fig. 16).

Figure 16- Progression pathway for human prostate cancer. *In* (Shen & Abate-Shen, 2010).



Stages of lesion progression from low-risk to high-risk prostate cancer. Initially the lesions develop as prostatic intraepithelial neoplasia (PIN) which is a precursor for prostate cancer. PIN is generally characterized at the histological level by the appearance of luminal epithelial hyperplasia, reduction in basal cells, enlargement of nuclei and nucleoli, cytoplasmic hyperchromasia, and nuclear atypia. Lesions of PIN tend to evolve to adenocarcinoma in which there is disruption of the basement membrane and invasion of the surrounding smooth muscle layer. Adenocarcinoma lesions progress to less-differentiated forms and eventually leading to metastization and castration-resistance forms of prostate cancer.

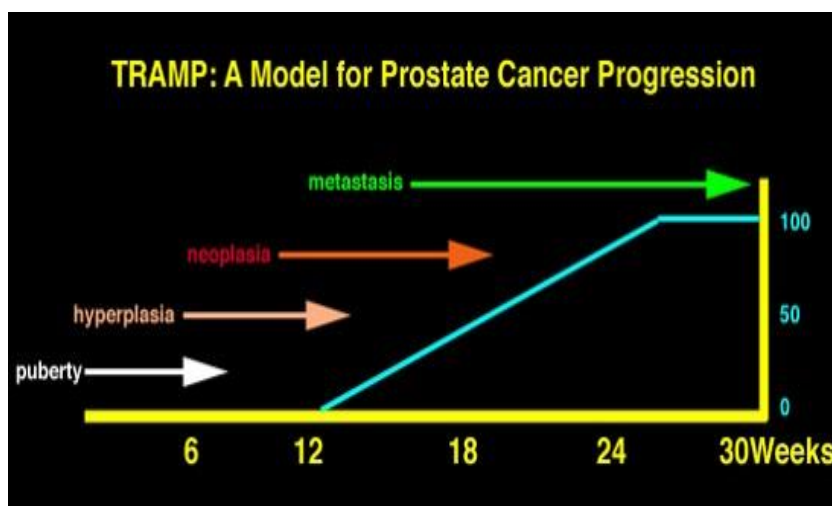
6.2.1 Mouse models of prostate cancer- TRAMP model

Over the years many models including cell lines, transplantable tumors, chemically and hormonally induced tumors and mouse transgenics, have been used to study prostate cancer pathophysiology, and to test strategies for prevention and treatment of this cancer.

The transgenic adenocarcinoma of the mouse prostate (TRAMP) model was generated by microinjection of a vector containing a regulatory sequence (rat probasin) to target simian virus 40 (SV40) (antigens T and t; Tag) early gene expression specifically to the prostatic epithelium (Greenberg et al., 1995). The antigen T (Tag) blocks the expression of tumor suppressor genes, Rb and p53 (Ludlow, 1993; Ali & DeCaprio, 2001), while the antigen t inhibits the function of phosphatase 2A protein (PP2A), whose activity has been implicated in several cellular mechanisms (Chen et al., 2004; Van Hoof & Goris, 2004).

The transgene expression can be detected as early as at 4 weeks of age (Fig.17). The initial lesion observed in these mice is a prostatic intraepithelial neoplasia (PIN) by 12 weeks of age which rapidly becomes invasive, developing lesions of adenocarcinoma, that arise at 24 weeks of age and can progress to less differentiated forms and even to metastasis formation, primarily in the pelvis lymph nodes and the lungs (Gingrich et al., 1996). Moreover, TRAMP mice have been shown to develop spontaneous mutations in the androgen receptor, leading to emergence of hormone-refractory disease (Gingrich, Barrios, Foster, & Greenberg, 1999; Han et al., 2001).

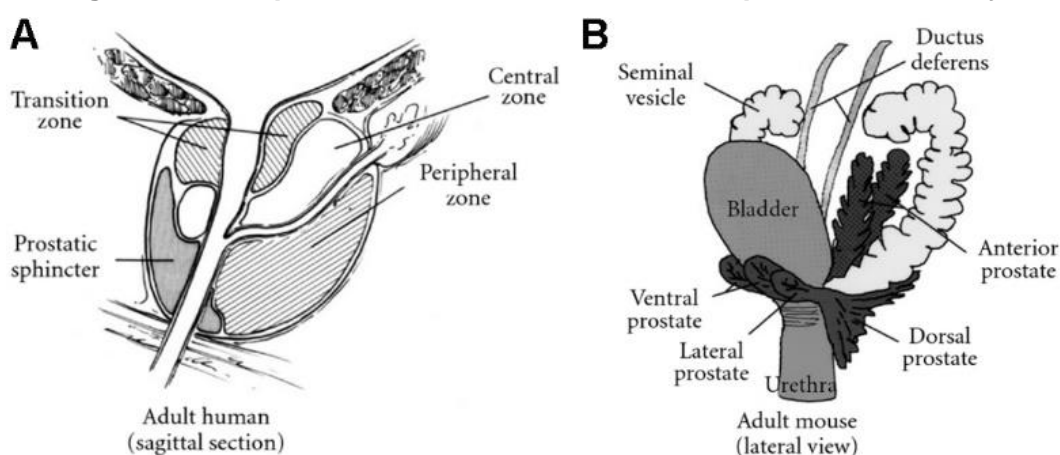
Figure 17- Prostate cancer development in the TRAMP model. *In* (Greenberg et al., found on TRAMP webpage).



The temporal pattern of transgene expression correlates with sexual maturity and is hormonally regulated by androgens. At 12 wk of age, the structures within the prostate histologically resemble mild to severe hyperplasia. Severe hyperplasia and adenocarcinoma is observed by 18 wk of age. At this time, invasion of epithelial cells into underlying smooth muscle and stroma can be observed. By the time the mice are 24-30 wk of age, they will all display primary tumors, progressing to less-differentiated lesions and to metastization at 30 wks of age.

The mouse prostate consists of multiple lobes that have distinct patterns of ductal branching, histological appearance, gene expression, and secretory protein expression (Cunha et al., 1987). These correspond to the ventral, lateral, dorsal, and anterior lobes. However, even though the organization of the prostate differs from humans to mice, the dorsolateral lobe is most analogous to the human peripheral zone, where prostate cancer develops in humans (Berquin, Min, Wu, Wu, & Chen, 2005). Therefore, despite the differences, the TRAMP model is considered a good model for studying prostate cancer progression, closely mimicking clinical prostate cancer with respect to progression, androgen independence, and biochemistry (Kaplan-Lefko et al., 2003).

Figure 18- Comparison of the human and mouse prostates anatomy.



Schematic illustration of the anatomy of the human prostate **A** and mouse prostate **B** (adapted from McNeal et al. (McNeal, 1969) and Cunha et al. (Cunha et al., 1987), respectively.).

6.3 Effects of Notch signaling in prostate tumor development

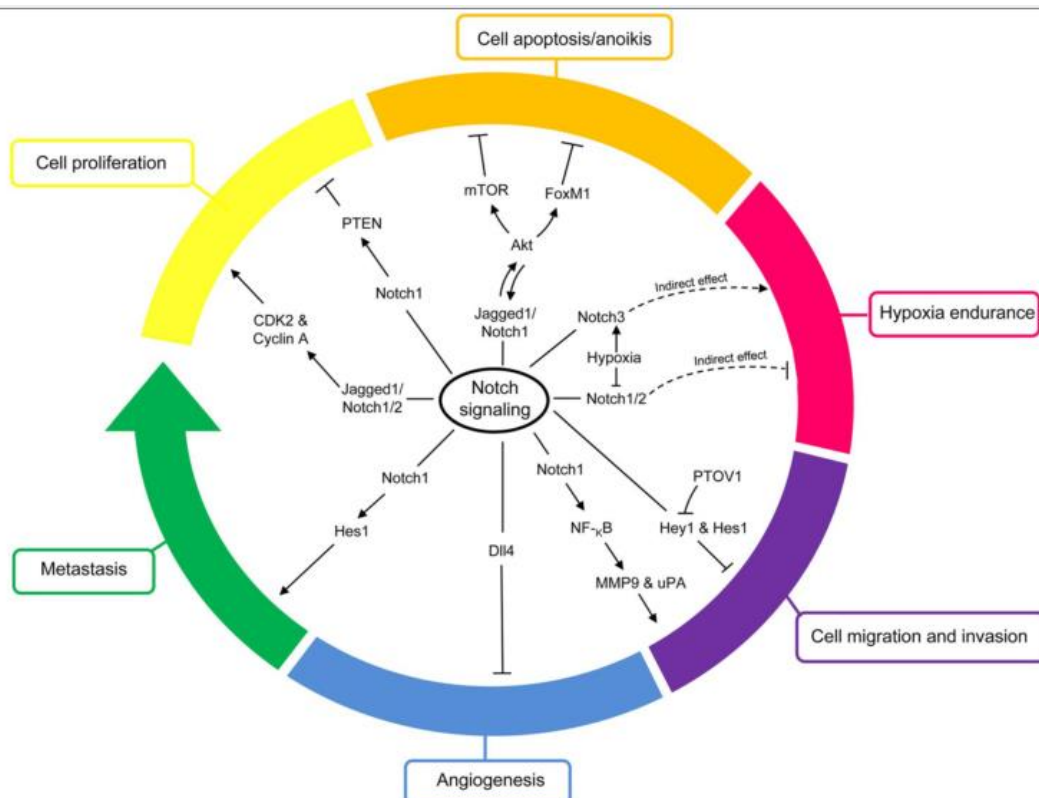
Similarly to breast tumors, prostatic tumors, also an endocrine dependent type of cancer, has also been associated with Notch signaling activation/over-expression. Emerging evidence has demonstrated that Notch expression is significantly higher in prostate cancer and dysregulation of Notch signaling contributes to tumor development and cancer metastasis (Deng et al., 2015). In prostate cancer cell lines, such as DU145, LNCaP and PC3, Notch1 is expressed at various levels (Shou, Ross, Koeppen, de Sauvage, & Gao, 2001). Moreover, Notch2 increased mRNA expression (Scorey et al., 2006) and protein levels (Martin, 2004) have been described in some prostate cancer cell lines. And, up-regulation of *Jagged2* and *Notch3* have also been described in prostate cancer cells with high metastatic potential (Ross et al., 2011). In the TRAMP model, *Notch1* mRNA levels rose upon metastasis to regional lymph nodes (Shou et al., 2001).

However, in human prostate samples, a databases analysis of mRNA expression showed decreased mRNA levels of *NOTCH1* and *HEY1* in prostate cancer compared to benign glands (Wang et al., 2006). Contrastingly, *NOTCH1* protein levels increased with increasing Gleason

grade (Bin Hafeez et al., 2009), and an increase in the frequency of NOTCH3 immunostaining was also observed in tumor biopsies with higher Gleason score (Danza et al., 2013). Moreover, *JAGGED1* mRNA expression levels were shown to be significantly higher in primary tumor and metastasis samples compared to normal samples (Yu et al., 2014). Likewise, high *JAGGED1* and *NOTCH1* protein levels were shown in advanced prostate cancers (Zhu, Zhou, Redfield, Lewin, & Miele, 2013) and higher *JAGGED1* expression is significantly associated with recurrence after radical prostatectomy, and poor prognosis (Santagata et al. 2004). Expression profiling studies also indicate that members of the Notch pathway were the foremost distinctive features of aggressive prostate cancers with high Gleason grade (True et al., 2006; Tomlins et al., 2007; Ross et al., 2011). Particularly, microdissected cancer cells with high metastatic potential displayed upregulated Notch ligand *JAGGED2*, the *NOTCH3* receptor, and the Notch target gene, Hairy enhancer of split family member, *HES6* (Ross et al., 2011).

Therefore, bearing in mind the contradictory evidence in mice (Shou et al., 2001), the preponderance of evidence supports upregulation over downregulation of Notch components with prostate cancer progression (Fig. 19).

Figure 19- Notch signaling in prostate cancer hallmarks. In (Deng et al., 2015).



Contradicting results have suggested Notch signaling to either promote or inhibit prostate cell proliferation, migration and invasion. Activation of Notch suppresses cell apoptosis, anoikis and angiogenesis, while promoting metastasis. Under hypoxic conditions, Notch signaling indirectly promotes hypoxia endurance in prostate cancer cells by sustaining cell proliferation.

6.3.1 Notch signaling regulation of prostatic tumor cell proliferation and apoptosis

The mechanisms exploited by Notch for oncogenic effects include regulation of cellular proliferation and apoptosis/cell survival (Fig.19). Notch1 activation has been shown to inhibit the proliferation of prostate cancer cells (Shou et al., 2001). Conversely, Wang et al. reported that inactivation of Notch1 in prostate led to enhanced cell proliferation, tufting, bridging and localized clusters of epithelial cells, resembling the phenotype of genetically engineered mouse models for prostate cancer (Wang et al., 2006).

Although some studies support the anti-proliferative role of Notch, others have suggested the opposite. Both down-regulation of Jagged1 and knocking down Jagged1 by siRNA transfection inhibited prostate cancer cell lines growth and proliferation (Zhang et al., 2006; Yu et al., 2014). Furthermore, knockdown of RBPJ led to reduced proliferation in PC3 cells (Yong, Sun, Henry, Meyers, & Davis, 2011).

Proliferation is tightly controlled by cell cycle regulation. It has been reported that down-regulation of Notch1 and Jagged1, retards S phase cell cycle progression, inhibiting cell growth in PC3 prostate cancer cell line by reducing CDK2 kinase and Cyclin A expression and up-regulating p27 expression, a CDK inhibitor (Zhang et al., 2006). However, in the same report, knockdown of Jagged1 exhibited a much stronger inhibitory effect on prostate cancer cell lines when compared to knockdown of Notch1. JAGGED1 has also been shown to directly regulate the cell cycle and induce proliferation by inducing cyclin D1 in breast cancer (Cohen et al., 2010), cyclin D1, cyclin E, and c-Myc in colon cancer (Dai et al., 2014). Similar pro-proliferative functions have also been reported for JAGGED1 and NOTCH3 in ovarian cancer (Choi et al., 2008).

Expectedly, Notch signaling can also affect cell death and there are several studies indicating anti-apoptotic functions for Notch and more specifically for Jagged1 ligand. Knockdown of Notch1 and Jagged1 reduced cell viability and induced apoptosis in the PC3 prostate cancer cell line mediated by inactivation of PI3K/Akt mTOR pathways (Wang et al., 2010). JAGGED1 has also been demonstrated to prevent spontaneous apoptosis in glioma cells (Purow et al., 2005).

Furthermore, increased Notch signaling has been shown to inhibit anoikis, via NF-KB and independently of Hes1, in transit amplifying luminal progenitors and stimulate proliferation of prostate luminal epithelial cells (Kwon et al., 2014). Anoikis is an important mechanism that may be used to prevent metastasis by triggering programmed cell death. Therefore, it was proposed that Notch signaling promotes proliferation of luminal cells, inhibits anoikis and enhances prostate cancer progression and metastasis.

The poor prognosis observed in aggressive tumors can also be directly associated with a role for Notch in the development of drug-resistance. Particularly, cultured breast cancer cells that acquire resistance to endocrine therapy have shown increased Notch signaling levels (Rizzo et al., 2008). Moreover, JAGGED1 ligand has also been shown to prevent chemotherapy-

induced cell death in lymphoma cells (Cao et al., 2014), ovarian cancer (Steg et al., 2011), and pancreatic cancer (Wang et al., 2009).

6.3.2 Notch signaling regulation of Cancer Stem Cells (CSCs)

In several tumor types a distinct subpopulation of cells termed “cancer stem cells” (CSCs), or cancer-initiating cells has been identified (Korkaya & Wicha, 2007). CSCs are characterized by self-renewal capacity, high clonogenic potential, and asymmetric division producing daughter stem and differentiated cancer cells (Medema, 2013). CSCs have also been described to have increased invasive potential, ability to resist to several anti-cancer treatments and often thought to be responsible for patient relapse and metastasis (Medema, 2013).

Notch signaling has also been reported to be important for both CSC maintenance and self-renewal in several tumor types (Espinoza, Pochampally, Xing, Watabe, & Miele, 2013). Notch1 and Notch4 have been reported to have increased activity in the breast CSC population, and conversely, inhibition of Notch signaling reduced stem cell activity *in vitro* and tumor formation *in vivo* (Patrawala et al., 2005; Wang, Li, Banerjee, & Sarkar, 2009; Harrison et al., 2010). Similarly, Notch activity has been described to be higher in the colon CSC population, driving apoptosis prevention (Sikandar et al., 2010). Moreover, Xing et al have also shown that Jagged2 was upregulated in bone marrow stroma under hypoxic conditions, which significantly promoted EMT and self-renewal of breast CSCs (Xing et al., 2011).

Particularly, JAGGED1 has also been associated to “stemness” in cancer, appearing to be the main ligand driving CSC dependent Notch signaling (Li, Masiero, Banham, & Harris, 2014). Accordingly, in breast cancer, high levels of *JAG1* and *NOTCH3* were reported to promote stem cell self-renewal and survival and to potentiate mammosphere formation *in vitro* (Sansone et al., 2007, 2007). Moreover, using mouse models with mammary-specific deletion of *Lfng*, an N-acetylglucosamine transferase that prevents Notch activation by Jagged ligands, that develop basal-like breast cancer, were shown to have higher Jagged1 activity and enhanced CSC proliferation (Xu et al., 2012). Furthermore, JAGGED1 expressed by both tumor and endothelial cells was reported to play an important role in glioma/glioblastoma-initiating cells (Zhu et al., 2011; Jeon et al., 2014). Soluble JAGGED1 produced by tumor-associated endothelial cells has been demonstrated to promote the CSC phenotype in human colorectal cancer cells (Lu et al., 2013).

More specifically in the prostate, genomic profiling results have identified *JAG1* transcription as one of the markers of stem cell-like prostate cancer cells (Duhagon, Hurt, Sotelo-Silveira, Zhang, & Farrar, 2010). Moreover, in another gene profiling study of DU145 prostate cancer cells, a subpopulation with CD133^{high}/CD44^{high}, both markers for cancer stem cells, was isolated and found to express high levels of Notch1, Jagged1, Dll1 and Dll3 (Oktem et al., 2014). Conversely, in human prostate cancer tissue samples, a subpopulation that conferred

docetaxel resistance, tumor-initiating capacity and that had increased numbers in metastatic tumors, presented marked up-regulation of Notch and Hedgehog signaling (Domingo-Domenech et al., 2012). Furthermore, in the the same study, combined targeted inhibition of Notch and Hedgehog signaling pathways significantly depleted this subpopulation, implicating a promising therapeutic strategy toward prostate cancer. In another report it was demonstrated that Notch1 overexpression led to proliferation, anoikis resistance and rescue of a prostatic cancer stem cell-like subpopulation (Kwon et al., 2014).

6.3.3 Notch signaling regulation of epithelial-to-mesenchymal transition (EMT), invasion and metastasis

Aggressive cancers are characterized by the ability of tumor cells to invade the surrounding tissues and to colonize distant organs (metastatic process). For efficient metastatic process, tumor epithelial cells make use of a reversible developmental program called EMT, during which loss of epithelial features (e.g., E-cadherin expression and cell-to-cell adhesion) and the acquisition of mesenchymal traits (e.g., Snail, Slug and twist transcription) enables tumor cells to invade, resist apoptosis, disseminate and to acquire stem-cell-like features (Hanahan & Weinberg, 2011; Kong, Li, Wang, & Sarkar, 2011; Lamouille, Xu, & Derynck, 2014). Similarly to the other cancer hallmarks, Notch signaling has also been extensively studied in this context (Espinoza et al., 2013) (Fig.19).

Notch signaling has been shown to cross-talk with several transcription and growth factors relevant to EMT, including Snail, Slug, and transforming growth factor Beta (TGF- β). Notch has been shown to promote EMT through the regulation of Snail: Over-expression of Notch-1 in immortalized endothelial cells *in vitro* induced Snail (Timmerman et al., 2004) which is thought to bind to E-boxes in the human *E-cadherin* promoter and repress *E-cadherin* gene expression (Becker et al., 2007); Notch1 activation was also shown to be able to induce EMT by stabilizing Snail protein under hypoxic conditions (Sahlgren, Gustafsson, Jin, Poellinger, & Lendahl, 2008). Additionally, it has been reported that Notch1 activation can directly stimulate the *Slug* promoter, resulting in the upregulation of Slug and initiation of EMT (Niessen et al., 2008). Furthermore, Notch signaling is often and aberrantly activated by hypoxia, which induces EMT during tumor progression, favoring cancer metastasis (Sahlgren et al., 2008).

A direct role for Jagged1 induced EMT has also been reported in several tumor settings. JAGGED1-induced signaling in breast cancer was shown to inhibit the epithelial phenotype by SLUG upregulation, promoting tumor growth and metastasis (Leong et al., 2007). Furthermore, it has been demonstrated that TGF- β is able to induce Jagged1 expression (Niimi, Pardali, Vanlandewijck, Heldin, & Moustakas, 2007) and that TGF- β -induced EMT can be blocked by either Hey1 or Jagged1 knockdown and pharmacological inactivation of Notch (Zavadil, Cermak, Soto-Nieves, & Böttlinger, 2004). Moreover, the Jagged1/Notch2 axis was described to be highly upregulated in treatment-resistant pancreatic cancer cells, which was associated

with EMT phenotype by controlling Snail, Slug and Zeb1 transcription factors (Wang et al., 2009). It was also reported that JAGGED1 is able to increase tumor migratory and invasive behavior of breast cancer, by inducing the urokinase-type plasminogen activator (uPA), a well-known marker of recurrence and metastasis (Shimizu et al., 2011). Lastly, JAGGED1 has also been shown to be involved in the tissue specificity of breast cancer dissemination since it has been described to have significant roles in metastasis to the bone and brain (Sethi, Dai, Winter, & Kang, 2011; Xing et al., 2013).

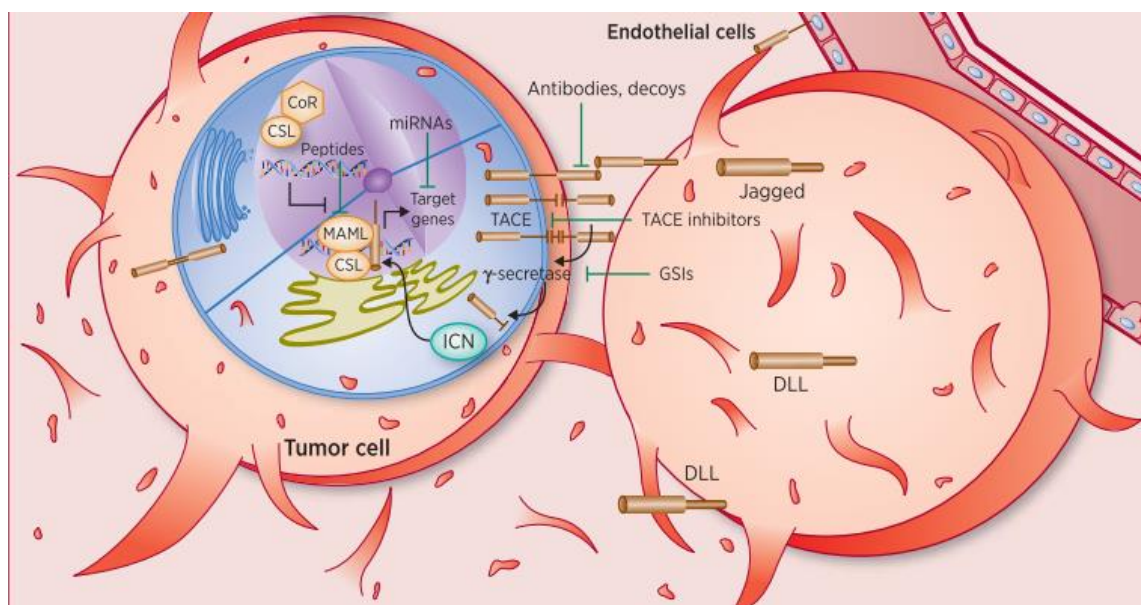
More specifically in the case of prostate cancer, high JAGGED1 expression has been clinically associated with metastasis development and recurrence (Santagata et al., 2004) and with regulation of migration/invasion via NF- κ B (Wang et al., 2010). Recent data also showed that JAGGED1 and NOTCH1 expression increases dramatically in high-grade and metastatic prostate cancers compared to primary lesions (Zhu et al., 2013). Moreover, overexpression of NOTCH1, in both human tissue samples and cultured prostate cancer cell lines, promoted tumor invasion (Bin Hafeez et al., 2009). In the same study, knockdown of Notch1 in PC3 and 22Rv1 cells significantly attenuated cell invasion by decreasing the expression of extracellular proteins involved in cell invasion, including matrix metalloproteinase-9 (MMP9) and urokinase plasminogen activator (uPA) (Bin Hafeez et al., 2009) which are NF- κ B downstream genes. Furthermore, treatment with DAPT, a Notch inhibitor, down-regulated Hes1 and decreased cell motility in prostatic cancer cell lines (Scorey et al., 2006). Finally, Jagged2/Notch3/Hes6 axis was shown to be highly up-regulated in microdissected prostate cancer cells with high metastatic potential (Ross et al., 2011).

In recent years, EMT has also been linked with stem-like signatures in prostate cancer cells, characterized by increased expression of Notch-1, Sox2, Nanog and Oct4, (Kong et al., 2010). Similarly, epithelial cells from a primary prostate tumor can undergo EMT with activation of embryonic programs of epithelial plasticity, including Notch, and switch from a stable, epithelial phenotype to a motile, mesenchymal phenotype (Sethi, Macoska, Chen, & Sarkar, 2010).

7. Targeting the Notch signaling pathway as a therapeutic approach to cancer

Despite its disputable role as oncogene or tumor suppressor, Notch signaling has been profoundly studied in the pathogenesis of cancer and therefore has become a target for diagnostic and pharmacological intervention. Even though no FDA-approved drugs currently exist that target the Notch pathway, several therapeutics have been developed to target different aspects of this pathway for both hematologic and solid malignancies (Fig. 20).

Figure 20- Potential cancer therapeutics that target Notch signaling. *In* (Previs, Coleman, Harris, & Sood, 2015).



Potential cancer therapeutics that target Notch signaling include antibodies, peptides, miRNAs, TACE inhibitors, and GSIs. Notch can function as a tumor suppressor or is oncogenic and activate/inhibit different downstream targets depending on the malignancy and microenvironment.

7.1 Gamma- and alfa-secretase inhibitors (GSIs and ASIs)

GSIs were initially developed to reduce amyloid- β protein aggregates in Alzheimer's disease (Wong et al., 2004). Subsequently they were found to be an attractive potential treatment for cancers involving active Notch signaling because proteolytic cleavage of NOTCH receptors by the presenilin/gamma-secretase complex is a necessary step for signaling activation. They were initially tested in T-ALL cell lines and later in prostate, breast, lung and xenografts, and found to suppress cancer growth (Weng et al., 2004; Dang, Kawaguchi, Carbone, & Hue, 2005; Zhang et al., 2006; Rizzo et al., 2008; Balasubramanian et al., 2008). Several GSI molecules have reached clinical trials and even phase 2 trials alone or in combination with other drugs (Previs et al., 2015). However it soon became evident that GSIs caused toxicity in Notch-dependent tissues, particularly in the gastrointestinal tract, due to alterations in the differentiation of intestinal stem cells that caused accumulation of secretory goblet cells, and

the thymus (Wong et al., 2004; van Es et al., 2005). As a result, inhibition of the pathway using GSIs alone may not become a viable therapeutic choice in the future.

Targeting of Notch signaling is not restricted to the use of GSIs. Alfa-Secretase inhibitors (ASIs), or TACE inhibitors, that act upon the ADAM10/17 metalloproteases, which mediate receptor S2 cleavage, are also available (Zhou et al., 2006) and currently being tested (Purow, 2012). However, ASIs will probably manifest the same toxicity problems as GSIs, since it inhibits pan-Notch signaling.

7.1.1 Therapeutic Notch inhibition in prostate cancer

Of all the clinical trials on going using Notch inhibitors there is one specific for prostate cancer patients. It combines the anti-androgen bicalutamide with a GSI in patients with recurrent prostate cancer after prostatectomy or prostate radiation therapy. Recently published results from two Phase I clinical trials with GSIs reported that these drugs were well tolerated and there was potential clinical benefit in brain tumor (glioma), colorectal adenocarcinoma and melanoma patients. However, no benefits have been reported for prostate cancer patients (Tolcher et al., 2012; Krop et al., 2012).

7.2 Specific targeting of Notch pathway components

Other approaches have emerged to selectively inhibit the Notch pathway. Antibodies binding the receptors Notch1 and Notch2 have been generated by using phage display technology, that act mainly by stabilizing the negative regulatory region of the receptors and protecting against proteolytic cleavage, thus inhibiting the production of ICN1/2 (intracellular domains) (Wu et al., 2010). Other antibodies directed against the ligand Delta-like 4, have been used experimentally and shown to inhibit cancer cell proliferation (Noguera-Troise et al., 2006; Ridgway et al., 2006).

Another approach utilized synthetic peptides that specifically block NICD1 binding to RBPJ, by mimicking MAML1 but lacking its active domains. Moellering et al. generated a synthetic, cell-permeable, α -helical peptide (SAHM1) that blocks MAML1 recruitment and NOTCH-mediated transcription as it binds with high affinity to the interface on the NOTCH-CSL transactivation complex. Tested *in vivo* in a Notch1 driven mouse leukemia model, and *in vitro* in human T-ALL cell lines, the peptide strongly inhibited NOTCH-mediated cell proliferation and leukemia progression while avoiding gastrointestinal toxicity (Moellering et al., 2009).

These agents could avoid toxicity because they do not affect signaling by other Notch receptors (Notch2, 3, or 4), and/or because they spare other GSI targets outside of the Notch pathway.

7.3 Notch decoys

Soluble extracellular fractions of Notch ligands and receptors have also been developed to inhibit the pathway in a dominant-negative manner, consequently acting as decoys.

A soluble Dll4 fusion protein (sDll4-Fc) that works by binding Notch receptors and preventing their activation by endogenous Dll4 was first used to inhibit tumor growth by promoting an abnormalization of the neo-vasculature, as previously mentioned (Noguera-Troise et al., 2006; Scehnet et al., 2007). A Notch1 decoy was shown to decrease tumor cell viability in xenograft models (Funahashi et al., 2008). More recently, a Notch1 decoy that specifically blocks Jagged mediated interactions was shown to inhibit xenograft growth by an anti-angiogenic and anti-maturation functions, leading to restricted tumor vessel perfusion and thus functionality (Kangsamaksin et al., 2014).



**EXPERIMENTAL
WORK**



Chapters I-IV

**Chapter I –
Endothelial
Jagged1
antagonizes Dll4
regulation of
endothelial
branching and
promotes vascular
maturation
downstream of
Dll4/Notch1.**

Ana-Rita Pedrosa,
Alexandre Trindade, Ana-
Carina Fernandes,
Catarina Carvalho, Joana
Gigante, Ana Teresa
Tavares, Rodrigo
Diéguez-Hurtado, Hideo
Yagita, Ralf H. Adams,
António Duarte.

Published in *Arterioscler
osis, Thrombosis, and
Vascular Biology*.

2015;35(5):1134-1146.

DOI:

10.1161/ATVBAHA.114.

1. Abstract

Objective—Notch signaling controls cardiovascular development and has been associated with several pathological conditions. Among its ligands, Jagged1 and Dll4 were shown to have opposing effects in developmental angiogenesis, but the underlying mechanism and the role of Jagged1/Notch signaling in adult angiogenesis remain incompletely understood. The current study addresses the importance of endothelial Jagged1-mediated Notch signaling in the context of adult physiological angiogenesis and the interactions of Jagged1 and Dll4 on angiogenic response and vascular maturation processes.

Approach and Results— The role of endothelial Jagged1 in wound healing kinetics and angiogenesis was investigated with endothelial-specific *Jag1* gain-of-function and loss-of-function mouse mutants (*eJag1OE* and *eJag1cKO*). To study the interactions between the 2 Notch ligands, genetic mouse models were combined with pharmacological inhibition of Dll4 or Jagged1, respectively. Jagged1 overexpression in endothelial cells increased vessel density, maturation, and perfusion, thus accelerating wound healing. The opposite effect was seen in *eJag1cKO* animals. Interestingly, Dll4 blockade in these animals led to an increase in vascular density but induced a greater decrease in perivascular cell coverage. However, Jagged1 inhibition in *Dll4* gain-of-function (*eDll4OE*) mutants, with reduced angiogenesis, further diminished angiogenic growth and hampered perivascular cell coverage. Our findings suggest that as Dll4 blocks endothelial activation through Notch1 signaling, it also induces Jagged1 expression. Jagged1 then blocks Dll4 signaling through Notch1, allowing endothelial activation by vascular endothelial growth factor and endothelial layer growth. Jagged1 also initiates maturation of the newly formed vessels, possibly by binding and activating endothelial Notch4. Importantly, mice administered with a Notch4 agonistic antibody mimicked the mural cell phenotype of *eJag1OE* mutants without affecting angiogenic growth, which is thought to be Notch1 dependent.

Conclusions—Endothelial Jagged1 is likely to operate downstream of Dll4/Notch1 signaling to activate Notch4 and regulate vascular maturation. Thus, Jagged1 not only counteracts Dll4/Notch in the endothelium but also generates a balance between angiogenic growth and maturation processes in vivo.

Key Words: angiogenesis factor; Jagged1 protein; Notch proteins; wound healing.

2. Introduction

Increasing evidence indicates the importance of Notch signaling in the development and homeostasis of the vascular system as well as in the pathogenesis of several diseases. The Notch signaling pathway comprises 4 different transmembrane receptors (Notch1–4) and 5 ligands (Delta like 1, 3, and 4 and Jagged1 and 2). Binding of a Notch ligand to a receptor triggers a series of conformational changes and cleavages of the receptors. These lead to the release and translocation of the Notch intracellular domain to the nucleus where it controls the expression of a variety of target genes depending on cell type and on biological context (Schweisguth, 2004). The *Dll4* and *Jag1* (encoding Jagged1) genes were shown to be fundamental in developmental angiogenesis. Dll4 ligand is required for normal arterial patterning in the embryo (Duarte et al., 2004) and was also shown to have a major antiangiogenic effect in wound healing in the adult (Trindade et al., 2012). *Jag1*-null mouse mutants die at E11.5 because of heart defects and abnormal development of the yolk sac and head vasculature (Xue et al., 1999). Moreover, mutations in the human *JAG1* gene cause Alagille syndrome, which comprises complex cardiac defects and vascular anomalies (Li, Miano, Cserjesi, & Olson, 1996). However, little is known about the function of Jagged1 in adult neoangiogenesis. Dll4 is predominantly expressed in the endothelium of capillaries and arteries (Shutter et al., 2000), whereas Jagged1 is expressed in both endothelial and vascular smooth muscle cells (vSMCs) (Villa et al., 2001). During developmental angiogenesis in the postnatal mouse retina, Dll4 is detected in endothelial tip cells at the distal end of sprouting vessels (Claxton & Fruttiger, 2004). In contrast, Jagged1 is found in stalk cells at the sprout base (Benedito et al., 2009). A recent study has suggested that Dll4 and Jagged1 have opposite effects in mouse retinal vascular development. In this setting, Jagged1 acts as a positive regulator of sprouting and tip cell formation because of its ability to antagonize Dll4/Notch signaling, which acts as a negative regulator of these processes (Benedito et al., 2009). Previous work has also shown that endothelial Jagged1 is indispensable for the development of neighboring vascular smooth muscle (High et al., 2008), which has been attributed to the induction of mural cell differentiation through Notch3 (Liu et al., 2009) and RBP-Jkappa (Doi et al., 2006) activation. Despite considerable progress in understanding vascular morphogenesis during development, few studies have targeted in vivo angiogenesis in adult physiological settings. In mammals, physiological angiogenesis occurs mainly during tissue regeneration, such as in healing wounds, and in the female reproductive cycle. In particular, the wound healing assay constitutes a fast, easy, and reliable in vivo model of physiological angiogenesis for studying the molecular mechanisms involved in the formation and remodeling of vascular structures (Eming et al., 2007). During regeneration, the vascular network at the wound edges expands through sprouting into the granulation tissue, which has increased oxygen and nutrient demand. Vascular endothelial growth factor (VEGF) is the main pro-angiogenic signal controlling this process (Carmeliet, 2003). Through the analysis of

wound healing kinetics, vessel morphology, and gene expression in endothelial *Jag1* or *Dll4* mutants treated with ligand-specific antagonists, we provide the first evidence for an important pro-angiogenic role of endothelial Jagged1 in adult regenerative angiogenesis. Moreover, we present evidence supporting a synergistic effect of both ligands on mural cell recruitment and propose a new mechanism by which Dll4/Notch1 signaling promotes the recruitment of perivascular cells through the upregulation of *Jag1* and Notch4 activation in endothelial cells (ECs).

3. Materials and Methods

3.1 Experimental animals

All the procedures involving animals used in this study were approved by the Ethics and Animal Welfare Committee of the Faculty of Veterinary Medicine of Lisbon. Animals were housed in ventilated propylene cages with sawdust as bedding, in a room with temperature between 22°C and 25°C and a 12-hours-light/12-hours-dark cycle. The mice were fed standard laboratory diet.

To obtain the gain-of-function mutants, heterozygous Tet-O-Jag mice were crossed with a line of heterozygous Tie-2-rtTA mutant mice. The double heterozygous offspring obtained, Tet-O-Jag; Tie-2-rtTA, were administered doxycycline (4mg/ml in drinking water from week 4), in order to activate the overexpression of *Jag1* under the control of the *Tie-2* promoter. Control mice had the same *Jag1* gain-of-function genotype but were not induced with doxycycline.

The loss-of-function mutant is a conditional “knock-out” where the coding region for the DSL (Delta-Serrate-Lag2) region of *Jag1* (exon 4) is flanked by loxP sites- *Jag1lox/lox* line (Kiernan, Xu, & Gridley, 2006) (B6; 129S-*Jag1 tm2Grid/J*; The Jackson Laboratory). *Jag1lox/+* mice were crossed with VE-Cadherin-Cre-ERT2 mice (Alva et al., 2006) in order to obtain a *Jag1lox/lox* VE-Cadherin-Cre-ERT2 mouse line. *Jag1* null endothelial mutants were generated upon treatment with tamoxifen (50mg/kg daily IP for 5 days, starting one week before the experiment). Control mice had the same *Jag1* loss-of-function genotype but were not induced with tamoxifen.

Endothelial specific *Dll4* gain-of-function mutant mice (*eDll4OE*) were obtained as previously reported (Trindade et al., 2008).

3.2 Wounding procedures

Skin biopsy wounds (4mm diameter) were performed in the dorsum of anaesthetized animals as previously described (Chigurupati et al., 2007; Trindade et al., 2012). Shortly, the back hair of the mouse was shaved and two full- thickness wounds were created on each mouse by excising the skin and the underlying *panniculus carnosus* with a 4 mm dermal biopsy punch. Wounds were measured on day 0, to serve as reference, and periodically at each 24 h from that point onwards. Wounds were considered to be ellipsoid in shape and measurements of

the larger (l) and smaller (s) diameters of each wound were made with a calliper. The areas of each wound were calculated using the formula $(l/2)*(s/2)*\pi$, and transformed into percentage relative to day 0 (100%).

Blocking anti-Dll4 antibody (Anti-Dll4) (Yamanda et al., 2009) was administered by intraperitoneal injection at the dosage of 8 mg/kg at day 0 and day 3 of the experiment, to both *eJag1cKO* (*eJag1cKO* + Anti-Jag1) and respective control mice (Ctrl+ Anti-Dll4). Control mice were administered an equal volume of PBS.

Blocking anti-Jagged1 antibody (Anti-Jag1) (Elyaman et al., 2007) was administered at the dosage of 8 mg/kg at day 0 and day 3 of the experiment, to both *eDll4OE* (*eDll4OE* + Anti-Jag1) and respective control mice (Ctrl+ Anti-Jag1). An extra control mice group were administered an equal volume of PBS (Ctrl).

Notch4 agonist (Sekine et al., 2012) was administered at the dosage of 8 mg/kg at day 0 and day 3 of the experiment to WT mice. WT mice alone were administered an equal volume of PBS.

3.3 Tissue preparation and immunofluorescence

Wound tissue biopsies collected at day 7 after injury were fixed with 4% paraformaldehyde (PFA) solution at 4°C for 1h, cryoprotected in 15% sucrose, embedded in 7,5% gelatin, frozen in liquid nitrogen and cryosectioned at 10 and 20µm.

Immunostaining was performed using the following protocol: tissue slides were permeabilized in 3% H₂O₂ methanol solution for 30 min and PBS-Triton 0,1% solution 2x 10 min; blocking was performed for 1h (room temperature) either with 2% BSA + 5% Goat serum in PBS-W 0,1% solution or with 5% BSA in PBS-W 0,1% solution (for primary antibodies made in goat); after blocking, slides were incubated over-night at 4°C with specific primary antibodies followed by 1h incubation at room-temperature with fluorescently-tagged specific secondary antibodies (Invitrogen).

To examine wound vascular density and vessel maturity, judged by the degree of recruitment of smooth muscle cells and pericytes, double fluorescent immunostaining of platelet endothelial cell adhesion molecule (PECAM-1), alpha smooth muscle actin (α -SMA) and Pdgfr- β , respectively, was performed on tissue sections. The primary antibodies used were rat monoclonal anti-mouse PECAM-1 (BD Pharmingen, San Jose, CA), mouse monoclonal anti-SMA Cy3 conjugate (Sigma Aldrich, USA), rabbit monoclonal anti-PDGFR β (Cell signaling Technology) and the secondary antibody was anti-rat conjugated with Alexa Fluor 488 and anti-rabbit conjugated with Alexa Fluor 594 (Invitrogen, Carlsbad, CA). Nuclei were counterstained with 4',6-diamidino-2-phenylindole dihydrochloride hydrate (DAPI; Molecular Probes, Eugene, OR).

To assess vascular perfusion, avertin (2,5%) anesthetized mice were injected with biotin-conjugated lectin from *Lycopersicon esculentum* (100µg in 100µl of PBS; Sigma, St. Luis, MO)

via caudal vein and allowed to circulate for 5 minutes before we perfused the vasculature transcardially with 4% PFA in PBS for 3 minutes. Wound samples were collected and processed as described above. Tissue sections (20 μ m) were stained with rat monoclonal anti-mouse PECAM-1, followed by Alexa 594 goat anti-rat IgG (Invitrogen, Carlsbad, CA). Biotinylated lectin was visualized with Streptavidin-Alexa 488 (Invitrogen, Carlsbad, CA). The images were obtained and processed as described above. Wound perfusion area was quantified by determining the percentage of PECAM-1-positive structures that were co-localized with Alexa 488 signals.

In order to visualize vascular extravasation, avertin anesthetized mice were injected with 1% Evans Blue dye solution (Sigma, St. Luis, MO) via caudal vein, and perfused transcardially 5 minutes later with 4% PFA in PBS for 3 minutes. Wound tissue sections (20 μ m) were stained with rat monoclonal anti-mouse PECAM-1, followed by Alexa 488 goat anti-rat IgG. Extravasation was visualized by observing Evans Blue red fluorescence in contrast with green fluorescent vascular structures (Gratton et al., 2003). Wound vascular extravasation area was quantified by determining the wound section field of Evans Blue red positive signal per vessel area (given by vascular density measurements).

Additional primary antibodies used were rabbit anti-Hey1 or Hey2 (Milipore), rabbit anti-N1ICD (Cell signalling Technology), rabbit anti-N3ICD and goat anti-N4ICD (Santa Cruz Biotechnology).

Fluorescent immunostained sections of the granulation wound tissue (Stadelmann, Digenis, & Tobin, 1998) (angiogenic fronts) were examined under a Leica DMRA2 fluorescence microscope with Leica HC PL Fluotar 10, 20X and 40X/0.5 NA dry objectives (Leica, Heidelberg, Germany), captured using Photometrics CoolSNAP HQ, (Photometrics, Friedland, Denmark), and processed with Metamorph 4.6-5 (Molecular Devices, Sunnyvale, CA). The high-magnification confocal images were obtained using a Carl Zeiss LSM 780 confocal microscope with Zeiss 40X (LD C-Apo) NA 1.10 water immersion objective, and captured using ZEN 2012 Black edition software (Carl Zeiss, Jena, Germany). Morphometric analyses were performed using the NIH ImageJ 1.37v program (NIH, Bethesda, MA, USA).

For immunostaining quantification a defined window (26,5 cm wide per 17,6 cm height) was used and applied to select an area from the wound front in each image. In sequenced images the area selected at the wound front was moved along the vascular plexus in order to be able to collect and analyze windows from all areas of the wound edges. Pixel intensity measurements (determined by the percentage of white pixels per field after transforming the RGB images into binary files) were then applied to each selected window using Image J. In the case of co-localization quantification (SMA, Pdgfr- β , Hey1/2, Lectin and NICDs stainings) pixel intensity measurements were applied but to intact RGB images in order to quantify overlaying signals from two different channels.

3.4 Quantitative transcriptional analysis

Wound samples were collected at the endpoint of each experiment and prepared for FACS sorting. ECs and Mural cells were sorted directly into the lysis buffer of the RNeasy Micro Kit (Qiagen). Total RNA was isolated according to manufacturer's protocol. A total of 100 ng RNA per reaction was used to generate cDNA with the SuperScript III First Strand Synthesis Supermix Q RT-PCR Kit (Invitrogen, CA). Relative quantification real-time PCR analysis was performed as described (Trindade et al., 2008) using Sybergreen Fastmix ROX dye (Qiagen). Primer pair sequences are available on request. The housekeeping gene β -actin was used as endogenous control.

3.5 Flow cytometry

For flow cytometric analysis and sorting of ECs (Lin- (cd45- ter119-) cd31+) and mural cells (Lin- (cd45- ter119-) cd146+ cd31-) (Crisan, Corselli, Chen, & Péault, 2012), 2 wound samples were collected per each animal and finely dissected into small pieces (2-4 mm). Then, the samples were digested with collagenase (Sigma) incubation at 37°C, with agitation, for 4h30 min. DNase I (Sigma) was added during digestion to eliminate DNA residues. After washing, digested cells were then subjected to immunostaining with anti-mouse ter-119 PE-Cy7, anti-mouse cd45 PE-Cy7 (Affymetrix, eBioscience), anti-mouse cd31 FITC and anti-mouse cd146 PE (BD Pharmingen). After washing, cells were sorted in FACS Aria III cytometer and analyzed using BD FlowJo software (Version 10.0, BD Bioscience).

For demarcating and sorting ECs and mural cells, first standard quadrant gates were set, subsequently to differentiate cd31+ (>10³ log FITC fluorescence) and cd146+ (>10 log PE fluorescence) cells from the Lineage negative population (\leq 10² log PE-Cy7 fluorescence).

3.6 Statistical analysis

Data processing was carried out using the Statistical Package for the Social Sciences software, version 17.0 (SPSS v. 17.0; Chicago, IL). Statistical analyses were performed using Mann-Whitney-Wilcoxon test and Student's t-test. All results are presented as mean \pm SEM. *P*-values < 0.05, <0.01 and <0.001 were considered significant (indicated in the figures with *) and highly significant (indicated with ** and ***), respectively.

4. Results

4.1 Endothelial Jagged1 accelerates wound healing by promoting angiogenesis and vessel maturation

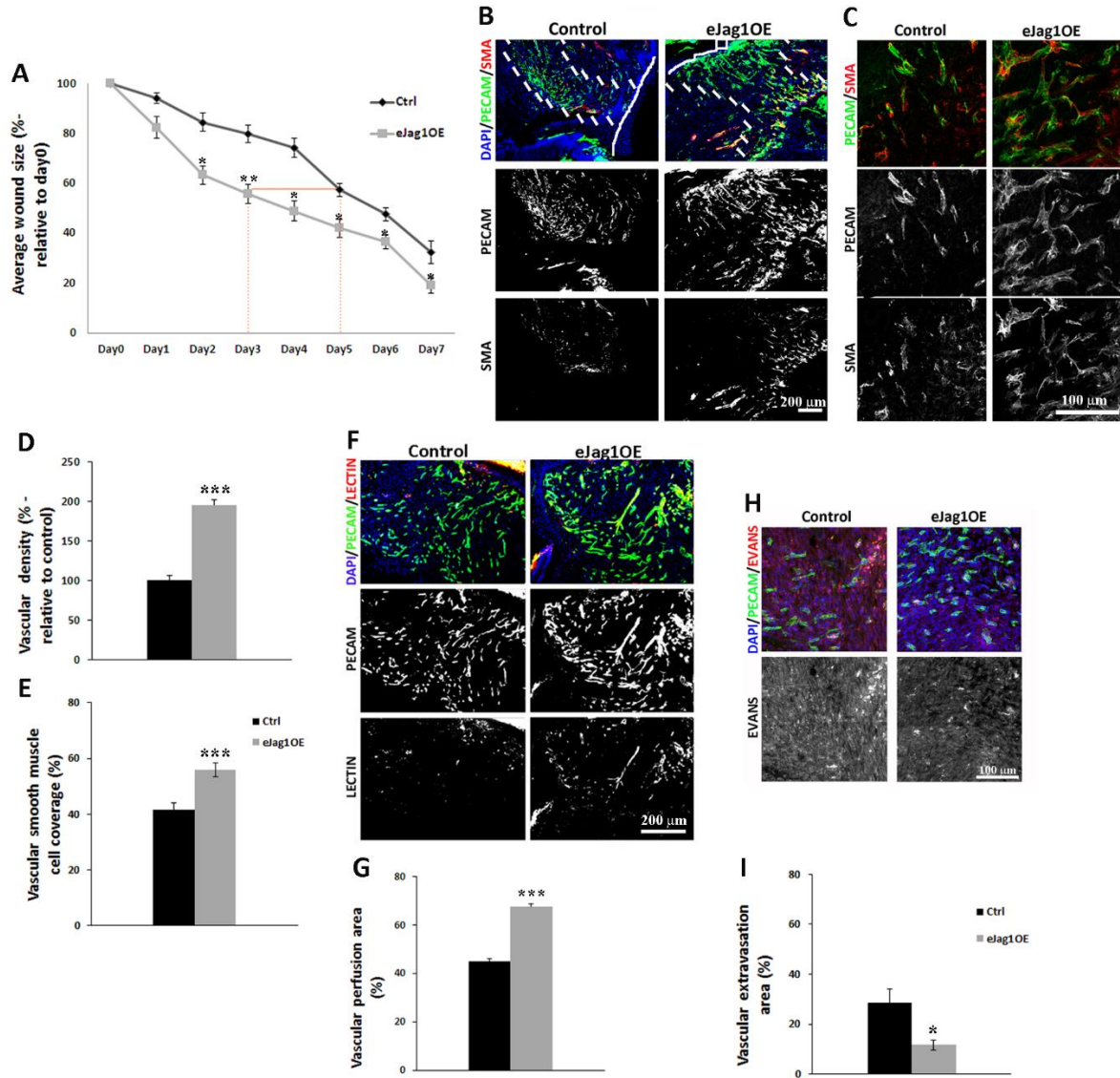
To better characterize the role of Jagged1/Notch signaling during adult physiological angiogenesis, wound healing kinetics were analyzed in endothelial-specific *Jag1* gain-of-function and loss-of-function mutant mice. EC-specific *Jag1* overexpression (endothelial-specific *Jag1* gain-of-function or conditional overexpression [*eJag1OE*]) led to significantly accelerated wound healing from day 2 of recovery onward relative to control animals. Accordingly, closing of *eJag1OE* wounds occurred 2 days faster on average (Figure I.1A). In contrast, loss of endothelial *Jag1* (endothelial-specific *Jag1* loss-of-function or conditional knockout [*eJag1cKO*]) led to significantly delayed healing from day 2 of recovery with an average 2-day delay in the healing process (Figure I.2A).

To address whether the altered wound closure kinetics observed in these EC-specific mutants was indeed associated with altered vessel growth, the vascular morphology of the samples collected at end point (day 7 of recovery) was examined. Blood vessel endothelium in the wounded area was visualized by immunostaining against PECAM-1, whereas α -SMA and Pdgfr- β were used to reveal perivascular cell and pericyte coverage, respectively, and thereby analyze vessel maturation (Figures I.1B, I.1C, I.2B, and I.2C and Suppl. Figure I.1A and I.1B). In *eJag1OE* mutants, we observed higher vascular density (Figure I.1B–I.1D) as well as an increase in vSMC (Figure I.1B, I.1C, and I.1E) and pericyte coverage (Suppl. Figure I.1A and I.1B). As shown in detail in Figure I.1C, the newly formed vasculature in *eJag1OE* mutants displayed highly branched networks and exhibited a greater maturation state, as indicated by the abundance of both perivascular cells and pericytes present. The opposite was seen in *eJag1cKO* mutant wounds, which showed a significant decrease in vascular density (Figure I.2B–I.2D) as well as in the number of perivascular cells (Figure I.2B, I.2C, and I.2E) and pericyte coverage (Suppl. Figure I.1C and I.1D). At high magnification, the vasculature of *eJag1cKO* wounds was sparse and with few SMCs (Figure I.2C) and pericytes attached (Suppl. Figure I.1C and I.1D).

We also evaluated wound vessel functionality by analyzing biotinylated lectin perfusion and Evans' blue dye vascular leakage (Figures I.1F, I.1H, I.2F, and I.2H). As shown in Figure I.1F and I.1G, overexpression of *Jag1* in the endothelium was associated with an increase in the amount of perfused, lectin-containing vessels. At the same time, Evans' blue extravasation was significantly reduced in comparison with controls (Figure I.1H and I.1I), suggesting an overall improvement in the functionality of newly formed vessels. Conversely, endothelial *Jag1* loss of function led to a significant decrease in vascular perfusion (Figure I.2F and I.2G) and to an increase in extravasation per vessel area (Figure I.2H and I.2I). Taken together, endothelial *Jag1* overexpression led to the formation of a dense, mature, and more functional wound vascular plexus, whereas endothelial *Jag1* loss of function led to a sparse, immature,

and poorly functional vessel network. These results establish that endothelial *Jag1* expression is responsible for modulating vascular growth and maturation during in vivo regenerative angiogenesis, which, in turn, affects wound closure kinetics.

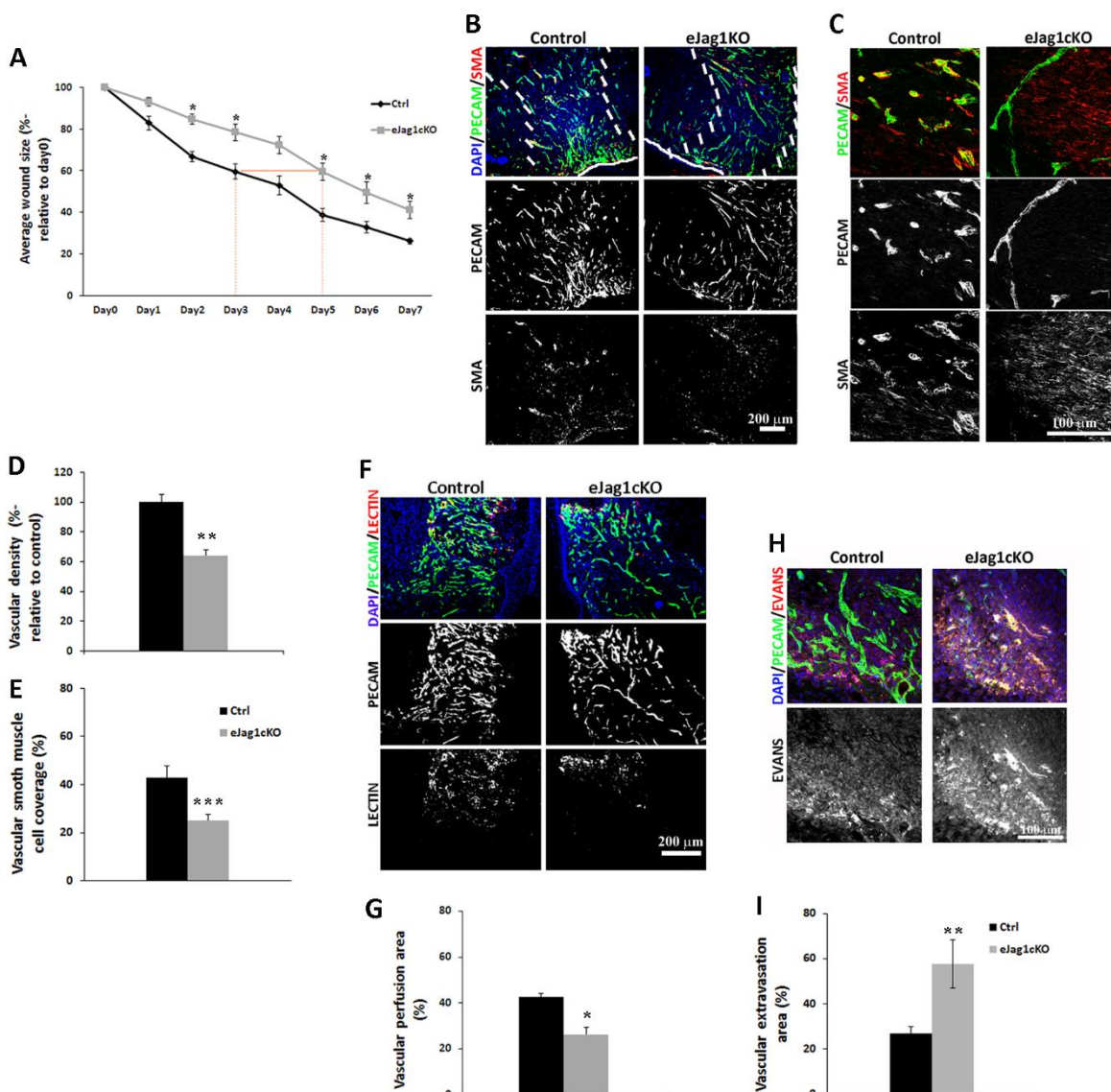
Figure I.1- Effect of endothelial *Jag1* overexpression in wound healing.



A, Progression of average wound size relative to day 0 in 2 mouse groups, *Jag1* gain-of-function mutants *eJag1OE* (Tet-O-Jag Tie2-rtTA+) and controls (Tet-O-Jag Tie2-rtTA-). Overexpression of *Jag1* led to an increase in the healing rate of dermic wounds, with an average 2-day advance in comparison with controls (as demonstrated by the orange line). **B**, Immunostaining images ($\times 10$ amplification) of samples collected at day 7, marked for PECAM-1 (green) and SMA (red), to evaluate vascular density and vascular smooth muscle cell coverage, respectively. Continuous white line marks the base of epidermis and the space between dashed lines marks the angiogenic fronts. **C**, High- magnification ($\times 40$ amplification) confocal imaging showing in detail the vascular phenotype of *eJag1OE* mutants, consisting of an increased number of vessels, as seen by PECAM-1+ signal, and increased vessel coverage by SMA+ cells, compared with the controls. **D**, Percentage of vascular density (relative to control=100%) is increased in endothelial *Jag1* overexpression mutants, as shown by PECAM-1 labeling. **E**, Percentage of vascular smooth muscle coverage, showing increased levels of SMA on

eJag1OE mutant vasculature, relative to controls. **F**, Lectin (red) and PECAM-1 (green) immunostaining ($\times 20$ amplification) of samples collected at end point, to evaluate the colocalization of both signals, indicative of vessel perfusion. **G**, Percentage of perfusion area in the total vascular area (given by vascular density measurements) showing increased lectin labeling in endothelial *Jag1* overexpression mutants. **H**, Evans' blue (red) and PECAM-1 (green) confocal immunostaining images ($\times 20$ amplification) showing the extravasation areas. **I**, Percentage of vascular extravasation area in the total vascular area showing reduced leakage, or Evans' blue staining, in the *eJag1OE* mutant vasculature, relative to controls. 4'-6-Diamidino-2-phenylindole (DAPI; blue) stains nuclei. Results are representative of 2 independent experiments, each with $n=4$ mice per group. Error bars represent SEM; * $P<0.05$; ** $P<0.01$; and *** $P<0.001$.

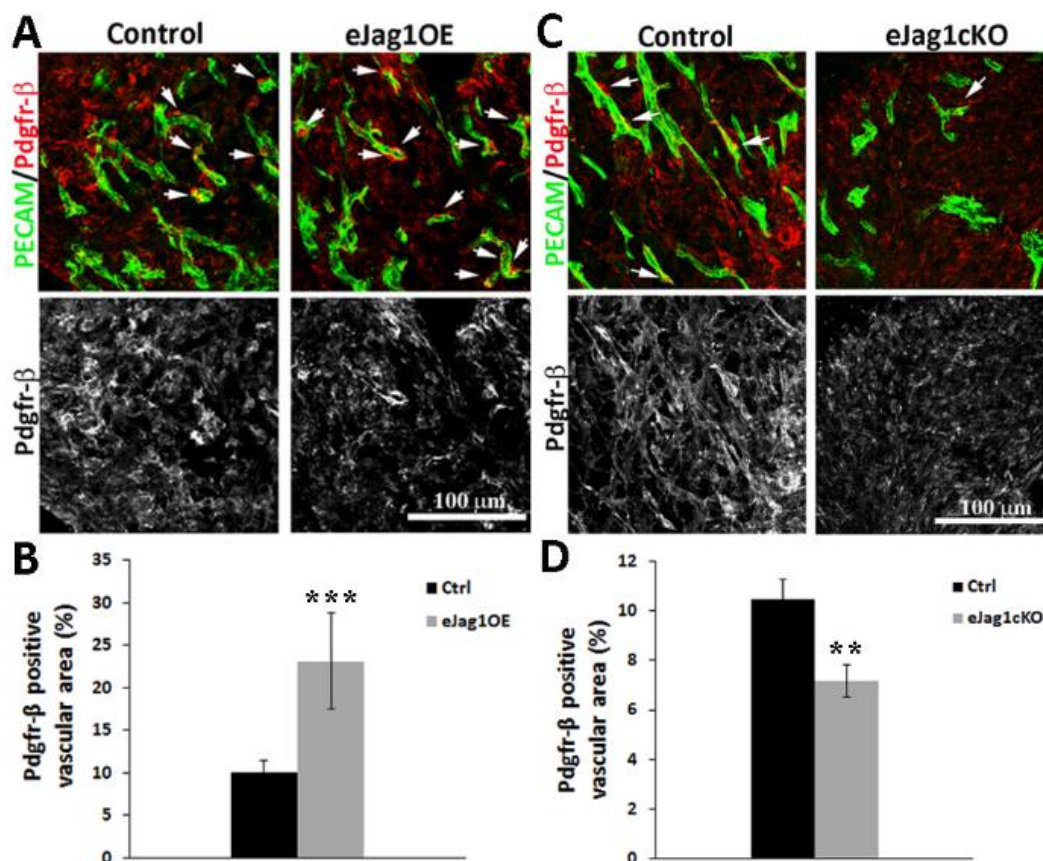
Figure I.2- Effect of endothelial *Jag1* loss of function in wound healing.



A, Progression of average wound size relative to day 0 in 2 mouse groups, *Jag1* loss-of-function mutants *eJag1cKO* (*Jag1lox/lox* Cre+) and controls (*Jag1lox/lox* Cre-). Loss of *Jag1* led to a decrease in the healing rate of dermic wounds, mutant mice showing an ≈ 2 -day delay in comparison with the control group (as demonstrated by the orange line). **B**, Immunostaining images ($\times 10$ amplification) marked for PECAM-1 (green) and SMA (red), to evaluate vascular density and vascular smooth muscle cell (vSMC)

coverage of samples collected at day 7. Continuous white line marks the base of epidermis and the space between dashed lines marks the angiogenic fronts. **C**, High-magnification ($\times 40$ amplification) confocal imaging, showing in detail the vascular phenotype observed in *eJag1*cKO mutants, consisting of decreased number of vessels and an almost complete absence of perivascular SMA⁺ cells. **D**, Percentage of vascular density (relative to controls=100%) showing that loss of endothelial *Jag1* expression led to decreased PECAM-1 labeling. **E**, Percentage of vSMC coverage, showing a lower SMA staining in the *eJag1*cKO vasculature. **F**, Lectin (red) and PECAM-1 (green) immunostaining ($\times 20$ amplification) of samples collected at end point, to evaluate the colocalization of both signals, indicative of vessel perfusion. **G**, Percentage of perfused area in the total vascular area (given by vascular density measurements) showing decreased lectin labeling in the endothelial *Jag1* loss-of-function vasculature. **H**, Evans' blue (red) and PECAM-1 (green) confocal immunostaining ($\times 20$ amplification) images showing the extravasation areas. **I**, Percentage of vascular extravasation area in the total vascular area, showing increased Evans' blue staining in the *eJag1*cKO mutants. 4',6-Diamidino-2-phenylindole (DAPI; blue) stains nuclei. Results are representative of 2 independent experiments, each with $n=5$ mice per group. Error bars represent SEM; * $P<0.05$; ** $P<0.01$; and *** $P<0.001$.

Supplemental Figure I.1- Immunostaining for Pdgfr- β in *eJag1*OE and *eJag1*cKO mutants.



A, and **C**, High-magnification confocal immunostaining images (40x amplification) of Pdgfr- β (red) and PECAM-1 (green) in *eJag1*OE (**A**) and *eJag1*cKO mutants (**C**) versus respective controls. **B**, and **D**, Percentage of Pdgfr- β -positive vascular area (relative to control; white arrows) showing increased and

decreased positive area in OE and KO mutants, respectively. Error bars represent SEM; * represents $p < 0.05$; ** represents $p < 0.01$; *** represents $p < 0.001$.

4.2 Regulation of angiogenic gene expression by Jagged1/Notch Signaling

To better understand the molecular mechanisms behind the vascular phenotypes observed in *eJag1OE* and *eJag1cKO* mutants, we performed quantitative reverse transcriptase polymerase chain reaction analysis of selected genes involved in angiogenesis (Figure I.3). RNA was extracted from EC (Lin⁻ (ter119-cd45⁻) cd31⁺) and mural cell (Lin⁻ (ter119-cd45⁻) cd146⁺) FACS sorted from wound samples collected at the experimental end point (i.e, day 7 of recovery; Figure I.3A). In ECs (Figure I.3B), *Jag1* transcript levels were largely increased (3-fold) in *eJag1OE* mutant samples and significantly reduced in *eJag1cKO* animals. In contrast, *Dll4* was upregulated in *eJag1cKO* and downregulated in *eJag1OE* mutants. Transcript levels for *Pdgfb* (encoding PDGF-B, the endothelial ligand for PDGFR β) and *Tek* (encoding the Tie2 receptor tyrosine kinase), which control the recruitment of perivascular cells and vascular permeability (Thomas & Augustin, 2009; Winkler, Bell, & Zlokovic, 2010), respectively, were downregulated in *eJag1cKO* mutants and increased in gain-of-function mutants. The same was the case for the mRNAs encoding VEGF receptor-2 (*Vegfr2/Kdr/Flk1*) and 3 (*Vegfr3/Flt4*) (Figure I.3B).

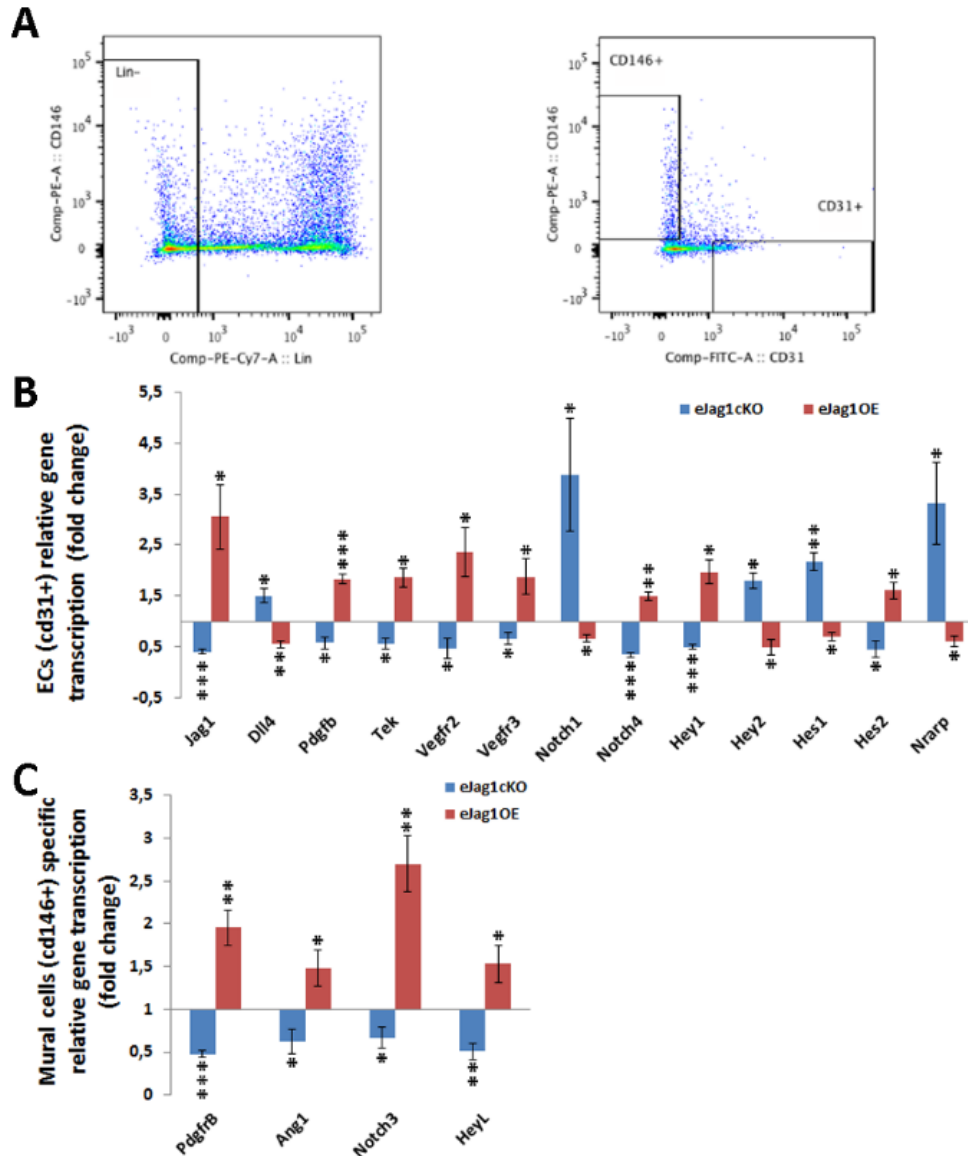
About known Notch effectors, we observed that *Hey2* and *Hes1* transcript levels were augmented in *eJag1cKO* samples and downregulated in *eJag1OE*. However, *Hey1* and *Hes2* were upregulated in *eJag1OE* and reduced in *eJag1cKO* wound ECs. *Nrarp*, a gene that is known to be rapidly upregulated in response to Dll4/Notch signaling, was strongly upregulated in the absence of endothelial *Jag1* and downregulated in the *Jag1* gain-of-function samples. The Notch receptor gene *Notch 4* was upregulated in *eJag1OE* wounds, whereas in *eJag1cKO* only *Notch1* was upregulated, and *Notch4* was robustly and significantly reduced.

Furthermore, mural cell-specific transcription analysis (Figure I.3C) revealed a downregulation of *PdgfrB* (encoding PDGFR β), *Ang1* (perivascular ligand for Tie2 receptor), *Notch3* receptor, and *HeyL* (perivascular cell notch effector) in *eJag1cKO* and an upregulation in *eJag1OE* mutants wounds.

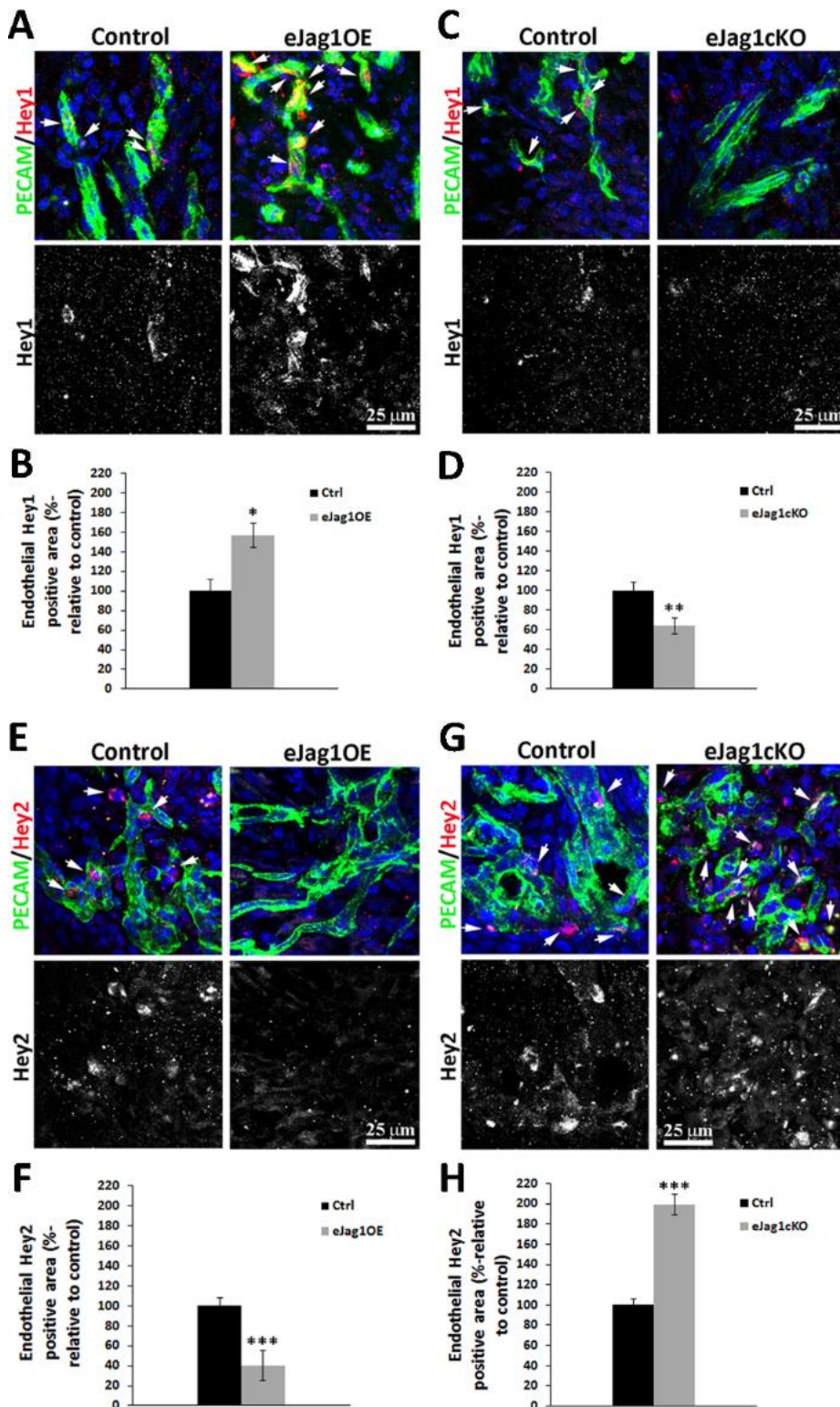
To obtain additional validation on the specific modulation of Notch effectors by endothelial Jagged1, immunofluorescence was performed for the main endothelial Notch effectors Hey1 and Hey2 (Figure I.4). Confirming the transcription results, it is clear from the quantification of double positive signal for the effectors with PECAM that in the *eJag1OE* wound vasculature there is increased Hey1 (Figure I.4A and I.4B) and decreased Hey2 (Figure I.4E and I.4F) levels. In contrast, *eJag1cKO* mutant vasculature presented decreased levels of Hey1 (Figure I.4C and I.4D) and increased levels of Hey2 effector (Figure I.4G and I.4H).

These results indicate that *Jag1* modulation in the endothelium is able to elicit changes in the expression profiles of Notch receptors and effectors as well as in genes controlling angiogenesis and the recruitment of mural cells.

Figure I.3- Gene expression analysis in *eJag1OE* and *eJag1cKO* mutants.



RNA was isolated from wound samples collected at the end point, and gene transcript analysis was performed by quantitative real-time reverse transcriptase polymerase chain reaction for genes involved in angiogenesis. **A**, Endothelial cell (ECs) (Lin⁻ (cd45⁻ ter119⁻) cd31⁺) and mural cells (Lin⁻ (cd45⁻ ter119⁻) cd146⁺ cd31⁻) sorted populations for specific gene transcription analysis. **B**, EC-specific relative gene transcription. **C**, Mural cell-specific relative gene transcription. Gene transcript levels were normalized to PECAM-1 mRNA levels, and the house-keeping gene β -actin was used as endogenous control. Blue bars represent the gene expression levels of samples collected from *eJag1cKO* mutants, and red bars the gene expression levels from *eJag1OE* mutants, relative to the respective controls. Error bars represent SEM; *P<0.05; **P<0.01; and ***P<0.001.

Figure I.4- Immunostaining for Hey1 and Hey2 in *eJag1OE* and *eJag1cKO* mutants.

A and **C**, High magnification confocal immunostaining images ($\times 40$ amplification) of Hey1 (red) and PECAM-1 (green) in *eJag1OE* (**A**) and *eJag1cKO* mutants (**C**) vs respective controls. **B** and **D**, Percentage of endothelial Hey1-positive area (relative to control= 100%; white arrows) showing increased and decreased positive area in OE and KO mutants endothelial cells (ECs), respectively. **E** and **G**, Confocal immunostaining images ($\times 40$ amplification) of Hey2 (red) and PECAM-1 (green) in *eJag1OE* (**E**) and *eJag1cKO* mutants (**G**) vs respective controls. **F** and **H**, Percentage of endothelial Hey2-positive area (relative to control=100%; white arrows) showing decreased and increased positive

area in OE and KO mutants ECs, respectively. 4',6-Diamidino-2-phenylindole (DAPI; blue) stains nuclei. Error bars represent SEM; * $P < 0.05$; ** $P < 0.01$; and *** $P < 0.001$.

4.3 Blocking Dll4 in endothelial *Jag1* knockout mice rescues angiogenesis but not mural cell coverage

The results obtained in the wound healing assays performed in *Jag1* mutants together with previous results from our laboratory describing a role for Dll4 in wound healing angiogenesis (Trindade et al., 2012) gave rise to the hypothesis that the loss of endothelial *Jag1* enables more robust Dll4/Notch signaling. In the absence of Jagged1, more Notch receptors would be left available to be activated by Dll4, which has a strong antiangiogenic function and might thereby cause a delay in wound healing (Trindade et al., 2012). Conversely, in *eJag1OE* animals, the pro-angiogenic phenotype might be associated with decreased Dll4/Notch signaling.

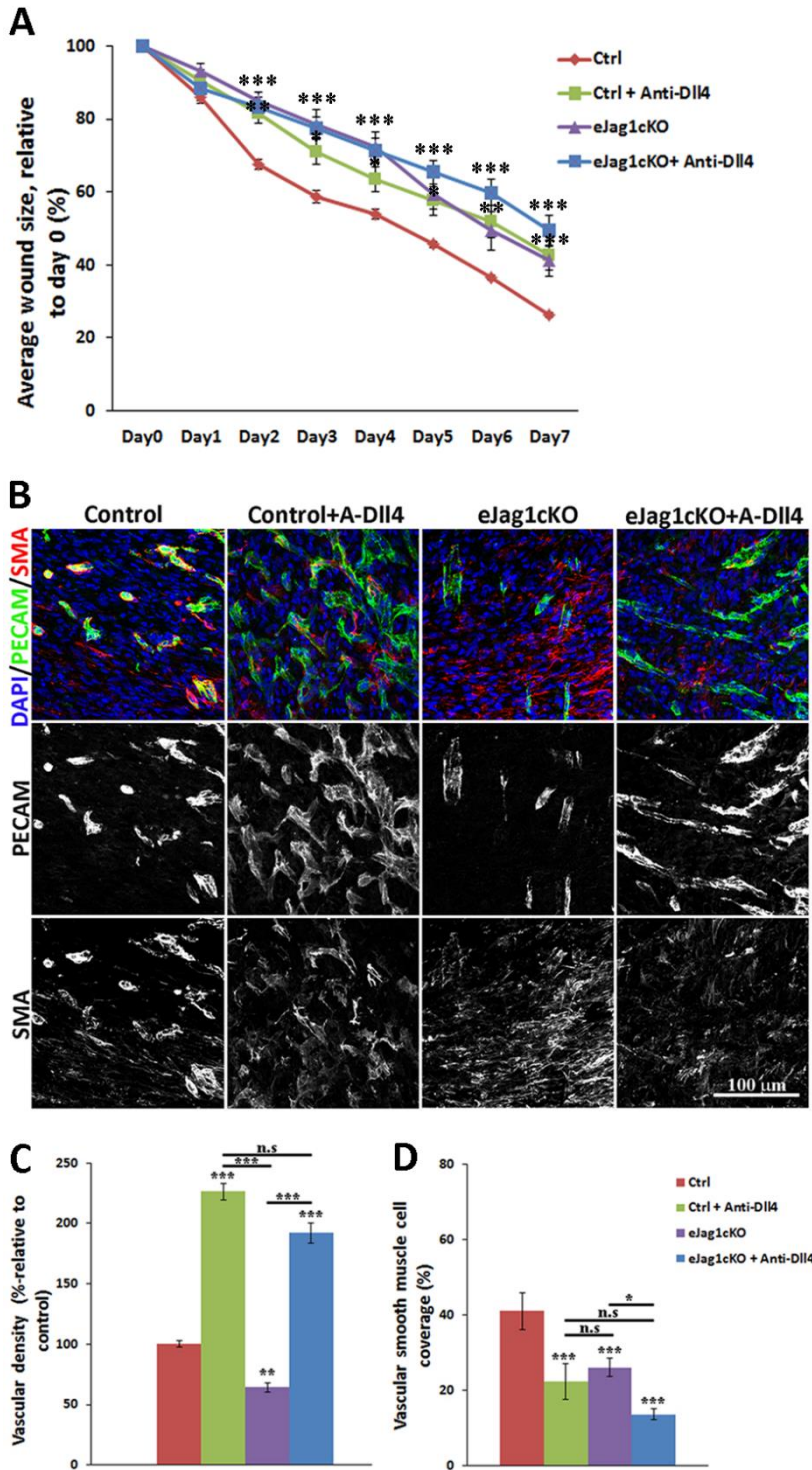
We therefore wanted to determine whether the *eJag1cKO* phenotype was mainly because of upregulation of Dll4/Notch signaling. We performed wound healing assays in *eJag1cKO* mutant mice treated with anti-Dll4 blocking antibody (anti-Dll4). As shown in Figure I.5, anti-Dll4 administration increased the angiogenic growth of the endothelium, in both control (control+anti-Dll4) and *eJag1cKO* (*eJag1cKO*+anti-Dll4) mouse groups but led to significantly delayed wound healing kinetics (Figure I.5A). Morphological and quantitative analysis of the wound vasculature (Figure I.5B) clearly showed an increase in the vascular density on antibody blockade of Dll4 (Figure I.5C). Strikingly, anti-Dll4 administration failed to rescue the defective mural cell (Figure I.5B and I.5D) and pericyte (Suppl. Figure I.2A and I.2B) coverage in *eJag1cKO* mutant mice. In fact, smooth muscle cell coverage showed a significant decrease on Dll4 blockade (Figure I.5B and I.5D) indicating that the reduced vascular maturation in *eJag1cKO* animals was further aggravated by treatment with anti-Dll4. Moreover, overall functionality of the newly formed vasculature was diminished by Dll4 blockade, as indicated by reduced perfusion (Suppl. Figure I.2C and I.2D) and increased leakiness (Suppl. Figure I.2E and I.2F). No evident anti-Dll4-induced effects were observed during the experimental period in tissues other than the skin vasculature (data not shown).

With regard to ECs and mural cell-specific gene expression (Suppl. Figure I.3), we observed downregulation of Notch-related genes both in extra control mouse group (control+anti-Dll4) as in *eJag1cKO* (*eJag1cKO*+Anti-Dll4) mouse groups treated with anti-Dll4 antibody. Administration of anti-Dll4 to *eJag1cKO* mutants reverted the upregulation of *Dll4*, *Notch1*, *Hey2*, *Hes1*, and *Nrarp* observed previously in these mutant mice (Suppl. Figure I.3A). Also, as expected, blockade of Dll4 alone (control+anti-Dll4) led to a downregulation of *Jag1* transcript levels, confirming the previously obtained results indicating that *Jag1* expression was downstream of Dll4/Notch signaling (Trindade et al., 2012). In addition, we observed a

downregulation response in the transcription of mural cell-specific genes (Suppl. Figure I.3B) in all analyzed mouse groups.

In summary, these observations indicate that *Jag1* and *Dll4* have opposing effects on regenerative angiogenesis in the adult organism. However, the data suggest a synergistic function of the 2 ligands in vessel maturation and perivascular cell recruitment to nascent vessels.

Figure I.5- Endothelial *Jag1* loss of function combined with administration of anti-Dll4 antibody in wound healing assay.



A, Progression of average wound size relative to day 0 in 4 mouse groups: controls (*Jag1lox/lox Cre*⁻), control treated with anti-Dll4 antibody (control+A-Dll4), *Jag1* loss-of-function mutants (*eJag1cKO Jag1lox/lox Cre*⁺), and *eJag1cKO* treated with anti-Dll4 antibody (*eJag1cKO+A-Dll4*).

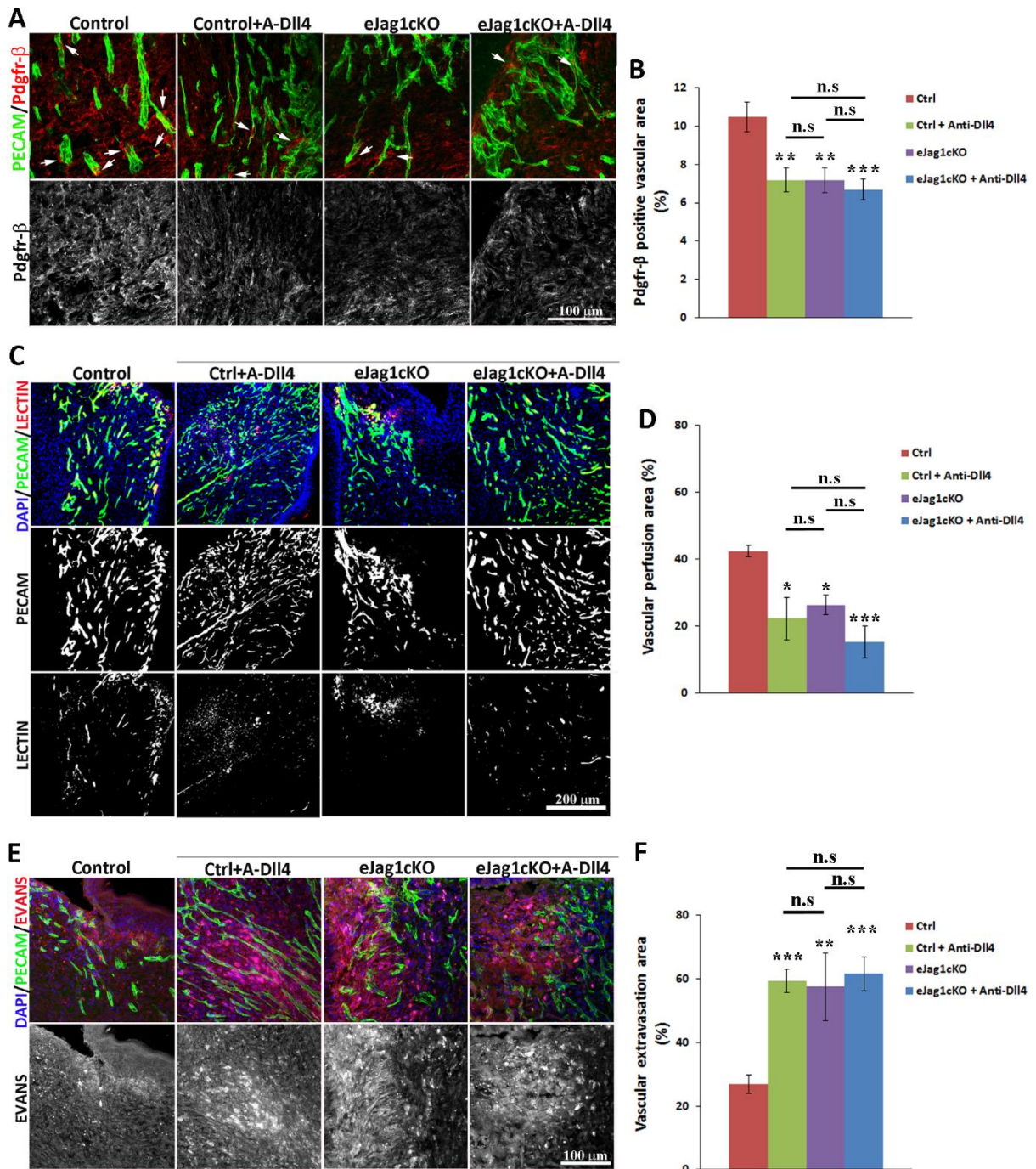
B, Confocal immunostaining images (×40 amplification) marked for PECAM-1 (green) and SMA (red), to evaluate vascular density and vascular smooth muscle cell (vSMC) of samples collected at day 7.

C, Percentage of vascular density (relative to control=100%) showing that the administration of anti-Dll4 either to control (ctrl+A-Dll4) or to *eJag1cKO*

(*eJag1cKO+A-Dll4*) mice led to an increase in vascular density. **D**, Percentage of vSMC coverage demonstrating that anti-Dll4 administration decreased the SMA+ perivascular coverage

of control (ctrl+A-DII4) mice and caused an even more pronounced decrease in *eJag1*KO mutants treated (e*Jag1*KO+A-DII4). 4',6-Diamidino-2-phenylindole (DAPI; blue) stains nuclei. Results are representative of 2 independent experiments, with n=5 in the control group, n=5 (e*Jag1*KO), and n=4 in each anti-DII4- treated group. Error bars represent SEM; **P*<0.05; ***P*<0.01; and ****P*<0.001.

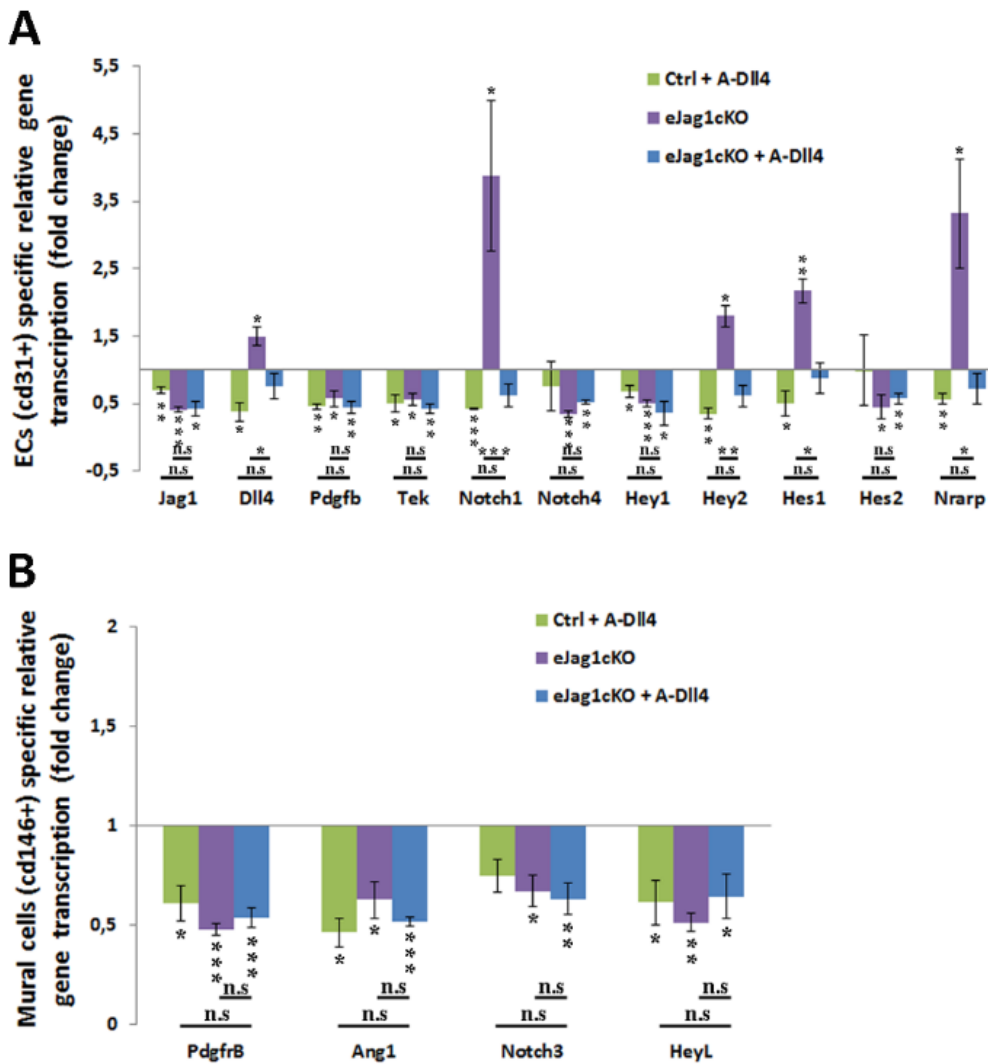
Supplemental Figure I.2- Pericyte vascular coverage, vascular perfusion and extravasation analyses in wound samples from endothelial *Jag1* loss-of-function mice treated with Anti-DII4 antibody.



A, Pdgfr-β (red) and PECAM-1 (green) confocal immunostaining images (40x amplification) of samples collected at end-point, in four mouse groups: controls (*Jag1*lox/lox Cre-), control treated with Anti-DII4

antibody (Control+A-Dll4), Jag1 loss-of-function mutants (*eJag1cKO -Jag1lox/lox Cre+*), and *eJag1cKO* treated with Anti-Dll4 antibody (*eJag1cKO+A-Dll4*). White arrows indicate positive Pdgfr- β cells along the vascular wall. **B**, Percentage of Pdgfr- β -positive vascular area showing decreased positive area in all mouse groups, relative to control. **C**, Lectin (red) and PECAM (green) immunostaining (20x amplification), the co-localization of which indicates the level of vessel perfusion. **D**, Percentage of perfused vessels in the vascular area (given by vascular density measurements) showing a decrease in vascular functionality in all mouse groups. **E**, Evans' Blue (red) and PECAM-1 (green) confocal immunostaining images (20x amplification) showing the extravasation areas. **F**, Percentage of vascular extravasation area in the total vascular area, showing increased vascular leakage in all mouse groups. Results are representative of 2 independent experiments, with n=5 in the control group and in *eJag1cKO*, n=4 in each Anti-Dll4 mouse group. Error bars represent SEM; * represents p<0.05; ** represents p<0.01; *** represents p<0.001.

Supplemental Figure I.3- Gene expression analyses in *eJag1cKO* treated with Anti-Dll4 antibody.



RNA was isolated from wound samples collected at the end-point, and gene transcription analysis was performed by quantitative real-time RT-PCR for genes involved in Notch signaling. **A**, ECs (Lin- (cd45-ter119-) cd31+) sorted population relative gene transcription. **B**, Mural cells (Lin- (cd45-ter119-) cd146+

cd31-) sorted population relative gene transcription. Gene transcript levels were normalized to PECAM-1 mRNA levels, and the house-keeping gene β -actin was used as endogenous control. Green bars represent the relative gene expression of the samples collected from control mice treated with Anti-Dll4 (ctrl +A-Dll4), the purple bars represent the relative gene expression levels from *eJag1*KO mutants (previously shown in figure I.3), and the blue bars represent the relative gene expression from *eJag1*KO mutants treated with Anti-Dll4 (*eJag1*cKO + A-Dll4) relative to the control group. Error bars represent SEM; * represents $p < 0.05$; ** represents $p < 0.01$; *** represents $p < 0.001$.

4.4 Vascular maturation in endothelial-specific Dll4 gain-of-function or conditional overexpression mice is impaired by Jagged1 blockade

The results described to date show that Dll4 inhibition in *eJag1*cKO mice further diminishes the mural cell coverage of the vascular plexus formed during wound healing. Previous work done by our group has established that endothelial-specific overexpression of Dll4 (endothelial-specific Dll4 gain-of-function or conditional overexpression [*eDll4*OE]) induces an increase in vSMC coverage of the vasculature (Trindade et al., 2012). To better understand the interaction between Dll4 and Jagged1 signaling in the vessel maturation process, we treated *eDll4*OE mutants with an anti-Jagged1 blocking antibody and analyzed the effect of this inhibition on wound healing.

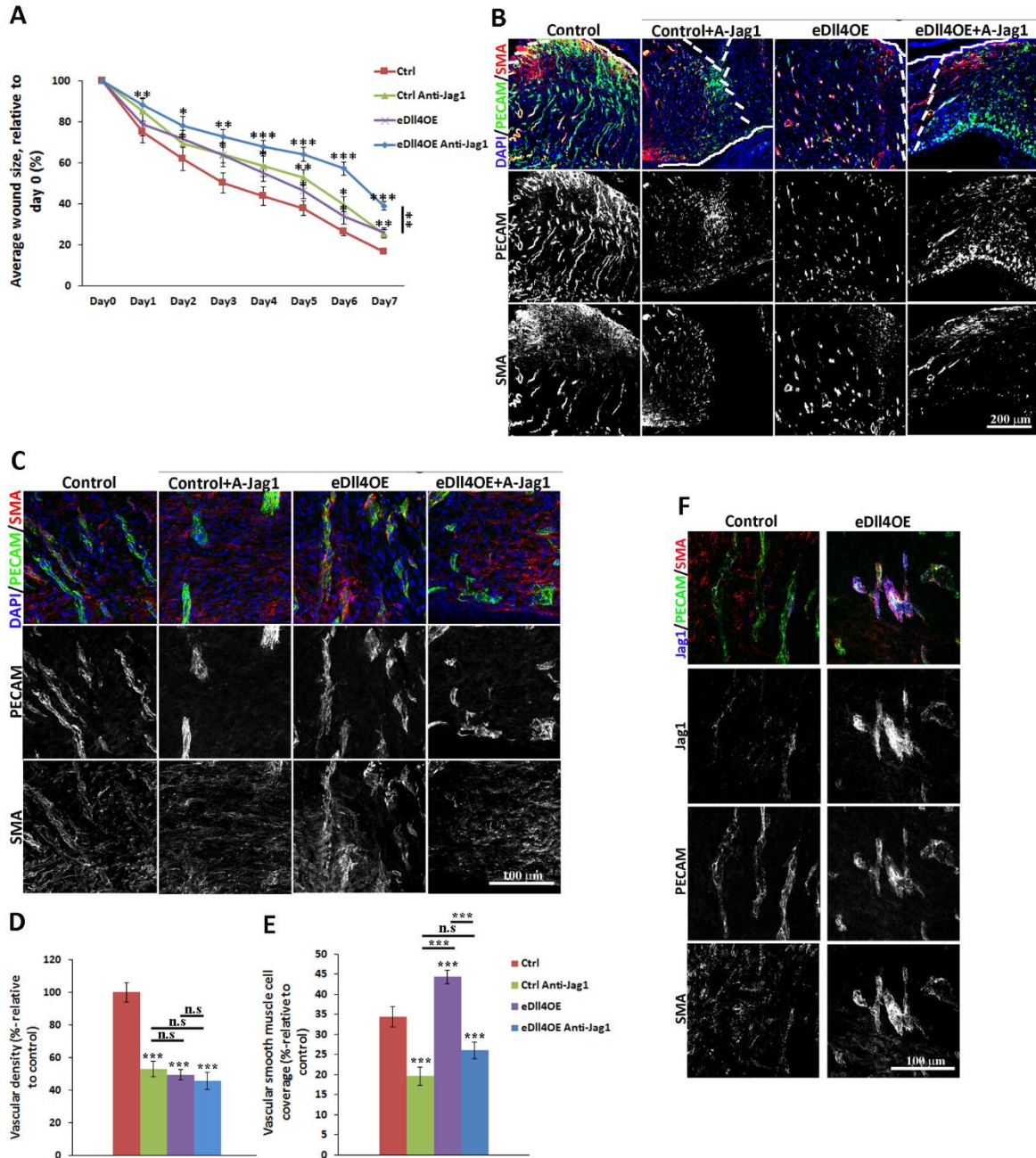
In accordance with our previous study (Trindade et al., 2012), Dll4 overexpression in the endothelium led to a significant delay in wound closure relative to controls (Figure I.6A). This reduction in the healing ability was phenocopied by Jagged1 inhibition in control animals (control+ Anti-Jag1), which argued further for opposing roles of *Dll4* and *Jag1*. In addition, treatment of *eDll4*OE mutants with anti-Jagged1 antibody severely impaired tissue regeneration suggesting that inhibition of Jagged1 further hampers growth and function of the dermal vasculature. No evident anti-Jag1-induced effects were observed during the experimental period in tissues other than the vasculature (data not shown).

Microscopical analysis of the vasculature at high magnification revealed that both Dll4 overexpression and Jagged1 inhibition were able to induce a significant decrease in the vascular density of the granulation tissue. This effect was most pronounced after Jagged1 inhibition in *eDll4*OE mutant mice (Figure I.6B–D), which suggested that Dll4 overexpression and Jagged1 blockade have additive antiangiogenic effects.

Moreover, *eDll4*OE mutant vasculature displayed a high ratio of coverage by SMA+ cells (Figure I.6B and I.6C) and pericytes (Suppl. Figure I.4A and I.4B), despite the reduced vascular density observed. Conversely, Jagged1 antibody inhibition significantly reduced the proportion of vessels covered by vSMCs (Figure I.6E) and pericytes (Suppl. Figure I.4A and I.4B) in both controls and *eDll4*OE animals. These results argue that Jagged1-mediated signaling is indispensable for the proper mural cell recruitment and sustainment of SMC and pericyte coverage during adult physiological angiogenesis. Moreover, the observed loss of maturation

may be responsible for the diminished vascular perfusion and increased extravasation in animals treated with Jagged1 blocking antibody (Suppl. Figure I.4C–F).

Figure I.6- Endothelial-specific Dll4 overexpression combined with administration of anti-Jagged1 antibody in wound healing assay.



A, Progression of average wound size relative to day 0 in 4 mouse groups: control, control treated with anti-Jagged1 antibody (control+A-Jag1), endothelial-specific Dll4 overexpression (*eDll4OE*), and *eDll4OE* treated with anti-Jagged1 antibody (*eDll4OE*+A-Jag1). **B**, Immunostaining images ($\times 20$ amplification) for PECAM-1 (green) and SMA (red), used to evaluate vascular density and perivascular coverage of samples collected at day 7. Continuous white line marks the base of epidermis and dashed lines mark the angiogenic fronts. **C**, Confocal immunostaining images ($\times 40$ amplification) showing the perivascular phenotype in detail; control mice treated with anti-Jagged1 antibody have consistently less

vessels, as seen by PECAM-1+ signal, and an almost complete absence of SMA staining associated with the vessel wall; note that *eDII4OE* mutant vessels seem to be enlarged because of the high number of SMA+ cells associated with the vessel wall. In *eDII4OE* mutants treated with anti-Jagged1 antibody, wound vessels are thinner than in *eDII4OE* and control mice, with less SMA+ perivascular cells. **D**, Percentage of vascular density (relative to control=100%) showing decreased PECAM-1 staining in all groups compared with the controls. **E**, Percentage of vascular smooth muscle cell coverage, showing PECAM-1/SMA+ signal is highly increased in *eDII4OE* mutants; this phenotype is strongly reversed by blocking Jagged1 signaling, both in control and in mutant animals. **F**, High magnification (×40 amplification) confocal imaging of Jagged1 staining in the vessels of *eDII4OE* mutants, showing strong Jagged1 levels in vessels with higher SMA+ coverage compared with the control. 4',6-Diamidino-2-phenylindole (DAPI; blue) stains nuclei. Results are representative of 1 experiment, with n=7 in the control and *eDII4OE* groups and n=8 in the control and *eDII4OE* treated with anti-Jagged1 antibody groups. Error bars represent SEM; **P*<0.05; ***P*<0.01; and ****P*<0.001.

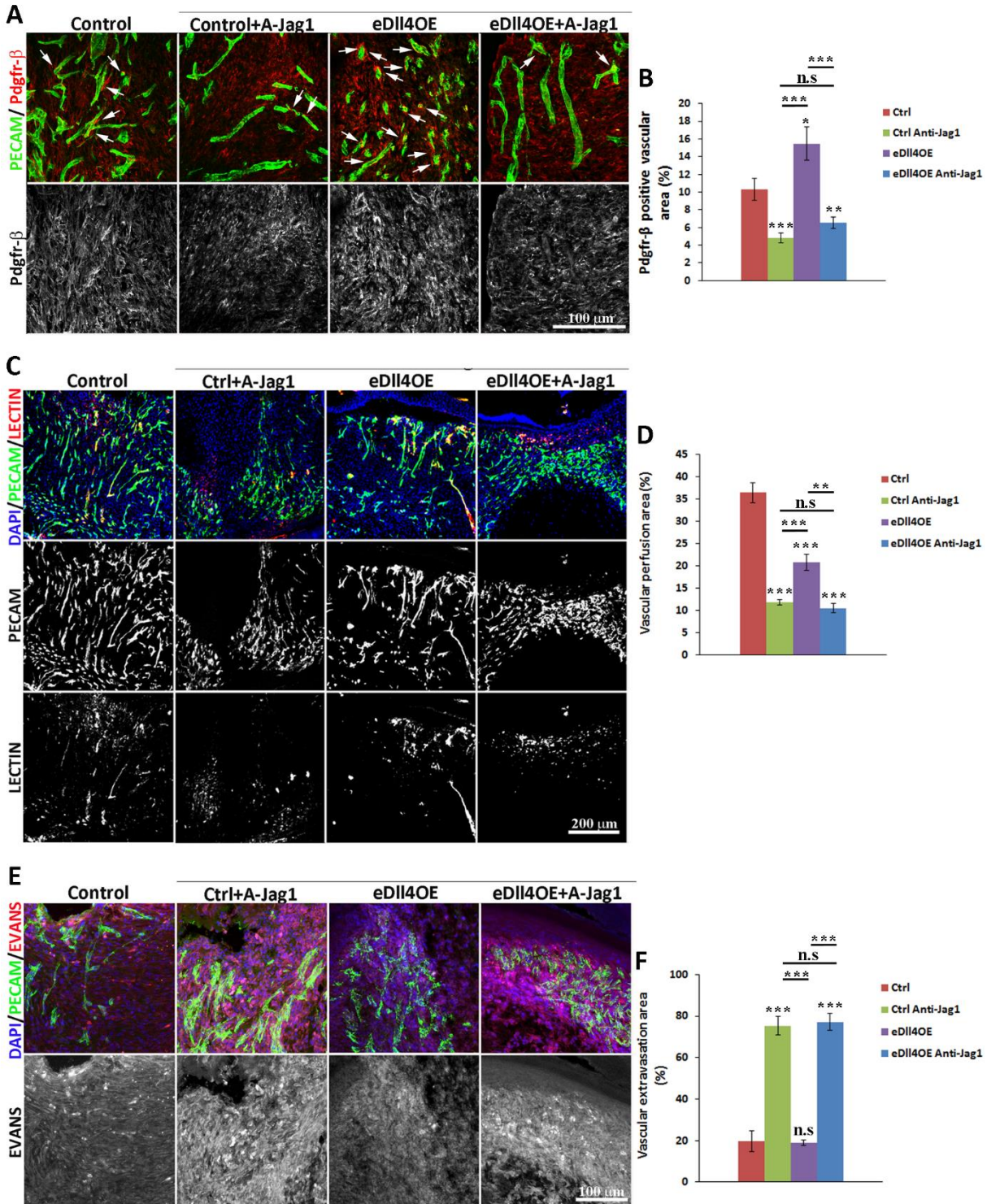
Transcription analysis revealed that inhibition of Jagged1 in *eDII4OE* mutants reverted the upregulation of *Jag1*, *Pdgfb*, *Tek*, *Notch4*, and *Hey1* (Suppl. Figure I.5A), and of *Pdgfr-β*, *Ang-1*, *Notch3*, and *HeyL* (Suppl. Figure I.5B), that was observed in these animals. This suggests that the transcription of these genes is directly regulated by Jagged1. Conversely, inhibition of Jagged1 in *eDII4OE* mutants (*eDII4OE*+anti-*Jag1*) maintained the upregulation of *DII4*, *Notch1*, *Hey2*, and *Nrarp* genes (Suppl. Figure I.5A).

In line with previous findings suggesting that *Jag1* expression is positively regulated by DII4 (Trindade et al., 2012) and with the observed Jagged1 upregulation (Suppl. Figure I.5A), immunostaining for Jagged1 in *eDII4OE* mutant vasculature showed much greater intensity in comparison with controls (Figure I.6F). This suggests that Jagged1 is a downstream effector of DII4/Notch signaling in the endothelium.

4.5 Endothelial Jagged1 activates Notch3 receptor in perivascular cells and Notch4 in ECs

It has been proposed that Jagged1 signals through Notch3 in perivascular cells (Liu et al., 2009). To confirm this, we immunostained the intracellular domain of Notch3 (N3ICD) in the wound samples from mutants that presented increased recruitment of mural cells: *eJag1OE* and *eDII4OE*. Endothelial *Jag1* overexpression mutants presented increased perivascular N3ICD positive staining compared with the respective controls (Suppl. Figure I.6A and B), measured as double positive staining for SMA and N3ICD. Conversely, administration of anti-Jagged1 to control animals (control+anti-*Jag1*) led to decreased N3ICD positive staining, whereas *eDII4OE* mutants presented increased staining (Suppl. Figure I.6C and D). Predictably, blocking Jagged1 in *eDII4OE* (*eDII4OE*+anti-*Jag1*) reversed the increased staining observed in the mutants, bringing N3ICD to levels comparable with control animals (Suppl. Figure I.6C and D).

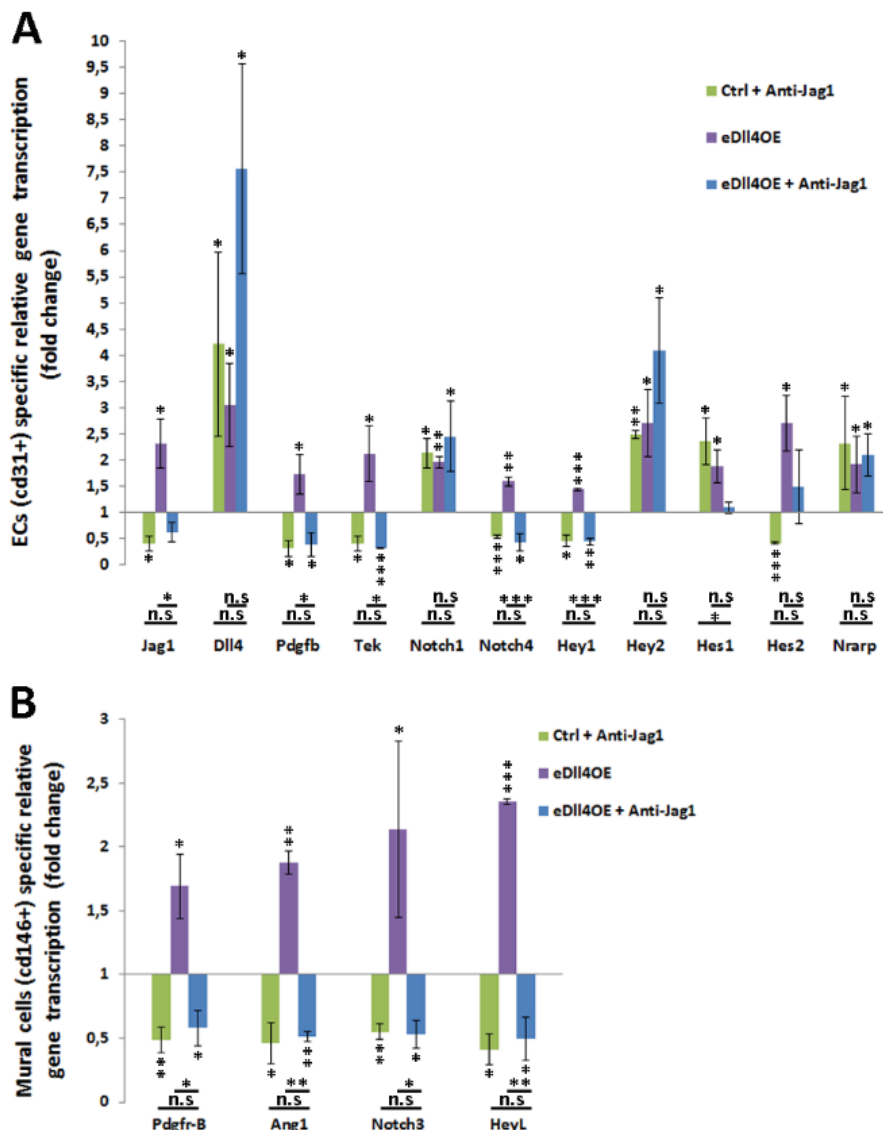
Supplemental Figure I.4- Pericyte vascular coverage, vascular perfusion and extravasation analyses in wound samples from endothelial-specific *Dll4* over-expression mutant mice treated with Anti-Jagged1 antibody.



A, Pdgfr-β (red) and PECAM-1 (green) confocal immunostaining images (40x amplification) of samples collected at end-point, in five mouse groups: control, control treated with Anti-Jagged1 (Ctrl+Anti-Jag1), *eDII4OE* and *eDII4OE* treated with Anti-Jagged1 (*eDII4OE*+Anti-Jag1). **B**, Percentage of Pdgfr-β positive vascular area showing decreased positive area in Ctrl+Anti-Jag1 and *eDII4OE*+Anti-Jag1 mouse groups, but increased area in *eDII4OE* mutants, relative to control. **C**, Lectin (red) and PECAM (green) immunostaining (20x amplification) of samples collected at end-point, indicative of vessel

perfusion levels. **D**, Percentage of perfused vessels in the total vascular area (given by vascular density measurements); vascular functionality is decreased in the groups treated with Anti-Jagged1. **E**, Evans' Blue (red) and PECAM (green) confocal immunostaining images (20x amplification) showing the extravasation areas. **F**, Percentage of vascular extravasation area of the total vascular area showing that Anti-Jagged1-treated mice have much higher extravasation levels than the respective controls. Results are representative of 2 independent experiments, with n=3+2 in the control and *eDII4OE* groups and n=4+3 in the control and *eDII4OE* treated with Anti-Jagged1 groups. Error bars represent SEM; * represents p<0.05; ** represents p<0.01; *** represents p<0.001.

Supplemental Figure I.5- Gene expression analyses in *eDII4OE* treated with Anti-DII4 antibody.



RNA was isolated from wound samples collected at the end-point, and gene transcription analysis was performed by quantitative real-time RT-PCR for genes involved in Notch signaling. **A**, ECs (Lin- (cd45- ter119-) cd31+) sorted population relative gene transcription. **B**, Mural cells (Lin- (cd45- ter119-) cd146+ cd31-) sorted population relative gene transcription. Gene transcript levels were normalized to PECAM-1 mRNA levels, and the house-keeping gene β -actin was used as endogenous control. Green bars

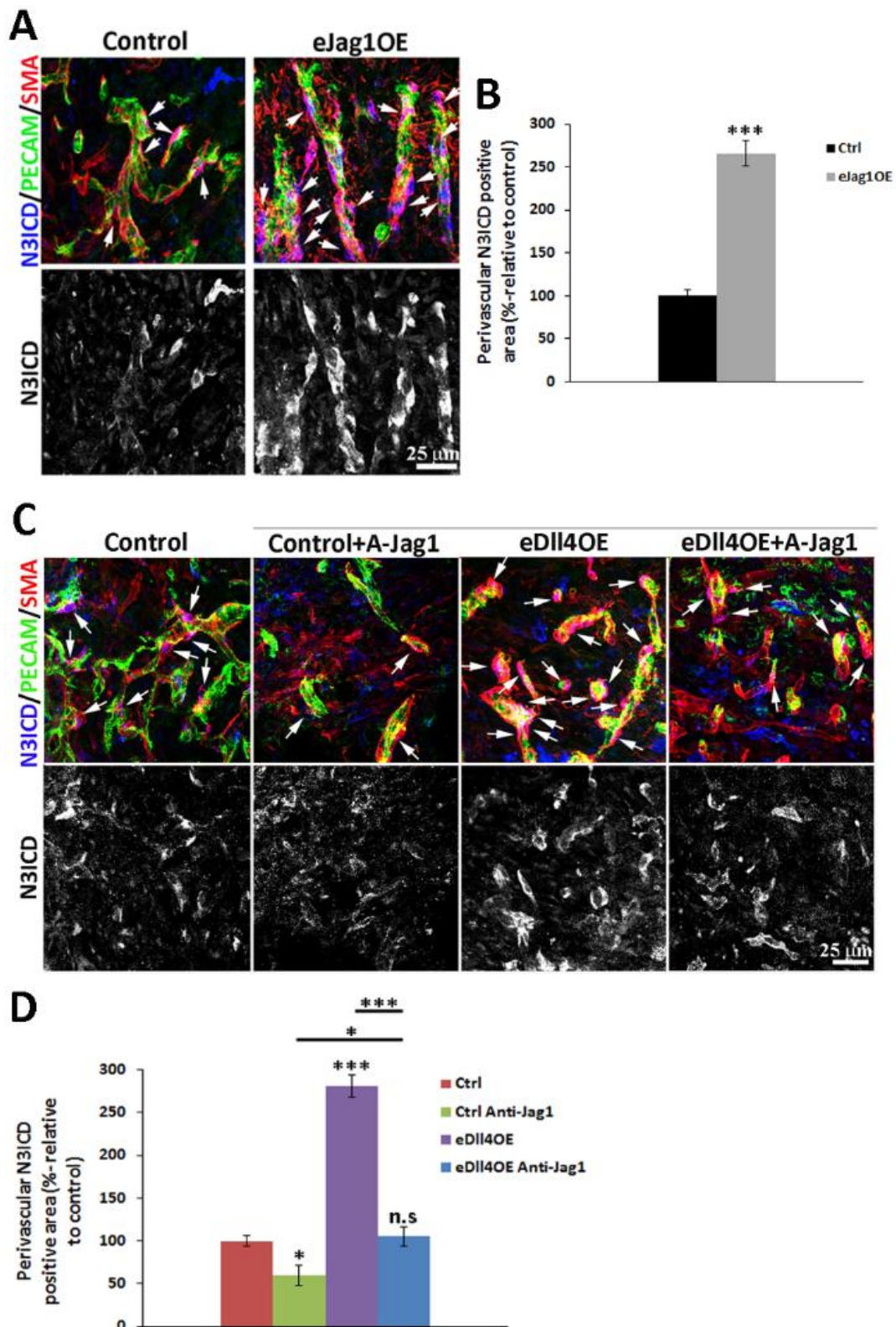
represent the relative gene expression of the samples collected from control mice treated with Anti-Jagged1 (ctrl +A-Jag1), the purple bars represent the relative gene expression levels from *eDII4OE* mutants and the blue bars represent the relative gene expression from *eDII4OE* mutants treated with Anti-Jagged1 (*eDII4OE* + A-Jag1) relative to the control group. Error bars represent SEM; * represents $p < 0.05$; ** represents $p < 0.01$; *** represents $p < 0.001$.

Despite the evidence for the ability of Jagged1 to activate perivascular Notch3, the endothelial Notch receptor(s) for Jagged1 remained unknown. Both Notch1 and Notch4 are prominently expressed in ECs (Villa et al., 2001), therefore to better understand the downstream signaling elicited by endothelial Jagged1, immunofluorescence staining for the intracellular domains of Notch1 (N1ICD) and Notch4 (N4ICD) was performed in wound samples from *eJag1* mutants (Figure I.7). *Jag1* overexpression led to a significant decrease in the amount of PECAM-1+ vessels showing activation of Notch1 (double positive N1ICD/PECAM-1 vessels; Figure I.7A and I.7B). The opposite effect was seen in *eJag1cKO* mutants where the proportion of N1ICD+ vessels was increased relative to controls (Figure I.7E and I.7F). Surprisingly, levels of activated Notch4 (N4ICD) were increased in *eJag1OE* mutants (Figure I.7C and D), whereas conditional deletion of *Jag1* in the endothelium was associated with a decrease in the colocalization of N4ICD and PECAM-1 staining (Figure I.7G and H).

We also quantified endothelial N1ICD in *eJag1cKO* animals treated with anti-DII4 and N4ICD in *eDII4OE* mutants treated with anti-Jagged1 (Suppl. Figure I.7). Anti-DII4 administration reversed the increase of ECs with cleaved (active) Notch1 in *eJag1cKO* samples (Suppl. Figure I.7A and B). Likewise, anti-Jagged1 administration significantly reduced the N4ICD-positive area in the *eDII4OE* endothelium (Suppl. Figure I.7C and D). Moreover, anti-DII4 administered either to control (control+anti-DII4) or *eJag1cKO* (*eJag1cKO*+anti-DII4) mouse groups also led to reduced levels of active endothelial Notch4 (Suppl. Figure I.8A and B). In the same manner, administration of anti-Jagged1 either to control (control+anti-Jag1) or *eDII4OE* (*eDII4OE*+anti-Jag1) mouse groups also showed a sustained increase in active endothelial Notch1 (Suppl. Figure I.8C and D).

These results argue that Jagged1 is able to trigger Notch4 receptor activation in ECs, whereas the receptor Notch1 seems to be preferentially activated by DII4.

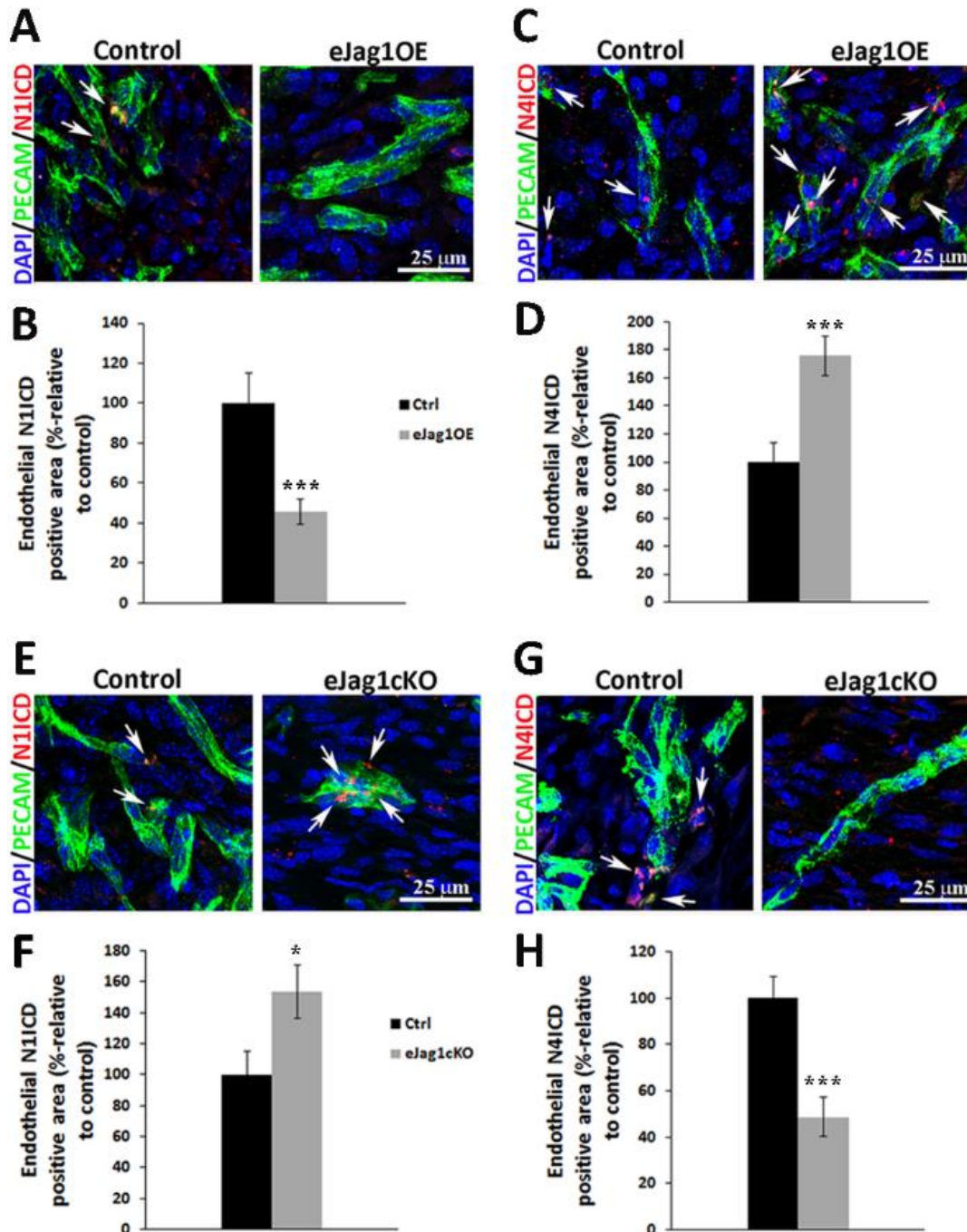
Supplemental Figure I.6- Immunostaining for Notch3 intra-cellular domain (N3ICD) in wound tissues of *eJag1OE* and Anti-Jag1-treated *eDII4OE* mutants.



A and **C**, Confocal immunostaining images (40x amplification) of PECAM (green), SMA (red) and N3ICD (blue) in *eJag1OE* mutants and Anti-Jagged1-treated *eDII4OE* mutants, respectively; co-staining (pink colour) labels the localization of cleaved Notch3 in perivascular cells (white arrows). **B**, Percentage of perivascular N3ICD-positive area (relative to control=100%) is increased in *eJag1OE* animals relative

to controls. **D**, Percentage of perivascular N4ICD-positive area (relative to control=100%); N4ICD is decreased in Ctrl+A-Jag1 while highly increased in *eDII4OE* mutants. Error bars represent SEM; * represents $p < 0.05$; ** represents $p < 0.01$; *** represents $p < 0.001$.

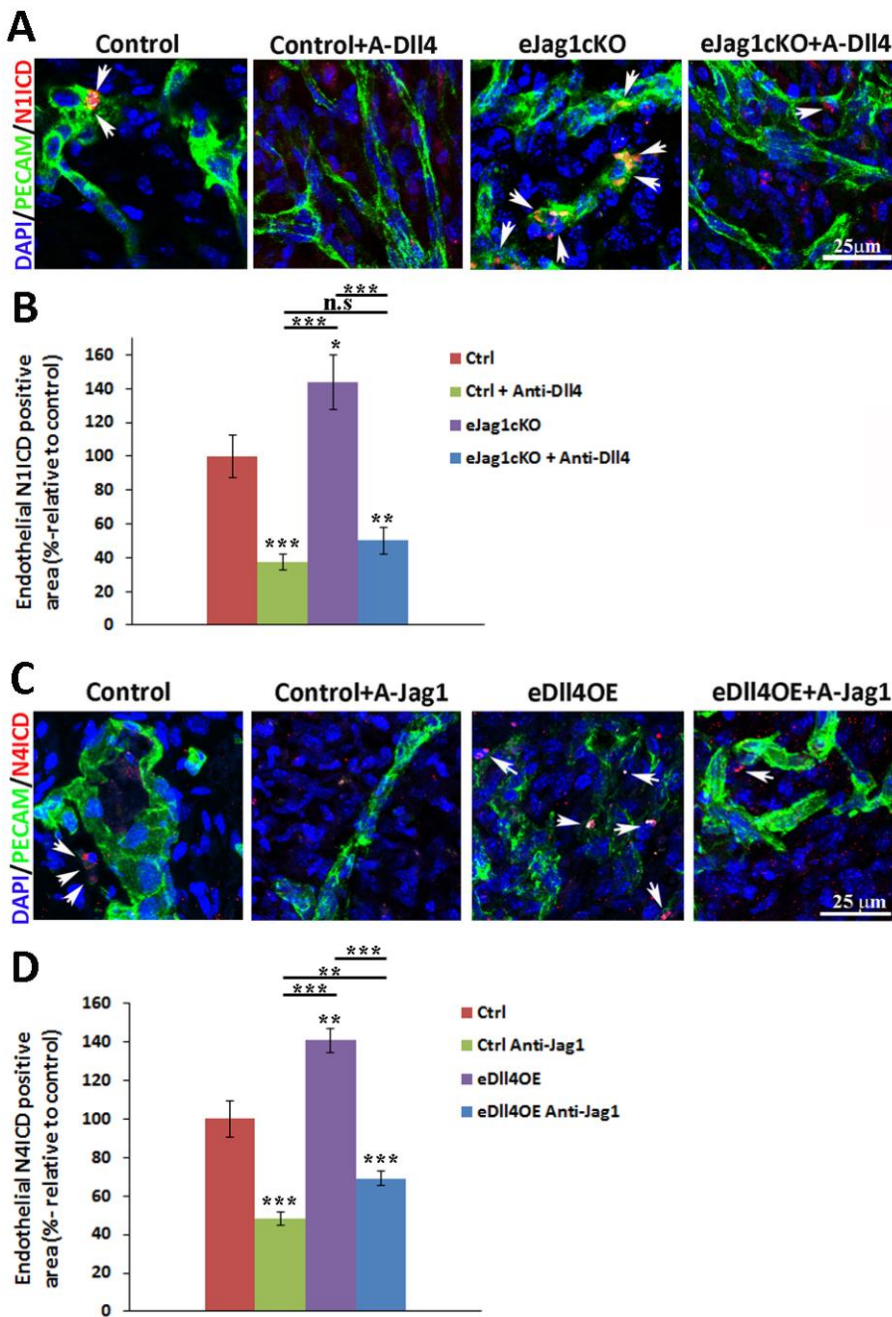
Figure I.7- Immunostaining of Notch1 and Notch4 intracellular domains (N1ICD and N4ICD) in *eJag1OE* and *eJag1cKO* mutants.



A and **C**, Highmagnification confocal immunostaining images ($\times 40$ amplification) of *eJag1OE* mutants vs controls, marked for PECAM-1 (green) and N1ICD (red) on the **left**, and PECAM-1 (green) and N4ICD (red) on the **right**, respectively. **B**, Percentage of endothelial N1ICD-positive area (relative to control=100%; white arrows) showing decreased N1ICD in mutants endothelial cells (ECs). **D**, Percentage of endothelial N4ICD-positive area (relative to control=100%) showing increased N4ICD in

mutant ECs. **E** and **G**, Confocal immunostaining images ($\times 40$ amplification) of *eJag1cKO* mutants vs controls, labeled for PECAM-1 (green) and N1ICD (red) on the **left**, and PECAM-1 (green) and N4ICD (red) on the right. **F**, Percentage of endothelial N1ICD-positive area (relative to control=100%), demonstrating increased N1ICD in mutant ECs. **H**, Percentage of endothelial N4ICD positive area (relative to control, 100%), showing the decreased colocalization of N4 activated form with ECs (white arrows) in the mutants. 4',6-Diamidino-2-phenylindole (DAPI; blue) stains nuclei. Error bars represent SEM; * $P < 0.05$; ** $P < 0.01$; and *** $P < 0.001$.

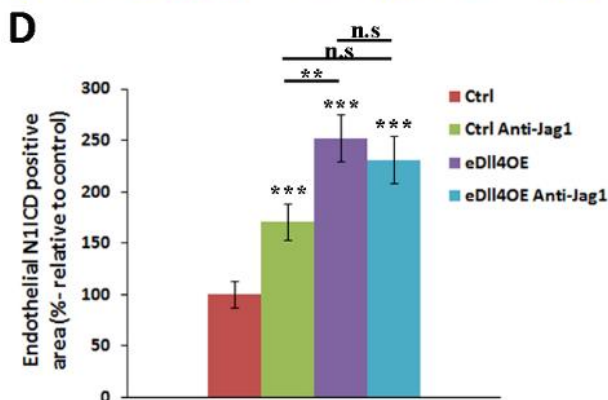
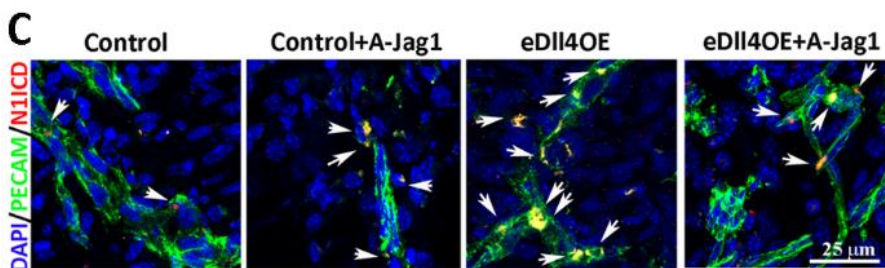
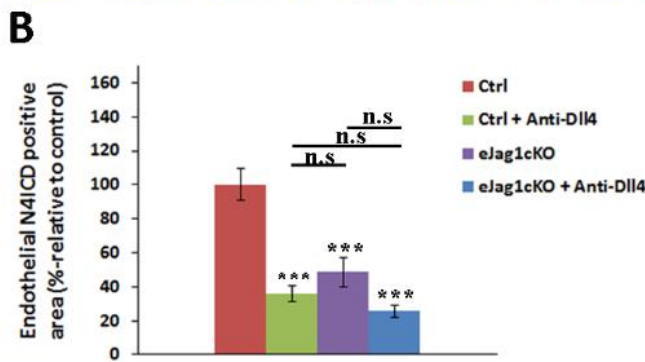
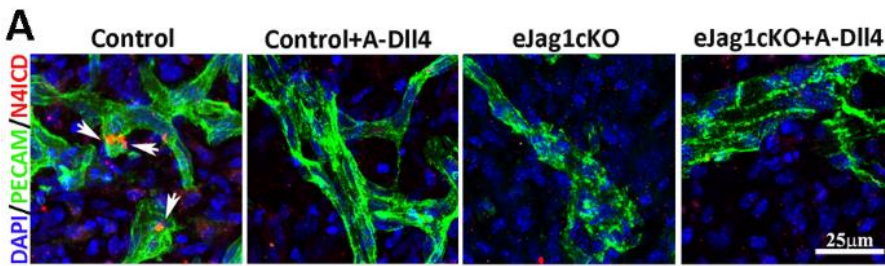
Supplemental Figure I.7- Immunostaining of Notch1 and Notch4 intra-cellular domains (N1ICD and N4ICD) in wound tissues of Anti-Dll4-treated *eJag1cKO* and Anti-Jag1-treated *eDll4OE* mutants.



A, Confocal immunostaining images (40x amplification) of four mice groups: controls (Control-*Jag1lox/lox* Cre-), control treated with anti-Dll4 antibody (Control+A-Dll4), *Jag1* loss-of-function mutants (*eJag1cKO*-*Jag1lox/lox* Cre+), and *eJag1cKO* treated with anti-Dll4 antibody (*eJag1cKO*+A-Dll4); PECAM-1 (green) and N1ICD (red) co-staining labels the localization of cleaved Notch1 in endothelial cells (white arrows). **B**, Percentage of endothelial N1ICD-positive area (relative to control=100%); All mouse groups present decreased active endothelial Notch1 receptor. **C**, Confocal immunostaining images (40x amplification) of wound tissue sections from four different groups of

animals: controls, control animals treated with Anti-Jagged1 (Control+A-Jag1), eDII4OE mutants (eDII4OE) and eDII4OE mutants treated with Anti-Jagged1 (eDII4OE+A-Jag1); the co-localization of PECAM (green) and N1ICD (red) indicates the presence of N1ICD in endothelial cells ECs (white arrows). **D**, Percentage of endothelial N1ICD-positive area (relative to control-100%); N1ICD is highly increased in all mouse groups. DAPI (blue) stains nuclei. Error bars represent SEM; * represents $p < 0.05$; ** represents $p < 0.01$; *** represents $p < 0.001$.

Supplemental Figure I.8- Immunostaining for Notch4 and Notch1 intra-cellular domains (N4ICD and N1ICD) in wound tissues of Anti-DII4 treated eJag1cKO and Anti-Jag1-treated eDII4OE mutants, respectively.



A, Confocal immunostaining images (40x amplification) of four mice groups: controls (Control-*Jag1^{lox/lox}* Cre-), control treated with anti-DII4 antibody (Control+A-DII4), Jag1 loss-of-function mutants (*eJag1cKO*-*Jag1^{lox/lox}* Cre+), and *eJag1cKO* treated with anti-DII4 antibody (*eJag1cKO*+A-DII4); PECAM-1 (green) and N4ICD (red) co-staining labels the localization of cleaved Notch4 in endothelial cells (white arrows). **B**, Percentage of endothelial N4ICD-positive area (relative to control=100%); All mouse groups present decreased active endothelial Notch4 receptor. **C**, Confocal immunostaining images

(40x amplification) of wound tissue sections from four different groups of animals: controls, control

animals treated with Anti-Jagged1 (Control+A-Jag1), *eDII4OE* mutants (*eDII4OE*) and *eDII4OE* mutants treated with Anti-Jagged1 (*eDII4OE*+A-Jag1); the co-localization of PECAM (green) and N1ICD (red) indicates the presence of N1ICD in endothelial cells ECs (white arrows). **D**, Percentage of endothelial N1ICD-positive area (relative to control-100%); N1ICD is highly increased in all mouse groups. DAPI (blue) stains nuclei. Error bars represent SEM; * represents $p < 0.05$; ** represents $p < 0.01$; *** represents $p < 0.001$.

4.6 Administration of a Notch4 agonist to wild-type mice accelerates wound healing by promoting vessel maturation without affecting angiogenic growth

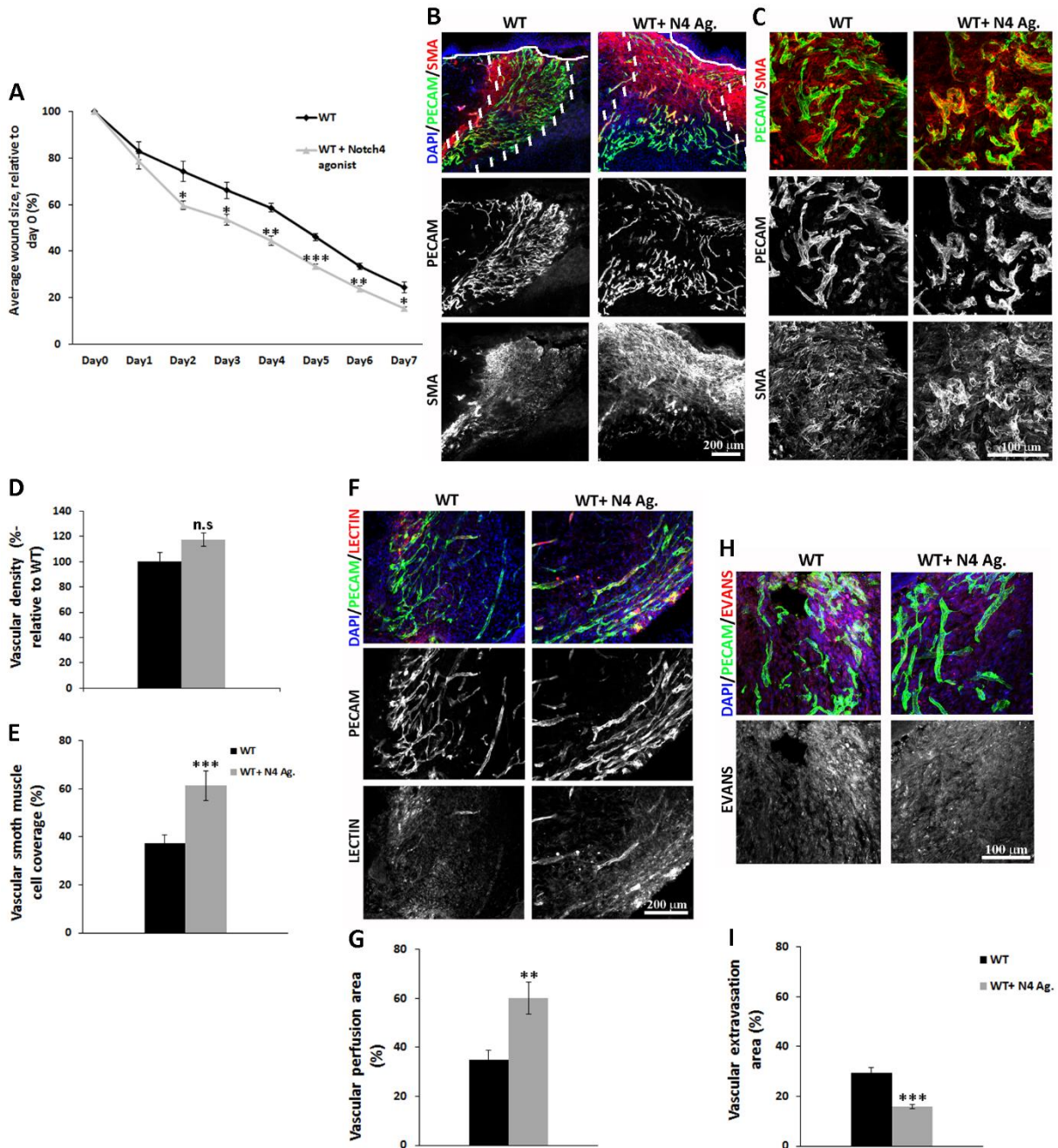
To provide independent evidence of the role of Notch4 in the vascular response and to better ascertain whether indeed endothelial Notch4 also contributes to the vascular maturation process, we administered a Notch4 agonistic antibody to wild-type (WT) mice and evaluated the healing response. Administration of a Notch4 agonist to WT mice (WT+N4 Agonist) led to significantly accelerated wound healing from day 2 of recovery (Suppl. Figure I.9A). Analysis of the wound vasculature revealed that despite no significant change had been observed in vascular density (Suppl. Figure I.9B–D), animals injected with the agonist presented increased coverage of SMA+ cells (Suppl. Figure I.9A, B, and E) and pericytes (Suppl. Figure I.10). Moreover, the newly formed vasculature of Notch4 agonist injected mice presented increased perfusion (Suppl. Figure I.9F and G) and decreased leakage (Suppl. Figure I.9H and I), consistent with an increased maturation status.

Transcription analysis further supported our previous results, with the same set of genes that were upregulated in *eJag1OE* also being upregulated in WT+ N4 agonist mice (Suppl. Figure I.11A). This group of genes included all the analyzed genes involved in recruitment of perivascular cells, such as *Pdgfb*, *Pdgfr- β* , *Tek*, and *Ang-1*. It also included *Jag1*, *Notch4*, *Notch3*, *Hey1*, and *HeyL*. Contrastingly, *Dll4*, *Notch1*, and *Hey2* transcription levels showed no significant changes in the WT+ N4 agonist group.

Accordingly to the transcription analysis, Notch4 agonist injected animals showed increased endothelial Hey1 positive area (Suppl. Figure I.11B and C), whereas no significant differences were observed on Hey2 staining (Suppl. Figure I.11D and E).

These results reinforce the evidence for the role of endothelial Jagged1/Notch4 signaling in the process of vascular maturation.

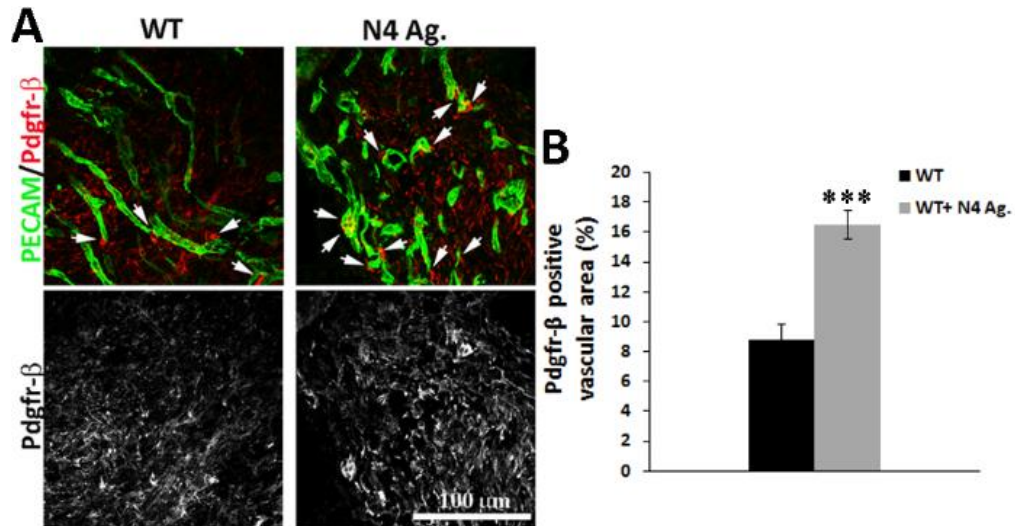
Supplemental Figure I.9- Notch4 Agonist treated WT mice in wound healing assay.



A, Progression of average wound size relative to day 0 in WT and WT mice administered a Notch4 Agonist (WT+ N4 Ag.) **B**, Immunostaining images (10x amplification) for PECAM-1 (green) and SMA (red), used to evaluate vascular density and perivascular coverage of samples collected at day 7. Continuous white line marks the base of epidermis and the space between dashed lines marks the angiogenic fronts. **C**, Confocal immunostaining images (40x amplification) showing the perivascular phenotype in detail; Notch4 agonist injected mice display no difference in vascular growth, as seen by PECAM-1+ signal, but an increased SMA staining associated with the vessel wall. **D**, Percentage of vascular density (relative to control=100%) showing no significant PECAM-1 staining between mice groups. **E**, Percentage of vSMC coverage, showing PECAM-1/SMA+ signal is highly increased in WT+ N4 Ag. Animals. **F**, Lectin (red) and PECAM-1 (green) immunostaining (20X amplification) of samples collected at end-point, to evaluate the co-localization of both signals, indicative of vessel perfusion. **G**, Percentage of perfusion area in the total vascular area (given by vascular density measurements)

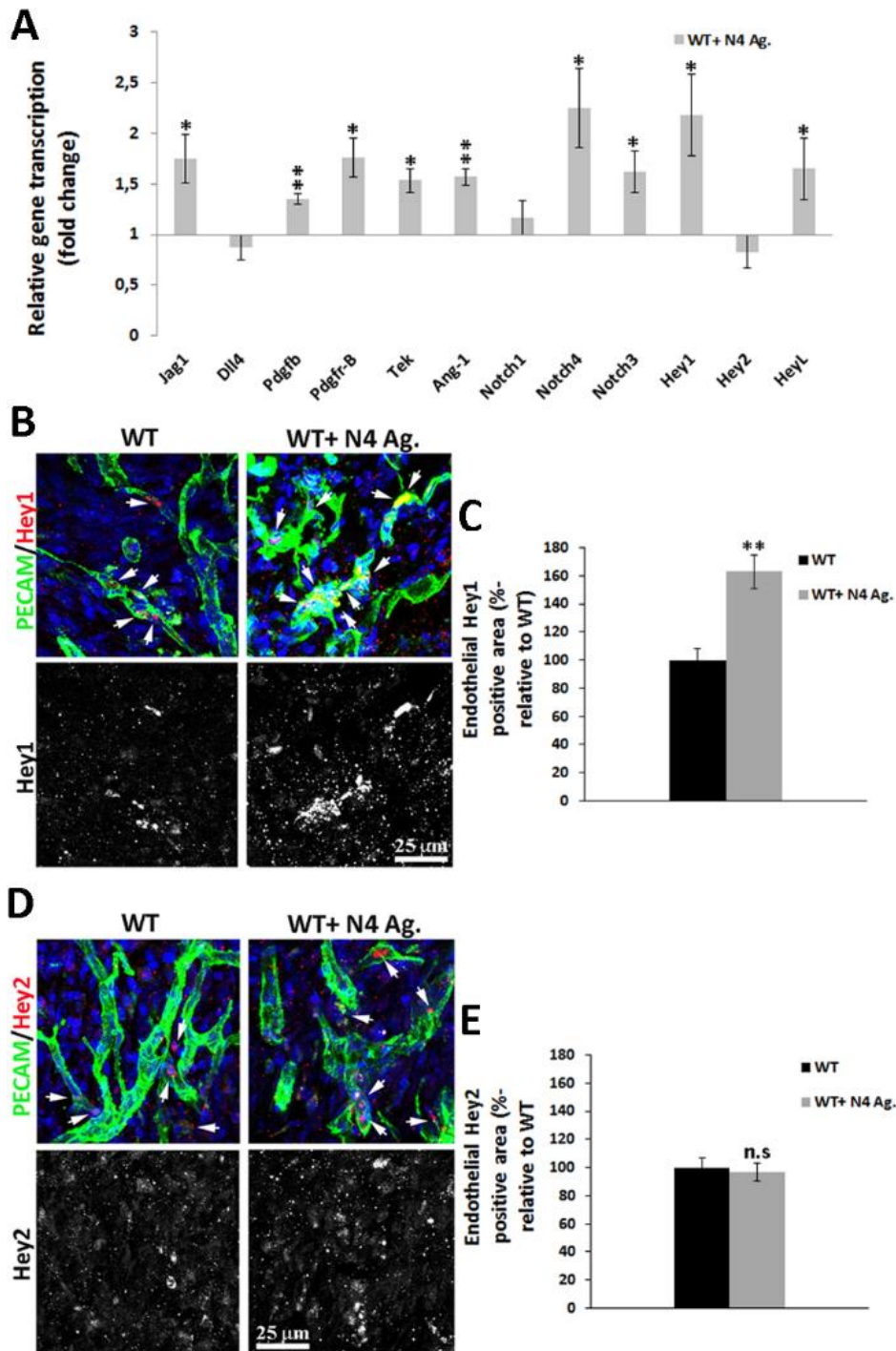
showing increased lectin labeling in Notch4 agonist administered mice. **H**, Evans' Blue (red) and PECAM-1 (green) confocal immunostaining images (20x amplification) showing the extravasation areas. **I**, Percentage of vascular extravasation area in the total vascular area showing reduced leakage, or Evans' Blue staining, in the WT+ N4 Ag. vasculature, relative to WT alone. DAPI (blue) stains nuclei. Results are representative of 1 experiment, with n=6 in each mouse group. Error bars represent SEM; * represents $p < 0.05$; ** represents $p < 0.01$; *** represents $p < 0.001$.

Supplemental Figure I.10- Pericyte vascular coverage in WT mice treated with a Notch4 agonist.



A, Pdgfr- β (red) and PECAM-1 (green) confocal immunostaining images (40x amplification) of samples collected at end-point in WT mice versus Notch4 agonist treated WT mice (WT+N4 Ag.). White arrows indicate positive Pdgfr- β cells along the vascular wall. **B**, Percentage of Pdgfr- β -positive vascular area showing increased positive area in WT+N4 Ag., relative to WT alone. Error bars represent SEM; *** represents $p < 0.001$.

Supplemental Figure I.11- Gene expression analysis and immunostaining for Hey1 and Hey2 in Notch4 agonist treated WT mice.



A, RNA was isolated from wound samples collected at the end-point, and gene transcription analysis was performed by quantitative real-time RT-PCR for genes involved in Notch signaling. Gene transcript levels were normalized to PECAM-1 mRNA levels, and the house-keeping gene β -actin was used as endogenous control. Grey bars represent the relative gene expression of the samples collected from Notch4 agonist treated WT mice (WT+N4 Ag.), relative to the WT group. **B** and **D**, High-magnification confocal immunostaining images (40x amplification) of Hey1 and Hey2 (red), respectively, and PECAM-1 (green) in WT+N4 Ag. Animals versus WT group alone. **C**, Percentage of endothelial Hey1-positive

area, (relative to control=100%; white arrows) showing increased positive area in Notch4 Agonist treated mice. **E**, Percentage of endothelial Hey2-positive area, (relative to control=100%; white arrows) showing no significant staining quantification in WT and N4 agonist treated mice. Error bars represent SEM; * represents $p < 0.05$; ** represents $p < 0.01$; *** represents $p < 0.001$.

5. Discussion

This article addresses the role of Jagged1/Notch signaling and its relation to the other major Notch ligand, Dll4, during angiogenic processes related to skin wound healing. In particular, our results establish that the pro-angiogenic role of *Jag1* observed in developmental processes (Benedito et al., 2009) is also relevant for regenerative angiogenesis in the adult. We found that endothelial *Jag1* overexpression improved the healing rate of dermal wounds and was associated with an increase in the density, maturation, and functionality of the newly formed vasculature, whereas endothelial-specific *Jag1* knockout had the opposite effect. VEGF receptors were upregulated in *eJag1OE* mutants and downregulated in *eJag1cKO* samples. This finding is consistent with previously published work (Benedito et al., 2009) showing that Jagged1 can promote VEGF signaling by upregulating the levels of *Vegfr3* and *Vegfr2*.

Given our previous studies with endothelial-specific *Dll4* mutants (Trindade et al., 2012), the *eJag1cKO* loss-of-function endothelial phenotype is similar to that observed in *eDll4OE* mutants, whereas the *eJag1OE* phenotype corresponds to that observed in *eDll4cKO* mutants. Dll4 blockade with an anti-Dll4 antibody led to delayed wound healing, in accordance with our previous study where we showed the same wound healing kinetics using either endothelial-specific Dll4 loss-of-function mutant mice or administration of a soluble Dll4-Fc fusion protein (Trindade et al., 2012). Administration of anti-Dll4 to *eJag1cKO* mutants led to a further delay in wound healing and significantly increased vascular density, demonstrating the opposing roles of the 2 Notch ligands in the endothelium, Dll4 antiangiogenic and Jagged1 pro-angiogenic.

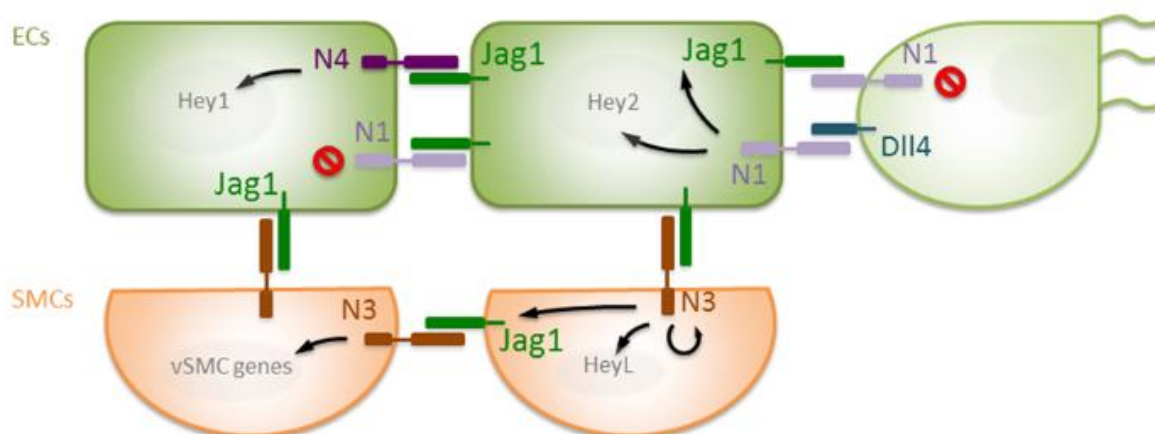
In addition, our new data show that Jagged1 and Dll4 have also overlapping functional roles in the vasculature, as both ligands contributed to increased vSMC and pericyte coverage and reduced vascular leakage during wound healing angiogenesis. We propose that Jagged1/Notch signaling might be directly responsible for maturation processes in a newly formed vascular plexus acting downstream of Dll4. This is supported by the observation that the perivascular phenotype observed in *eDll4OE* mutants is linked to the downstream upregulation of *Jag1*, which was visible both at the transcript level and at the protein level, as shown in Figure I.5F. Accordingly, treatment of *eDll4OE* mutants with anti-Jagged1 antibody led to decreased recruitment of mural support cells. In line with our observations, High et al (High et al., 2008) have shown that endothelial-specific *Jag1* knockout mutant embryos have striking deficits in vascular smooth muscle, whereas endothelial Notch1 activation and arterial-venous differentiation seemed normal. They also showed that endothelial *Jag1* mutant embryos are phenotypically distinct from embryos in which Notch signaling is inhibited in the

endothelium. Therefore, the primary role of endothelial Jagged1 may be to potentiate the development and differentiation of neighboring vSMCs. Thus, Jagged1 not only counteracts Dll4/Notch in the endothelium but also generates a balance between angiogenic growth and maturation processes. Our observations also suggest that endothelial Jagged1 negatively regulates the transcription and activation of Notch1, whereas it positively controls the transcription and activation of Notch4. Our colocalization analysis suggests that Jagged1 might be unable to trigger substantial Notch1 activation. Accordingly, a recent study (Yoon et al., 2013) demonstrated that in vitro cultivation of ECs in high glucose conditions causes increased angiogenesis because of Jagged1 overexpression and inhibition of Notch1. Conversely, *eJag1cKO* mutants, where the transcript levels of *Dll4* were upregulated, showed a significant increase in N1ICD-positive endothelium. This increase was reverted by blocking Dll4 with anti-Dll4 antibody. In addition, antibody blocking of Jagged1 failed to revert the increased active endothelial Notch1 observed in *eDll4OE* mouse mutants, suggesting that Notch1 is mainly activated by Dll4. In fact, the embryonic lethal phenotype observed in *Notch1*^{-/-} mice is similar to that of *Dll4*^{-/-} embryos (Swiatek et al., 1994; Duarte et al., 2004; Benedito et al., 2008). From the analysis of endothelial N4ICD in the *eJag1* mutants, where endothelial N4ICD positive area is higher in *eJag1OE* mutants and lower in *eJag1cKO*, it seems that Jagged1 is able to activate Notch4 in the endothelium, as previously suggested (Uyttendaele et al., 2000; Emuss et al., 2009). Moreover, the vasculature of *eDll4OE* mutants, where *Jag1* expression is high, has increased numbers of N4ICD positive ECs, which are not observed when Jagged1 signaling is blocked. Moreover, blocking of Dll4 in either control (control+anti-Dll4) or *eJag1cKO* (*eJag1cKO*+anti-Dll4) mice also led to decreased endothelial activation of Notch4, which was expected because of the downstream downregulation of *Jag1* transcript levels that is observed in these mice.

Furthermore, we have also showed that administering a Notch4 agonistic antibody to WT mice accelerated the healing response, similar to what was observed in *eJag1OE* mutants. Vasculature analysis of the injected mice showed no alteration in vascular density but sustained increase in vSMC and pericyte coverage, suggesting this receptor to be mainly involved in the vascular maturation response. Therefore, these results support the hypothesis that the pro-angiogenic phenotype observed in *eJag1OE* mutants can be a consequence of, first, inhibiting Notch1 activation, resulting in increased angiogenic growth, and second, activating Notch4, which in turns drives vascular maturation. In addition, the immunofluorescence and transcription analysis of both *eJag1* mutants and Notch4 agonist-administered mice suggest that activation of Notch4 by endothelial Jagged1 results in the transcription of specific target genes, namely *Hey1* (Manderfield et al., 2012). Conversely, the other major Notch effector, *Hey2*, was upregulated in *eJag1cKO* and in *eDll4OE* mutants, which in both cases is likely to be a consequence of increased Dll4/Notch1 signaling.

Evidence for a role of Notch and, more specifically, Jagged1 in endothelial contact-dependent recruitment of SM progenitor cells in vivo was provided by the deletion of Notch signaling activity in neural crest–derived smooth muscle progenitors (High et al., 2007) and in experiments where *Jag1* was deleted specifically in ECs (High et al., 2008). Thus, endothelial Jagged1 is also able to bind Notch3 on neural crest–derived smooth muscle progenitors, which leads to the lateral induction of Jagged1/Notch signaling and directs the expression of *HeyL* and other signals laterally into the growing circumferential wall, as suggested by Liu et al. (Liu et al., 2009). Here, we show the ability of endothelial Jagged1 to activate perivascular Notch3. We have detected increased levels of N3ICD in SMCs in both *eJag1OE* and *eDII4OE* mutants. Moreover, administration of anti-Jagged1 to *eDII4OE* mutants brought N3ICD levels back to control levels. Most importantly, these results suggest that Jagged1/Notch4 endothelial signaling can also contribute to the assembly of a SMC layer by regulating the transcription of key components of pathways associated with vascular maturation and perivascular cell recruitment. In particular, these data point at the ANG-1/TIE-2 and PDGF-B/PDGFR β pathways as possible targets of Jagged1/Notch signaling, as has been previously suggested (Jin et al., 2008). Nonetheless, further studies are required to distinguish the roles of Jagged1/Notch4 and Jagged1/Notch3 signaling in the process of vascular maturation. In our proposed model (Figure I.8), endothelial Jagged1 acts downstream of DII4/Notch1 to produce 2 distinct effects. First, Jagged1 is responsible for antagonizing DII4 ability to bind to and activate Notch1 in tip cells, creating a negative feedback loop in the regulation of endothelial branching, as described in the developing retina (Benedito et al., 2009). Second, by activating Notch4 in ECs and Notch3 in vSMCs, Jagged1 positively regulates vascular maturation downstream of DII4/Notch1 signaling.

Figure I.8- Proposed model for Jagged1/Notch signaling in wound angiogenesis.



Endothelial DII4, mainly expressed in tip cells (Claxton & Fruttiger, 2004), activates Notch1 in adjacent cells leading to the transcription of specific Notch effectors (namely *Hey2*) and upregulating endothelial *Jag1* transcription and expression. Moreover, Jagged1 is responsible for antagonizing DII4 ability to bind to and activate Notch1 in tip cells, creating a negative feedback loop in the regulation of endothelial

branching (Benedito et al., 2009). Furthermore, endothelial Jagged1 positively regulates vascular maturation by 2 possible mechanisms: by activating endothelial Notch4 leading to the transcription of specific Notch effectors (namely *Hey1*); and by activating Notch3 in vascular smooth muscle cells (Liu et al., 2009).

6. Conclusions

In conclusion, this study is the first to demonstrate the pro-angiogenic role of endothelial Jagged1 in adult physiological angiogenesis and the synergistic roles of endothelial Jagged1 and Dll4 on vascular maturation. Also, it is the first study to reveal Jagged1 as a potential therapeutic target. We have previously presented results showing that low dosage inhibition of Dll4 function could produce a pro-angiogenic phenotype, while maintaining an intact network of functional blood vessels (Trindade et al., 2012). This approach might enable faster wound healing and regenerative processes. The current results establish that increased endothelial expression of Jagged1 has a more profound pro-angiogenic effect that promotes healing processes by increasing vessel density but also improved maturation of the newly formed wound vasculature. This goes way beyond what Dll4 targeting/inhibition alone can achieve. Activation of Jagged1 expression may well prove potentially useful in situations where vascular function is a limiting factor in patient recovery, like in ischemia or wound healing. In the case of diabetic retinopathy, increased Jagged1 signaling could be used to stabilize and promote the maturation of nascent blood vessels, which could help to reduce edema and hypoxia of retinal tissues in this condition. However, blocking Jagged1 is likely to be useful in cases where it is desirable to limit vascular growth such as in antiangiogenic cancer therapy.

**Chapter II -
Endothelial
Jagged1 promotes
solid tumor
growth through
both pro
angiogenic and
angiocrine
functions.**

Ana-Rita Pedrosa,
Alexandre Trindade,
Catarina Carvalho, José
Graça, Sandra Carvalho,
Maria C. Peleteiro, Ralf
H. Adams and António
Duarte.

Published in *Oncotarget*
2015; 6(27).
DOI:10.18632/oncotarge
t.4380

1. Abstract

Angiogenesis is an essential process required for tumor growth and progression. The Notch signaling pathway has been identified as a key regulator of the neo-angiogenic process. Jagged1 (*Jag1*) is a Notch ligand required for embryonic and retinal vascular development, which direct contribution to the regulation of tumor angiogenesis remains to be fully characterized.

The current study addresses the role of endothelial Jagged1-mediated Notch signaling in the context of tumoral angiogenesis in two different mouse tumor models: subcutaneous Lewis Lung Carcinoma (LLC) tumor transplants and the autochthonous Transgenic Adenocarcinoma of the Mouse Prostate (TRAMP).

The role of endothelial Jagged1 in tumor growth and neo-angiogenesis was investigated with endothelial-specific *Jag1* gain- and loss-of-function mouse mutants (*eJag1OE* and *eJag1cKO*). By modulating levels of endothelial *Jag1*, we observed that this ligand regulates tumor vessel density, branching, and perivascular maturation, thus affecting tumor vascular perfusion. The pro-angiogenic function is exerted by its ability to positively regulate levels of *Vegfr-2* while negatively regulating *Vegfr-1*. Additionally, endothelial Jagged1 appears to exert an angiocrine function possibly by activating Notch3/Hey1 in tumor cells, promoting proliferation, survival and epithelial-to-mesenchymal transition (EMT), potentiating tumor development. These findings provide valuable mechanistic insights into the role of endothelial Jagged1 in promoting solid tumor development and support the notion that it may constitute a promising target for cancer therapy.

Keywords: jagged1, notch, TRAMP, tumor angiogenesis, angiocrine.

2. Introduction

Since Folkman's seminal insight of treating cancer by cutting its blood supply (Folkman, 1971) much effort has been devoted to understand the underlying molecular mechanisms that drive tumor angiogenesis. It is well established that tumor growth is restricted in an early avascular phase, and that, to be able to progress and develop it requires an angiogenic switch (Hanahan & Folkman, 1996).

Tumor angiogenesis is initiated when endothelial cells respond to local stimuli and migrate towards the growing mass. This migration results in the formation of tubular structures that ultimately recruit perivascular support cells in order to create a well-established neo-vasculature that allows tumor development and eventual metastization (Hanahan & Folkman, 1996).

Many signaling pathways have been identified as key contributors to the neo-angiogenic process. Among them is the Notch signaling pathway, an evolutionary conserved signaling system that regulates proliferation, differentiation, cell-fate determination, progenitor and stem-cell self-renewal, in both embryonic and adult tissues (Duarte et al., 2004; Schweisguth, 2004). The Notch pathway is composed of 5 ligands (Jagged1, Jagged2, and Delta-like 1, 3, and 4) and 4 receptors (Notch 1–4). Ligand–receptor interactions promote the cleavage of the Notch receptors, releasing the Notch intracellular domain (NICD), which is then translocated to the nucleus where it binds a transcriptional repressor and ultimately leads to the transcription of downstream target genes, such as several helix–loop–helix transcription factors (*Hey* and *Hes* gene families among others) (Schweisguth, 2004).

The Notch ligand, Dll4, is required for normal arterial patterning in the embryo (Duarte et al., 2004) and has a major effect in solid tumor growth (Noguera-Troise et al., 2006; Ridgway et al., 2006). This effect of targeting Dll4 is apparently paradoxical as it inhibits tumor growth by triggering excessive angiogenesis, that results in poorly functional vessels (Sainson & Harris, 2007).

However, despite the extensive characterization of the role of Dll4 in tumor vasculature, the contribution of other Notch ligands, like Jagged1, is less well studied. *Jag1*-null mouse mutants die at E11.5 due to heart defects and abnormal development of the yolk sac and head vasculature (Xue et al., 1999). Moreover, mutations in the human *JAG1* gene cause Alagille syndrome, which comprises complex cardiac defects and vascular anomalies (Spinner et al., 2001). Additionally, in the developing retina (Benedito et al., 2009) endothelial Jagged1 has been shown to have a pro-angiogenic function, opposite to that of Dll4. This pro-angiogenic function has also been demonstrated in an adult physiological setting, where it promotes wound healing by the ability to antagonize Dll4/Notch1 endothelial branching while positively regulating vascular maturation through activation of endothelial Notch4 and perivascular Notch3 (Pedrosa et al., 2015a). Jagged1 is expressed in the vasculature, as well as in many other tissues. In the context of tumor angiogenesis two reports suggest that tumor cells

expressing Jagged1 can act in a pro-angiogenic manner: induction of the Notch ligand Jagged1 by growth factors (via MAPK) in head and neck squamous cell carcinoma was shown to trigger Notch activation in neighboring endothelial cells and promote capillary-like sprout formation (Zeng et al., 2005), and Jagged1 expressed in breast tumor cells can influence tumor angiogenesis (Funahashi et al., 2008). Similarly, in the context of lymphoma, a specific population of lymphoma cells was shown to up-regulate endothelial Jagged1, through the secretion of FGF4, which in turn up-regulates Notch2 and consequently Hey1 in the tumor cells promoting growth, aggressiveness and resistance to chemotherapy (Cao et al., 2014). Finally, a specific Notch1 decoy, that blocks both Jagged ligands interactions with Notch1, was shown to decrease xenograft growth by an anti-angiogenic effect and by the ability to destabilize pericyte-ECs interactions (Kangsamaksin et al., 2014).

Therefore, the direct role of endothelial Jagged1 in tumor angiogenesis has not yet been thoroughly described. With this purpose, we have fully characterized tumor growth and progression, and the associated vascular phenotype and cellular metabolic consequences in endothelial *Jag1* mutants in two different mouse tumor models: subcutaneous Lewis Lung Carcinoma (LLC) tumor transplants and in the autochthonous transgenic adenocarcinoma of the mouse prostate (TRAMP) (Greenberg et al., 1995; Gingrich et al., 1999).

Here we demonstrate for the first time the effect of directly modulating endothelial Jagged1 in tumor angiogenesis and growth, confirming that loss of endothelial *Jag1* has a strong anti-angiogenic effect that inhibits tumor growth and the acquisition of an invasive phenotype. Moreover, we have shown that endothelial Jagged1 regulates prostatic tumor cell proliferation and de-differentiation by activating Notch3 and consequently up-regulating Hey1 in tumor cells. The results obtained clearly raise the possibility of applying anti-Jagged1 therapies to cancer treatment.

3. Materials and Methods

3.1 Experimental animals

All the procedures involving animals used in this study were approved by the Ethics and Animal Welfare Committee of the Faculty of Veterinary Medicine of Lisbon. All animals were housed in ventilated propylene cages with sawdust as bedding, in a room with temperature between 22°C and 25°C and a 12-hours-light/12-hours-dark cycle. The mice were fed standard laboratory diet.

To obtain the gain-of-function mutants, heterozygous Tet-O-Jag mice were crossed with a line of heterozygous Tie-2-rtTA mutant mice. The double heterozygous offspring obtained, Tet-O-Jag; Tie-2-rtTA, were administered doxycycline (4mg/ml in drinking water from week 4), in order to activate the overexpression of *Jag1* under the control of the *Tie-2* promoter. One control group contained mice with the same *Jag1* gain-of-function genotype that were not induced with doxycycline. Another control group consisted of TRAMP.Tet-O-*Jag1*.Tie-2-rtTA- mice

administered with doxycycline to discard possible doxycycline driven effects. No differences in tumor growth dynamics or tumor vascular phenotypes were found between the two control groups (data not shown).

The loss-of-function mutant is a conditional “knock-out” where the coding region for the DSL (Delta-Serrate- Lag2) region of *Jag1* (exon 4) is flanked by loxP sites- *Jag1lox/lox* line (Kiernan et al., 2006) (B6; 129S-*Jag1 tm2Grid/J*; The Jackson Laboratory). *Jag1lox/+* mice were crossed with VE-Cadherin-Cre-ERT2 mice (Monvoisin et al., 2006) in order to obtain a *Jag1lox/lox* VE-Cadherin-Cre-ERT2 mouse line. *Jag1* null endothelial mutants were generated upon treatment with tamoxifen (50mg/kg daily IP for 5 days, starting one week before the experiment). One control group had the same *Jag1* loss-of-function genotype but were not induced with tamoxifen. Another control group consisted of TRAMP.*Jag1lox/lox* VE-Cadherin-Cre-ERT2- mice administered with tamoxifen to discard possible tamoxifen specific effects. No differences in tumor growth dynamics or tumor vascular phenotypes were found between the control groups (data not shown).

3.2 LLC subcutaneous tumor model

Lewis Lung Carcinoma (LLC) (ATCC® CRL- 1642TM) (Bertram & Janik, 1980) cells were cultured in RPMI 1640 medium (Gibco 21875-034) supplemented with 10% foetal bovine serum (Gibco 10270-106) and 1% penicillin/ streptomycin (Gibco 15140-122) in 100mm tissue culture dishes (Corning 734-1705) coated with poly-D-Lysine Hydrobromide (Sigma P7280) at 37 °C in a humidified atmosphere of 95% air and 5% CO₂. When cells reached sub confluence, they were detached by 5 min treatment with 0,25% trypsin-EDTA (Gibco 25200-056) and resuspended in PBS to a cell concentration of 1×10⁷/ml. For the transplant tumor model, cells (1×10⁶/mouse) were inoculated subcutaneously, in the right flank with the mouse under anesthesia (2,5% avertin).

3.3 Tissue preparation and immunohistochemistry

Subcutaneous tumor transplants were collected at day 14th after LLC injection and, in the TRAMP model, prostates were dissected at 18 or 24 weeks of age.

For histopathological analysis, prostates were fixed in 10% buffered formalin solution for 48 h, dehydrated in alcohol, cleared in xylene, embedded in paraffin, sectioned at 3µm and stained with hematoxylin (Fluka AG Buchs SG Switzerland) and eosin Y (Sigma, St. Louis, MO). The sections were then analysed blindly by a pathologist (CP) and scored according to the literature (Kaplan-Lefko et al., 2003). Tumor samples from both models, were also fixed with 4% paraformaldehyde (PFA) solution at 4°C for 1h, cryoprotected in 15% sucrose, embedded in 7,5% gelatin, frozen in liquid nitrogen and cryosectioned at 10 and 20µm.

Immunofluorescence was performed using the following protocol: tissue slides were permeabilized in 3% H₂O₂ methanol solution for 30 min and PBS-Triton 0,1% solution 2x 10

min; blocking was performed for 1h (room temperature) either with 2% BSA + 5% Donkey serum in PBS-W 0,1%; after blocking, slides were incubated over-night at 4°C with specific primary antibodies followed by 1h incubation at room-temperature with fluorescently-tagged specific secondary antibodies.

For PSMA staining, rabbit monoclonal anti-PSMA4 (Abcam, Cambridge, UK) was used.

To examine vascular density and vessel maturity a rat monoclonal anti-mouse PECAM-1 (BD Pharmingen, San Jose, CA) and a mouse monoclonal anti-SMA Cy3 conjugate (Sigma Aldrich, USA), combined with a donkey anti-rat conjugated with Alexa Fluor 488 (Invitrogen, Carlsbad, CA) were used. Nuclei were counterstained with 4', 6'-diamidino-2-phenylindole dihydrochloride hydrate (DAPI; Molecular Probes, Eugene, OR). Vascular density is equivalent to the percentage of each tumor section field occupied by a PECAM-1-positive signal (as determined by the percentage of black pixels per field after transforming the RGB images into binary files). Similarly, as a measure of vascular maturity, mural cell recruitment was assessed by quantifying the percentage of PECAM-1- positive structures lined by α -SMA-positive cells. For pericyte coverage rabbit monoclonal anti- PDGFR β (Cell signaling Technology) was used. Similarly to mural cell recruitment analysis, coverage was assessed by quantifying the percentage of PECAM-1-positive structures lined by pdgfr- β positive cells.

To assess vascular perfusion, avertin (2,5%) anesthetized mice were injected with biotin-conjugated lectin from *Lycopersicon esculentum* (100 μ g in 100 μ l of PBS; Sigma, St. Luis, MO) via caudal vein and allowed to circulate for 5 minutes before perfusing the vasculature transcardially with 4% PFA in PBS for 3 minutes. Slides were stained with rat monoclonal anti-mouse PECAM-1, followed by Alexa 594 goat anti-rat IgG (Invitrogen, Carlsbad, CA). Biotinylated lectin was visualised with Streptavidin-Alexa 488 (Invitrogen, Carlsbad, CA). Tumor perfusion area was quantified by determining the percentage of PECAM-1-positive structures that were co- localized with Alexa 488 signals.

To analyse vascular extravasation, avertin anesthetized mice were injected with 1% Evans Blue dye solution (Sigma, St. Luis, MO) via caudal vein, and perfused transcardially 5 minutes later with 4% PFA in PBS for 3 minutes. Tissue sections were stained with rat monoclonal anti-mouse PECAM-1, followed by Alexa 488 goat anti-rat IgG. Tumor vascular extravasation area was quantified by determining the tumor section field of Evans Blue red positive signal per vessel area (given by vascular density measurements).

For evaluation of hypoxic levels a rabbit anti- Hif1 α antibody was used (Abcam, Cambridge, UK). Additionally, HypoxyprobeTM-1 Plus Kit (Hypoxyprobe, Inc, USA) was used to detect cells with low oxygen pressure (pO₂ = 10 mmHg), in paraffin embedded sections.

For quantification of cellular apoptosis and proliferation, a rabbit anti-active caspase3 (Cell signaling Technology) and an Alexa-570 conjugated mouse anti- Ki67 (eBiosciences Inc., CA, USA) antibodies were used.

For the assessment of epithelial to mesenchymal transition, an Alexa-488 conjugated mouse anti-E-cadherin and a goat polyclonal anti-Snail (Abcam, Cambridge, UK) antibodies were used, respectively.

Additional primary antibodies used were goat anti-Jagged1 (Sigma), rat anti-Vegfr-2 (Cell signalling Technology), Alexa-488 conjugated rabbit anti- NG-2 (Milipore) rabbit anti-Hey1 (Milipore), rabbit anti- N3ICD and goat anti-N4ICD (Santa Cruz Biotechnology). Additional secondary antibodies used were Alexa-647 donkey anti-goat, anti-rat and anti-rabbit (Invitrogen, Carlsbad, CA).

Instrument details- Fluorescent immunostained sections from tumor transplants were examined under a Leica DMRA2 fluorescence microscope with Leica HC PL Fluotar 10X, 20X and 40X/0.5 NA dry objectives (Leica, Heidelberg, Germany), captured using Photometrics CoolSNAP HQ, (Photometrics, Friedland, Denmark), and processed with Metamorph 4.6-5 (Molecular Devices, Sunnyvale, CA). Fluorescent immunostained sections from prostatic tumors, due to the tissue complexity, were obtained using a Carl Zeiss LSM 710 confocal microscope with either Zeiss 20X (Plan-Apochromat) NA 0.80 dry objective or 40X (EC Plan-Neofluor) NA 1.30 oil immersion objective, and captured using ZEN 2010 software (Carl Zeiss, Jena, Germany). Morphometric analyses were performed using the NIH ImageJ 1.37v program (NIH, Bethesda, MA, USA). H&E stained sections were examined under a Olympus BX51 microscope with Olympus 10X/0.30 NA and 40X/0.75 NA dry objectives and captured with coupled Olympus DP21 photographic equipment (Olympus Iberia, Inc).

3.4 Quantitative transcriptional analysis

For whole prostate analysis, tumor samples were collected at the endpoint of each experiment and snap frozen for RNA extraction (Qiagen, Hilden, Germany). For ECs and vSMCs specific analysis, samples were collected at the endpoint of each experiment and prepared for FACS sorting. ECs and mural cells were sorted directly into the lysis buffer of the RNeasy Micro Kit (Qiagen). Total RNA was isolated according to manufacturer's protocol. A total of 100 ng RNA per reaction (ECs and vSMCs) and 400 ng per reaction (whole prostate) was used to generate cDNA with the SuperScript III First Strand Synthesis Supermix Q RT-PCR Kit (Invitrogen, CA). Relative quantification real-time PCR analysis was performed as described (Trindade et al., 2008) using Sybergreen Fastmix ROX dye (Qiagen). Primer pair sequences are available on request. The housekeeping gene β -actin was used as endogenous control.

3.5 Flow cytometry

For flow cytometric analysis and sorting of ECs (Lin- (cd45- ter119-) cd31+) and mural cells (Lin- (cd45- ter119-) cd146+ cd31-) (Crisan et al., 2012), prostates were collected and finely dissected into small pieces (2-4 mm). Then, the samples were digested into 1 ml solution of 1% collagenase (Sigma) and 2,4U/ml of dispase (Gibco, Life Technologies) incubation at 37°C,

with agitation, for 2h30 min. DNase I (Sigma) was added during digestion to eliminate DNA residues. After washing, digested cells were then subjected to immunostaining with anti-mouse ter-119 PE-Cy7, anti-mouse cd45 PE-Cy7 (Affymetrix, eBioscience), anti-mouse cd31 FITC and anti-mouse cd146 PE (BD Pharmingen). After washing, cells were sorted in FACS Aria III cytometer and analyzed using BD FlowJo software (Version 10.0, BD Bioscience).

For demarcating and sorting ECs and mural cells, first standard quadrant gates were set, subsequently to differentiate cd31+ (>103 log FITC fluorescence) and cd146+ (>10 log PE fluorescence) cells from the Lineage negative population (≤ 102 log PE-Cy7 fluorescence).

3.6 Statistical analysis

All data processing (except most common prostatic lesion) was carried out using the Statistical Package for the Social Sciences software, version 17.0 (SPSS v. 17.0; Chicago, IL). Statistical analyses were performed using Mann-Whitney-Wilcoxon test and Student's t-test.

Scores of the most common histopathological prostatic lesions were analyzed with the GLM procedure of Statistical Analysis System (SAS Institute Inc. v.9.1.3 2009; Cary, USA). The analyses were carried out within group, with a linear model including the effects of time (weeks 18 and 24), endothelial *Jag1* modulation (*eJag1OE* and *eJag1cKO* vs. respective controls) and their interaction.

All results are presented as mean \pm SEM. *P*-values < 0.05, <0.01 and <0.001 were considered significant (indicated in the figures with *) and highly significant (indicated with ** and ***), respectively.

4. Results

4.1 Modulation of endothelial *Jag1* interferes with the growth of LLC subcutaneous tumor transplants

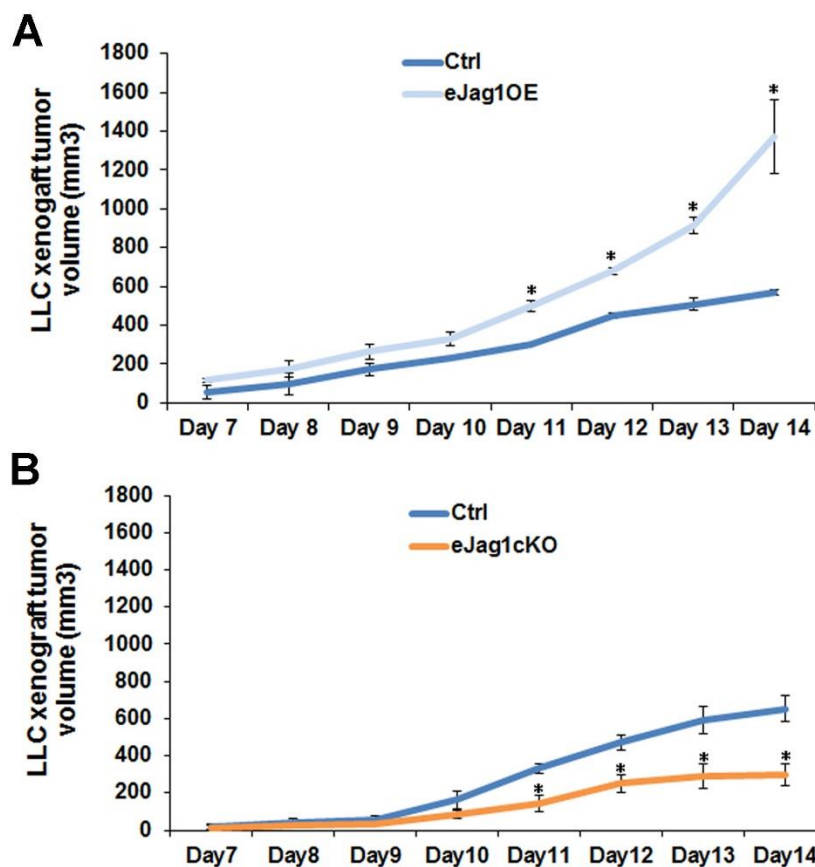
To evaluate the contribution of endothelial Jagged1 to tumor angiogenesis, LLC cells were subcutaneously implanted in the dorsum of endothelial specific *Jag1* gain- (*eJag1OE*) and loss-of-function mouse mutants (*eJag1cKO*). Tumor volumes (mm³) were measured from day seven after the subcutaneous injection until day fourteen.

Endothelial specific *Jag1* overexpression led to significantly accelerated growth of subcutaneous tumors, from day eleven after injection, with a final tumor volume more than two-fold larger (1370 mm³) than that of the respective controls (570 mm³) (Figure II.1A). In contrast, loss of endothelial *Jag1* led to significantly delayed tumor growth, from day eleven after injection (Figure II.1B). The average final tumor volume in the endothelial *Jag1* loss-of-function mutants was only 300 mm³, less than half of that of the respective controls (650 mm³).

4.2 Endothelial Jagged1 contributes to prostate cancer development and progression

After verifying that modulation of endothelial *Jag1* caused such significant alterations in the growth of LLC subcutaneous tumor transplants, we investigated its effect in an autochthonous tumor model. For this end, we crossed the endothelial *Jag1* mutants to a mouse model of prostate adenocarcinoma (TRAMP) (Greenberg et al., 1995), which spontaneously develop prostatic lesions from 8 weeks of age (Kaplan-Lefko et al., 2003). The TRAMP endothelial specific *Jag1* mutants, TRAMP.e*Jag1*OE and TRAMP.e*Jag1*cKO, were sacrificed at 18 and 24 weeks of age, for early and late stages of prostate cancer development, and the prostates collected for analysis.

Figure II.1- LLC transplant tumor volume in endothelial specific *Jag1* mutants.



A. Progression of LLC transplant tumor volume, from day 7 of subcutaneous injection, in endothelial specific *Jag1* over-expression mutants (Tet-O-Jag Tie2-rtTA+) relative to the respective controls (Tet-O-Jag Tie2-rtTA-). *Jag1* over-expression mutants present an accelerated growing rate of subcutaneous tumors, with a final tumor volume of more than double of the respective controls. **B.** Progression of LLC transplant tumor volume, from day 7 of subcutaneous injection, in endothelial specific *Jag1* Knock-out mutants (*Jag1*lox/lox Cre+) and controls (*Jag1*lox/lox Cre-). Loss of *Jag1* led to a decrease in the growing rate of subcutaneous tumors, with a final tumor volume of less than half of the respective controls. Results are representative of 2 independent experiments, each with $n = 6$ mice per group. Error bars represent SEM; * represents $p < 0.05$; ** represents $p < 0.01$; *** represents $p < 0.001$.

Endothelial specific *Jag1* over-expression TRAMP mice presented increased prostate weights relative to the respective controls (TRAMP Ctrl) at both early and late stages of prostate tumor development (Figure II.2A). Accordingly, loss of endothelial *Jag1* caused decreased total prostate weights due to reduction of the tumors, relative to TRAMP Ctrl mice, both in early and late stages (Figure II.2B). Noticeably, the prostate weights of TRAMP.e*Jag1*cKO did not differ significantly from those of WT animals, indicating a most considerable reduction in tumor growth.

Histopathological analysis was carried out blindly and the tumors scored according to the following categories: Normal (0), prostatic intraepithelial neoplasia [PIN (1)], well differentiated adenocarcinoma [WDA (2)], moderately differentiated adenocarcinoma [MDA (3)], poorly differentiated adenocarcinoma [PDA (4)], or phylloides-like cancer [PHY (5)] (Kaplan-Lefko et al., 2003). The prostatic lesions evolve in a progressive manner, with different lobes of the prostate presenting different stages of tumor development. Endothelial overexpression of *Jag1* caused an overall acceleration of prostate cancer progression (Figure II.2C, D and F; Suppl. Figure II.1A). At an early stage, even though there was no statistically significant difference in the most common lesion score between TRAMP.e*Jag1*OE and the respective controls (Figure II.2C), it was observed that, in the controls, the majority of animals (70%) presented lesions of PIN (Suppl. Figure II.1A), while in the e*Jag1*OE group, the majority (85,7%) already had evolved to lesions of WDA. Similarly, at a late stage, it was observed a statistically significant difference in the most common lesion score (Figure II.2C) between the mouse groups: 100% of control mice (TRAMP Ctrl) presented lesions of WDA and few animals progressed to advanced stages of prostatic adenocarcinoma (Figure II.2C and D), while the TRAMP.e*Jag1*OE group presented a greater percentage of animals that progressed to advanced stages of prostatic adenocarcinomas (Figure II.2C) (33% lesions of MDA, 22% of PDA and 30% PHY lesions).

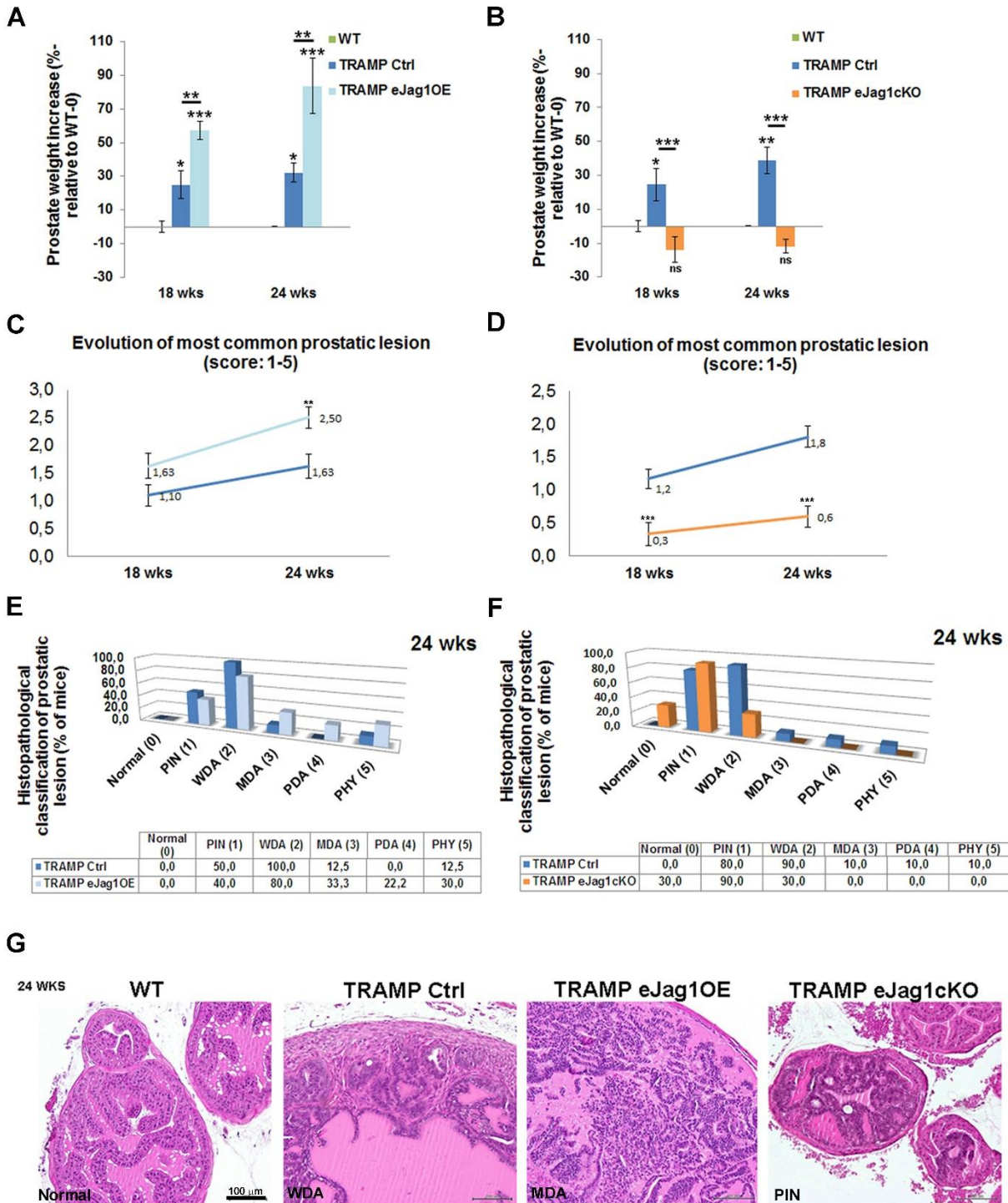
In contrast, TRAMP.e*Jag1*cKO mutant mice presented a statistically significant inhibition of prostate tumor progression (Figure II.2C, E and G; Suppl. Figure II.1B). At an early stage of tumor development (18wks), the respective control group presented a mean score of the most common lesion of 1.2 (Figure II.2D) with 66,7% of animals revealing lesions of WDA (suppl. Figure II.1B), while the e*Jag1*cKO mouse group presented a mean score of 0.3 (Figure II.2D) with 44,4% animals still showing no lesions (Normal), and the majority (77,8%) progressing only to lesions of PIN (Suppl. Figure II.1B). At a later stage, the same kind of response was observed with WDA in 90% of control animals, while only 30% of e*Jag1*cKO evolved to WDA, being the majority (90%) of this latest group classified mainly with lesions of PIN (Figure II.2F and G).

From the analysis of the most common lesion per animal it was also clear that there was no statistical interaction between the genotype and respective control groups throughout the evolution of the lesions (Figure II.2C and D), in either TRAMP.e*Jag1*cKO or TRAMP.e*Jag1*OE.

This means that the effect of modulating endothelial *Jag1* remained constant in time (evolution of tumor progression).

To gain additional confirmation of the differences in the progression and severity of prostatic lesions we immunostained the prostate samples for PSMA, a known marker of prostate cancer progression (Su, Huang, Fair, Powell, & Heston, 1995). Consistently with the prostate weight and histopathological classification data, TRAMP.e*Jag1*OE presented very strong immunostaining for PSMA in the prostatic tissue, while TRAMP.e*Jag1*cKO presented very weak signal, compared with controls (TRAMP Ctrl) (Suppl. Figure II.1C).

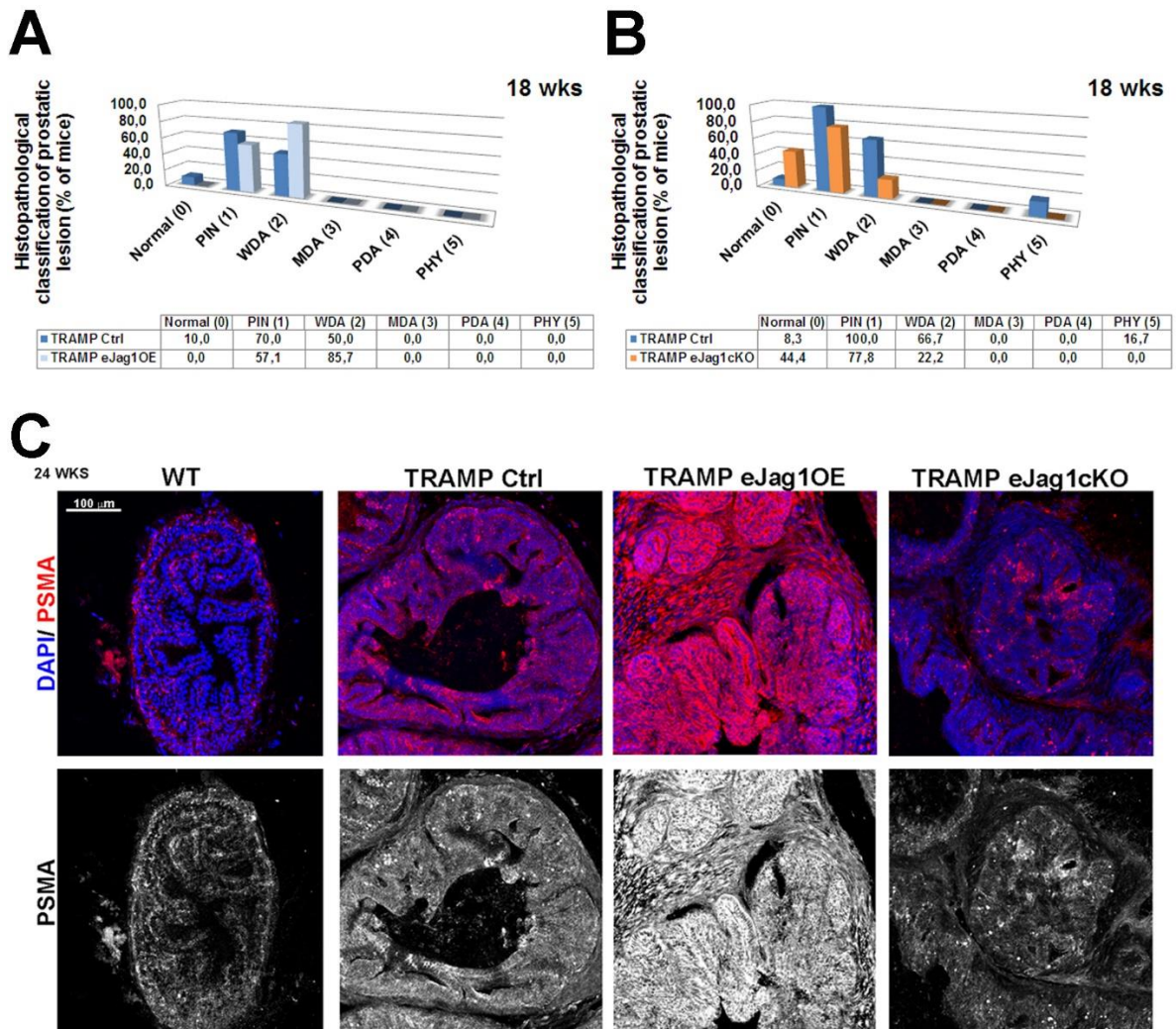
Figure II.2- Modulation of endothelial Jag1 in TRAMP mice.



A. Prostate weight increase (in %, relative to WT-0) in TRAMP Ctrl (Tet-O-Jag Tie2-rtTA-) and TRAMP.eJag1OE (Tet-O-Jag Tie2-rtTA+) mutants, in early (18 wks) and late (24 wks) stages of prostate tumor development. In both stages TRAMP.eJag1OE present higher prostate weight increase either relative to WT, as to TRAMP Ctrl mice groups. **B.** Prostate weight increase (in %, relative to WT-0) in TRAMP Ctrl (*Jag1lox/lox* Cre-) and TRAMP.eJag1cKO (*Jag1lox/lox* Cre+) mutants, in early (18 wks) and late (24 wks) stages of prostate tumor development. In both stages TRAMP.eJag1cKO present lower prostate weight increase than TRAMP Ctrl mice group. **C.** and **D.** Evolution of most common prostatic lesion of TRAMP.eJag1OE and TRAMP. eJag1cKO mutants, respectively, and controls, based on histopathological classification of prostatic lesions according to the following score (1-5): Normal (0);

prostatic intraepithelial neoplasia [PIN (1)]; well differentiated adenocarcinoma [WDA (2)]; moderately differentiated adenocarcinoma [MDA (3)]; poorly differentiated adenocarcinoma [PD (4)]; or phylloides-like cancer [PHY (5)]. TRAMP.e*Jag1*OE present a higher score evolution than controls, whereas TRAMP.e*Jag1*cKO present a lower one. **E.** and **F.** Frequency distribution (% of mice) of histopathological classification of prostatic lesions at 24 weeks of age in TRAMP.e*Jag1*OE and TRAMP.e*Jag1*cKO, respectively, versus controls. **G.** H & E representative images of the histopathological classification in WT (no lesions), TRAMP Ctrl (WDA), TRAMP. e*Jag1*OE (MDA) and TRAMP.e*Jag1*cKO (PIN) mice. Results are representative of $n = 12$ per mice group for each time point. Error bars represent SEM; * represents $p < 0.05$; ** represents $p < 0.01$; *** represents $p < 0.001$.

Supplemental Figure II.1- Modulation of endothelial *Jag1* in TRAMP mice.

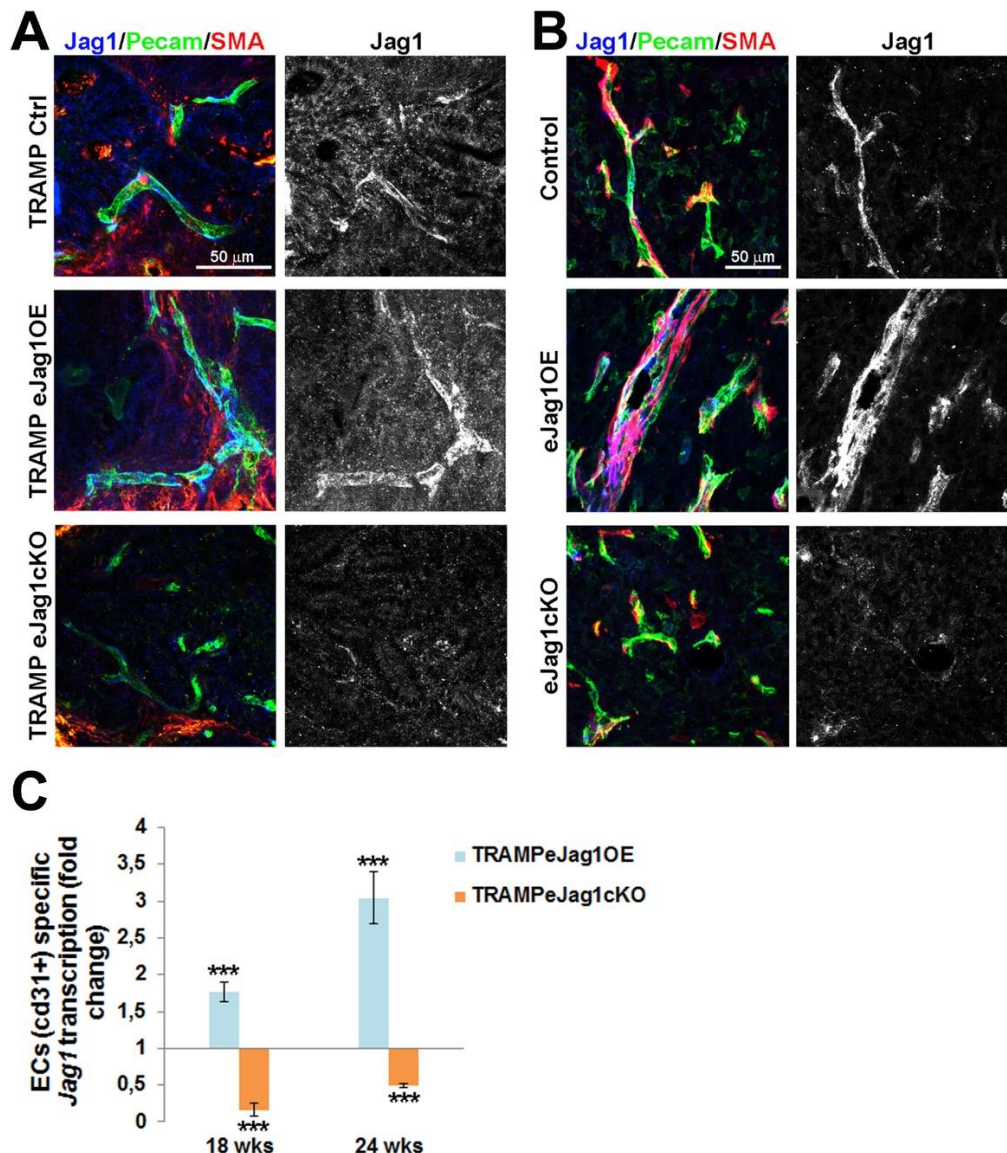


A and **B.** Frequency distribution (% of mice) of histopathological classification of prostatic lesions at 18 weeks of age in TRAMP.e*Jag1*OE and TRAMP.e*Jag1*cKO mutants, respectively, versus controls. **C.** Representative images of prostate specific membrane antigen (PSMA) (red) immunostaining demonstrating increased positive signal in TRAMP.e*Jag1*OE while decreased positive staining in TRAMP.e*Jag1*cKO mutants relative to controls (TRAMP Ctrl). DAPI (blue) stains nuclei.

4.3 Endothelial Jagged1 has a pro-angiogenic function in tumor development

Efficient modulation of endothelial Jagged1 was achieved in our conditional gain-of-function and knock-out mutants as demonstrated by the increased and decreased *Jag1* transcription levels in ECs and the increased and decreased fluorescence levels of Jagged1 co-localized with PECAM-1, respectively (Suppl. Figure II.2).

Supplemental Figure II.2- *Jag1* expression and transcription in endothelial-specific *Jag1* mutants.



A and **B**. Representative confocal immunostaining images (40x amplification) marked for Jag1 (blue), Pecam (green), and SMA (red) to evaluate specific modulation of endothelial Jag1 in TRAMP and LLC tumor samples, respectively. DAPI (blue) stains nuclei. **C**. ECs specific *Jag1* transcription analysis in TRAMP.eJag1 prostates. Error bars represent SEM; ** represents $p < 0.01$; *** represents $p < 0.001$.

To address whether the altered growth of subcutaneous LLC tumor transplants and prostate cancer development and progression observed in these EC-specific mutants was indeed associated with altered vessel growth, the vascular morphology of the tumors was examined.

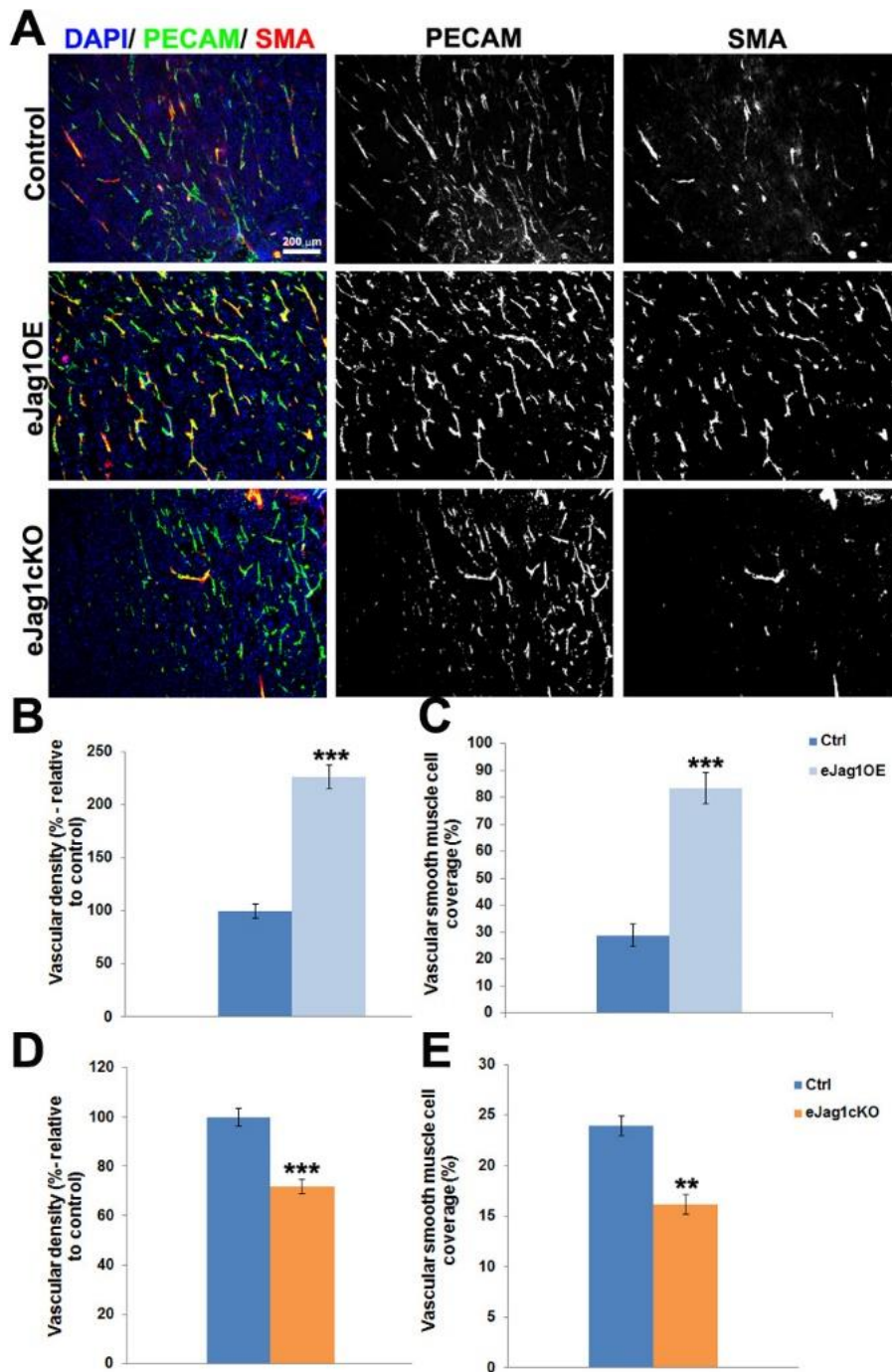
The endothelium was visualized by immunostaining against PECAM-1, while α -SMA was used to reveal perivascular cell coverage and thereby analyze vessel maturation. In *eJag1OE* mutants, tumor vasculature was denser in both LLC tumor transplants (Suppl. Figure II.3A and B) and prostate tumors (Figure II.3A and B), with increased number of endothelial branching points (Figure II.3A and C). Regarding perivascular coverage, it was observed, despite the abundant SMA positive signal from the stroma surrounding each prostatic gland, that *eJag1OE* tumor vasculature presented considerably more smooth muscle cells attached to the endothelial wall than the respective controls (Figure II.3A and D; Suppl. Figure II.3A and C). Not surprisingly, tumor vasculature of *eJag1cKO* mutants was the opposite of what was observed in the gain-of-function mutants: sparser (Suppl. Figure II.3A and D; Figure II.3A and E), with reduced ramification (Figure II.3F), and decreased number of perivascular SMA positive cells (Suppl. Figure II.3A and E; Figure II.3A and G). From Figure II.3 it is also clear that there are no major differences in tumor vasculature between early (18 wks) and late (24 wks) stages of prostate tumor development.

Tumor endothelial pericyte coverage was also investigated by immunostaining for *pdgfr- β* and *ng-2* (Winkler et al., 2010). Interestingly, no significant differences were observed in pericyte coverage with any of the markers, in either TRAMP.*eJag1OE* or TRAMP.*eJag1cKO* relative to the respective controls (Suppl. Figure II.4A-C). In contrast, in the LLCs transplant model, we observed significantly increased and decreased levels of endothelial *pdgfr- β* coverage in OE mutants and KO mutants, respectively (Suppl. Figure II.5).

Tumor vessel functionality in terms of perfusion and leakage was also analyzed by biotinylated lectin perfusion and Evans' Blue dye, respectively (Figure II.4 and suppl. Figure II.6). Over-expression of *Jag1* in the endothelium was associated with an increased number of perfused, lectin-containing vessels, whereas endothelial *Jag1* loss-of-function led to a significant decrease in vessel perfusion relative to the respective controls. Moreover, Evans' Blue extravasation was significantly reduced in *eJag1OE* mutants while *eJag1cKO* mutants presented an increased vascular extravasation area. These differences in tumor vascular phenotypes were observed in both tumor models used, prostatic tumors [early (18wks) and late (24 wks) stages, Figure II.4] as well as LLC subcutaneous tumor transplants (Suppl. Figure II.6).

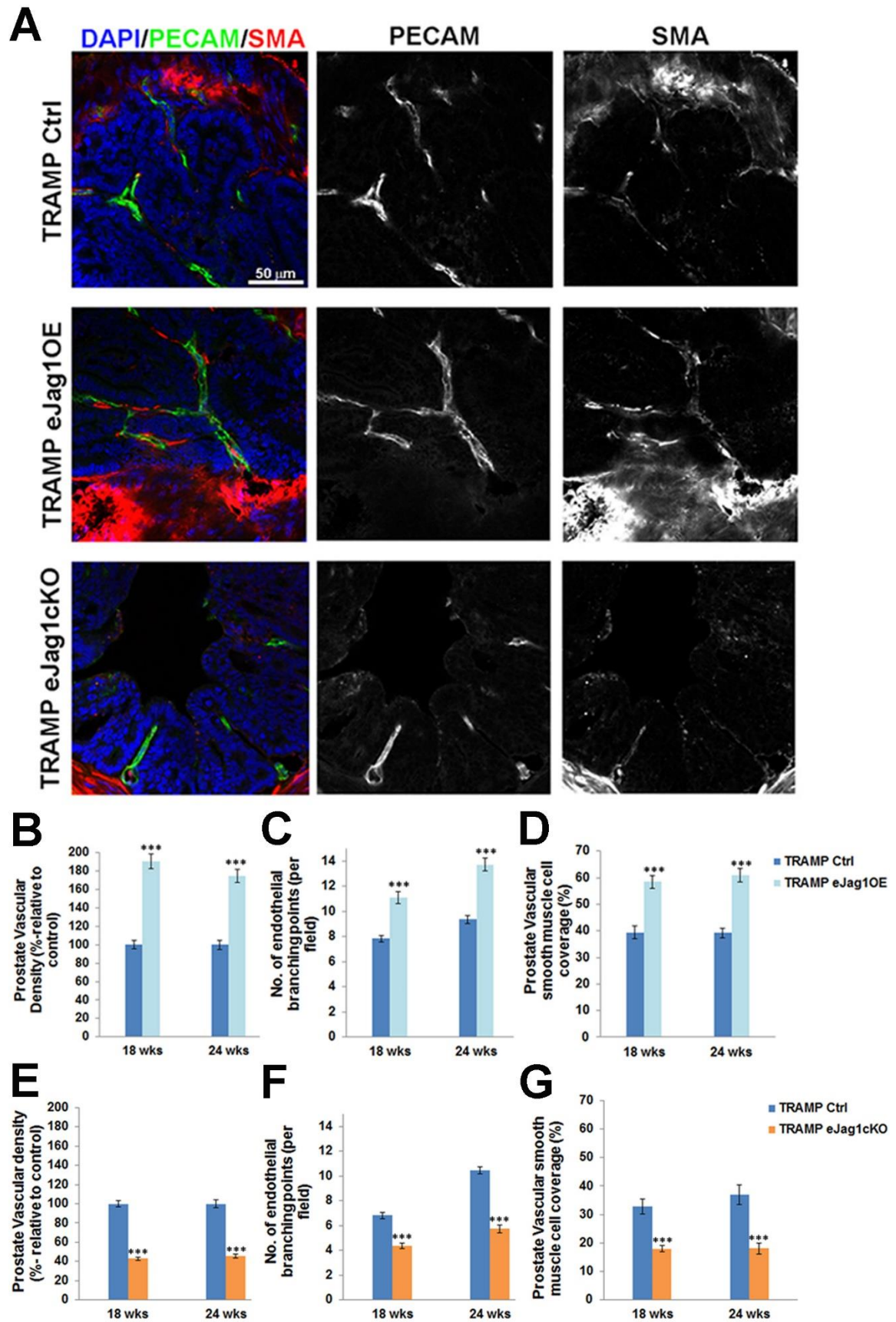
Taken together, endothelial *Jag1* over-expression led to the formation of a dense, mature, and more functional tumor vascular plexus, that contributes to increased tumor growth and progression. Conversely, endothelial *Jag1* loss-of-function led to a sparse, immature, and poorly functional neo-vessel network that substantially inhibits tumor growth.

Supplemental Figure II.3- LLC xenograft tumor vascular phenotype in endothelial specific *Jag1* mutants.



A. Representative immunostaining images (10x amplification) marked for PECAM-1 (green) and SMA (red), to evaluate vascular density and vSMC of xenograft samples. **B.** Percentage of vascular density (relative to control=100%) is increased in endothelial *Jag1* over-expression mutants as shown by PECAM-1 labeling. **C.** Percentage of vascular smooth muscle coverage, showing increased levels of SMA on *eJag1OE* mutant vasculature, relative to controls. **D.** Percentage of vascular density (relative to control=100%) is decreased in endothelial *Jag1* knock-out mutants. **E.** Percentage of vascular smooth muscle coverage, showing decreased levels of SMA on *eJag1cKO* mutant vasculature, relative to controls. DAPI (blue) stains nuclei. Error bars represent SEM; ** represents $p < 0.01$; *** represents $p < 0.001$.

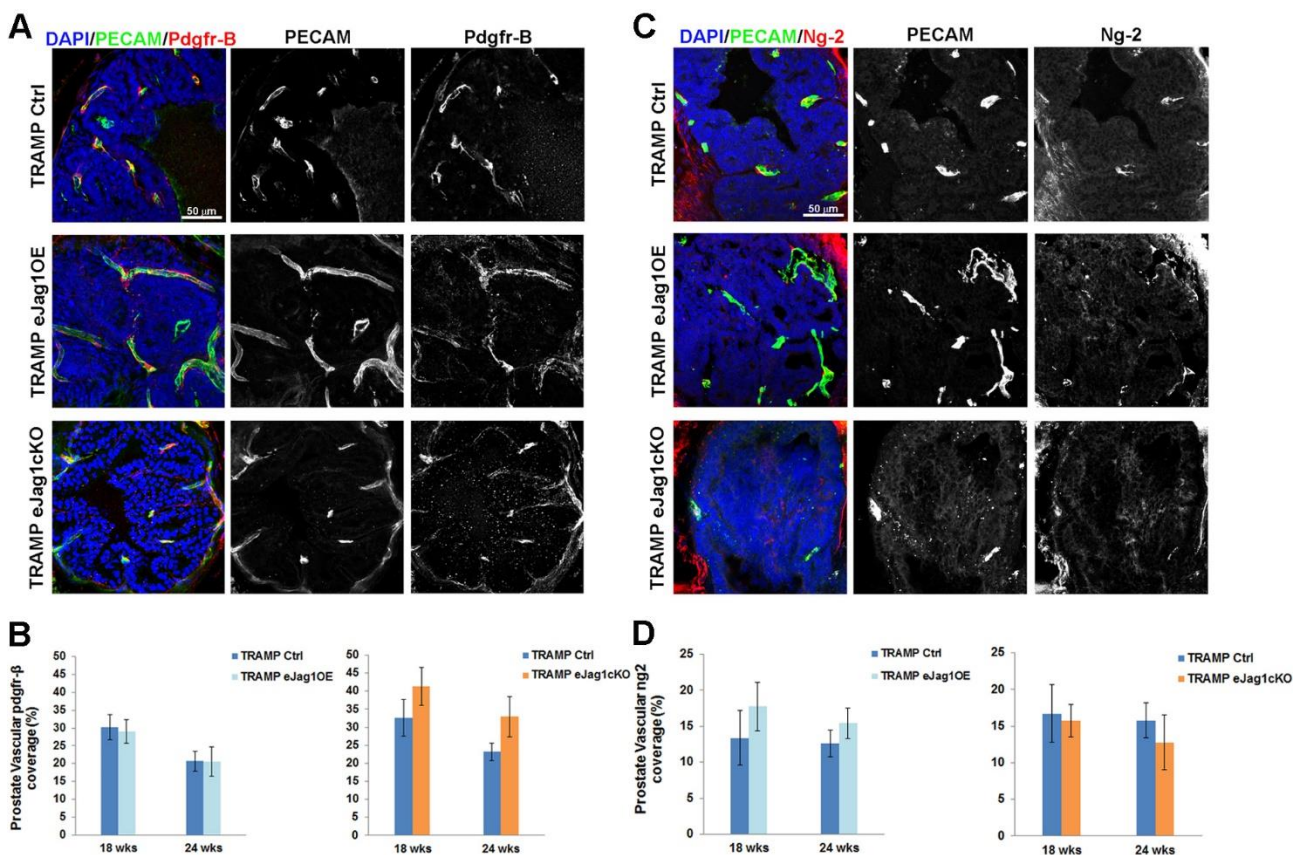
Figure II.3- Prostate tumor vascular phenotype in TRAMP endothelial-specific Jag1 mutants.



A. Representative confocal (one z layer) immunostaining images (40x amplification) marked for PECAM-1 (green) and SMA (red), to evaluate vascular density and vSMC of prostate samples. B.

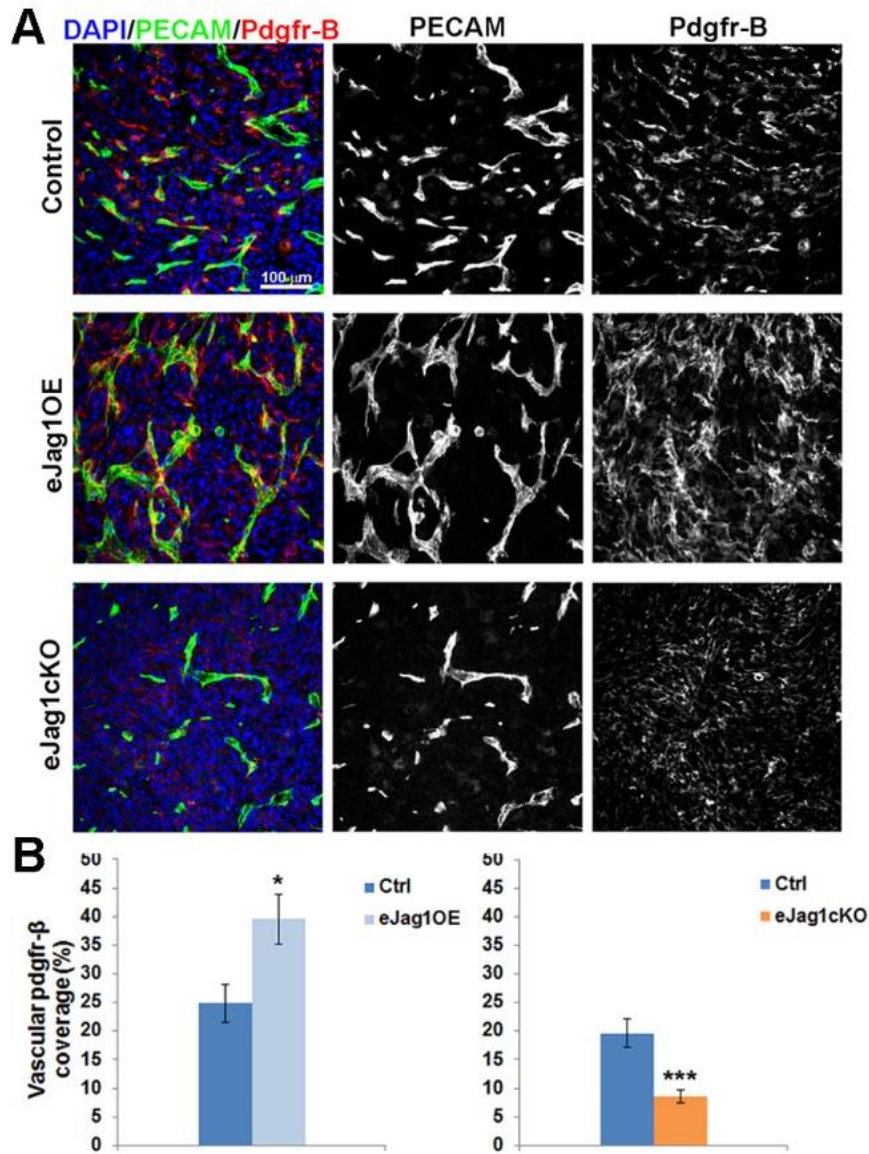
Percentage of vascular density (relative to control = 100%) is increased in TRAMP endothelial *Jag1* over-expression mutants as shown by PECAM-1 labeling. **C.** Number of endothelial branching points, demonstrating increased branching in TRAMP.e*Jag1*OE relative to controls. **D.** Percentage of vascular smooth muscle coverage, showing increased levels of SMA on TRAMP *eJag1*OE mutant vasculature, relative to controls. **E.** Percentage of vascular density (relative to control=100%) is decreased in TRAMP endothelial *Jag1* knock-out mutants. **F.** Number of endothelial branching points, demonstrating decreased branching in TRAMP.e*Jag1*cKO relative to controls. **G.** Percentage of vascular smooth muscle coverage, showing decreased levels of SMA on TRAMP *eJag1*cKO mutant vasculature, relative to controls. DAPI (blue) stains nuclei. Error bars represent SEM; * represents $p < 0.05$; ** represents $p < 0.01$; *** represents $p < 0.001$.

Supplemental Figure II.4- Prostate tumor endothelial pericyte coverage in TRAMP endothelial-specific *Jag1* mutants.



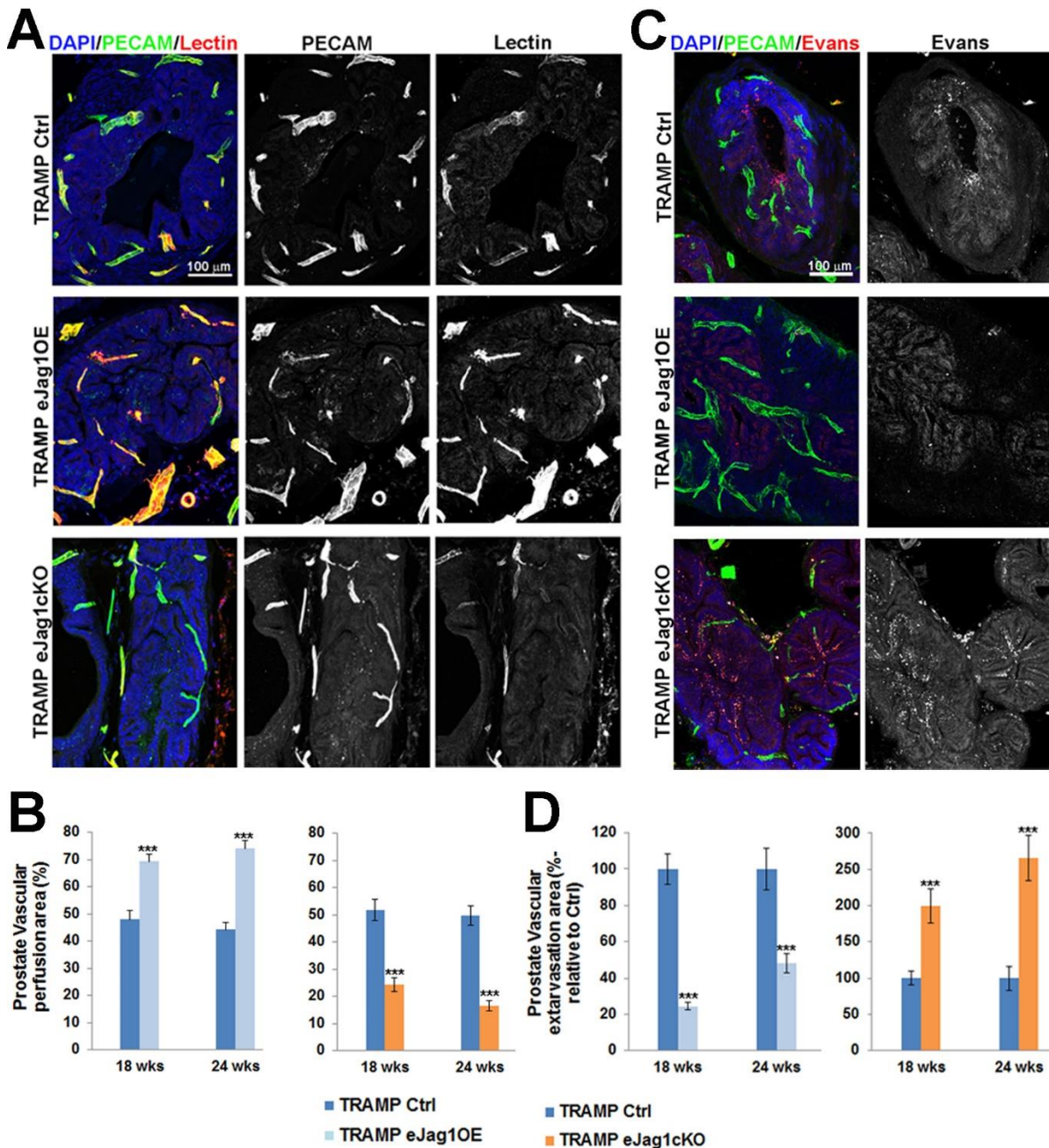
A. Representative confocal immunostaining images (40x amplification) marked for PECAM-1 (green) and Pdgfr-β (red), to evaluate pericyte vascular coverage of prostate samples. **B.** Percentage of prostate vascular Pdgfr-β coverage in TRAMP.e*Jag1*OE and KO mutants showing no significant difference from the controls. **(C)** Representative confocal immunostaining images (40x amplification) marked for PECAM-1 (green) and Ng-2 (red), to evaluate pericyte vascular coverage of prostate samples. **D.** Percentage of prostate vascular Ng-2 coverage in TRAMP.e*Jag1*OE and KO mutants showing no significant difference from the controls.

Supplemental Figure II.5- LLC xenograft tumor endothelial pericyte coverage in endothelial-specific *Jag1* mutants.



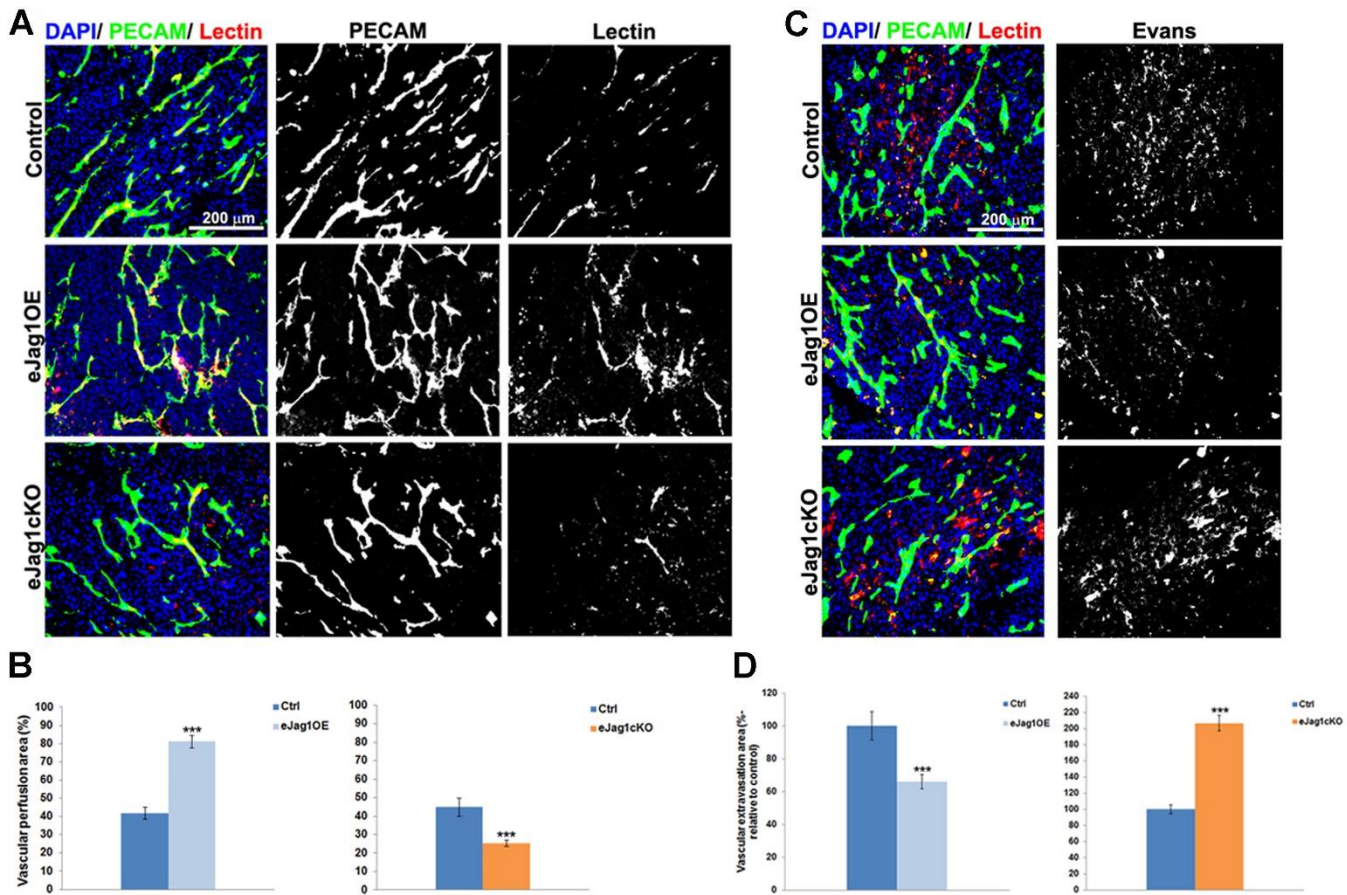
A. Representative immunostaining images (20x amplification) marked for PECAM-1 (green) and Pdgfr- β (red), to evaluate pericyte vascular coverage of LLCs tumor samples. **B.** Percentage of vascular Pdgfr- β coverage in e*Jag1*OE and KO mutants showing increased and decreased coverage relative to the controls, respectively. DAPI (blue) stains nuclei. Error bars represent SEM; ** represents $p < 0.01$; *** represents $p < 0.001$.

Figure II.4- Prostate tumor vascular perfusion and extravasation in TRAMP endothelial-specific Jag1 mutants.



A. Lectin (red) and PECAM-1 (green) confocal immunostaining (20x amplification) (maximum intensity projections) of TRAMP.eJag1OE and TRAMP.eJag1cKO mutants, to evaluate the co-localization of both signals, indicative of vessel perfusion. **B.** Percentage of perfused area in the total vascular area (given by vascular density measurements) showing increased and decreased lectin labeling in the endothelial Jag1 over-expression and loss-of-function vasculature, respectively. **C.** Evans' Blue (red) and PECAM-1 (green) confocal immunostaining (20x amplification) images (maximum intensity projections) showing the extravasation areas. **D.** Percentage of vascular extravasation area in the total vascular area, showing decreased Evans' Blue staining in TRAMP.eJag1OE, and increased in TRAMP.eJag1cKO mutants. DAPI (blue) stains nuclei. Error bars represent SEM; *** represents $p < 0.001$.

Supplemental Figure II.6- LLC xenograft tumor vascular perfusion and extravasation in endothelial specific *Jag1* mutants.



A. Lectin (red) and PECAM-1 (green) immunostaining (20x amplification) of *eJag1OE* and *eJag1cKO* mutants xenografts, to evaluate the co-localization of both signals, indicative of vessel perfusion. **B.** Percentage of perfused area in the total vascular area (given by vascular density measurements) showing increased and decreased lectin labeling in the endothelial *Jag1* over-expression and loss-of-function vasculature, respectively. **C.** Evans' Blue (red) and PECAM-1 (green) immunostaining (20x amplification) images showing the extravasation areas. **D.** Percentage of vascular extravasation area in the total vascular area, showing decreased Evans' Blue staining in *eJag1OE*, while increased in *eJag1cKO* mutants. DAPI (blue) stains nuclei. Error bars represent SEM; *** represents p<0.001.

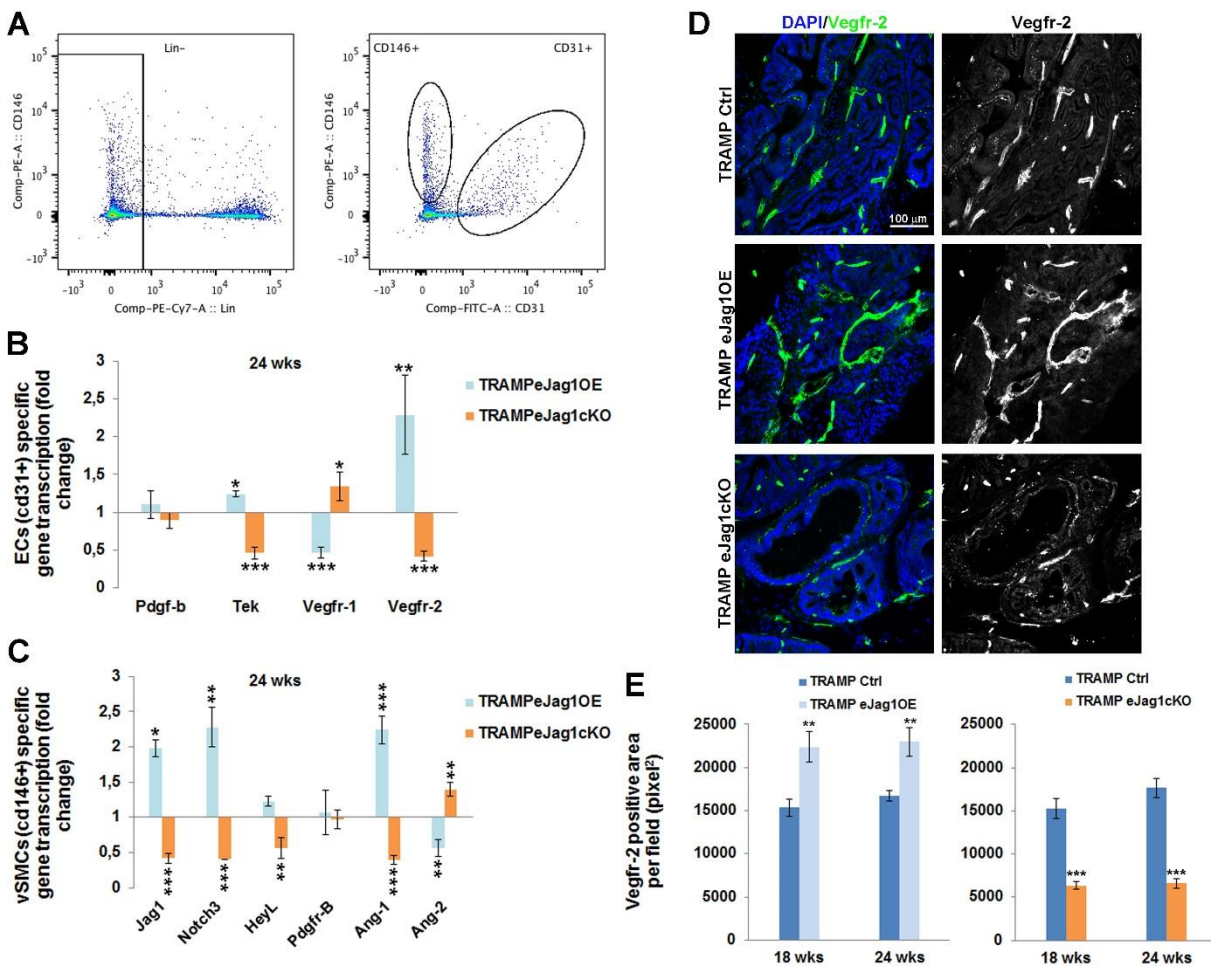
4.4 Endothelial Jagged1 elicits changes in the transcription profile of angiocrine factors of endothelial and perivascular tumor associated cells

In order to better understand the molecular mechanisms behind the tumor vascular phenotypes observed in *eJag1OE* and *eJag1cKO* mutants, we performed RT-qPCR analysis of selected genes (Figure II.5). RNA was extracted from ECs (Lin- (ter119-cd45-) cd31+) and vSMC cells (Lin- (ter119-cd45-) cd146+cd31-) FACS sorted from prostate samples collected at early and late stages of tumor development (Figure II.5A).

ECs specific gene transcription (Figure II.5B and Suppl. Figure II.7A), revealed that the levels for *Pdgfb* transcription, encoding PDGF-B, the endothelial ligand for PDGFR β , which controls

the recruitment of pericytes, was not significantly altered in either of the mutants (Figure II.5B), even though a significant down-regulation in *eJag1cKO* early stage prostate samples was observed (Suppl. Figure II.7A). *Tek* (encoding the Tie2 receptor tyrosine kinase) which regulates vascular permeability and maturation (Vikkula et al., 1996) was downregulated in *eJag1cKO* mutants and increased in gain-of-function mutants at both time points. Regarding vascular endothelial growth factor receptor-1 (*Vegfr1/Flt1*) transcription in prostate tumor samples we observed a down-regulation in TRAMP.*eJag1OE* and an up-regulation in TRAMP.*eJag1cKO*. In contrast, *Vegfr-2 (Vegfr2/Kdr/Flk1)* levels were positively modulated by endothelial Jagged1, with up-regulation and down-regulation in OE and KO prostate samples, respectively.

Figure II.5- Transcription profile of angiocrine factors by endothelial and perivascular tumor associated cells in TRAMP endothelial-specific *Jag1* mutants.



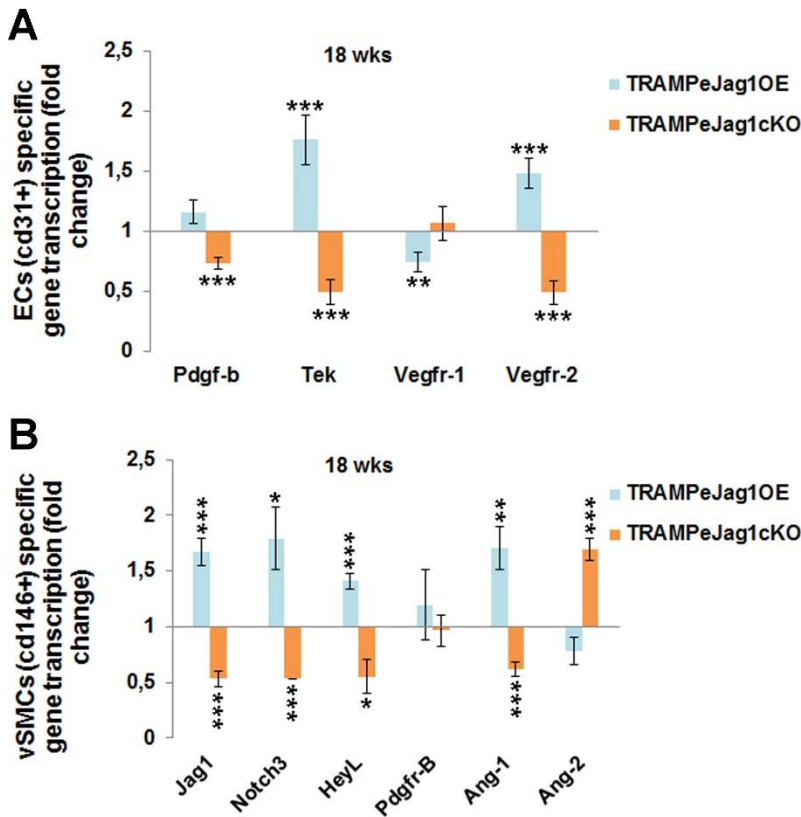
RNA was isolated from prostates collected at the end-point, and gene transcript analysis was performed by quantitative real-time RT-PCR for genes involved in angiogenesis. **A.** ECs (Lin- (cd45- ter119-) cd31+) and vSMCs (Lin- (cd45- ter119-) cd146+cd31-) sorted populations for specific gene transcription analysis. **B.** ECs specific relative gene transcription. **C.** vSMCs specific relative gene transcription. Gene transcript levels were normalized to PECAM-1 mRNA levels, and the house-keeping gene β -actin was used as endogenous control. Blue bars represent the gene expression levels of samples collected from

*eJag1*OE mutants, and orange bars the gene expression levels from *eJag1*cKO mutants, relative to the respective controls. **D.** Representative images of Vegfr-2 immunofluorescence (green) (20x amplification) in TRAMP endothelial-specific *Jag1* mutants. **E.** Quantification of Vegfr-2 positive area per field (pixel²) demonstrating increased stained areas in TRAMP.*eJag1*OE and decreased staining in TRAMP.*eJag1*cKO relative to respective controls. DAPI (blue) stains nuclei. Error bars represent SEM; * represents $p < 0.05$; ** represents $p < 0.01$; *** represents $p < 0.001$.

Furthermore, mural cell specific transcription analysis (Figure II.5C and Suppl. Figure II.7B) revealed a downregulation of *Jag1*, *Notch3* and *HeyL* (perivascular cell Notch effector) in *eJag1*cKO and an upregulation in *eJag1*OE mutants prostates. Additionally, *PdgfrB* (encoding PDGFR β) levels were not altered in response to endothelial Jagged1 modulation, as already demonstrated by protein staining for the receptor. *Ang1* (perivascular ligand for Tie2 receptor), was up-regulated in OE and down-regulated in KO mutants. On the contrary, *Ang2* (antagonistic ligand for Tie2 receptor) was down-regulated in OE and up-regulated in KO mutant.

These results indicate that *Jag1* modulation in the endothelium is able to elicit changes in the expression profiles of angiocrine factors that regulate angiogenesis and the recruitment of mural cells.

Supplemental Figure II.7- Transcription profile of angiocrine factors by endothelial and perivascular tumor associated cells in TRAMP endothelial-specific *Jag1* mutants at 18 weeks of age.



RNA was isolated from prostates collected at the endpoint, and gene transcript analysis was performed by quantitative real-time RT-PCR for genes involved in angiogenesis. **A.** ECs specific relative gene transcription. **B.** vSMCs specific relative gene transcription. Gene transcript levels were normalized to PECAM-1 mRNA levels, and the house-keeping gene β -actin was used as endogenous control. Blue bars represent the gene expression levels of samples collected from

*eJag1*OE mutants, and orange bars the gene expression levels from *eJag1*cKO mutants, relative to the respective controls. Error bars represent SEM; * represents $p < 0.05$; ** represents $p < 0.01$; *** represents $p < 0.001$.

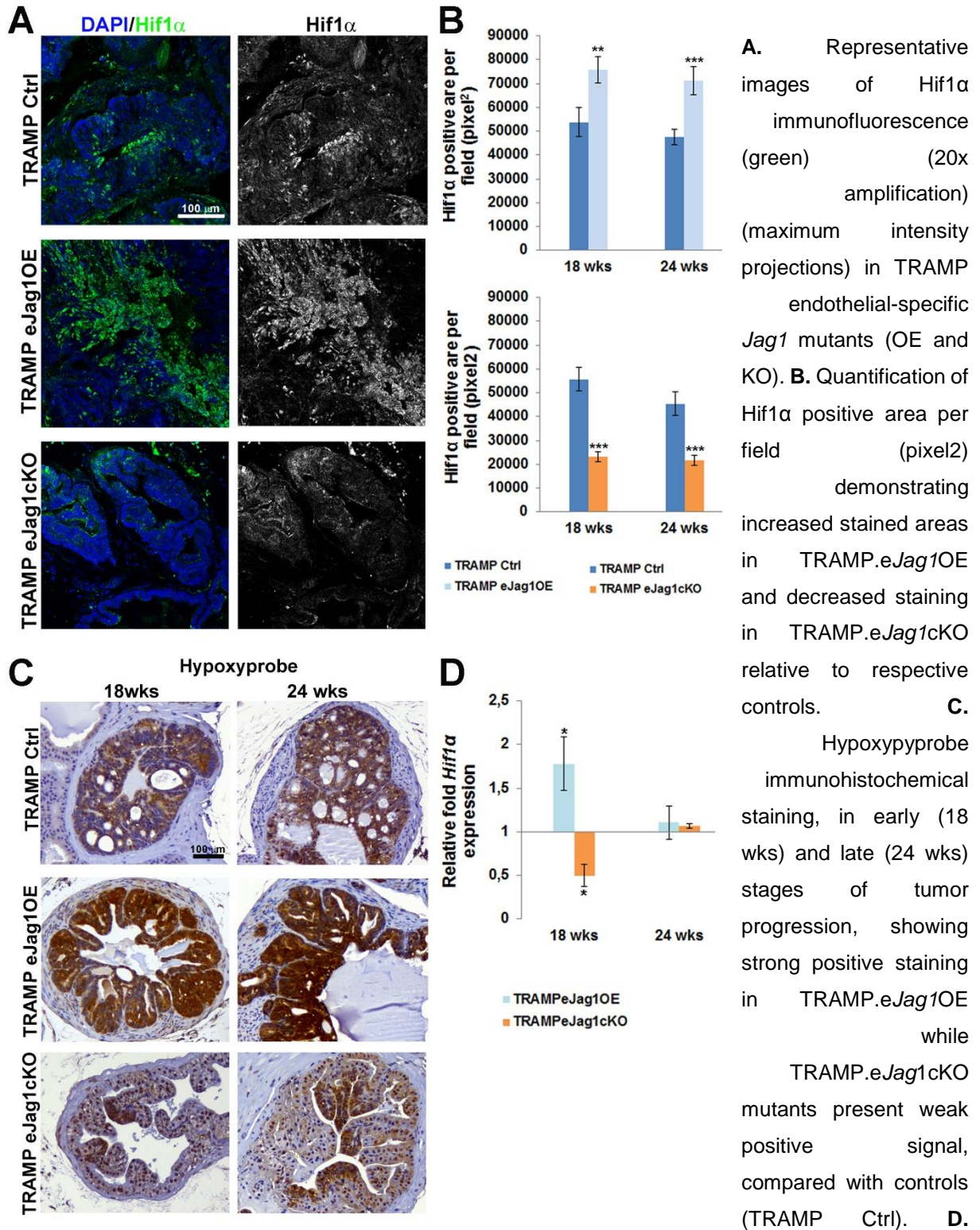
4.5 Modulation of neo-vasculature of prostatic tumors leads to alterations in local hypoxic levels

After characterizing the neo-vasculature of two different tumor models in endothelial *Jag1* specific mutants, we aimed to understand how the different vascular phenotypes were able to cause such significant differences in progression of prostatic cancer in mice. Therefore, in order to evaluate tumor hypoxia, immunostaining for Hif1 α was performed in prostatic samples from TRAMP *eJag1* mutants. As can be observed in Figure II.6A and B, *eJag1*OE mutants presented increased levels of Hif1 α , whereas *eJag1*cKO show decreased levels, relative to the respective controls, in either early (18 wks) or late (24 wks) stages of tumor progression. In addition, hypoxyprobe was administered to mice prior to dissection in order to visualize the tumor areas with low oxygen pressure ($pO_2 = 10$ mmHg) (Figure II.6C). The response observed was consistent with Hif1 α staining in both TRAMP.*eJag1*OE, with stronger and extended areas of positive staining, and TRAMP.*eJag1*cKO mutants, that presented only weak and localized staining. Transcript levels of *Hif1 α* mRNA were also analyzed by qRT-PCR (Figure II.6D). *Hif1 α* mRNA levels varied in the same manner as the protein staining, with up-regulation in OE and down-regulation in KO mutants, but only in an early stage (18 wks). Surprisingly, in a late stage (24 wks) no differences were observed between the different mutants and the respective controls.

4.6 Endothelial Jagged1 induces proliferation and inhibits apoptosis in the surrounding tumor tissues

To better understand the metabolic changes in prostatic tumor development caused by altered vascular supply, cellular apoptosis and proliferation were addressed by immunostaining for active caspase 3 and ki67, respectively, on prostate samples from TRAMP.*eJag1* mutants (Figure II.7). Endothelial *Jag1* overexpression in TRAMP mice (TRAMP.*eJag1*OE) led to decreased apoptosis (Figure II.7A and B) and increased cellular proliferation (Figure II.7A and C). On the other hand, endothelial *Jag1* loss-of-function (TRAMP.*eJag1*cKO) resulted in increased cellular apoptosis (Figure II.7A and D) and decreased proliferation (Figure II.7A and E).

Figure II.6- Prostate tumor hypoxic levels in TRAMP endothelial-specific *Jag1* mutants.



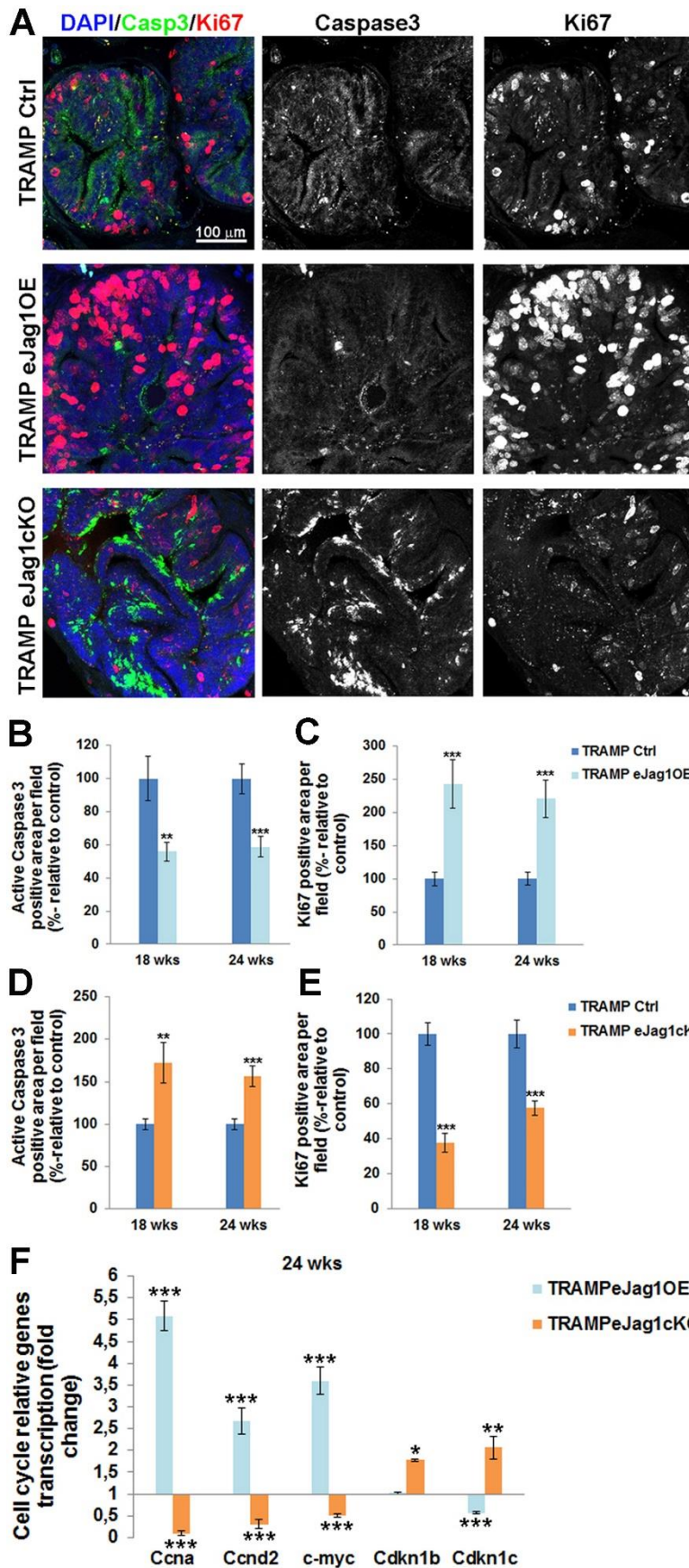
Moreover, we profiled the transcription of several important cell-cycle regulatory genes in TRAMP.e*Jag1* prostate samples (Figure II.7F). There was up-regulation and down-regulation of the cell-cycle stimulating genes, *Ccna* (encoding for Cyclin A), *Ccnd2* (encoding for CyclinD2), and *c-myc*, in OE and KO samples, respectively. Conversely, the opposite response was observed in the cell-cycle inhibitors, *Cdkn1b* (*p27*, encoding for Cyclin-Dependent Kinase Inhibitor 1B) and *Cdkn1c* (*p57*, encoding for Cyclin-Dependent Kinase Inhibitor 1C): in TRAMP.e*Jag1*OE prostate samples *Cdkn1c* was down-regulated while in TRAMP.e*Jag1*cKO both kinase inhibitors were up-regulated.

4.7 Modulation of endothelial *Jag1* leads to alterations in epithelial-to-mesenchymal transition (EMT)

Lastly, we intended to investigate if the alterations in vascular supply of the prostate tumors, and consequently altered metabolism of tumor cells, would contribute to increased and/or decreased pressure for the acquisition of an invasive phenotype and to epithelial-to-mesenchymal transition. To this purpose, we performed immunostaining for the epithelial adhesion marker, E-cadherin, and for Snail, a transcription factor known for the induction of EMT (Thiery, 2002), in the prostatic lesions of TRAMP mice.

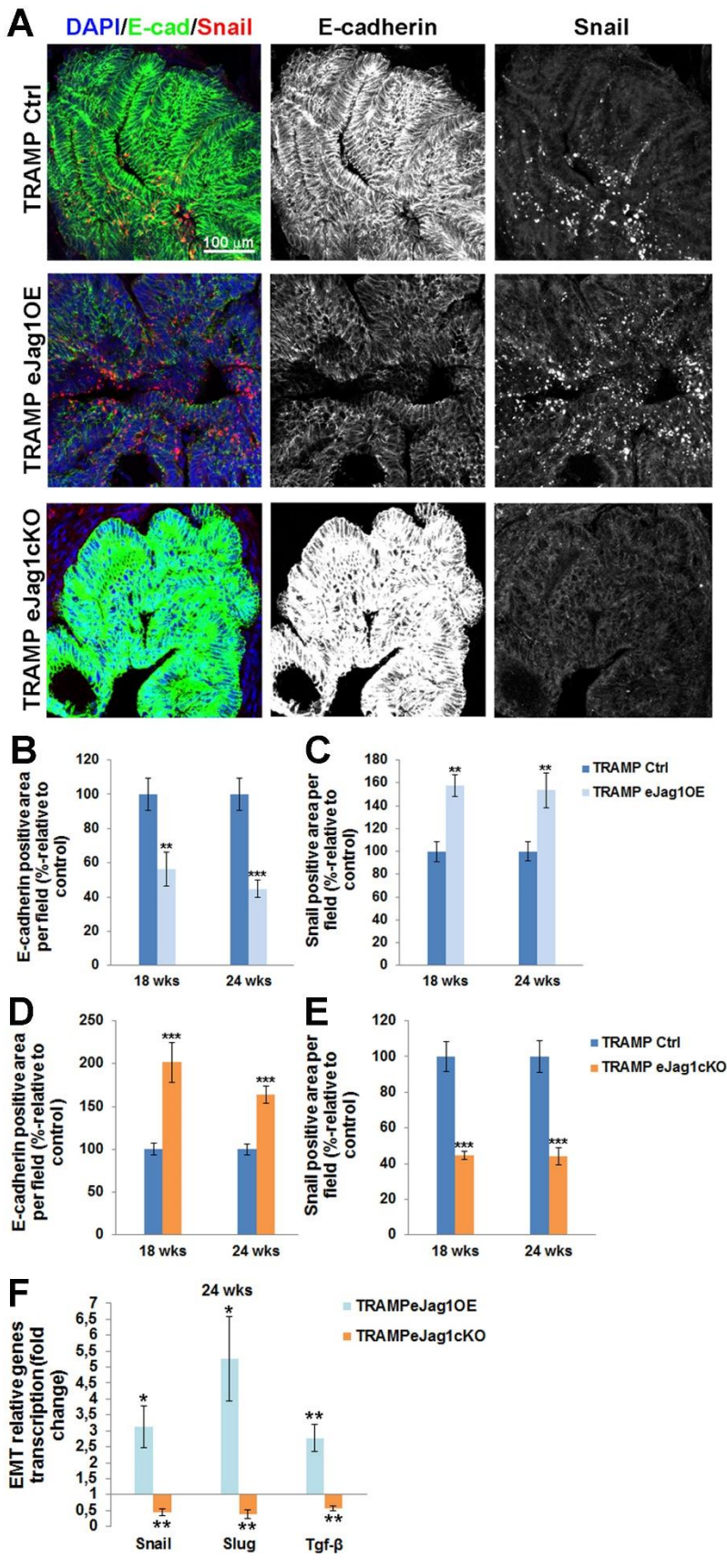
Over-expression of endothelial *Jag1* (TRAMP. e*Jag1*OE) was associated with substantial loss of E-cadherin expression (Figure II.8A and B) and increased expression of Snail (Figure II.8A and C) relative to the respective controls. Conversely, both *Snail* and *Slug* mRNA expression levels were increased in these mutants (Figure II.8F). In contrast, loss of endothelial *Jag1* (TRAMP. e*Jag1*cKO) was associated with increased E-cadherin expression (Figure II.8A and D) and decreased Snail expression (Figure II.8A and E), relative to the respective controls. In these mutants the levels of mRNA expression of both *Snail* and *Slug* were also decreased (Figure II.8F). We also analyzed *tgf-β* transcription levels, since it is a known Jagged1 dependent regulator of EMT (Zavadil et al., 2004), and observed increased and decreased transcription in OE and KO prostates, respectively (Figure II.8F).

Figure II.7- Prostate cellular apoptosis and proliferation in TRAMP endothelial-specific Jag1 mutants.



A. Representative images of active Caspase3 (green) and Ki67 (red) immunofluorescence staining (20x amplification) (maximum intensity projections) in TRAMP endothelial-specific *Jag1* mutants (OE and KO). **B.** Prostatic lesions of TRAMP.e*Jag1*OE mutants presented decreased percentage of active caspase3 positive area per field, relative to control (100%), either at 18 as at 24 weeks of age. **C.** Prostate samples from TRAMP.e*Jag1*OE presented increased percentage of Ki67 positive area per field, relative to control (100%), at both time points (18 and 24 wks). **D.** Prostatic lesions of TRAMP.e*Jag1*cKO mutants presented increased percentage of active caspase3 positive area per field, relative to control (100%), at 18 and 24 weeks of age. **E.** Prostate samples from TRAMP.e*Jag1*cKO presented decreased percentage of Ki67 positive area per field, relative to control (100%), at both time points (18 and 24 wks). **F.** Relative fold mRNA expression of cell cycle regulatory genes in TRAMP.e*Jag1*OE and TRAMP.e*Jag1*cKO mutants, at 24 weeks of age. DAPI (blue) stains nuclei. Error bars represent SEM; * represents $p < 0.05$; ** represents $p < 0.01$; *** represents $p < 0.001$.

Figure II.8- Epithelial-to-mesenchymal transition in prostate lesions of TRAMP endothelial-specific *Jag1* mutants.



A. Representative images of E-cadherin (green) and Snail (red) immunofluorescence staining (20x amplification) (maximum intensity projections) in TRAMP.eJag1OE and TRAMP.eJag1cKO mutants. **B.** Decreased percentage of E-cadherin per field in TRAMP.eJag1OE mutants, relative to respective controls (100%), at 18 and 24 weeks of age. **C.** Increased Snail positive area per field in OE mutants, relative to respective controls (100%). **D.** Increased percentage of E-cadherin per field in TRAMP.eJag1cKO mutants, relative to respective controls (100%), at 18 and 24 weeks of age. **E.** Decreased Snail positive area per field in KO mutants, relative to respective controls (100%). **F.** Relative fold of *Snail*, *Slug* and *Tgf-β* mRNA expression, demonstrating increased expression in the prostate of TRAMP.eJag1OE mutants whereas in TRAMP.eJag1cKO mutants prostate their expression is decreased at 24 weeks of age. DAPI (blue) stains nuclei. Error bars represent SEM; * represents $p < 0.05$; ** represents $p < 0.01$; *** represents $p < 0.001$.

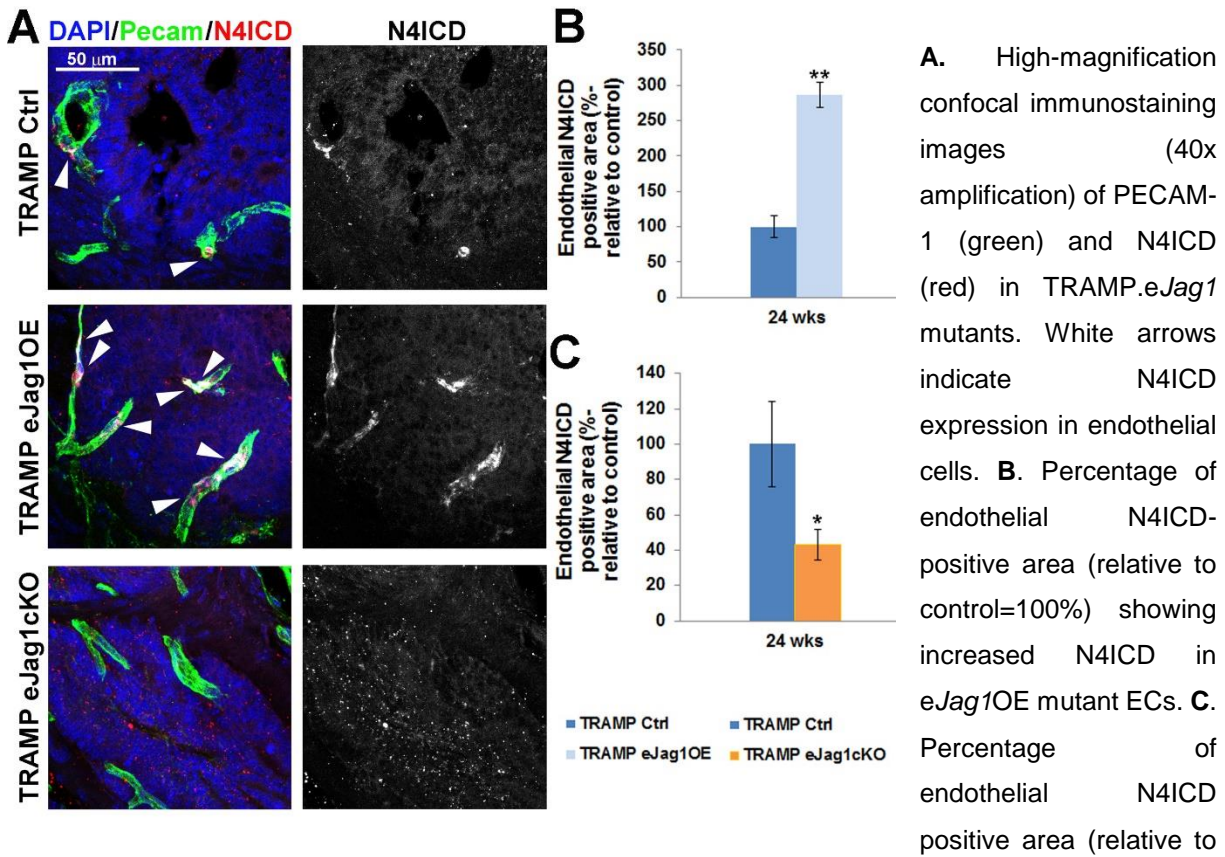
4.8 Endothelial Jagged1 exerts its angiogenic function through Notch4/Hey1 and its angiocrine function through Notch3/Hey1 influencing tumor cell proliferation and de-differentiation

Having previously established that endothelial Jagged1 is able to activate Notch4 in a physiological angiogenic response (Pedrosa et al., 2015a), we wanted to confirm this in a tumor setting. To do it, we immunostained the intracellular domain of Notch4 (N4ICD) in our TRAMP.*eJag1* mutants and co-localized it with PECAM to evaluate endothelial activation of Notch4 (Suppl. Figure II.8). In TRAMP. *eJag1*OE prostates we observed increased double positive staining for N4ICD and Pecam (Suppl. Figure II.8A and B) whereas in TRAMP.*eJag1*cKO prostates N4ICD staining was decreased in the endothelium (Suppl. Figure II.8A and C).

In our previous study (Pedrosa et al., 2015a), Hey1 was the main Notch effector found downstream of Jagged1/Notch4 signaling. Therefore we aimed to quantify Hey1 in the vasculature of *eJag1* mutants. As shown in Figure II.9, in TRAMP.*eJag1*OE mutants prostates there were increased levels of Hey1 staining in the endothelium, while in TRAMP.*eJag1*cKO prostates they were decreased (Figure II.9A and B). Interestingly, we observed increased and decreased Hey1 staining in tumor cells adjacent to the vessels (Figure II.9A and C), in OE and KO samples, respectively, relative to controls. Additionally, Hey1 modulation by endothelial Jagged1 was confirmed at the transcript level (Figure II.9D and E) in both ECs specific and whole prostate mRNA analysis. TRAMP.*eJag1*OE mutants presented *Hey1* up-regulation in ECs (Figure II.9D) and in whole prostate (Figure 9E), whereas *eJag1*cKO mutants presented a down-regulation response.

Given the significant activation of Notch signaling, by Hey1 transcription and expression, observed in tumor cells adjacent to the vasculature, we hypothesized that a specific Notch receptor was being activated by endothelial Jagged1. Endothelial Jagged1 has been shown to be able to activate Notch3 in adjacent perivascular cells (Liu et al., 2009). Additionally, high levels of Notch3 have been described in prostate cancer cells with high metastatic potential (Ross et al., 2011). Therefore, we hypothesized that endothelial Jagged1 could also be acting as an angiocrine factor activating Notch3 in adjacent tumor cells, and consequently regulating proliferation and de-differentiation. To test this hypothesis, we immunostained TRAMP.*eJag1* samples for N3ICD concomitantly with Ki67 and E-cadherin (Figure II.9F and G). TRAMP.*eJag1*OE mutants presented increased staining for N3ICD whereas *eJag1*cKO mutants presented decreased staining, relative to controls. Remarkably, as shown in Figure II.9F, the tumor areas that display activated Notch3 staining also have increased ki67 positive staining and loss of E-cadherin.

Supplemental Figure II.8- Immunostaining for Notch4 intra-cellular domains (N4ICD) in TRAMP.eJag1OE and eJag1cKO mutants.



control-100%), showing the decreased co-localization of N4 activated form with ECs (white arrows) in eJag1cKO mutants. DAPI (blue) stains nuclei. Error bars represent SEM; * represents $p < 0.05$; ** represents $p < 0.01$; *** represents $p < 0.001$.

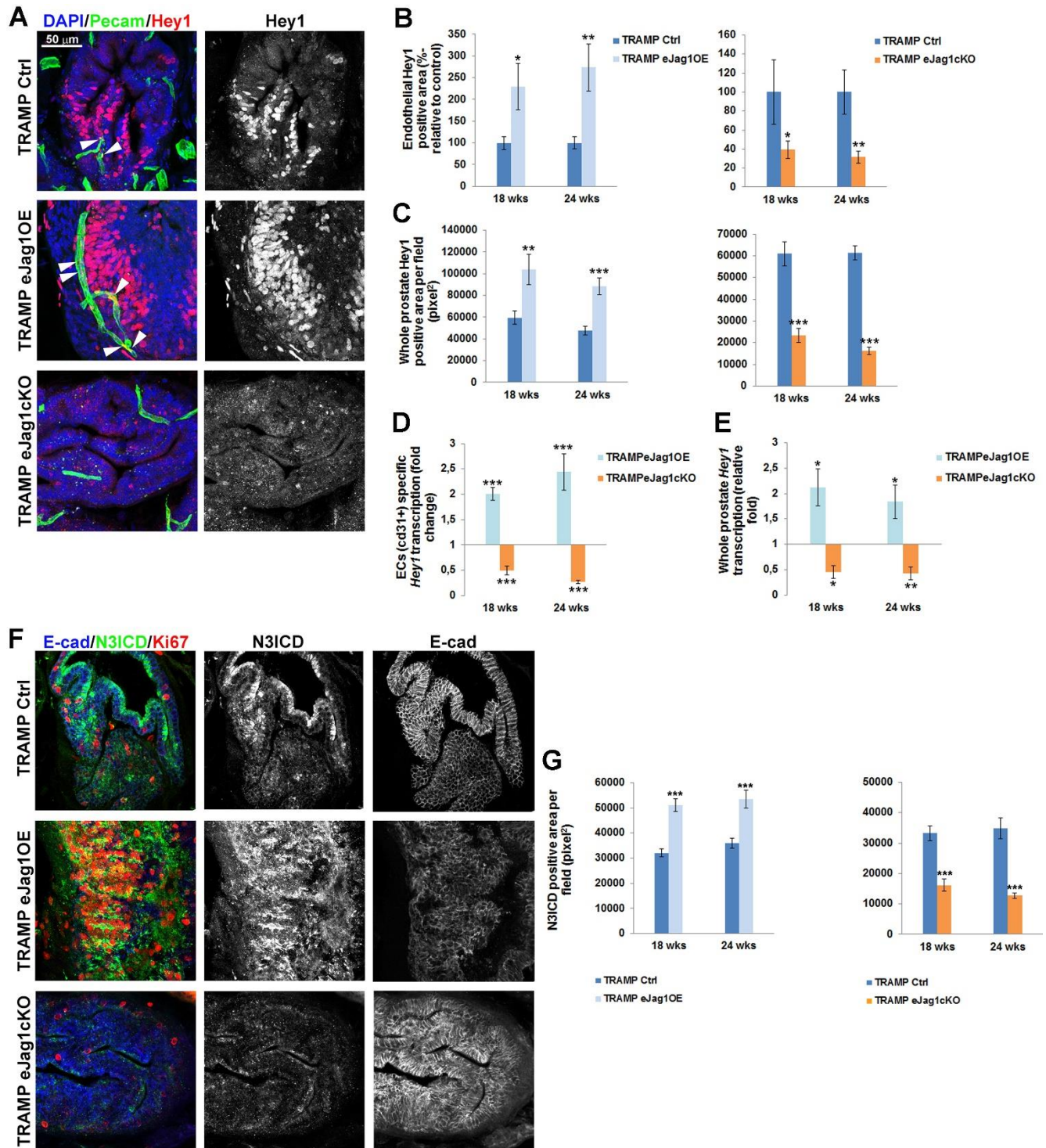
5. Discussion

In the last decades tumor angiogenesis has become a very active area of research, resulting in the introduction of anti-angiogenic drugs in cancer therapy, such as the anti-VEGF antibody bevacizumab (Hurwitz et al., 2004) and the tyrosine kinase inhibitors like sunitinib or sorafenib (Meadows & Hurwitz, 2012). Many other molecules have been investigated since for their effect on angiogenesis. Modulation of endothelial *Jag1* was previously shown to be crucial in developing retina vascularization (Benedito et al., 2009). The results presented here describe the effect of modulating endothelial *Jag1* in tumor angiogenesis and metabolism and consequently in tumor development and progression.

We observed that endothelial *Jag1* over-expression accelerated the growing rate of LLC subcutaneous tumor transplants and contributed to the progression and development of prostate cancer in TRAMP mice. This effect was associated with an increase in the density and branching of the tumor vessels. In contrast, endothelial *Jag1* loss-of-function delayed the growing rate of LLC subcutaneous transplants and inhibited the development of prostate lesions in TRAMP mice, by decreasing the density and branching of the tumor neo-vasculature.

This appears to be consistent with a report stating that increased tumor microvascular density (MVD) constitutes a bad prognostic indicator in several solid tumors that induce significant angiogenesis (Weidner, Carroll, Flax, Blumenfeld, & Folkman, 1993).

Figure II.9- Hey1 transcription and expression and Notch3 intracellular domain (N3ICD) expression in prostate lesions of TRAMP endothelial-specific *Jag1* mutants.



A. Representative images of Hey1 (red) and Pecam (green) immunofluorescence staining (40x amplification) (maximum intensity projections) in TRAMP.eJag1OE and TRAMP.eJag1cKO mutants. White arrows indicate Hey1 expression in endothelial cells. **B.** Quantification of endothelial Hey1 positive

area per field (%-relative to control) in TRAMP. *eJag1*OE (left) and TRAMP.*eJag1*cKO (right), demonstrating increased and decreased double positive staining for Hey1/Pecam in *eJag1* mutants, respectively. **C.** Quantification of whole prostate Hey1 positive area per field (pixel²), demonstrating increased and decreased areas in OE (left) and KO (right) mutants, respectively. **D.** and **E.** ECs specific and whole prostate Hey1 transcription analysis in TRAMP.*eJag1* prostates. **F.** Representative images of N3ICD (green), E-cadherin (blue) and Ki-67 (red) immunofluorescence staining (40x amplification) (maximum intensity projections) in TRAMP.*eJag1*OE and TRAMP.*eJag1*cKO mutants. **G.** Quantification of N3ICD positive area per field (pixel²), demonstrating increased and decreased areas, relative to controls, of *eJag1*OE and *eJag1*cKO prostates, respectively. DAPI (blue) stains nuclei. Error bars represent SEM; * represents $p < 0.05$; ** represents $p < 0.01$; *** represents $p < 0.001$.

From the observations in the TRAMP model, where there is a stepwise progression of tumor development, no major differences were observed in the vascular response between early (18 wks) and late (24 wks) stages, which is thought to be a consequence of the angiogenic switch occurring relatively early on the onset of prostatic lesions and therefore before 18 wks of age (Huss, Hanrahan, Barrios, Simons, & Greenberg, 2001). In this report we show that endothelial Jagged1 acts as a pro-angiogenic ligand in a tumor setting, after having recently demonstrated this effect in a regenerative setting (Pedrosa et al., 2015a), where Jagged1 antagonizes Dll4 regulation of endothelial branching, by its ability to block Dll4/Notch1 activation and thus by positively regulating Vegfr-2 transcription. Here, we have further validated and complemented the mechanistic process by which endothelial Jagged1 exerts its pro-angiogenic function, by showing that it not only positively regulates Vegfr-2 transcription and expression, but that it also negatively regulates Vegfr-1 transcription, specifically in ECs. Accordingly, a recent report using a Notch decoy that specifically blocks Jagged ligands mediated interaction (Kangsamaksin et al., 2014) has shown that the anti-angiogenic effect observed is likely due to increased secretion of the soluble form of Vegfr-1, and thus decreased Vegf/Vegfr-2 signaling.

In addition, in confirming the pro-angiogenic function of endothelial Jagged1 in tumors, we have identified a new role for it in promoting blood vessel maturation in tumor angiogenesis, since *eJag1*OE tumor vasculature presented increased coverage of SMA+ cells, whereas the vasculature of *eJag1*KO mutants presented the opposite phenotype. Moreover, the ECs and SMCs specific mRNA levels of *angpt1* (encoding angiopoetin1) and *tek* (encoding tie-2 receptor), respectively, members of one of the main signaling pathways involved in the recruitment of support cells to the vessel wall (Thomas & Augustin, 2009), also responded accordingly with modulation of *eJag1*. Additionally, endothelial Jagged1 was also able to positively regulate vSMC specific *Jag1* and *Notch3* and *HeyL* levels, supporting the existing model where activation of perivascular Notch3 and HeyL effector is essential for the assembly of a SM layer (Liu et al., 2009). The contribution of endothelial Jagged1 to vSMC recruitment has already been described in other angiogenic settings (High et al., 2008; Liu et al., 2009; Manderfield et al., 2012). Moreover, we have also suggested previously that the perivascular

phenotype observed in *eJag1* mutants can also be a consequence of Notch4 activation by endothelial Jagged1. Inclusive we have not only demonstrated increased and decreased levels of active Notch4 in OE and KO mutants, respectively, but also increased vessel maturation upon administration of a Notch4 specific agonist to WT mice (Pedrosa et al., 2015a). Here, we have further validated Notch4 as a strong endothelial receptor for Jagged1. In tumors, pericyte coverage decrease and perturbed associations between pericytes and endothelial layer have been described (Abramsson, 2002; Raza, Franklin, & Dudek, 2010). However, we found no significant alterations in pericyte number by *pdgfr-β* or *ng-2* immunostaining or changes in the levels of *pdgfr-β* mRNA in *eJag1* mutant's prostate tumor vasculature, suggesting that the observed changes in vascular maturation are independent of pericyte coverage. Nonetheless, in the LLCs transplant model, modulation of endothelial Jagged1 produced alterations in pericyte coverage, suggesting that the absence of effect on pericyte coverage by Jagged1 function modulation seems to be prostate specific. Similarly, the use of a Jagged specific Notch decoy (Kangsamaksin et al., 2014), presented the same perivascular phenotype as the one caused by endothelial Jagged1 loss-of-function.

Modulation of tumor angiogenesis and maturation by endothelial Jagged1 led to alterations in functionality and permeability of tumor vessels, which ultimately may lead to different hypoxic and metabolic responses of tumor cells. Over-expression of endothelial *Jag1* culminated in increased perfusion and decreased extravasation, while endothelial loss-of-function caused the tumor vasculature to be less perfused and leakier. This was likely to cause, respectively, increased and decreased delivery of oxygen to tumor cells. However, unexpectedly, quantification of Hif1 α protein and mRNA levels, as well as pimonidazole-thiol adducts formation by hypoxyprobe administration, indicates that OE and KO mutant prostatic tissues have increased and decreased hypoxic levels, respectively. It is known that Hif1 α is up-regulated in most prostate tumor tissues, compared with normal and benign prostate tissues (Zhong, Semenza, Simons, & De Marzo, 2004). Additionally, it is also established that prostate cancer cells have the ability to compensate the lack of oxygen by anaerobic glycolytic respiration (Higgins et al., 2009), which is able to persist upon neovascularization, suggesting that the glycolytic phenotype arises from genetic or epigenetic changes (Costello & Franklin, 2005).

It seems clear that from the early beginning of tumor epithelial transformation (demonstrated in lesions of TRAMP.*eJag1cKO*) the local concentration of oxygen drops in the affected areas. It is also clear that the oxygen concentration levels are inversely proportional to the degree of dysplasia. We have observed that endothelial Jagged1 contributes to tumor dysplasia through two distinct effects: a pro-angiogenic effect, increasing tumor vascular density, maturation and perfusion; and an angiocrine effect likely through Notch3/Hey1 stimulation of tumor cell proliferation. Therefore we propose that the angiogenic and angiocrine functions of endothelial Jagged1 both contribute to increase proliferation and reduce apoptosis leading to increased

consumption of local oxygen with consequent acidotic microenvironment conditions and increased hypoxia. Therefore the TRAMP.*eJag1OE* prostates, that present the most aggressive lesions, also present the lowest oxygen levels.

Moreover, numerous reports have also described a crosstalk between Notch and hypoxia signaling pathways (Pear & Simon, 2005). Inclusively, the existence of a negative feed-back loop has been suggested, in order to prevent excessive hypoxic gene induction, by the ability of Hey factors to repress Hif1 α induced gene expression (Diez et al., 2007). This negative feed-back loop may explain why *Hif1 α* mRNA levels were only altered in an early stage (18 wks) of prostate tumor development in TRAMP.*eJag1* mutants since at late stages (24 wks) modulation of *Hey1* mRNA levels may have caused a repressive effect.

The hyper-productive angiogenesis observed in the prostatic lesions of TRAMP.*eJag1OE* mutants, was associated with increased proliferation and survival of tumor cells and to the acquisition of a more invasive phenotype promoting de-differentiation and epithelial-mesenchymal transition. Accordingly, Jagged1 mediated activation is known to induce epithelial-mesenchymal transition (Leong et al., 2007). Conversely, the anti-angiogenic phenotype observed in TRAMP.*eJag1cKO* mutants was associated with reduced proliferation of tumor cells and increased apoptotic events that ultimately restricted invasiveness. Notably, endothelial Jagged1 regulated the transcription profile of several cell cycle regulatory genes: CyclinA, D2 and c-myc were positively regulated while the inhibitors of these kinases activity, Cdkn1b and c were negatively regulated by endothelial Jagged1 function. Similarly, previous studies have demonstrated that down-regulation of *Jag1* induces cell growth inhibition and S phase cell cycle arrest in prostate cancer cells (Zhang et al., 2006).

The metabolic changes observed in prostate tumor cells that arise from altered tumor angiogenic response may not only be a consequence of altered support of nutrients and oxygen, but can also be a consequence of paracrine signaling. In this work we have also unveiled a new angiocrine effect of the Jagged1 ligand. Endothelial Jagged1 not only up-regulated ECs specific Hey1 transcription and expression but also increased its expression in adjacent tumor cells. In twin slides, we could also observe that the same Hey1 positive tumor areas concomitantly expressed active Notch3, had increased tumor cell proliferation and presented loss of epithelial markers, suggesting a de-differentiation phenotype. Therefore, we suggest that endothelial Jagged1 is able to regulate tumor cell metabolism by its angiocrine function through Notch3/Hey1. Accordingly, Jagged1 expressing EC- tumor cell signaling has been described in the regulation of colorectal cancer (Lu et al., 2013), and in the ability of providing chemo resistance, aggressiveness to lymphoma cells by activating Notch2 and consequently Hey1 in these adjacent cells (Cao et al., 2014).

The angiocrine effect combined with the pro-angiogenic and pro-maturation function of endothelial Jagged1 may constitute an important therapeutic advantage over DLL4 based-therapies. Blockade of DLL4 was shown to lead to increased nonproductive tumor vasculature

inhibiting tumor growth (Noguera-Troise et al., 2006; Ridgway et al., 2006). However, long-term blockade of Dll4 was found to lead to the development of vascular neoplasms (Yan et al., 2010) and other toxicities (Smith D, Eisenberg P, Stagg R, Manikhas G, Pavlovskiy A, Sikic B, Kapoun A, Benner S. A First-In-human, phase I trial of the anti-DLL4 antibody (OMP-21M18) targeting c, 2010).

6. Conclusions

In summary, this study is the first to demonstrate the effect of directly modulating endothelial *Jag1* in tumor development. Notably, loss of endothelial *Jag1* not only had an inhibitory effect in the neo-angiogenic and maturation responses but also had an angiocrine effect, through inhibition of Notch3/Hey in tumor cells, restricting proliferation, increasing apoptosis, and preventing the acquisition of an invasive phenotype by tumor cells, therefore inhibiting growth and development of subcutaneous LLC tumor transplants and autochthonous prostatic tumors in mice. Thus, this report provides substantial support for the development of novel therapeutic strategies against cancer based on blocking endothelial Jagged1 function.

**Chapter III - Notch
signaling
dynamics in the
adult healthy
prostate and in
prostatic tumor
development.**

Ana-Rita Pedrosa^{*}, José
L. Graça^{*}, Sandra
Carvalho, Maria C.
Peleteiro, António Duarte
and Alexandre Trindade.

*These authors contributed
equally to this work

Published in *The
Prostate 2016.*
76(1); 80-96.
DOI:10.1002/pros.
2310

1. Abstract

Background- The Notch signaling pathway has been implicated in prostate development, maintenance and tumorigenesis by its key role in cell-fate determination, differentiation and proliferation. Therefore, we proposed to analyze Notch family members transcription and expression, including ligands (Dll1, 3, 4 and Jagged1 and 2), receptors (Notch1-4) and effectors (Hes1, 2, 5 and Hey1, 2, L), in both normal and tumor bearing mouse prostate to better understand the dynamics of Notch signaling in prostate tumorigenesis.

Methods- Wild type mice and Transgenic Adenocarcinoma of the mouse prostate model (TRAMP) mice were sacrificed at 18, 24 or 30 weeks of age and the prostates collected and processed for either whole prostate or prostate cell specific populations mRNA analysis and for protein expression analysis by immunohistochemistry and immunofluorescence.

Results- We observed that Dll1 and Dll4 are expressed in the luminal compartment of the mouse prostate, whereas Jagged2 expression is restricted to the basal and stromal compartment. Additionally, Notch2 and Notch4 are normally expressed in the prostate luminal compartment while Notch2 and Notch3 are also expressed in the stromal layer of the healthy prostate. As prostate tumor development takes place, there is up-regulation of Notch components. Particularly, the prostate tumor lesions have increased expression of Jagged1 and 2, of Notch3 and of Hey1. We have also detected the presence of activated Notch3 in prostatic tumors that co-express Jagged1 and ultimately the Hey1 effector.

Conclusions- Taken together our results point out the Notch axis Jagged1-2/Notch3/Hey1 to be important for prostate tumor development and worthy of additional functional studies and validation in human clinical disease.

Keywords: healthy prostate, prostate cancer, Notch, TRAMP, Jag1/2, Notch3, Hey1.

2. Introduction

The Notch pathway is a well conserved signaling pathway involved in cell-fate determination, differentiation and proliferation in a variety of tissues (Artavanis-Tsakonas et al., 1999). In mammals, this pathway is comprised of four different transmembrane receptors (Notch1-4) and five ligands (Delta like 1, 3, and 4 and Jagged1 and 2). Notch signaling initiates when a membrane-bound ligand on the sending cell binds to a receptor on the receiving cell. Ligand binding then drives a series of proteolytic cleavages that convert the full-length receptor into a smaller transcriptional activator, the notch intracellular domain (NICD), which is released from the cytoplasmic membrane and translocated to the nucleus. NICDs bind to RBPJ/CBP transcription factors to activate Notch target genes, including those encoding transcriptional repressors belonging to the Hairy and enhancer of split (HES) and the Hairy/enhancer-of-split related with YRPW motif (HEY) protein families (Hori, Sen, & Artavanis-Tsakonas, 2013).

The Notch pathway has been implicated in prostate development, maintenance and tumorigenesis (Carvalho, Simons, Eberhart, & Berman, 2014). The embryonic prostate rudiment, urogenital sinus (UGS), through complex and finely orchestrated proliferation, invasion, and differentiation, evolves into complex glands. The final maturation of the glands, providing the correct form and function, requires a series of cell-fate events that give rise to the main epithelial cell types, basal and luminal cells, surrounded by a layer of stromal smooth muscle cells (Wang et al., 2001). One of the first studies on Notch role in the prostate (Shou et al., 2001) demonstrated that *Notch1* mRNA was upregulated in embryonic and postnatal prostate epithelia and downregulated upon maturation of the gland. In adult mice, however, the expression levels of the receptors and consequently the functional role of the pathway appear to be different from those described during the neonatal stage. Both basal and luminal cells were described to express some Notch ligands and receptors but the expression was found to be higher in luminal cells (Valdez et al., 2012). In the same study, Notch activation in the mouse prostate induced proliferation of luminal cells, while having the opposite effect on basal cells. This observation supports a model wherein Notch ligands presented by basal epithelial cells activate the Notch pathway in adjacent luminal cells promoting differentiation and proliferation.

However this study only performed transcription analysis, therefore, there is lack of an extensive expression analysis to help understand the distribution of different Notch family components in the adult prostate.

Several studies have also addressed the role of Notch in prostate tumor development. High levels of expression of NOTCH1 and N1ICD (Notch1 intracellular domain) were detected in all four frequently studied human prostate cancer cell lines (PC3, DU145, 22Rn1, and LNCaP) (Shou et al., 2001). Other studies in either human or mice prostate cancer tissue provided evidence for Notch contribution to tumorigenesis: levels of NOTCH1 protein increased with increasing Gleason grade (Bin Hafeez et al., 2009); prostatic metastasis showing distinctly

elevated levels of JAGGED1 protein (Santagata et al., 2004); Notch signaling being the most distinguishing feature when comparing gene expression profiles from high-grade versus low-grade Gleason scores micro-dissected cancer cells (Ross et al., 2011); and cancer cells with metastatic potential showing upregulated Notch ligand JAGGED2 and NOTCH3 receptor (Ross et al., 2011).

Despite these studies, there is lack of a comprehensive analysis of expression that may serve as a basis for further functional studies regarding Notch in the prostate. Therefore, the aim of this study was to dissect Notch family transcription and expression, including ligands, receptors and effectors, in the normal and tumorigenic prostate tissue. We also intended to look into specific prostate cell population expression, providing novel insights into Notch signaling dynamics and identifying potential expression alterations in each prostate compartment between healthy prostate and prostate tumor.

3. Materials and Methods

3.1 Experimental animals

All the procedures involving animals used in this study have been approved by the Ethics and Animal Welfare Committee of the Faculty of Veterinary Medicine of Lisbon. All animals were housed in ventilated propylene cages with sawdust as bedding, in a room with temperature between 22°C and 25°C and a 12-hours-light/12-hours-dark cycle. The mice were fed standard laboratory diet.

3.2 Tissue preparation, immunohistochemistry and immunofluorescence

C57BL/6 (WT) and TRAMP (in C57BL/6 genetic background) mice were sacrificed at 18, 24 or 30 weeks of age and the prostates finely dissected and collected. For immunohistochemistry, prostates have been fixed in 10% buffered formalin for 48 h, dehydrated in alcohol, cleared in xylene, embedded in paraffin, and sectioned at 3µm.

Immunohistochemistry in (paraffin-embedded tissue sections) protocol- Tissue slides were deparaffinized and rehydrated using Xylene bath solutions (1x 10min, 1x 5min) and Alcohol bath solutions (100% - 2x 2min, 95% alcohol- 1x 4min, 75% alcohol – 1x 4min). Then permeabilized in 3% H₂O₂ distilled solution (or 3% H₂O₂ methanol solution, for Dll1) at 37°C for 15 min (in dark); antigen retrieval was performed, using either Citrate buffer (pH 6.0) or Tris-EDTA buffer (pH 9.0) solutions, (depending on the primary antibody used), washed in PBS-Triton 0,3% solution (except for Dll1, and Hes2); blocking was performed with 2% BSA in PBS solution; slides were then incubated over-night at 4°C with specific primary antibodies and then incubated 1h at room-temperature with specific secondary antibodies; DAB chromogen (ImmPACT™ DAB, Vector Laboratories) was applied to the tissue sections on the

slides, until reaction occurred and proper staining was reached; slides were counterstained by immersion in Mayer's Hematoxilin (Fluka AG Buchs SG) for 30 sec -1 min. Finally, tissue slides were dehydrated in bath solutions (Alcohol 95%, 100% - 2 min each, Xylene 2x 5 min) and mounted using Entellan (Merck Millipore).

The primary antibodies used are: rabbit anti-Notch1 (ab27526)/ Notch2 (ab8926)/ Notch3 (ab23426)/ Dll1 (ab76655)/ Dll4 (ab7280)/ Hes1 (ab71559)/ Hes2 (ab134685)/ Hes5 (ab25374)/ Hey L (ab78048) (Abcam); Synaptophysin (ab32127); rabbit anti- Notch4 (sc-5594)/ Jagged1 (sc-8303)/ Dll3 (sc-67270) (Santa Cruz Biotechnology); goat anti-Jagged2 (sc-34476) (Santa Cruz Biotechnology); rabbit anti-Hey1 (AB5714)/ Hey2 (AB5716) (Merck Millipore); These antibodies were previously validated in other reproductive tissues, both in male as in female, and published by our lab (Murta et al., 2013, 2014, 2014, 2015). Rabbit IgG (ab27478) (Abcam) and Goat IgG (sc-2028) (Santa Cruz Biotechnology) were used as negative controls. The secondary antibodies used are: Polyclonal Goat anti-Rabbit Immunoglobulins HRP (P0448) (Dako) and Donkey anti-Goat IgG-HRP (sc-2020) (Santa Cruz Biotechnology). Nuclei were counterstained with Mayer's haematoxylin.

Immunofluorescence protocol- For immunofluorescence analysis prostates were fixed in 4% paraformaldehyde (PFA) solution at 4°C for 1h, cryoprotected in 15% sucrose, embedded in 7,5% gelatin, frozen in liquid nitrogen and cryosectioned at 20µm. Tissue slides were permeabilized in 3% H₂O₂ methanol solution for 30 min and PBS-Triton 0,1% solution 2x 10 min; blocking was performed for 1h (room temperature) with 2% BSA + 5% Donkey serum in PBS-W 0,1% solution; after blocking, slides were incubated over-night at 4°C with specific primary antibodies followed by 1h incubation at room-temperature with fluorescently-tagged specific secondary antibodies (Invitrogen). The primary antibodies used are: goat anti-Jagged1 (J4127) (Sigma); goat anti-Jagged2 (sc-34476) (Santa Cruz Biotechnology); rabbit anti-CK5 (EP16001Y) (NOVUS Biologicals); rabbit anti-Hey1 (AB5714) (Merck Millipore) and rabbit anti-N3ICD (sc-5593) (Santa Cruz Biotechnology). The secondary antibodies used are: donkey anti-goat Alexa 594 and donkey anti-rabbit Alexa 488 (Invitrogen). Nuclei were counterstained with 4',6-diamidino-2-phenylindole dihydrochloride hydrate (DAPI; Molecular Probes).

Histopathological analysis was carried out blindly by a Veterinary Pathologist (Peleteiro M.C) and the tumors scored according to the literature (Kaplan-Lefko et al., 2003): Normal, prostatic intraepithelial neoplasia (PIN), well differentiated adenocarcinoma (WDA), moderately differentiated adenocarcinoma (MDA), poorly differentiated adenocarcinoma (PD), or phylloides-like cancer (PHY).

Instrument details- Immunohistochemistry stained sections were examined under a Olympus BX51 microscope with Olympus 10X/0.30 NA and 40X/0.75 NA dry objectives and captured with coupled Olympus DP21 photographic equipment (Olympus Iberia, Inc). Fluorescent immunostained sections were examined under a Leica DMRA2 fluorescence microscope with Leica HC PL Fluotar 10, 20X and 40X/0.5 NA dry objectives (Leica), captured using Photometrics CoolSNAP HQ, (Photometrics), and processed with Metamorph 4.6-5 (Molecular Devices).

3.3 Quantitative transcriptional analysis

For whole prostate transcription analysis WT benign prostate and TRAMP prostates were collected at the endpoint of each experiment and snap frozen for RNA extraction (Qiagen). First-strand cDNA was synthesized from total RNA using a SuperScript III FirstStrand Synthesis Supermix Q RT-PCR (Invitrogen).

For transcription analysis of cell specific populations, prostates from both WT and TRAMP mice were collected at the endpoint of each experiment and prepared for FACS sorting. Luminal, basal and stromal cells were sorted directly into the lysis buffer of the RNeasy Micro Kit (Qiagen). Total RNA was isolated according to manufacturer's protocol. A total of 100 ng RNA per reaction was used to generate cDNA with the above mentioned kit. Relative quantification real-time PCR analysis was performed as described (Trindade et al., 2008) using Sybergreen Fastmix ROX dye (Qiagen). The housekeeping gene β -actin was used as endogenous control. Gene-specific primer pairs used for quantification are provided in Annex I.

3.4 Flow cytometry

For flow cytometric analysis and sorting of Luminal (Lin⁻ (cd45⁻ cd31⁻ ter119⁻) Sca1⁻ cd49f⁺), Basal (Lin⁻ (cd45⁻ cd31⁻ ter119⁻) Sca1⁺ cd49f⁺) and Stromal cells (Lin⁻ (cd45⁻ cd31⁻ ter119⁻) Sca1⁺ cd49f⁻) (Lawson & Witte, 2007) prostates were finely dissected into small pieces (2-4 mm). The samples were then digested into 1 ml solution of 1% collagenase (Sigma) and 2,4U/ml of dispase (Gibco, Life Technologies) incubation at 37°C, with agitation, for 2h30 min. DNase I (Sigma) was added during digestion to eliminate DNA residues. After washing, digested cells were then subjected to immunostaining with anti-mouse ter-119 PE-Cy7, anti-mouse cd45 PE-Cy7, anti-mouse cd31 PE-Cy7 (Affymetrix, eBioscience), anti-mouse Sca1 FITC and anti-mouse cd49f PE (BD Pharmingen). After washing, cells were sorted in a FACS Aria III cytometer and analyzed using BD FlowJo software (Version 10.0, BD Bioscience).

For demarcating and sorting of Luminal, Basal and Stromal cell populations, first standard quadrant gates were set, subsequently to differentiate Sca1⁺ (>10³ log FITC fluorescence) and cd49f⁺ (>10³ log PE fluorescence) cells from the Lineage negative population (≤10² log PE-Cy7 fluorescence).

3.5 Statistical analysis

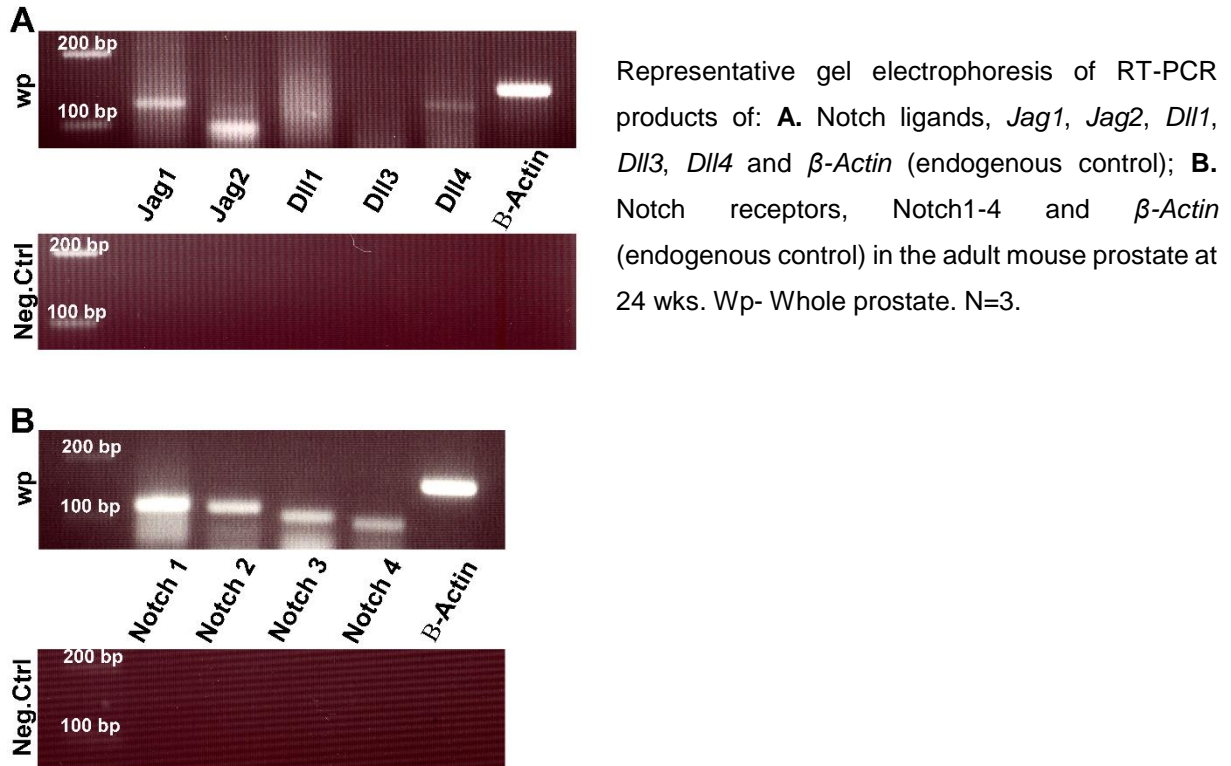
All data processing was carried out using the Statistical Package for the Social Sciences software, version 17.0 (SPSS v. 17.0). Statistical analyses were performed using Mann-Whitney-Wilcoxon test and Student's t-test.

Results are presented as mean ± SEM. *P*-values < 0.05, <0.01 and <0.001 were considered significant (indicated in the figures with *) and highly significant (indicated with ** and ***), respectively.

4. Results

4.1 Notch ligands and receptors are transcribed in the adult prostate

Since Notch signaling is required for normal prostate development and homeostasis (Leong & Gao, 2008) we first analyzed the transcription of Notch receptors and ligands in the adult prostate of WT mice at 24 weeks (wks) of age by qRT-PCR (Figure III.1). As shown in figure III.1A, the Notch ligands *Jag1* and *Jag2* were strongly transcribed while *Dll1* and *Dll4* were detected at lower levels and *Dll3* transcription was not detected. Additionally, all Notch receptors were transcribed in the healthy adult prostate (Figure III.1B).

Figure III.1- Transcription of Notch components in the healthy adult prostate tissue.

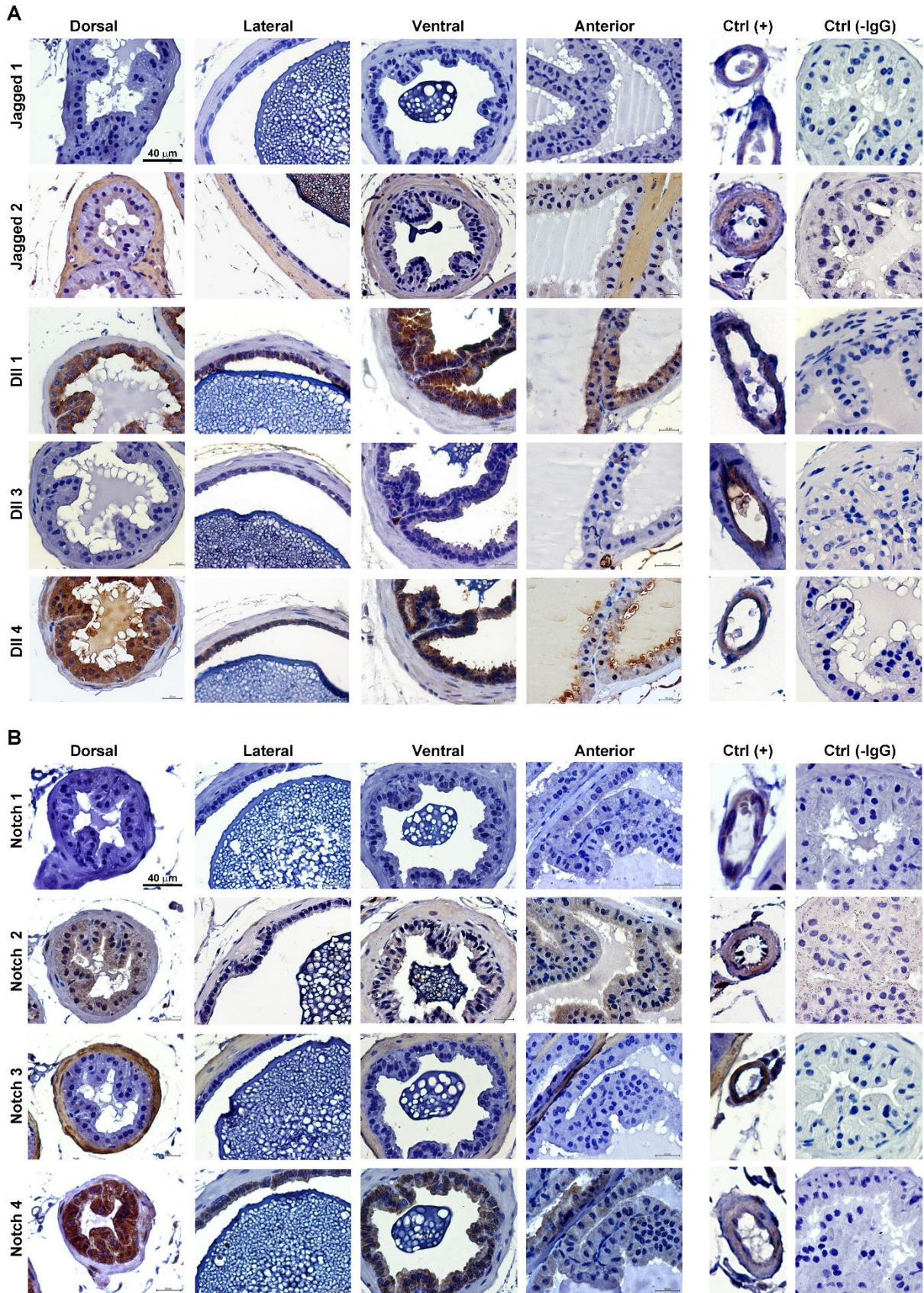
4.2 Notch components and effectors are expressed in all lobes of the adult prostate

Having observed that most of Notch components were transcribed in the adult prostate we looked at the protein expression of these same components by immunohistochemistry of the four different lobes of the mouse prostate (Dorsal, Lateral, Ventral and Anterior) at 24 weeks of age. The prostate vasculature was used as positive control for the staining given the known abundant expression of Notch components in blood vessels (Villa et al., 2001). All tested Notch components were found to be expressed either in the endothelial or perivascular layers of prostatic blood vessels, independently of prostatic epithelial staining.

As demonstrated in figure III.2A, while Jagged1 was absent, Jagged2 appeared strongly expressed in the smooth muscle layer of the prostatic glands in the healthy tissue of the four lobes of the mouse prostate. Regarding the Delta-like ligands, it was clear that Dll1 and Dll4 were expressed in the prostatic epithelium while Dll3 was expressed only in the vasculature. Regarding the Notch receptors (Figure III.2B), Notch1 expression was absent in all lobes of the prostate, while Notch2 appeared mildly expressed in both epithelial and stromal layers. Notch3 was highly expressed in the stromal layer, while completely absent from the epithelial layer. Lastly, Notch4 expression was restricted to the epithelial layer.

Figure III.2- Immunohistochemistry of Notch components in the four lobes (Dorsal, Lateral, Ventral and Anterior) of the healthy adult prostate.

WT Prostate



Positive immunostaining presented as brown color counterstained with haematoxylin. **A.** Notch ligands expression demonstrating absence of Jagged1 while Jagged2 appears marked in the smooth muscle layer surrounding each gland in all the different lobes of the adult prostate; Delta ligands expression is limited to Dll1 and Dll4 expression in the prostatic epithelium while Dll3 appears expressed only in the

vasculature. **B.** Notch receptors expression demonstrating complete absence of Notch1 protein in all prostate lobes, while Notch2 appears mildly expressed in both epithelium and mesenchymal layers of the prostate; Notch3 expression is restricted to the mesenchymal layer while Notch4 expression is restricted to the epithelial layer. Prostate vasculature serves as positive controls for the staining (Ctrl+) while IgGs against the species where the primary antibodies were produced were used as negative controls of the staining (Ctrl-IgG). N=2 for each adult age analyzed (18, 24 and 30 wks).

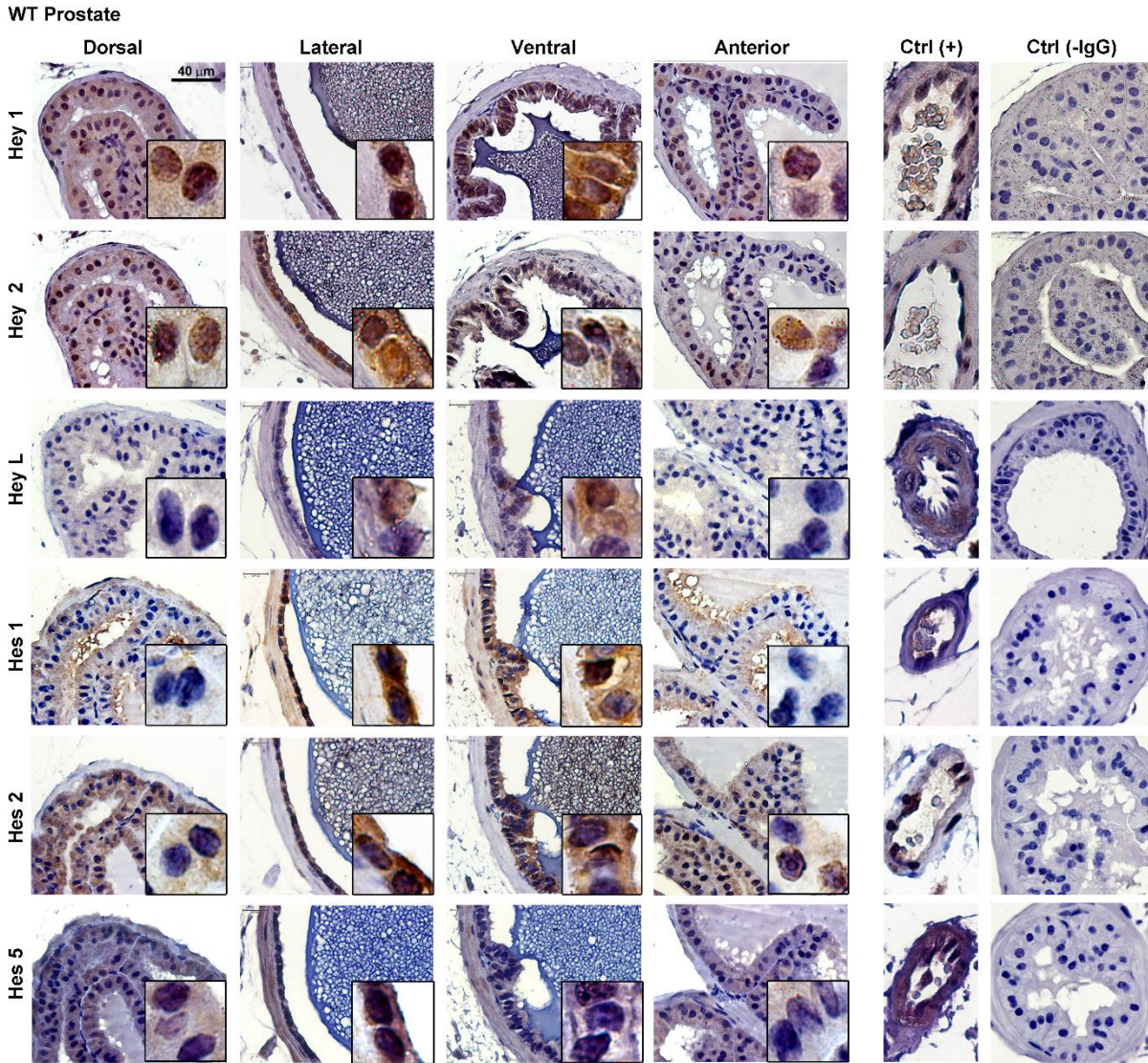
Given the high expression of Notch components we also looked for expression of Notch effectors, a potential indication of Notch pathway activation/function (Figure III.3). Looking at the Hey family members expression, it was clear that Hey1 and Hey2 presented nuclear localization, indicative of their function as Notch transcriptional regulators, in some epithelial cells, in all prostate lobes. Regarding HeyL, even though no expression was detected in the nucleus of the dorsal and anterior prostate, an occasional nuclear localization was identified in the lateral and ventral lobes. Hes1 and Hes2 appeared less clearly in the nuclei, with some occasional nuclear positive staining in the lateral, ventral and anterior lobes of the prostate. Lastly, Hes5 presented some positive staining in the cytoplasm but it was not detected in the nuclei in any prostate lobe. The expression data obtained was identical at 18 and 30 weeks of age and corroborated by qRT-PCR analysis (data not shown).

4.3 Prostatic tumor development is accompanied by up-regulation of Notch signaling pathway.

Notch signaling has been associated with prostatic tumor development (Carvalho et al., 2014), however there has been no previous study doing a comprehensive analysis of all Notch ligands, receptors and effectors expression in this scenario. Therefore, after observing the expression of the several Notch components in healthy murine prostate, we used the Transgenic Adenocarcinoma of the mouse prostate (TRAMP) (Greenberg et al., 1995) model to study the transcription and expression dynamics of Notch pathway components in the development of prostatic cancer. This model is broadly used and well established as the prostates of these mice progress through different preneoplastic and neoplastic lesions, similar to what occurs in man (Greenberg et al., 1995; Gingrich & Greenberg, 1996; Gingrich et al., 1999; Kaplan-Lefko et al., 2003). In an early stage, lesions of prostatic intraepithelial neoplasia (PIN) can be readily identified, which are characterized by epithelial crowding, stratification, cribriform structures, hyperchromatism, increased mitosis and apoptosis (Kaplan-Lefko et al., 2003). In a late stage, invasion takes place presenting well-differentiated adenocarcinomas (WDA) characterized by increased quantity of small glands and a desmoplastic response (Kaplan-Lefko et al., 2003). At a very late stage of prostatic tumor development in TRAMP mice phylloides-like and poorly differentiated adenocarcinoma lesions can be readily identified. The phylloides-like type of lesion is characterized by staghorn luminal patterns with hyper

cellular stroma, while the poorly differentiated adenocarcinoma lesions are characterized by anaplastic sheets of cells that may entrap normal glands (Kaplan-Lefko et al., 2003).

Figure III.3- Immunohistochemistry of Notch effectors in the four lobes (Dorsal, Lateral, Ventral and Anterior) of the healthy adult prostate.

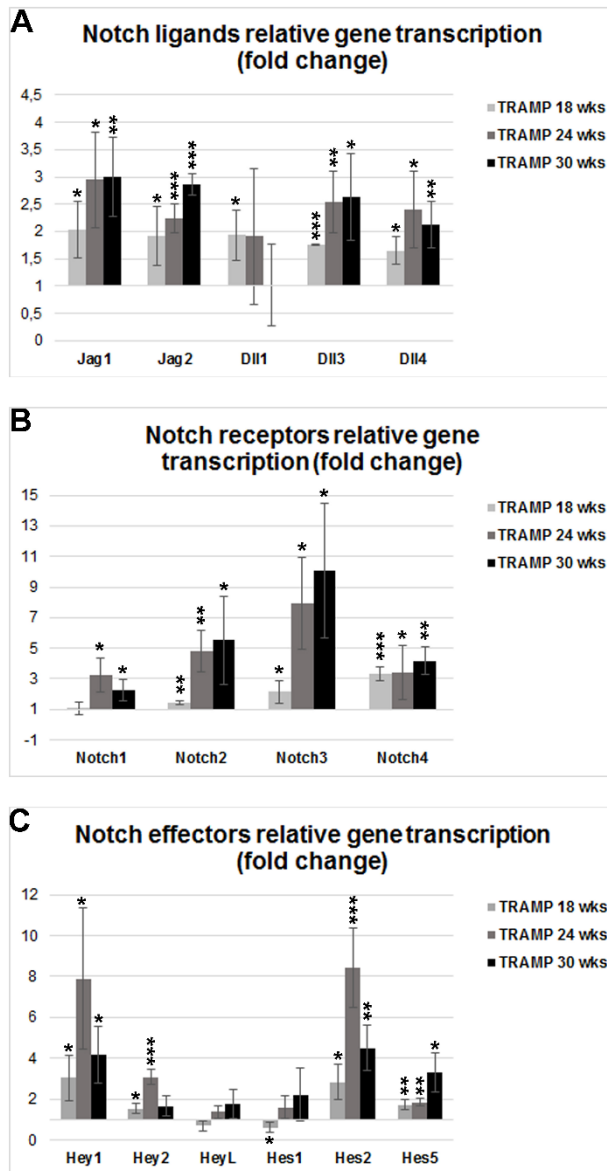


Positive immunostaining presented as brown color counterstained with haematoxylin. Hey1 and Hey2 present nuclear positive staining in all areas of the prostate. HeyL presented occasional cell-specific nuclear localization in the lateral and ventral prostate. Hes 1 and Hes2 also presented occasional nuclear staining while Hes5 is not detected in the nucleus. Prostate vasculature serves as positive controls for the staining (Ctrl+) while IgGs against the species where the primary antibodies were produced were used as negative controls of the staining (Ctrl+IgG). N=2 for each adult age analyzed (18, 24 and 30 wks).

Firstly, we analyzed the changes in gene transcription of whole prostate in TRAMP relative to WT mice at three different stages of tumor progression: 18 (early stage), 24 (late stage) and 30 weeks (very late stage) of age (Figure III.4). As seen in figure III.4A, all Notch ligands, with

exception of *Dll1*, displayed increased transcription as the tumors progressed. However, *Jag1* and *Jag2* were the most highly up-regulated ligands. In figure III.4B it can be observed that all Notch receptors (1-4) were up-regulated in TRAMP prostates in all stages of prostatic tumor development. Nevertheless, *Notch3* transcript levels were more highly up-regulated than the other receptors. Looking at the Notch effectors (figure III.4C), we observed that all were also up-regulated in response to tumor development, which exception of *HeyL* and *Hes1* but, remarkably, *Hey1* and *Hes2* clearly had the highest up-regulation response. Generally, the Notch up-regulation response tended to be more pronounced in late (24 wks) and very late (30 wks) stages of tumor development.

Figure III.4- Transcription analysis of whole prostate in TRAMP mice at three stages of tumor development (18, 24 and 30 wks of age).



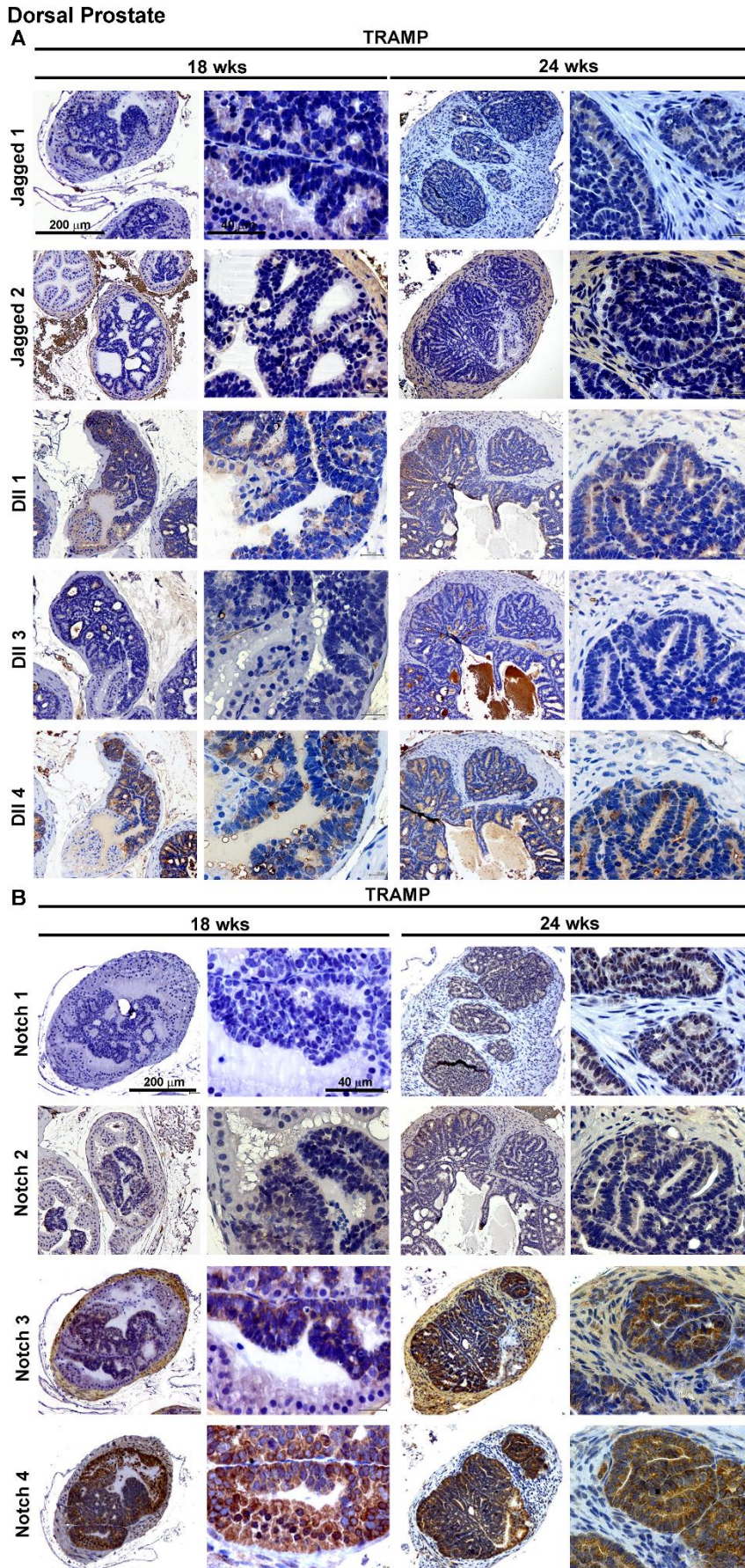
Comparative relative transcription analysis ($\Delta\Delta\text{CT}$) was performed, by RT-PCR, in whole prostates dissected at 18, 24 and 30 weeks of age from TRAMP mice and compared with WT prostates of the respective age. **A.** Notch ligands relative gene transcription revealing up-regulation of all ligands, with exception of *Dll1*, in all tumor stages; **B.** Notch receptors relative gene transcription demonstrating increased response in all Notch receptors; **C.** Notch effectors relative gene transcription exhibiting a similar up-regulation response in TRAMP prostates. β -actin was used as endogenous control. Error bars represent SEM; * represents $p < 0.05$; ** represents $p < 0.01$; *** represents $p < 0.001$. $N=3$ for each mice group and for each different age.

4.4 Early and late stages of prostatic tumor development are accompanied by significant changes in the expression of Notch components

After verifying that prostatic tumor development caused transcriptional changes in Notch signaling pathway components, we evaluated Notch pathway components expression in the various prostate lobes at the previously mentioned time points. We focused mainly on the dorsal prostate, because it is the lobe most consistently affected by the transgene expression in the TRAMP model (Kaplan-Lefko et al., 2003), whereas the other lobes can present slightly less evolved and aggressive lesions. As demonstrated in figure III.5A, both Jagged ligands were expressed in the affected areas of the dorsal prostate, with a clearly increased expression in WDA lesions (24 wks). These ligands were apparently absent from the epithelial layer in WT healthy prostate (Figure III.2A). The Delta-like ligands, Dll1 and Dll4 were also expressed in the affected dorsal areas, whereas Dll3, similarly to what was observed in healthy prostate, remained non-expressed. Looking at the other prostate lobes, lateral (Suppl. Figure III.1), ventral (Suppl. Figure III.2) and anterior (Suppl. Figure III.3), we observed a similar expression pattern for all the Notch ligands, with the exception of Jagged1 and Jagged2 that have reduced expression in these lobes when compared with the dorsal prostate (Figure III.5A).

Regarding Notch receptors, we observed that Notch1 was expressed only in lesions of WDA (24 wks) in the dorsal prostate (Figure III.5B). Notch2, Notch3 and Notch4, were all expressed in the tumor areas both in early and late stages, even though Notch2 expression was not as pronounced as Notch3 and 4. Remarkably, Notch3 was not expressed in the healthy prostatic epithelium of WT mice but was strongly expressed in the tumor areas. Similarly to what was observed in the Notch ligands analysis, the receptors also present a similar expression pattern in the lateral (Suppl. Figure III.4), ventral (Suppl. Figure III.5) and anterior (Suppl. Figure III.6) prostates.

Figure III.5- Immunohistochemistry of Notch components in the dorsal prostate of TRAMP mice at early (18 wks) and late (24 wks) stages of tumor development.

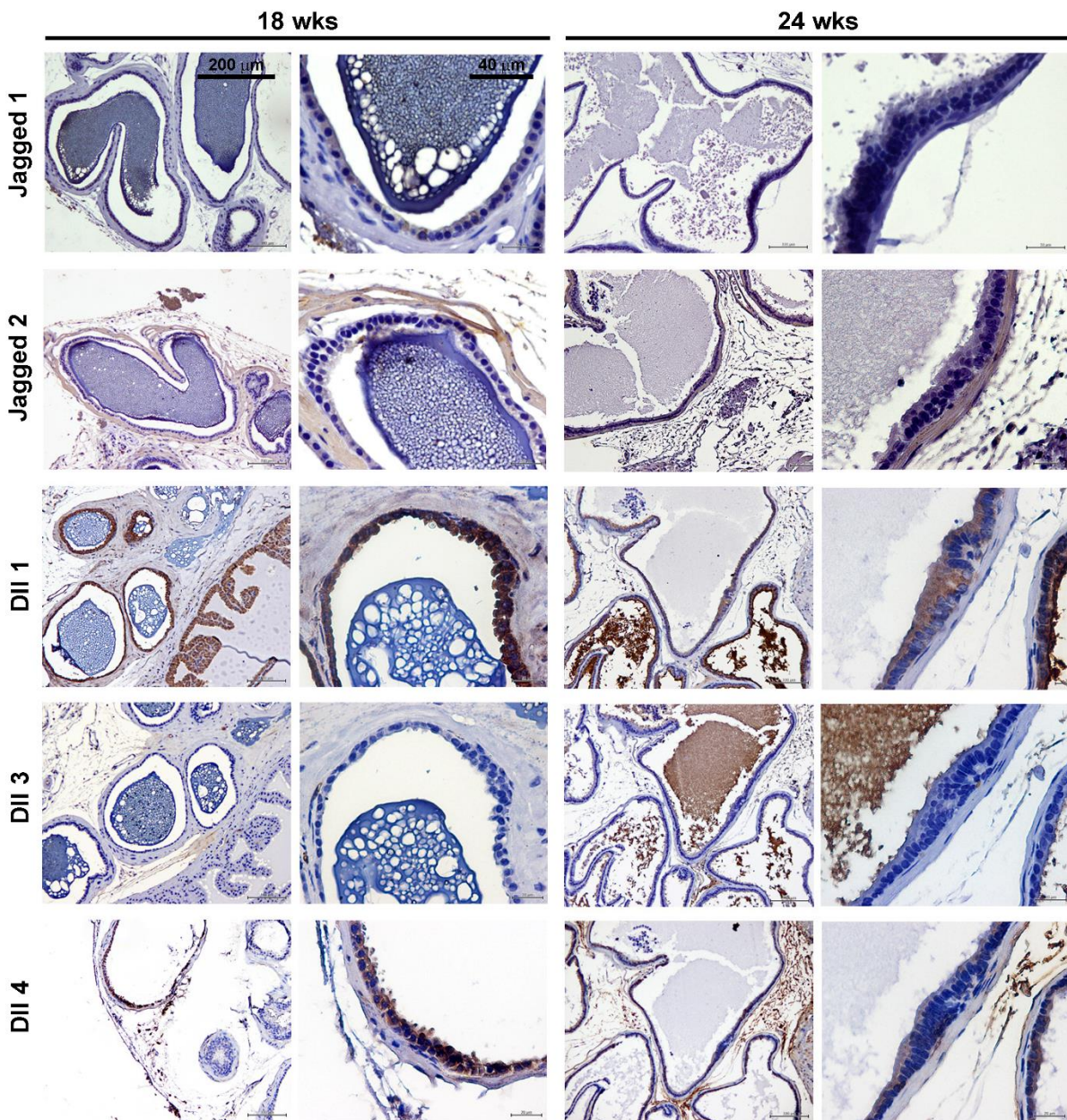


Positive immunostaining presented as brown color counterstained with haematoxylin. **A.** Notch ligands expression in dorsal prostate of TRAMP mice. All ligands, with the exception of Dll3 were expressed in the prostatic transformed epithelium. **B.** Notch receptors expression in dorsal prostate of TRAMP mice. Notch1 appeared expressed only in late stage lesions of WDA, whereas the other Notch receptors, Notch2, 3 and 4 were expressed in both early and late stage lesions. PIN- Prostatic Intraepithelial Neoplasia; WDA- Well differentiated Adenocarcinoma. N=4 for each time point.

Supplemental Figure III.1- Immunohistochemistry of Notch ligands in the lateral prostate of TRAMP mice at early (18 wks) and late (24 wks) stages of tumor development.

Lateral prostate

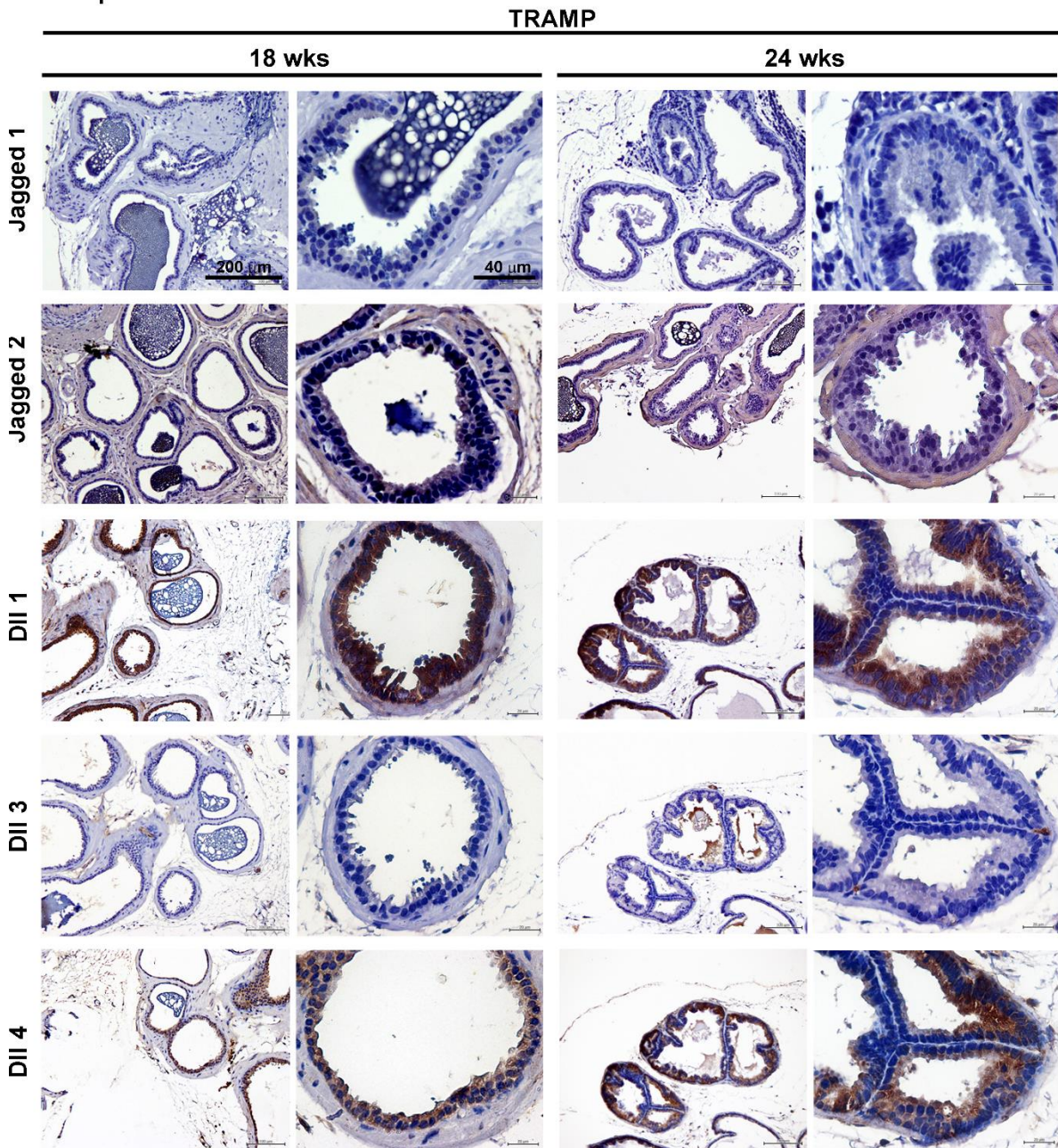
TRAMP



Positive immunostaining presented as brown color counterstained with haematoxylin. Jagged ligands, were expressed mildly, while Delta ligands, with exception of DII3, were strongly expressed in the prostatic transformed epithelium of the lateral prostate of TRAMP mice. N=4 for each time point.

Supplemental Figure III.2- Immunohistochemistry of Notch ligands in the ventral prostate of TRAMP mice at early (18 wks) and late (24 wks) stages of tumor development.

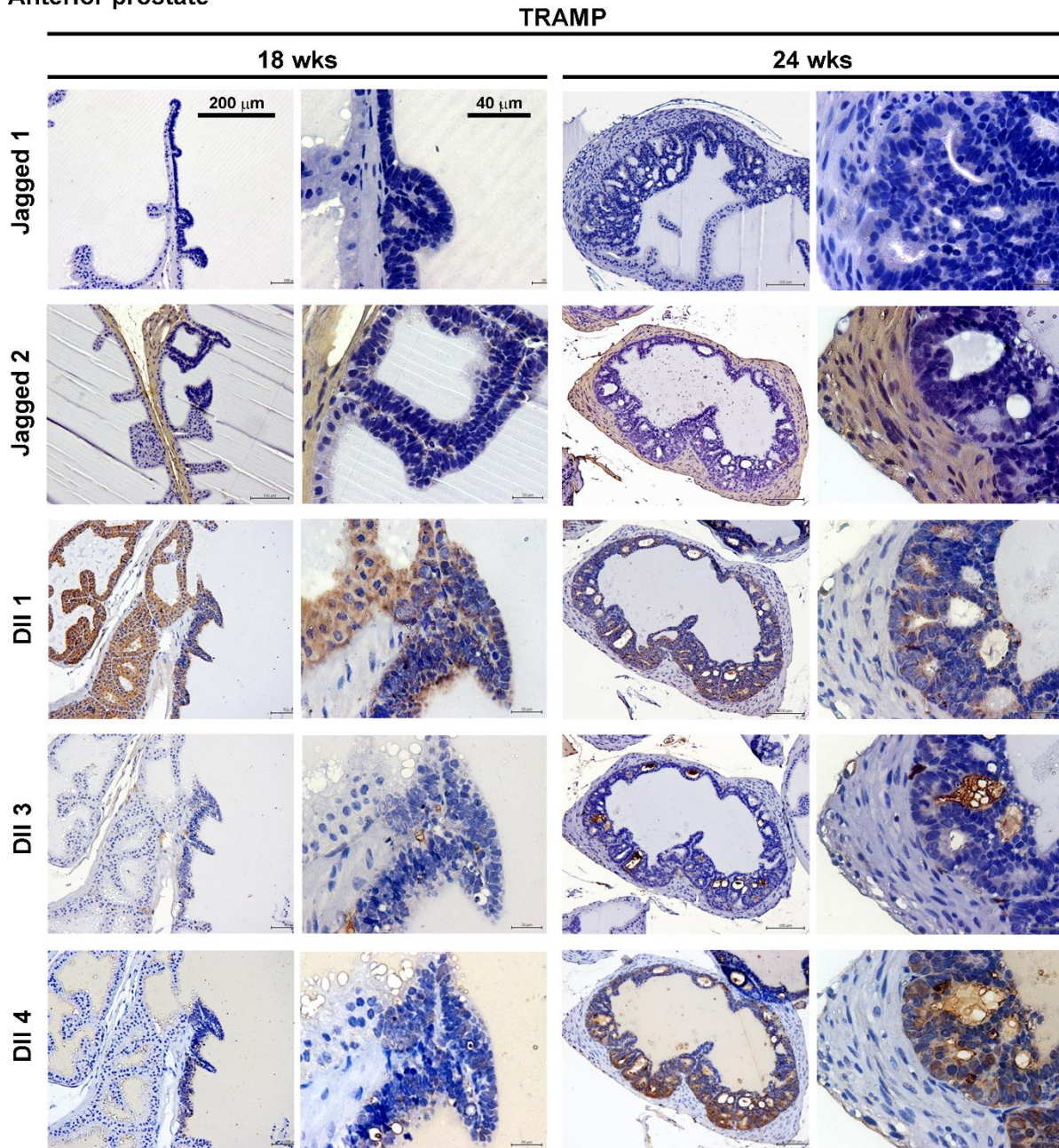
Ventral prostate



Positive immunostaining presented as brown color counterstained with haematoxylin. Jagged1 and DII3 weren't expressed while Jagged2, DII1 and DII4 were expressed in the prostatic dysplastic epithelium of the ventral prostate of TRAMP mice. N=4 for each time point.

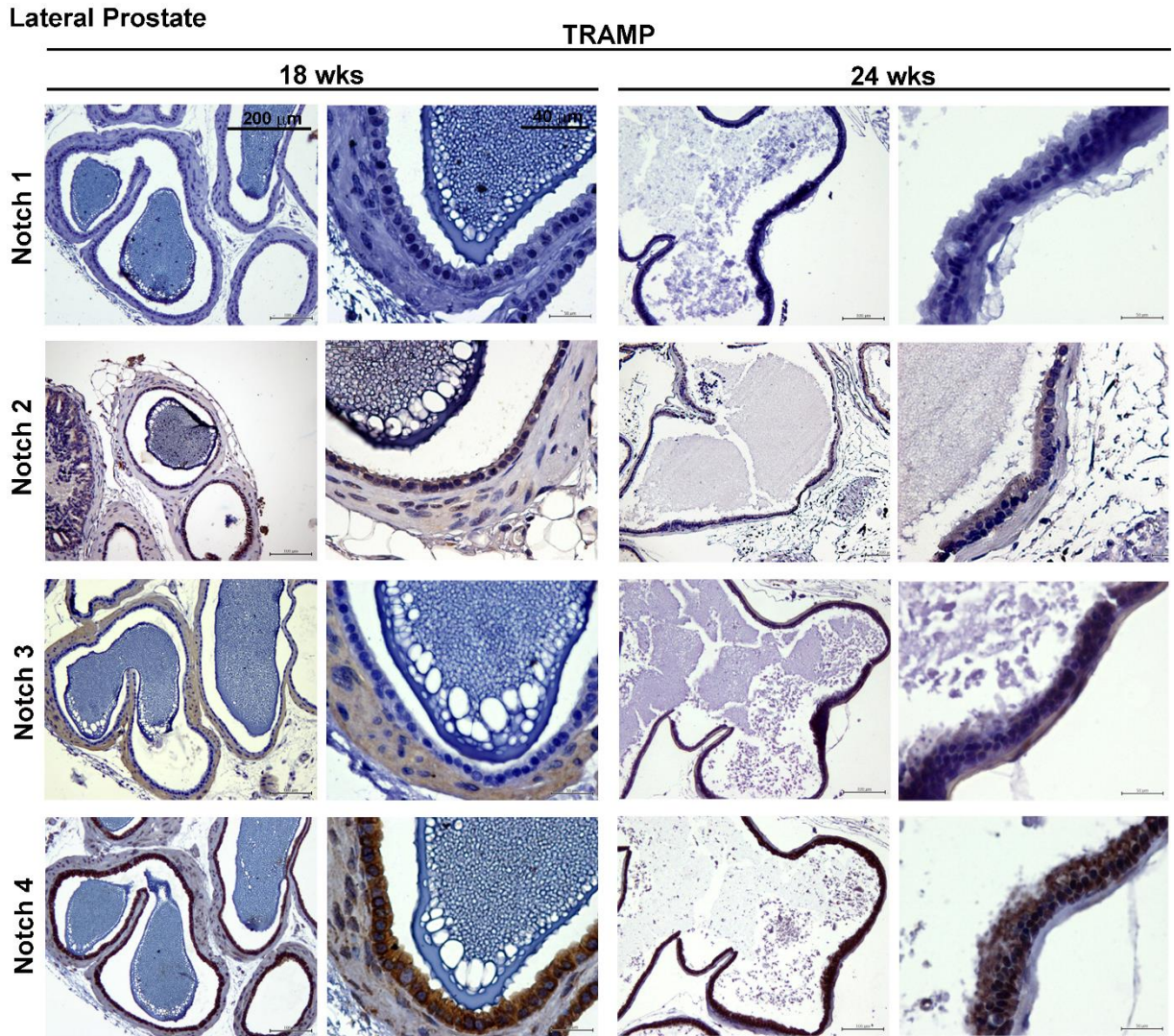
Supplemental Figure III.3- Immunohistochemistry of Notch ligands in the anterior prostate of TRAMP mice at early (18 wks) and late (24 wks) stages of tumor development.

Anterior prostate



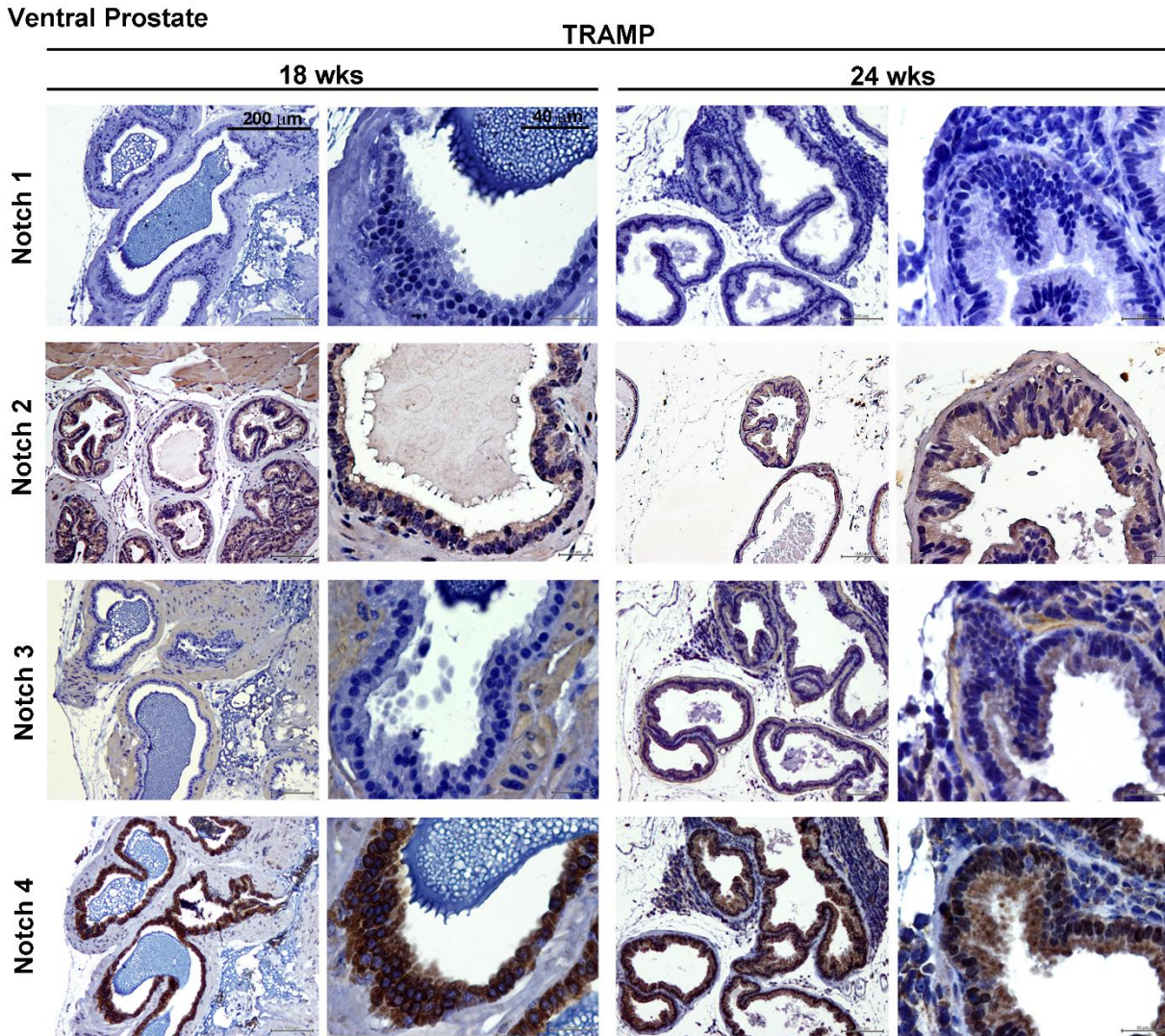
Positive immunostaining presented as brown color counterstained with haematoxylin. Jagged1, Jagged2 and DII3 seem not expressed while DII1 and DII4 were present in the prostatic dysplastic epithelium of the ventral prostate of TRAMP mice. N=4 for each time point.

Supplemental Figure III.4- Immunohistochemistry of Notch receptors in the lateral prostate of TRAMP mice at early (18 wks) and late (24 wks) stages of tumor development.



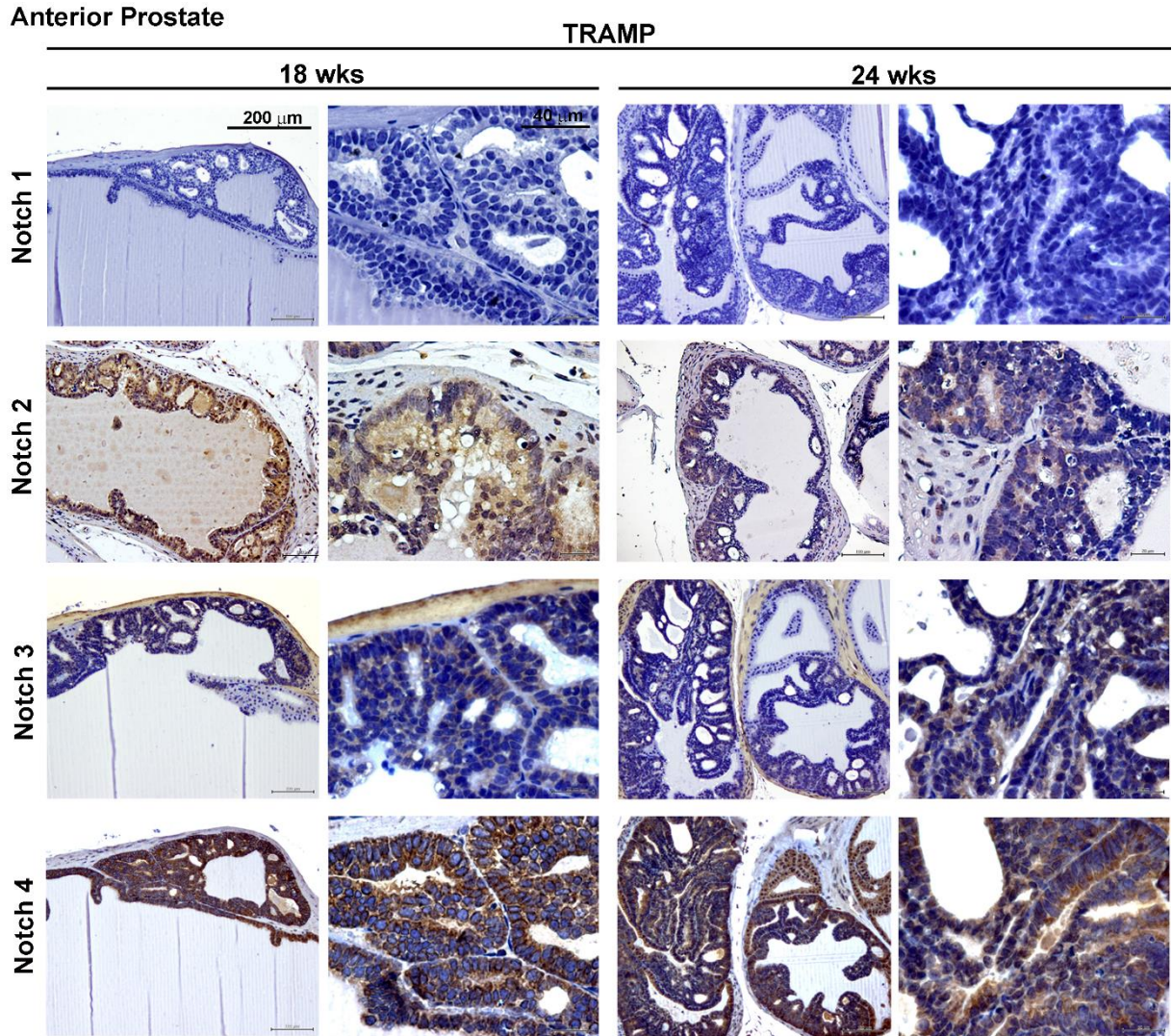
Positive immunostaining presented as brown color counterstained with haematoxylin. Notch1 failed to be expressed whereas the other Notch receptors, Notch2, 3 and 4 were expressed in both early and late stage lesions. N=4 for each time point.

Supplemental Figure III.5- Immunohistochemistry of Notch receptors in the ventral prostate of TRAMP mice at early (18 wks) and late (24 wks) stages of tumor development.



Positive immunostaining presented as brown color counterstained with haematoxylin. Notch1 failed to be expressed whereas the other Notch receptors, Notch2, 3 and 4 were expressed in both early and late stage lesions. N=4 for each time point.

Supplemental Figure III.6- Immunohistochemistry of Notch receptors in the anterior prostate of TRAMP mice at early (18 wks) and late (24 wks) stages of tumor development.



Positive immunostaining presented as brown color counterstained with haematoxylin. Notch1 failed to be expressed whereas the other Notch receptors, Notch2, 3 and 4 were expressed in both early and late stage lesions. N=4 for each time point.

4.5 Early and late stages of prostatic tumor development are accompanied by significant changes in the expression of Notch effectors

Given that TRAMP prostates presented altered expression of specific Notch ligands and receptors, we also looked into the expression of Notch effectors. As shown in figure III.6, it was observed that Hey1 was strongly detected in the epithelial nuclei of both early and late lesions of prostatic tumors. Despite this, in WDA lesions there were some dysplastic areas where Hey1 was not found in the nucleus. Hey2 presented nuclear staining in some cells, mainly in earlier lesions. HeyL failed to present nuclear expression in either time points. Hes1 and Hes2 presented nuclear positive staining in some affected cells mainly in WDA (24 wks) lesions. Lastly, and similarly to what was observed in the healthy prostate, Hes5 was only detected in the cytoplasm. Additionally, lateral (Suppl. Figure III.7), ventral (Suppl. Figure III.8) and anterior prostates (Suppl. Figure III.9) presented a very similar expression pattern for the Notch effectors: Hey1 being the one with a more pronounced expression in the tumor tissue; while Hes1 and Hes2 presented some nuclear staining mainly in early lesions (18 wks) of the ventral prostate (Suppl. Figure III.8).

4.6 Very late stages of prostatic tumor development also presented changes in Notch signaling expression

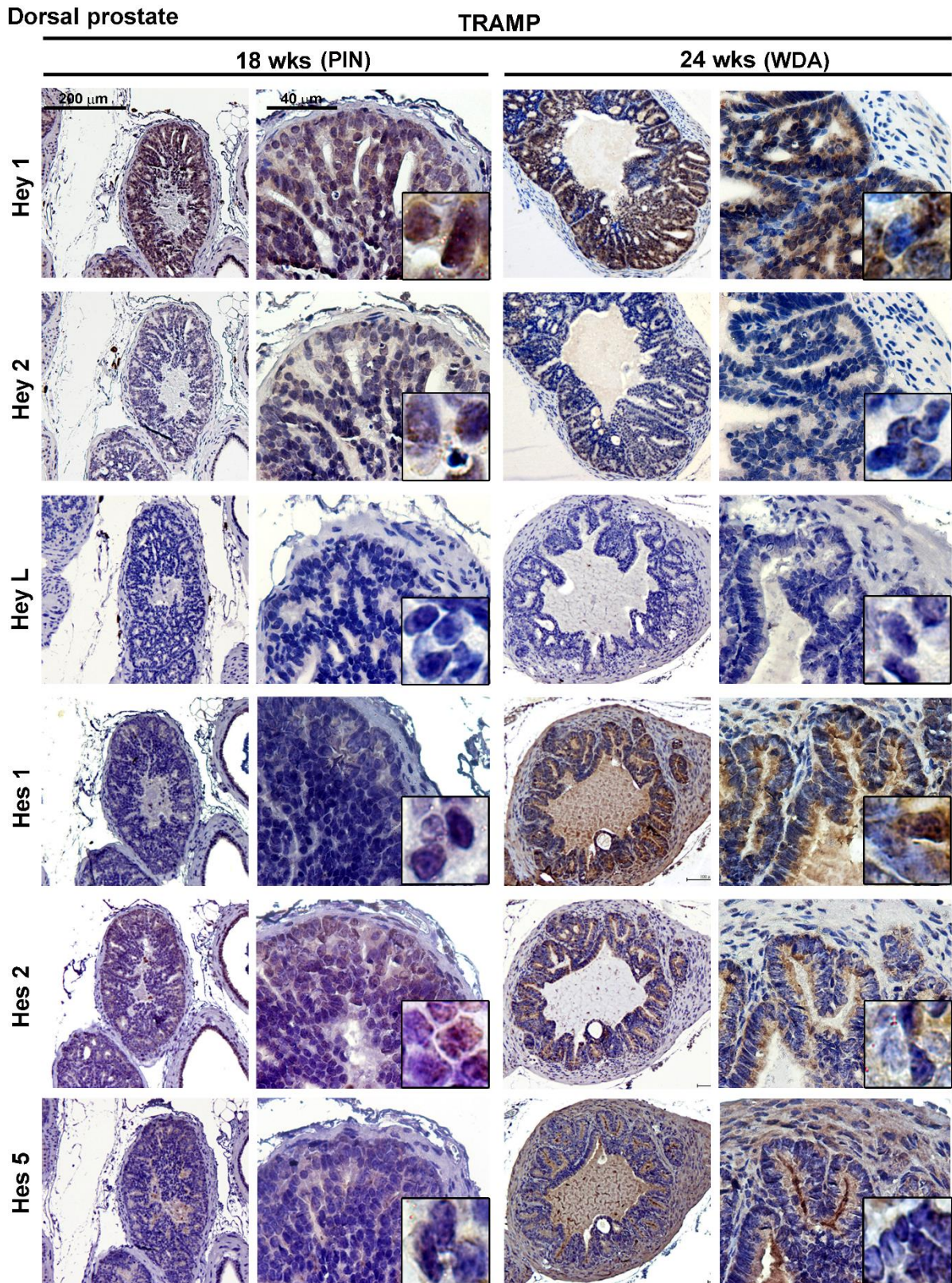
Figure III.7A demonstrates that Notch ligands expression in very late lesions of prostate tumor was very similar to what was observed in early (18 wks) and late (24 wks) stages. Jagged1 was highly expressed in these very advanced lesions, while Jagged2, unlike in earlier lesions, had practically null expression both in PHY and PDA. The Delta-like ligands, Dll1 and Dll4 retained the same expression pattern previously observed in earlier lesions as well as in healthy prostate. Dll3 also maintained its expression restricted to the vasculature that is clearly invading and proliferating in the PDA lesion.

Regarding Notch receptors that were presented in figure III.7B it was also observed a similar expression pattern to the previous analyzed stages of tumor progression. Notch1 presented mild expression in PHY lesions but that seemed to be null in PDA lesions. Notch2 also presented mild expression while Notch3 remained highly expressed in both types of very late stage lesions. Notch4, similarly to what was observed in earlier prostatic lesions and in healthy prostate tissue, remained strongly expressed.

Surprisingly, when we analyzed Notch effectors expression at this very late stage (Suppl. figure III.10), we observed no nuclear positive staining for any of the effectors tested.

We also marked the PDA lesions for Synaptophysin to access if the lesions had undergone neuroendocrine differentiation, as previously demonstrated for the majority of these lesions in TRAMP mice (Kaplan-Lefko et al., 2003). As observed in supplemental figure III.11 the presented lesions of PDA found in very late stages of tumor progression have undergone neuroendocrine differentiation, as they express synaptophysin marker.

Figure III.6- Immunohistochemistry of Notch effectors in the dorsal prostate of TRAMP mice at early (18 wks) and late (24 wks) stages of tumor development.

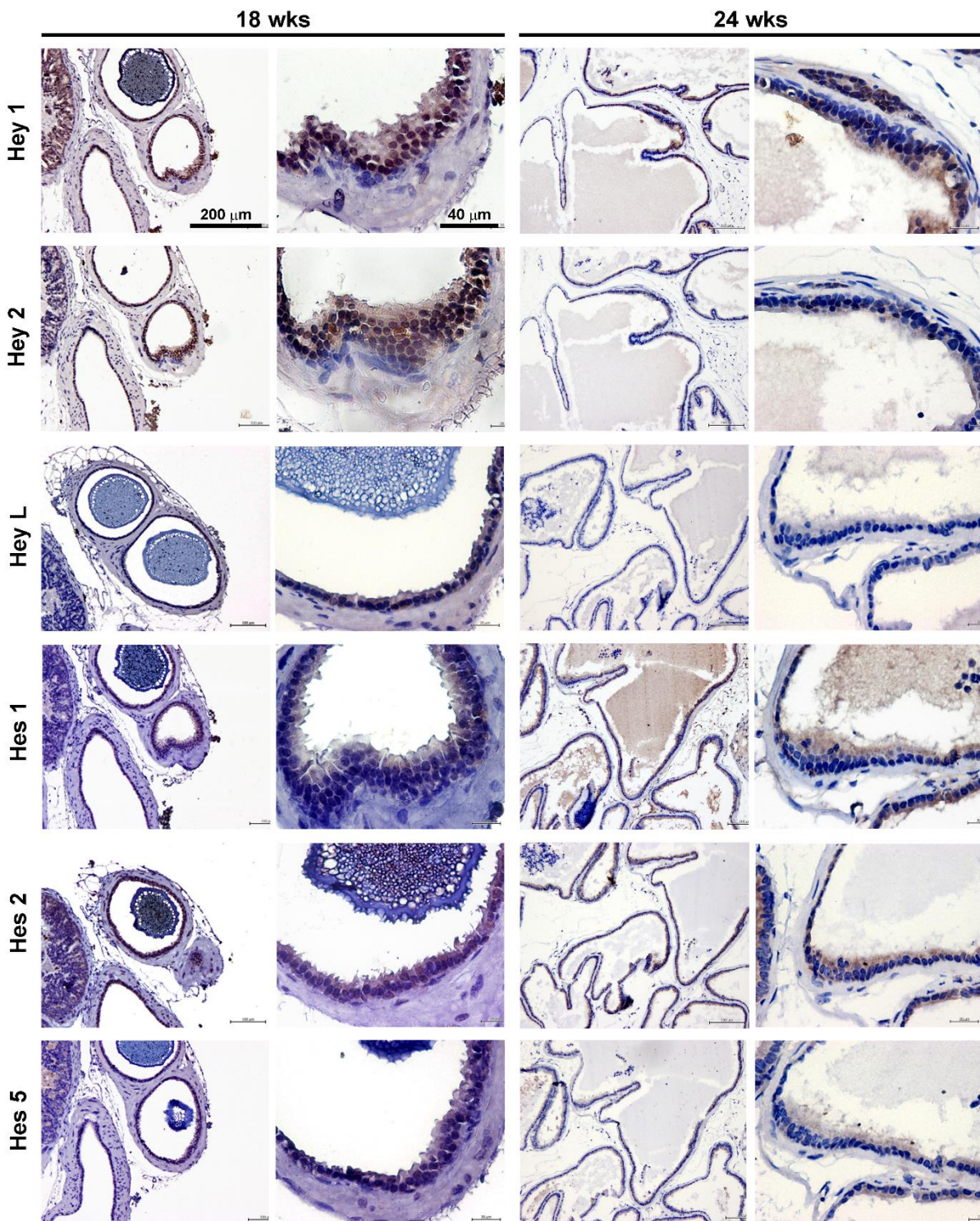


Positive immunostaining presented as brown color counterstained with haematoxylin. Hey1 presented the strongest nuclear expression in both time points. Hey 2, Hes1 and Hes2 were expressed in some dysplastic cells while HeyL and Hes5 were not detected in the nucleus. PIN- Prostatic Intraepithelial Neoplasia; WDA- Well differentiated Adenocarcinoma. N=4 for each time point.

Supplemental Figure III.7- Immunohistochemistry of Notch effectors in the lateral prostate of TRAMP mice at early (18 wks) and late (24 wks) stages of tumor development.

Lateral prostate

TRAMP

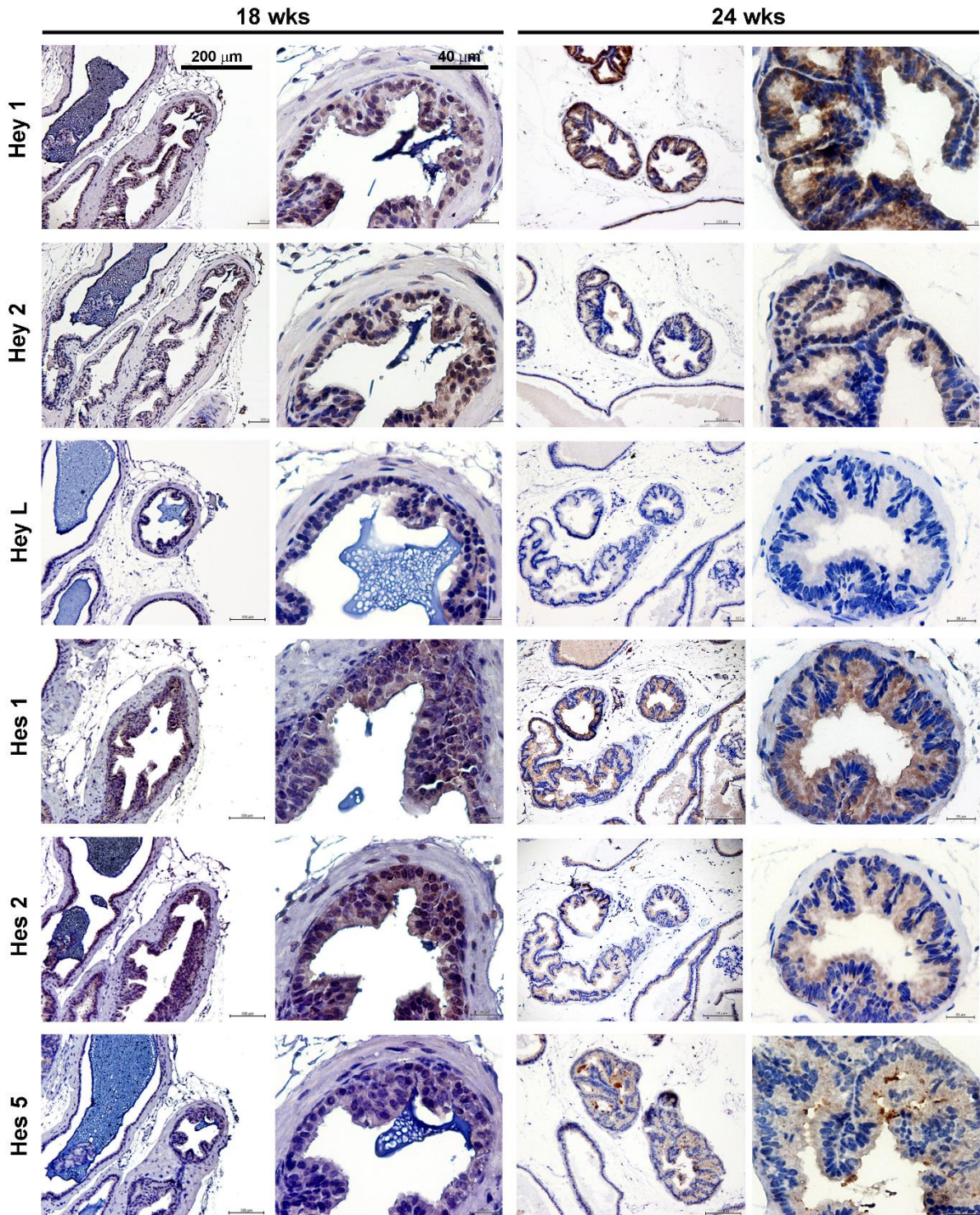


Positive immunostaining presented as brown color counterstained with haematoxylin. Hey1 was strongly expressed in the nuclei at both time points. Hey 2, Hes1 and Hes2 were expressed in some dysplastic cells mainly in early stage while HeyL and Hes5 were not detected in the nuclei. N=4 for each time point.

Supplemental Figure III.8- Immunohistochemistry of Notch effectors in the ventral prostate of TRAMP mice at early (18 wks) and late (24 wks) stages of tumor development.

Ventral prostate

TRAMP

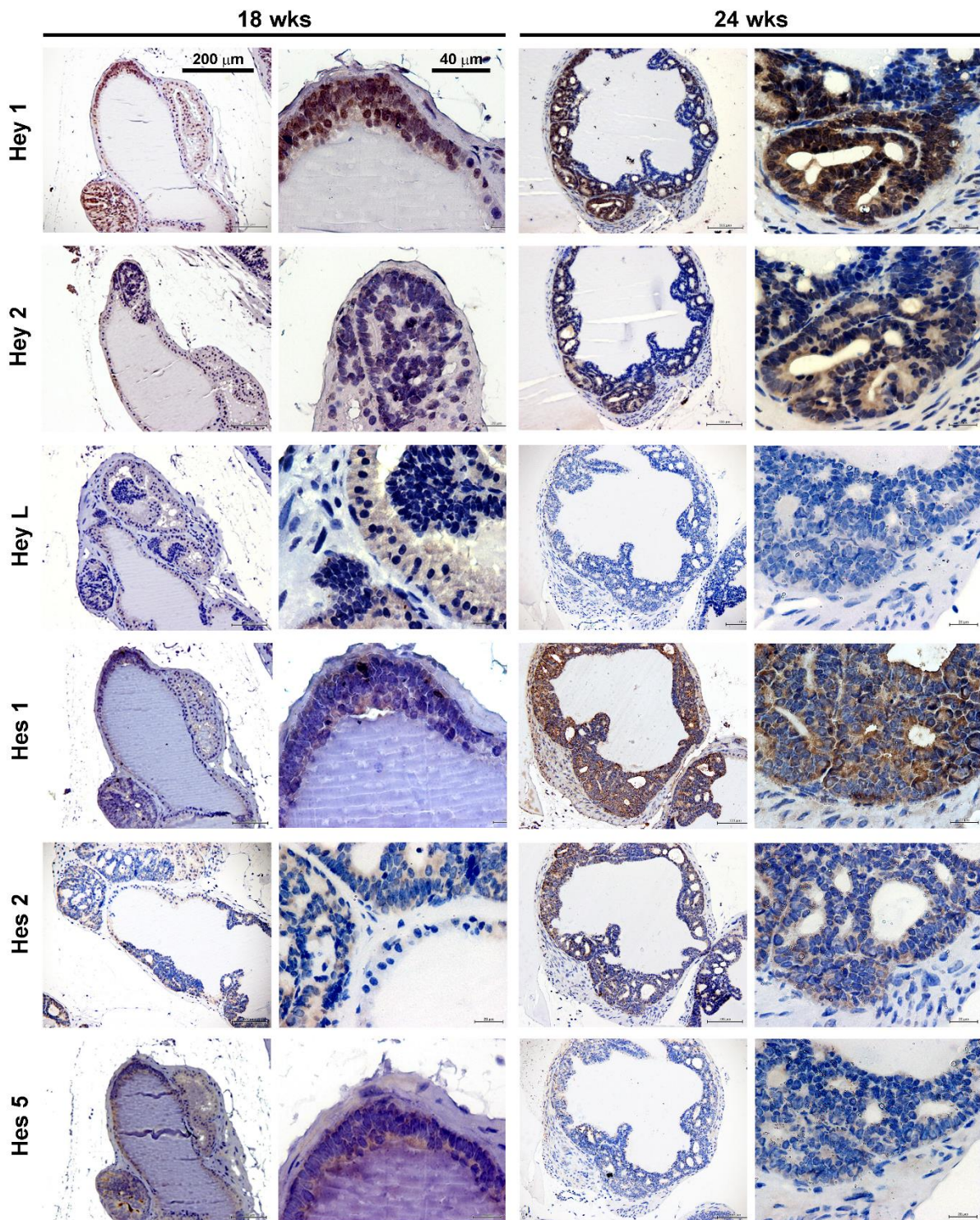


Positive immunostaining presented as brown color counterstained with haematoxylin. Hey1 and Hey2 were strongly expressed in the nuclei at both time points. Hes1 and Hes2 were expressed in some dysplastic cells only in early stage while HeyL and Hes5 were not detected in the nuclei. N=4 for each time point.

Supplemental Figure III.9- Immunohistochemistry of Notch effectors in the anterior prostate of TRAMP mice at early (18 wks) and late (24 wks) stages of tumor development.

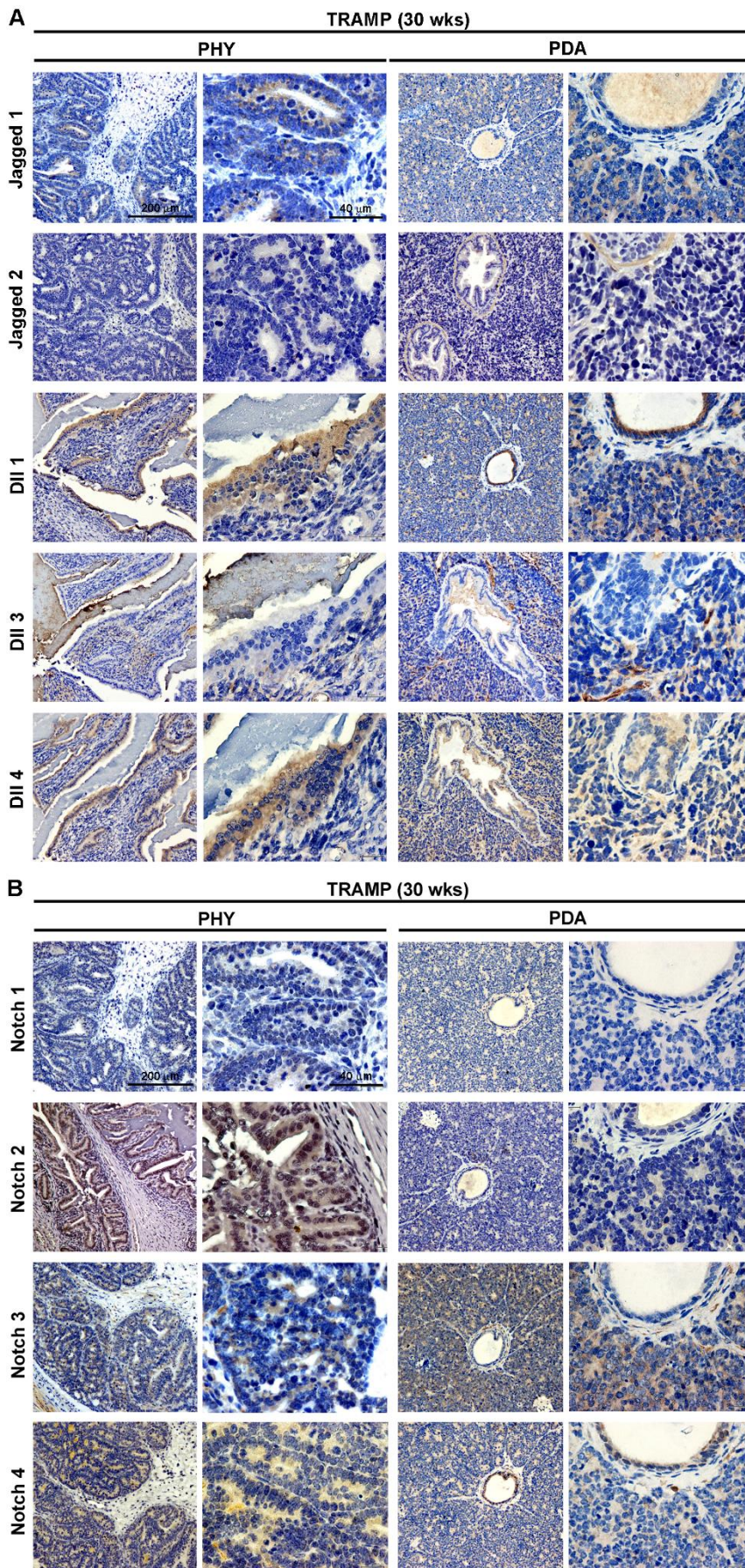
Anterior prostate

TRAMP



Positive immunostaining presented as brown color counterstained with haematoxylin. Hey1 was strongly expressed in the nuclei at both time points while Hey2 was also expressed but mildly. HeyL, Hes1, Hes2 and Hes5 were not detected in the nuclei in neither time points. N=4 for each time point.

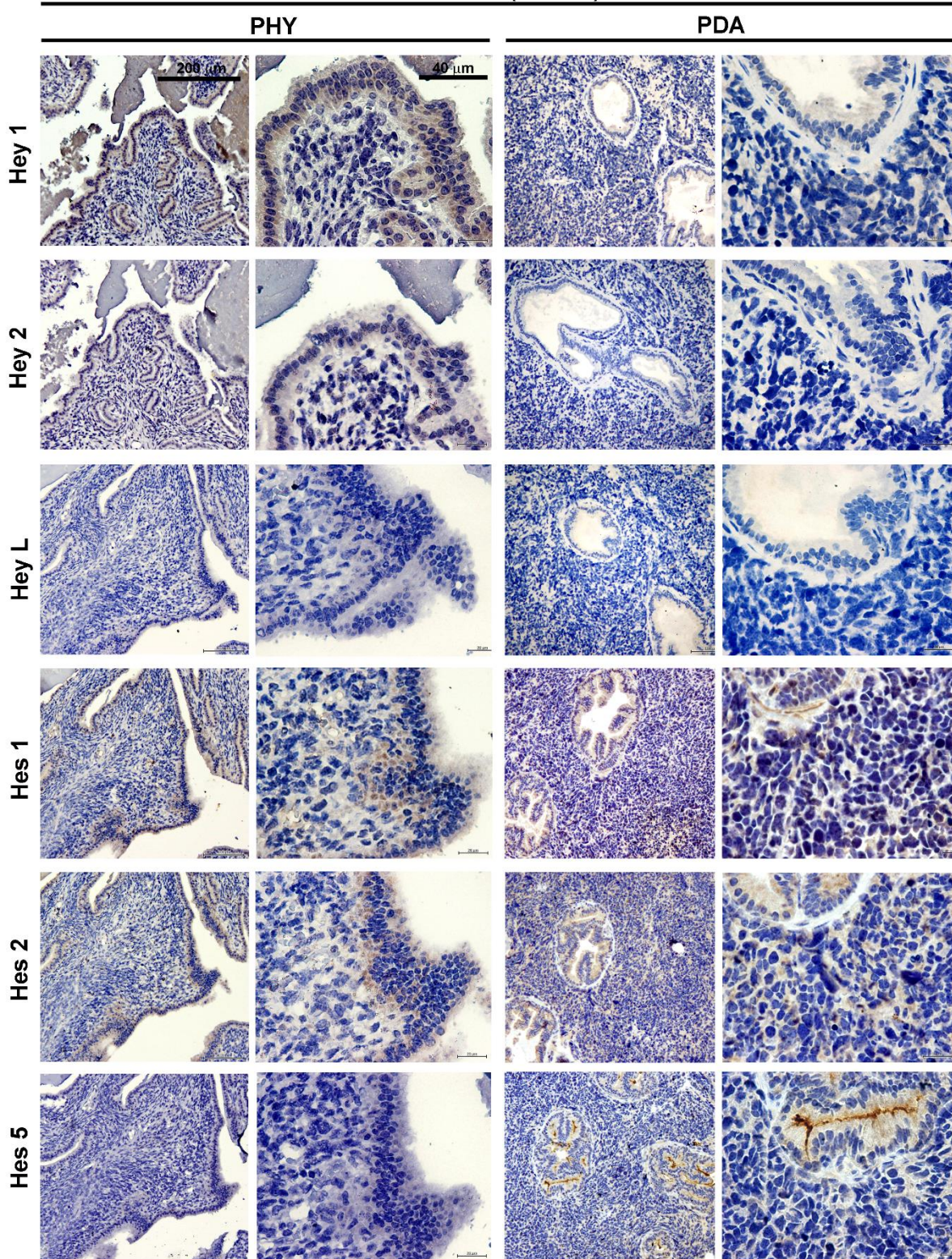
Figure III.7- Immunohistochemistry of Notch ligands and receptors in phylloides (PHY) and poorly differentiated adenocarcinoma (PDA) lesions of prostate cancer at 30 weeks of age.



Positive immunostaining presented as brown color counterstained with haematoxylin. (A) Notch ligands expression in PHY and PDA lesions of TRAMP prostates at 30 wks of age. Jagged1 presented strong expression, while Jagged2 presented practically null expression both in PHY and PDA. DII1 and DII4 showed to be expressed in both lesions unlike DII3 which was expressed only in the vasculature. (B) Notch receptors expression in PHY and PDA lesions of TRAMP prostates at 30 wks of age. Notch1 presented mild expression in PHY lesions but null expression in PDA lesions. Notch2 and Notch4 also presented mild expression while Notch3 was strongly expressed in both very late stage lesions. N=4.

Supplemental Figure III.10- Immunohistochemistry of Notch effectors in phylloides (PHY) and poorly differentiated adenocarcinoma (PDA) lesions of prostate cancer at 30 weeks of age.

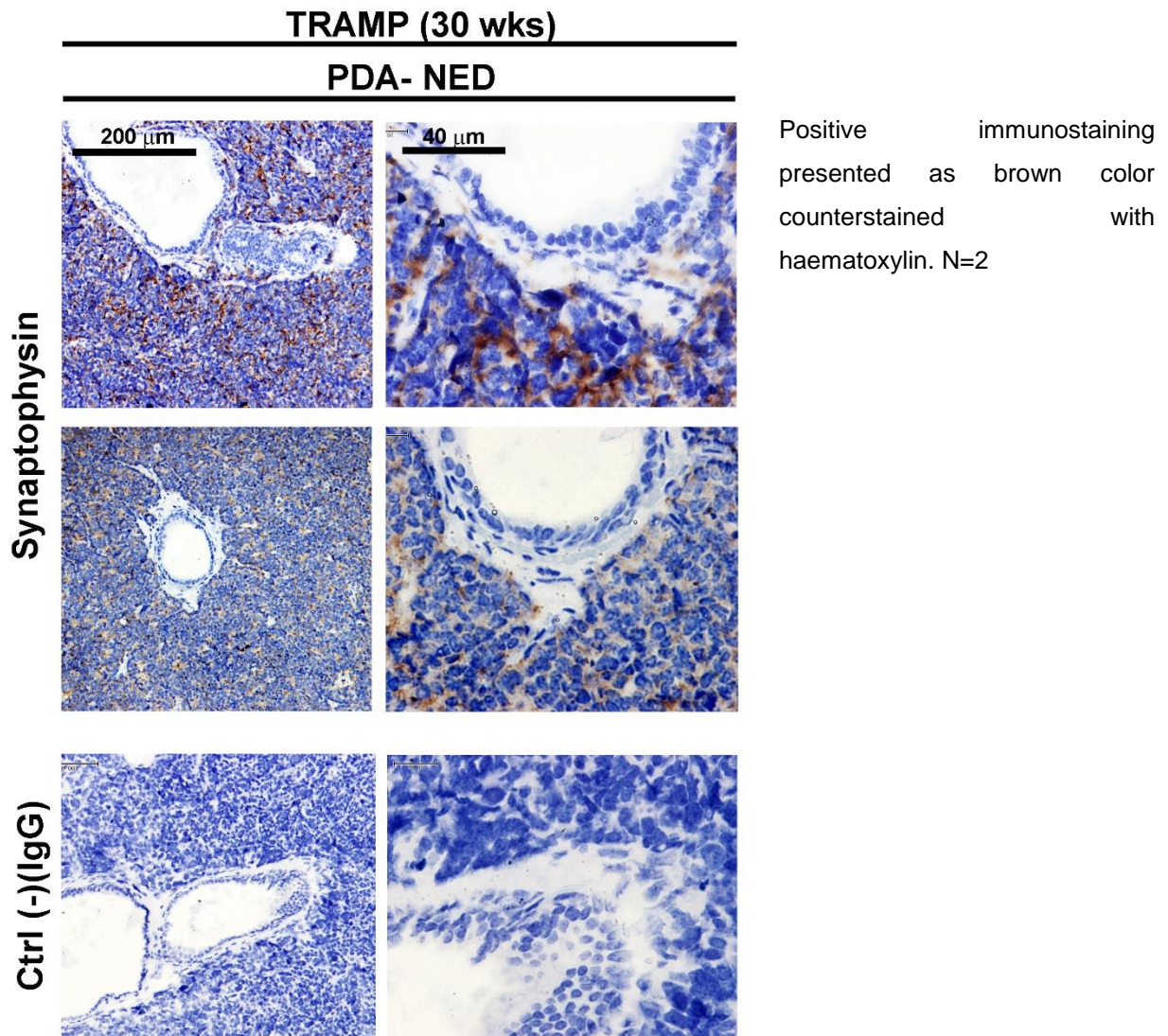
TRAMP (30 wks)



Positive immunostaining presented as brown color counterstained with haematoxylin. In these more advanced stages of prostate cancer progression the Notch effectors were not detected in the nucleus.

N=4.

Supplemental Figure III.11- Immunohistochemistry of Synaptophysin in poorly differentiated adenocarcinoma (PDA) lesions of prostate cancer at 30 weeks of age.



4.7 Notch signaling components are differentially transcribed and expressed in specific cell populations of the healthy and tumoral prostates.

After verifying that prostate tumor development caused significant up-regulation of specific Notch elements transcription and pronounced expression in the tumor tissues, we wanted to identify specific cell population (luminal, basal and stromal) expression changes. To achieve that aim, individual adult murine prostate cell populations were separated by FACS based on their surface antigenic expression profiles, as previously described (Lawson, Xin, Lukacs, Cheng, & Witte, 2007) (Figure III.8A). Subsequently, transcription analysis of the Jagged ligands, which were the only ligands that had a dynamic expression response in tumor development, receptors and effectors was performed.

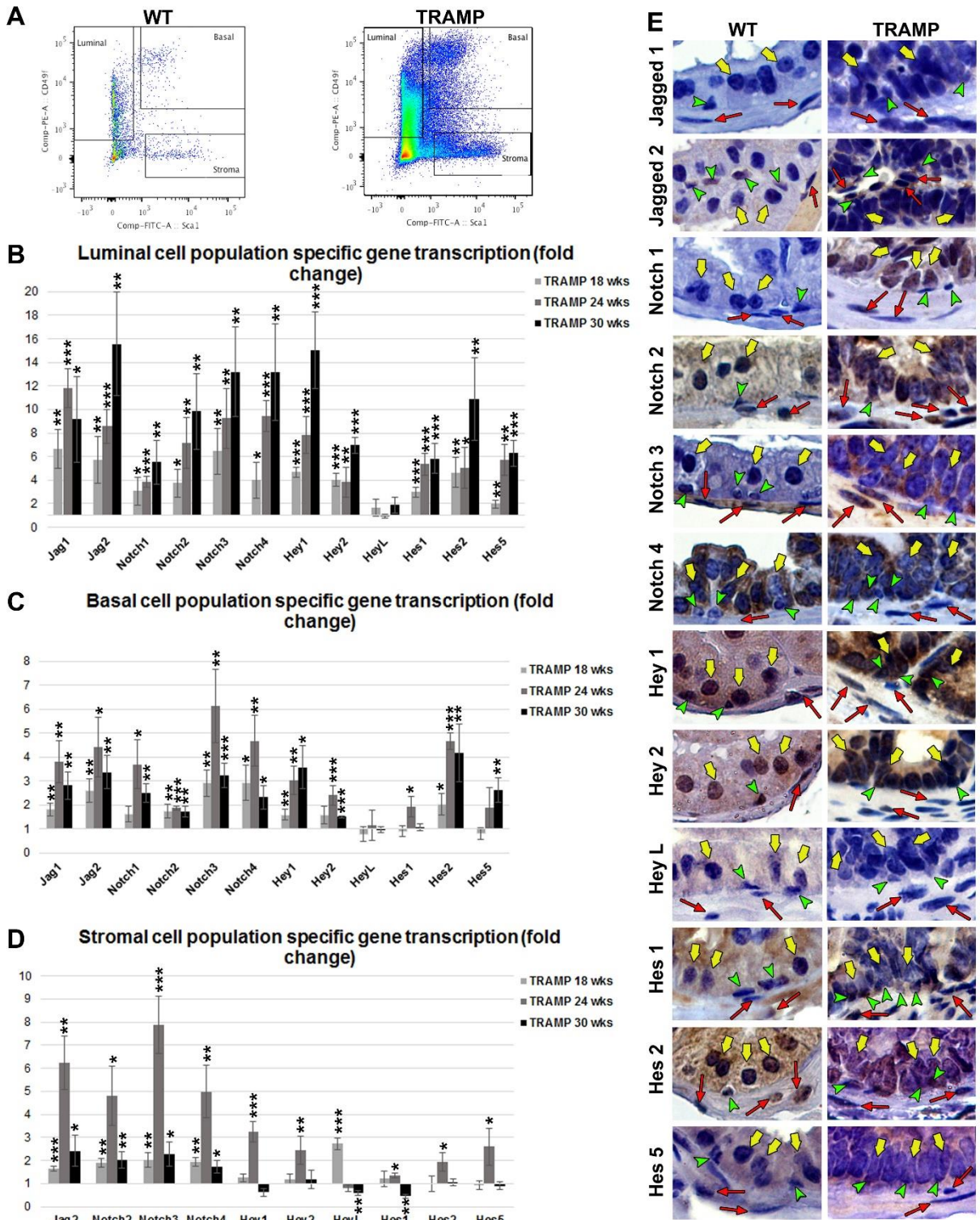
Luminal cell population specific analysis revealed that in luminal cells both Jagged ligands were highly up-regulated at both transcript (Figure III.8B) and protein levels (Figure III.8E-

yellow arrows) in prostate cancer development. The transcription of Notch receptors was found to be upregulated in luminal cells (Figure III.8B) of tumor lesions, especially *Notch3* and *Notch4*. However, at the protein level, Notch1 and Notch3 presented the strongest increased expression in TRAMP mice relative to WT (Figure III.8E- yellow arrows). Regarding luminal expression of Notch effectors, it was observed increased transcription of all effectors (Figure III.8B) with the exception of *HeyL*. *Hey1* and *Hes2* presented the highest mRNA up-regulation, but *Hey1* and *Hey2* were the effectors more consistently expressed in the luminal cells in both healthy and tumoral prostates (Figure III.8E), while *HeyL* and *Hes5* failed to present positive nuclear staining.

Basal cell population specific analysis (Figure III.8C and E - green arrows) demonstrated increased transcription of both Jagged ligands along the development of the tumor lesions. Notably, Jagged2 was also detected in WT basal cells, readily identified by their nuclear triangular or cuboidal shape, unlike Jagged1, which only appeared to be expressed in basal cells of TRAMP prostates (Figure III.8E- green arrows). To further validate the different expression patterns of Jagged ligands in basal cells, we immunostained these ligands together with CK5, a specific basal and intermediate cell marker (Wang et al., 2001) (Suppl. figure III.12). It was found the same expression pattern described previously: TRAMP prostates presenting Jagged1 increased expression, not only in luminal cells but also in CK5+ cells, while Jagged2 was detected in WT basal cells prostate but also presented increased expression in both luminal and basal TRAMP prostates. Similarly, all Notch receptors were upregulated at the mRNA level in TRAMP relative to WT mice (Figure III.8C), but *Notch3* presented the most pronounced response. At the protein level (Figure III.8E) it is clear that of all Notch receptors, only Notch2 was detected in basal cells of healthy prostates. Regarding the Notch effectors, once again *Hey1* and *Hes2* presented the highest mRNA up-regulation in basal cells of cancerous lesions (Figure III.8C). At the protein level (Figure III.8E-green arrows) only *Hey1*, *Hey2*, *Hes1* and *Hes2* were expressed in basal cell nuclei of healthy prostates, while mainly *Hey1* and *Hey2* were highly expressed in the tumor prostate lesions.

Lastly, stromal cell population specific analysis (Figure III.8D and E-red arrows) demonstrated increased transcript levels of *Jag2*, *Notch2*, *Notch3* and *Notch4* in stromal cells of cancerous prostate. However, only Jagged2, Notch2 and Notch3 were detected at the protein level in the stromal layer of healthy and tumor bearing prostates (Figure III.8E-red arrows). All the Notch effectors, with the exception of *HeyL*, were up-regulated in stromal cells of TRAMP relative to WT prostates, but mainly at a late stage of tumor development (24 wks) (Figure III.8D). Remarkably, *Hey1* was once again the Notch effector more prominently up-regulated in stromal population during prostate tumor development. Additionally, at the protein level, *Hey1* and *Hey2* were also strongly expressed in stromal cells of both healthy and tumor bearing prostates, while *Hes1* and *Hes2* were also detected mainly in tumor stromal cells, and finally *HeyL* and *Hes5* were not detected in either.

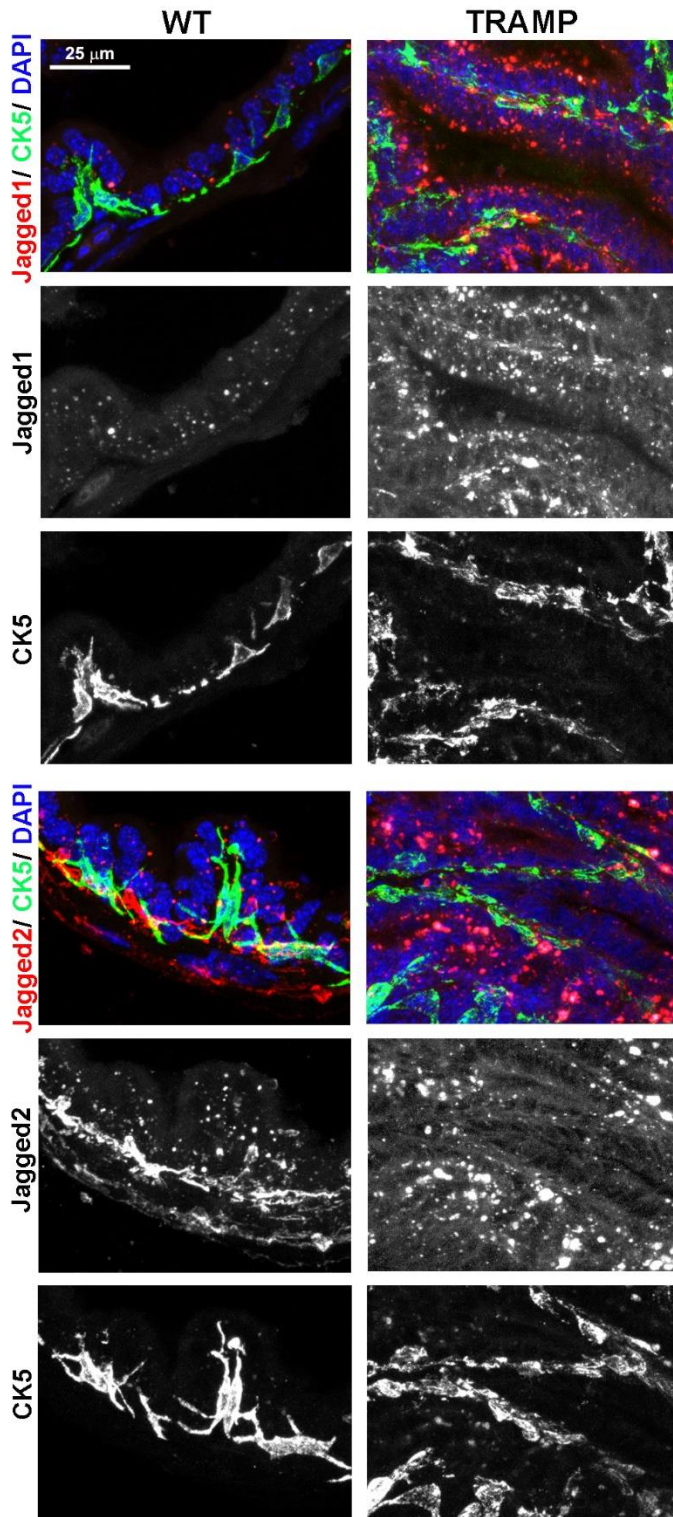
Figure III.8- Cell population specific transcription and expression analysis in prostate tumor development.



A. FACS plots of prostate cell population fractionation. Prostate basal, luminal and stromal cells are Lin⁻Sca1⁺CD49f⁺, Lin⁻Sca1⁻CD49f⁺, and Lin⁻Sca1⁺CD49f⁻, respectively in WT and TRAMP prostates. **B-D.** RNA was isolated from prostates collected at the end-point, and gene transcript analysis was performed by quantitative real-time RT-PCR for: **B.** luminal cells **C.** basal cells and **D.** stromal cells. Error bars represent SEM; * represents p<0.05; ** represents p<0.01; *** represents p<0.001. **E.** Immunohistochemistry of Notch signaling components and effectors showing cell population specific

staining. Yellow arrows indicate luminal cells; green arrowheads indicate basal cells; red arrows indicate stromal smooth muscle cells. N= 3 for each mice group (WT and TRAMP) and time point (18, 24 and 30 wks).

Supplemental Figure III.12- Immunofluorescence of Jagged1/2 and CK5 in healthy and tumorigenic prostates at 24 weeks of age.

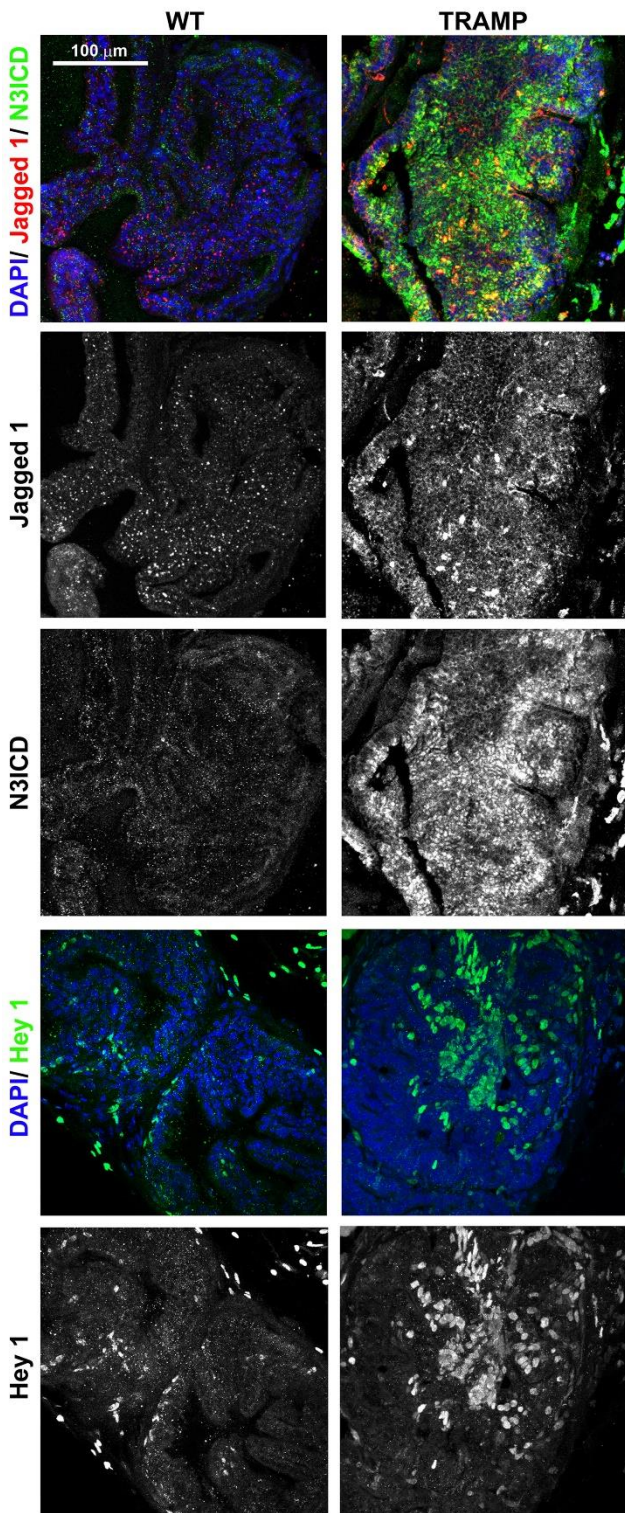


Healthy prostate of WT mice present absent Jagged1 expression in basal cells (CK5+ cells) whereas Jagged2 co-localizes with CK5 cells. Tumorigenic prostates of TRAMP mice present increased expression of both Jagged1 and Jagged2 ligands, which in both cases also co-localizes with CK5+ basal cells. N=2 for each mouse group.

4.8 The axis Jagged1/Notch3/Hey1 is highly activated in prostate tumor development

From the prostate cell population specific analysis in WT and TRAMP mice described previously, it seemed that Jagged1 and Notch3, that were completely absent from both luminal and basal cells in normal prostate, suffered a pronounced up-regulation at both transcript and protein levels. Since Jagged1 had already been described as a ligand for the Notch3 receptor (Liu et al., 2009), we immunostained WT and TRAMP prostates for Jagged1 and Notch3 intracellular domain (N3ICD), to detect activated Notch3. As can be observed in supplemental figure III.13, both Jagged1 and N3ICD presented strong positive staining in the same tumor areas. Furthermore, Hey1, the more prominently and consistently Notch effector upregulated in the tumor lesions, also presented strongly increased expression in the nuclei of TRAMP tumor lesions compared with WT prostates, further validating this Notch effector as the one more strongly correlated with prostate tumor development

Supplemental Figure III.13- Immunofluorescence of Jagged1, N3ICD and Hey1 in healthy and tumorigenic prostates.



Tumorigenic prostates of TRAMP mice present increased expression of Jagged1 ligand in areas where Notch3 is active (Notch3 intracellular domain), when compared with normal prostates of WT mice. Simultaneously the tumorigenic areas also present increased expression of Hey1 effector. N=2 for WT mice and N=4 for TRAMP mice.

5. Discussion

In this article we provide a comprehensive analysis of Notch pathway components expression in both healthy and tumor bearing mouse prostates. We have demonstrated that specific Notch components are expressed in the normal adult healthy prostate while others have their expression strongly increased along the prostate tumorigenic process, suggesting their involvement in prostatic tumor development.

In the healthy prostate of WT mice we detected transcription of all Notch components tested, except for *Dll3*. These results fall largely in line with the report of Valdez *et al.* (Valdez *et al.*, 2012) except for *Dll4* which was undetectable in either luminal or basal prostate cells in that report. Moreover, at the protein level we have observed that Dll1 and Dll4 ligands, Notch2 and Notch4 receptors, and Hey1, Hey2, Hes1 and Hes2 effectors are expressed in the luminal epithelial layer. Jagged2 is the Notch ligand with a more pronounced expression in the basal compartment of healthy prostates, alongside with Notch2 and Hey1, Hey2, Hes1 and Hes2. The stromal layer appears enriched for the ligand Jagged2, the receptors Notch2 and Notch3 and for the effectors Hey1, Hey2, Hes1 and Hes2. Valdez *et al.* (Valdez *et al.*, 2012) have observed high mRNA levels of *Jag1*, most specifically in basal cells, while *Dll1* and *Jag2* were transcribed at lower levels but preferentially in basal cells and *Dll3* and *Dll4* were undetectable in either luminal or basal prostate cells. Additionally they also found significant transcription of *Notch1* and *Notch2* receptors in both prostate basal and luminal cells and of *Notch3* in luminal cells, while the Notch target genes *Hes1*, *Hey1*, and *HeyL* were found to be transcribed in both basal and luminal compartments. Nevertheless, their results are only related to mRNA levels and should not be compared directly due to the possibility of post-transcriptional regulation. At the protein level, our results clearly demonstrate high expression levels of luminal Dll1, Dll4, Notch2 and Notch4, which can be speculated to play a role in the maintenance of the luminal differentiated state. In a similar glandular tissue, like the mammary gland, Notch signaling is believed to regulate luminal cell-fate commitment (Bouras *et al.*, 2008). In the basal compartment, Jagged2 and Notch2 are the key Notch members expressed, where they could be involved in restricting basal cell proliferation (Bouras *et al.*, 2008; Valdez *et al.*, 2012). Together these results suggest that specific expression patterns of Notch ligands and receptors in the different prostate cell compartments may exert a role in the homeostasis of the adult prostate providing new insights into the complex regulation that Notch signaling exerts in prostate cell proliferation and differentiation (Shahi, Seethammagari, Valdez, Xin, & Spencer, 2011; Valdez *et al.*, 2012).

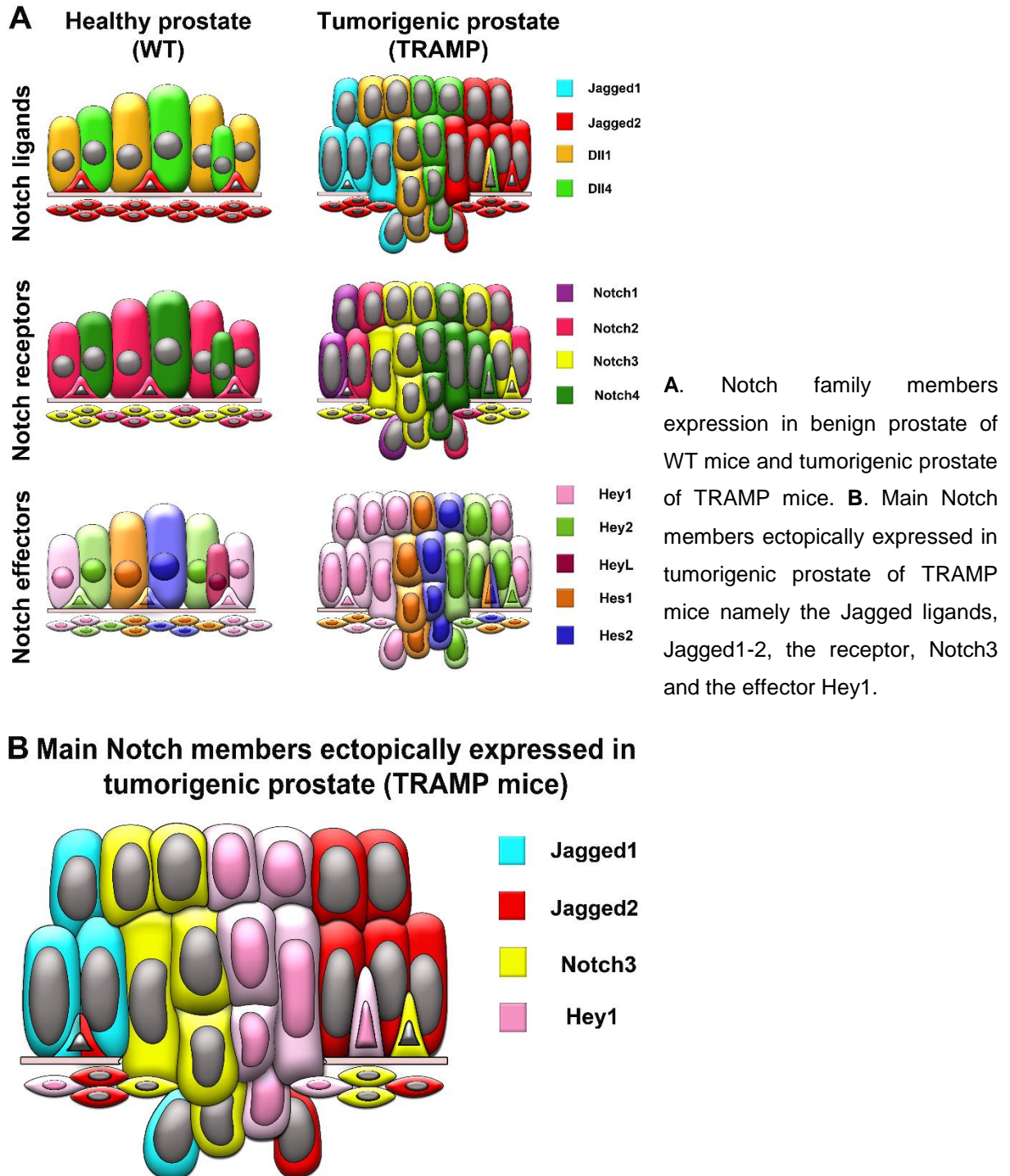
We have also profiled Notch member's expression during prostate tumor development (Figure III.9A). Even though we have found significant whole prostate mRNA upregulation of almost every Notch ligand (except Dll1), receptor and effector in TRAMP prostates relative to WT, there are specific ligands, receptors and effectors that seemed to be more relevant for the tumorigenic process. *Jag1* and *Jag2* were the ligands that suffered a higher upregulation at

the mRNA level of TRAMP vs WT prostates. Additionally they were also the Notch ligands that presented a dynamic expression change during prostate tumor development, given the fact that, unlike Dll1 and Dll4, they were not expressed in the luminal layer of healthy prostate even though Jagged2 was strongly expressed in the basal layer (Figure III.9A). The latest observation can lead to the speculation that Jagged2 may be involved in prostate cancer initiation and progression, given that deregulation of the basal cell lineage is a critical biological event for that process. Accordingly, Jagged2 increased expression has been described in cancer cells with high metastatic potential (Ross et al., 2011). Nevertheless, only Jagged1 remained to be strongly expressed in very late PDA and PHY lesions. Conversely, Jagged1 has been extensively described in the literature as of relevance for prostate tumor development by its increased expression in a variety of prostatic cancer cell lines (Scorey et al., 2006); the ability to regulate prostate cancer cell growth, apoptosis, migration and invasion (Zhang et al., 2006; Wang et al., 2010); and by its high levels of expression in metastatic and recurrent prostate cancer in humans (Santagata et al., 2004). In opposition, in a previous study *Jag1* was not detected by *in situ* hybridization in either WT or TRAMP prostates (Shou et al., 2001). Nevertheless, we mainly detected pronounced Jagged1 expression in late and very late stages of tumor development in TRAMP mice, with increased expression as the lesions progressed. Therefore, this discrepancy may be due to different stages of prostatic tumor analysis.

Regarding the Notch receptors, we also observed a strong upregulation of all the receptors either in whole prostate or in population specific analysis of TRAMP vs WT prostates. Nonetheless, Notch1 and Notch3 receptors, unlike Notch2 and Notch4, had a dynamic switch in their expression pattern, similar to what was observed with the Jagged ligands, given that they were not expressed in the healthy prostate (Figure III.9A). In the same line of evidence, Notch1 has been thoroughly studied in prostate tumor development, having been associated with malignant and metastatic prostate cells (Shou et al., 2001), described to be critical for prostate cancer cell growth and survival (Wang et al., 2010), invasion (Bin Hafeez et al., 2009) and chemoresistance (Ye et al., 2012). Controversially, Notch 1 activation has also been shown to have a tumor suppressive effect in prostate cancer by activating the PTEN suppressor gene (Whelan et al., 2009). The other Notch receptors have been less thoroughly studied so far: Notch2 increased mRNA expression (Scorey et al., 2006) and protein levels (Martin, 2004) have been described in some prostate cancer cell lines; and high levels of Notch3 have been described in prostate cancer cells with high metastatic potential (Ross et al., 2011). Despite the strongest evidence in the literature regarding the role of Notch1 in prostate tumor development, in our results, Notch3 was the most consistently and highly up-regulated and expressed Notch receptor. Additionally, the receptor Notch1 is known to be mainly activated by Delta-like ligands, Dll1 (Sörensen et al., 2009) and Dll4 (Benedito et al., 2009; Ding et al., 2012; Pedrosa et al., 2015a), unlike the Jagged ligands that have been described to be able to activate Notch3 in different settings (Liu et al., 2009; Ross et al., 2011;

Pedrosa et al., 2015a and b). Moreover, we have shown, by detecting increased N3ICD expression, that Notch3 is specifically activated in the TRAMP lesion areas, concomitantly with strong Jagged1 expression, providing a possible key Notch signaling axis of Jagged1/Notch3 in prostate tumor development.

Figure III.9- Models of Notch expression in healthy and cancerous murine prostate.



Lastly, we have also analyzed Notch effectors transcription and expression pattern in tumor lesions of TRAMP mice. We observed up-regulation of all Notch effectors in whole prostate transcription analysis, however *Hey1* and *Hes2* seemed to be more highly up-regulated, even in cell population specific analysis. Observing the protein expression of the effectors it was clear that especially *Hey1* but also *Hey2* were the effectors more strongly expressed in early (18 wks) and late stage (24 wks) prostatic tumor lesions (Figure III.9A), while *Hes2* presented positive nuclear expression only in some dysplastic cells. Additionally, immunofluorescence for *Hey1* has shown clearly increased nuclear expression in TRAMP tumor lesions, compared to WT prostates. Accordingly, amplification of the chromosome region comprising *Hey1* gene occurs in a large fraction of prostate cancers and correlates with aggressiveness of tumors (DeMarzo, Nelson, Isaacs, & Epstein, 2003). Unexpectedly, in very late lesions of PDA and PHY (30 wks) no nuclear expression was observed for any of the Notch effectors, even though there was strong expression of *Jagged1* ligand and *Notch3* receptor. This observation may be indicative of a Notch switch-down that may occur in very advanced stages of prostate cancer, prompting the tumor to become Notch independent. As demonstrated by Belandia *et al.* (Belandia *et al.*, 2005) *Hey1* co-localizes with androgen receptor in the epithelia of patients with benign prostatic hyperplasia, where it is found in both the cytoplasm and the nucleus. However *Hey1* is excluded from the nucleus in some human prostate cancers, raising the possibility that an abnormal *Hey1* subcellular distribution may have a role in the aberrant hormonal responses observed in prostate cancer. Moreover, the PDA lesions observed presented neuroendocrine differentiation, which in clinical tumors is associated with aggressive tumors and hormone refractory disease (Sun, Niu, & Huang, 2009; Vashchenko & Abrahamsson, 2014), which further supports the hypothesis presented by Belandia *et al.* (Belandia *et al.*, 2005) and our expression results regarding Notch effectors in very advanced lesions of prostatic tumors.

Furthermore, the strong expression of *Jagged2* and *Notch3* in benign stromal compartment as their pronounced up-regulation and expression in stromal TRAMP prostate (Figure III.9A), may be crucial for the invasion process that takes place in WDA or more advanced lesions of prostate cancer as similarly demonstrated in prostate cancer cells with high metastatic potential (Ross *et al.*, 2011).

6. Conclusions

Collectively, our data from both WT and TRAMP mouse prostates demonstrate that the main Notch components ectopically expressed in the prostate tumorigenic process (Figure III.9B) are the *Jagged* ligands, *Jagged1* and *Jagged2*, the *Notch3* receptor and the *Hey1* effector. Therefore, this extensive study has not only brought a new comprehensive view of Notch expression in healthy and neoplastic prostates, but also provides new insights into key Notch

components that may play a significant functional role in prostate tumor development. We suggest the Notch axis Jagged1-2/Notch3/Hey1 to be of high relevance for prostate tumor development, thereby, justifying additional functional studies.

**Chapter IV -
Targeting
Jagged1/2 is a
new promising
therapeutic
approach for
prostate cancer.**

Ana-Rita Pedrosa,
Alexandre Trindade,
Sandra Carvalho, Maria
C. Peleteiro, Joana
Gigante, Jim West and
António Duarte.

Manuscript in preparation

1. Abstract

The Notch signaling pathway has been implicated in cancer development, namely in prostate tumorigenesis, by its key role in cell-fate determination, differentiation and proliferation. Jagged1 (*Jag1*) is a Notch ligand that plays an important role in both physiological and pathological conditions, namely in embryonic and retinal vascular development, skin wound healing and tumor associated angiogenesis, while Jagged2 (*Jag2*) was first identified as required for craniofacial, limb and T cell development. Jagged1 is known to be expressed in the vasculature, and its increased expression in the glandular epithelium has been associated with cancer development and even considered to be a marker of bad prognosis and high metastatic potential in breast and prostate cancers. Up-regulation of Jagged2 has been described in prostate cancer cells with metastatic potential.

The purpose of our study was to investigate the potential therapeutic application of blocking Jagged ligands in prostate tumor therapy. To achieve it we administered a blocking anti-Jagged1/2 antibody to transgenic adenocarcinoma of the mouse prostate model (TRAMP) mice. The mice were sacrificed at 18 and 24 weeks of age, which correspond to early and late stages of tumor development, respectively, and the prostates were collected and analyzed regarding several parameters.

We observed that blocking Jagged1/2 has an inhibitory effect on the development of prostate tumors in all its stages. The tumor vasculature showed decreased density, with the presence of immature, leaky and non-functional blood vessels. We also detected increased tumor cell apoptosis and decreased proliferation. Moreover, anti-Jagged1/2 antibody treatment blocked the de-differentiation process by inhibiting the loss of luminal identity, the proliferation of the basal cell compartment and epithelial-to-mesenchymal transition. Additionally, treatment also restricted prostatic cancer stem-like cell proliferation and survival. These functions were achieved by decreasing Notch3 activation and Hey1 expression. The combination of all these different effects caused a strong inhibition of tumor progression, indicating that targeting Jagged1/2 may be a new promising therapeutic approach to prostate cancer.

Keywords: Jagged1; Jagged2; Notch; TRAMP; prostate cancer.

2. Introduction

The Notch signaling pathway has been extensively characterized in its role in cell-fate determination, differentiation, proliferation, progenitor and stem-cell self-renewal, in a diversity of embryonic and adult tissues (Artavanis-Tsakonas et al., 1999; Schweisguth, 2004). The Notch pathway is composed of 5 ligands (Jagged1, Jagged-2, and Delta-like 1, 3, and 4) and 4 receptors (Notch 1–4). Notch receptors are transmembrane molecules that consist of an N-terminal extracellular (NEC) fragment and a C-terminal transmembrane-intracellular subunit (Blaumueller et al., 1997). The Notch pathway is normally activated upon interactions with ligands, which are also transmembrane proteins containing EGF-like repeats. Upon ligand–receptor interactions, cleavage of the Notch receptors is promoted by ADAM10/17 metalloproteases, followed by a third cleavage mediated by the presenilin- γ -secretase complex. This series of events releases the intracellular portion of the Notch receptor (termed ICD), which is then translocated to the nucleus where it binds a transcriptional repressor leading to the transcription of downstream target genes, such as several helix–loop–helix transcription factors (*Hey* and *Hes* gene families among others)(Schweisguth, 2004).

Ligand-induced Notch signaling has been implicated in various aspects of cancer biology, with an associated oncogenic or tumor suppression function depending on the context (Ntziachristos et al., 2014). In the prostate, the contribution of Notch signaling to tumorigenesis is still not clear. Different laboratories consistently detected increased expression levels of NOTCH1 and NICD1 in all four frequently studied human prostate cancer cell lines (PC3, DU145, 22Rn1, and LNCaP)(Shou et al., 2001; Bin Hafeez et al., 2009). In these cell lines, knockdown of NOTCH1 levels by small interfering RNA inhibited cell invasion (Bin Hafeez et al., 2009) survival, and proliferation (Zhang et al., 2006). Controversially, a previous work had shown that Notch pathway activation, through engineered overexpression of NICD, also had a growth inhibitory effect (Shou et al., 2001). In the mouse, in the TRAMP- Transgenic Adenocarcinoma of the mouse prostate model, increased Notch1 mRNA levels were detected upon metastization to regional lymph nodes (Shou et al., 2001). However, in humans, an mRNA expression analysis of databases showed decreased levels of NOTCH1 and HEY1 in prostate cancer compared to benign prostate samples (Wang et al., 2006). In contrast, studies on protein levels, have found increasing levels of Notch pathway members in human cancers: levels of NOTCH1 and NOTCH3 protein increased with increasing Gleason grade (Bin Hafeez et al., 2009; Danza et al., 2013); prostatic metastases showed distinctly elevated levels of JAGGED1 protein, when compared to localized tumor or benign tissue (Santagata et al., 2004); moreover, tumors with highest levels of JAGGED1 were least likely to be cured by radical prostatectomy, suggesting that JAGGED1 contributes to the ability of these cancers to metastasize prior to surgery (Santagata et al., 2004); Notch signaling was the most distinguishing feature when comparing gene expression profiles from high-grade versus low-grade Gleason scores microdissected cancer cells (Ross et al., 2011); and ultimately, cancer

cells with metastatic potential showed upregulation of the Notch ligand JAGGED2 and NOTCH3 receptor (Ross et al., 2011). Notch signaling also plays an important role in tumor angiogenesis, one of the hallmarks of cancer (Hanahan & Weinberg, 2011). Notably, a Notch decoy that specifically blocks Jagged ligand interactions inhibited xenograft tumor growth by an anti-angiogenic phenotype (Kangsamaksin et al., 2014). Moreover, in the prostate, endothelial *Jag1* was shown to be able to significantly inhibit tumor development by inhibiting angiogenesis, maturation of the vessels and by an angiocrine function regulating prostate tumor cell proliferation and de-differentiation (Pedrosa et al., 2015b).

The contradictory information about Notch signaling contribution to prostate cancer development may be related to different levels of Notch activation and even to different receptors and ligands equilibrium, since both may result in different downstream effects, as demonstrated previously in other settings (Benedito et al., 2009; Trindade et al., 2012; Pedrosa et al., 2015a). Nevertheless, the preponderance of evidence supports upregulation rather than downregulation of Notch components with mouse and human prostate cancer progression. Consequently, pan-Notch inhibitors and therapeutic antibodies targeting one or more of the Notch receptors have been investigated for cancer therapy (Ntziachristos et al., 2014). However, the use of the previous approaches has lifted many important questions, due to the broad Notch expression in several other tissues, leading to aggressive secondary effects, such as gastro-intestinal and liver toxicity, as well as a great rate of Notch receptors mutations identified in cancer. Therefore an effort has been made in the field to narrow the Notch targets used in cancer therapy.

Considering the vast correlation data existing between Jagged1 expression and prostate cancer progression, and the finding of our lab that both Jagged ligands are ectopically expressed in prostatic lesions of the TRAMP prostate (unpublished data) we proposed to investigate the therapeutic potential of a blocking Jagged1/2 antibody in prostate cancer.

3. Materials and Methods

3.1 Experimental animals

All the procedures involving animals used in this study were approved by the Ethics and Animal Welfare Committee of the Faculty of Veterinary Medicine of Lisbon. All animals were housed in ventilated propylene cages with sawdust as bedding, in a room with temperature between 22°C and 25°C and a 12-hours-light/12-hours-dark cycle. The mice were fed standard laboratory diet.

3.2 Therapeutic Intervention Trials

For intervention trials TRAMP mice were administered once a week (IP) with 20mg/Kg (during a 6 week period) of Anti-Jagged1/2 antibody (TRAMP Anti-Jag1/2) while the other TRAMP

mice group received an equal dosage of IVIG (which consists of the excipient in which the antibody was diluted) (TRAMP).

In the early intervention trial antibody administration began at 12 and extend until 18 weeks of age, while the late intervention trial began at 18 weeks and extend until 24 weeks of age.

3.3 Tissue preparation and immunohistochemistry

TRAMP (in C57BL/6 genetic background) mice were sacrificed at 18 and 24 weeks of age and the prostates finely dissected and collected.

For histopathological analysis, prostates were fixed in 10% buffered formalin solution for 48 h, dehydrated in alcohol, cleared in xylene, embedded in paraffin, sectioned at 3µm and stained with hematoxylin (Fluka AG Buchs SG Switzerland) and eosin Y (Sigma, St. Louis, MO). The sections were then analysed blindly by a pathologist (CP) and scored according to the literature (Kaplan-Lefko et al., 2003). Tumor samples were also fixed with 4% paraformaldehyde (PFA) solution at 4°C for 1h, cryoprotected in 15% sucrose, embedded in 7,5% gelatin, frozen in liquid nitrogen and cryosectioned at 10 and 20µm.

Immunofluorescence was performed using the following protocol: tissue slides were permeabilized in 3% H₂O₂ methanol solution for 30 min and PBS-Triton 0,1% solution 2x 10 min; blocking was performed for 1h (room temperature) either with 2% BSA + 5% Donkey serum in PBS-W 0,1%; after blocking, slides were incubated over-night at 4°C with specific primary antibodies followed by 1h incubation at room-temperature with fluorescently-tagged specific secondary antibodies.

To examine vascular density and vessel maturity a rat monoclonal anti-mouse PECAM-1 (BD Pharmingen, San Jose, CA) and a mouse monoclonal anti-SMA Cy3 conjugate (Sigma Aldrich, USA), combined with a donkey anti-rat conjugated with Alexa Fluor 488 (Invitrogen, Carlsbad, CA) were used. Nuclei were counterstained with 4', 6'-diamidino-2-phenylindole dihydrochloride hydrate (DAPI; Molecular Probes, Eugene, OR). Vascular density is equivalent to the percentage of each prostate section field occupied by a PECAM-1-positive signal (as determined by the percentage of black pixels per field after transforming the RGB images into binary files). Similarly, as a measure of vascular maturity, mural cell recruitment was assessed by quantifying the percentage of PECAM-1-positive structures lined by α-SMA-positive cells.

To assess vascular perfusion, avertin (2,5%) anesthetized mice were injected with biotin-conjugated lectin from *Lycopersicon esculentum* (100µg in 100µl of PBS; Sigma, St. Luis, MO) via caudal vein and allowed to circulate for 5 minutes before perfusing the vasculature transcardially with 4% PFA in PBS for 3 minutes. Slides were stained with rat monoclonal anti-mouse PECAM-1, followed by Alexa 594 goat anti-rat IgG (Invitrogen, Carlsbad, CA). Biotinylated lectin was visualised with Streptavidin-Alexa 488 (Invitrogen, Carlsbad, CA). Prostate perfusion area was quantified by determining the percentage of PECAM-1-positive structures that were co-localized with Alexa 488 signals.

To analyse vascular extravasation, avertin anesthetized mice were injected with 1% Evans Blue dye solution (Sigma, St. Luis, MO) via caudal vein, and perfused transcardially 5 minutes later with 4% PFA in PBS for 3 minutes. Tissue sections were stained with rat monoclonal anti-mouse PECAM-1, followed by Alexa 488 goat anti-rat IgG. Prostate vascular extravasation area was quantified by determining the tumor section field of Evans Blue red positive signal per vessel area (given by vascular density measurements).

For evaluation of hypoxic levels a rabbit anti-Hif1 α antibody was used (Abcam, Cambridge, UK). For quantification of cellular apoptosis and proliferation, a rabbit anti-active caspase3 (Cell signaling Technology) and an Alexa-570 conjugated mouse anti-Ki67 (eBiosciences Inc., CA, USA) antibodies were used.

For the assessment of epithelial to mesenchymal transition, an Alexa-488 conjugated mouse anti-E-cadherin and a goat polyclonal anti-Slug and anti-Snail (Abcam, Cambridge, UK) antibodies were used, respectively.

For analysis of the prostate cellular populations, a chicken anti-CK8 (Abcam) for luminal cells, a rabbit anti-p63 for basal cells and a rabbit anti-CK5 (Novus) for intermediate cells were used. Additional primary antibodies used were rat anti-Androgen Receptor (Abcam), rabbit anti-N3ICD (Santa Cruz), rabbit anti-Hey1 (Milipore) and rat anti-CD44 (BD Pharmingen). Additional secondary antibodies used were Alexa-488 or 594 donkey anti-goat, anti-rat, anti-rabbit and anti-chicken (Invitrogen, Carlsbad, CA).

3.4 Instrument details

Fluorescent immunostained sections from prostatic tumors, due to the tissue complexity, were obtained using a Carl Zeiss LSM 710 confocal microscope with either Zeiss 20X (Plan-Apochromat) NA 0.80 dry objective or 40X (EC Plan-Neofluor) NA 1.30 oil immersion objective, and captured using ZEN 2010 software (Carl Zeiss, Jena, Germany). Morphometric analyses were performed using the NIH ImageJ 1.37v program (NIH, Bethesda, MA, USA).

H&E stained sections were examined under a Olympus BX51 microscope with Olympus 10X/0.30 NA and 40X/0.75 NA dry objectives and captured with coupled Olympus DP21 photographic equipment (Olympus Iberia, Inc).

3.5 Quantitative transcriptional analysis

For whole prostate analysis, tumor samples were collected at the endpoint of each experiment and snap frozen for RNA extraction (Qiagen, Hilden, Germany). LSCs were sorted directly into the lysis buffer of the RNeasy Micro Kit (Qiagen). Total RNA was isolated according to manufacturer's protocol. A total of 75 ng RNA per reaction (LSCs) and 400 ng per reaction (whole prostate) was used to generate cDNA with the SuperScript III First Strand Synthesis Supermix Q RT-PCR Kit (Invitrogen, CA). Relative quantification real-time PCR analysis was performed as described (Trindade et al., 2008) using Sybergreen Fastmix ROX dye (Qiagen).

Primer pair sequences are available on request. The housekeeping gene β -actin was used as endogenous control.

3.6 Flow cytometry

For flow cytometric analysis and sorting of LSCs (Lin^- (cd45^- $\text{cd31}^-\text{ter119}^-$) $\text{Sca1}^{\text{hi}}\text{cd49f}^{\text{hi}}$), prostates were finely dissected into small pieces (2-4 mm). Then, the samples were digested into 1 ml solution of 0,1% collagenase (Sigma) and 2,4U/ml of dispase (Gibco, Life Technologies) incubation at 37°C, with agitation, for 2h30 min. DNase I (Sigma) was added during digestion to eliminate DNA residues. After washing, digested cells were then subjected to immunostaining with anti-mouse ter-119 PE-Cy7, anti-mouse cd45 PE-Cy7, anti-mouse cd31 PE-Cy7 (Affymetrix, eBioscience), anti-mouse Sca1 FITC and anti-mouse cd49f PE (BD Pharmingen). After washing, cells were sorted in a FACS Aria III cytometer and analyzed using BD FlowJo software (Version 10.0, BD Bioscience).

For demarcating and sorting of LSCs population, first standard quadrant gates were set, subsequently to differentiate Sca1^{hi} ($>10^{3.5}$ log FITC fluorescence) and cd49f^+ ($>10^3$ log PE fluorescence) cells from the Lineage negative population ($\leq 10^2$ log PE-Cy7 fluorescence).

3.7 Statistical analysis

All data processing (except most common and most severe prostatic lesion) was carried out using the Statistical Package for the Social Sciences software, version 17.0 (SPSS v. 17.0; Chicago, IL). Statistical analyses were performed using Mann-Whitney-Wilcoxon test and Student's t-test.

Scores of the most common and most severe histopathological prostatic lesions were analyzed with the GLM procedure of Statistical Analysis System (SAS Institute Inc. v.9.1.3 2009; Cary, USA). The analyses were carried out within group, with a linear model including the effects of time (weeks 18 and 24) and treatment (TRAMP Anti-Jag1/2 vs. respective controls- TRAMP) and their interaction.

All results are presented as mean \pm SEM. *P*-values < 0.05 , <0.01 and <0.001 were considered significant (indicated in the figures with *) and highly significant (indicated with ** and ***), respectively.

4. Results

4.1 Administration of a blocking antibody against Jagged1 and Jagged2 inhibited prostate tumor development and progression

To evaluate the efficacy of a blocking antibody directed against both Jagged1 and Jagged2 ligands we performed a therapeutic intervention trial using a transgenic murine model of prostate adenocarcinoma (TRAMP)(Greenberg et al., 1995), which spontaneously develop prostatic lesions from 8 weeks of age (Kaplan-Lefko et al., 2003). The therapeutic trial was performed in two different time points: from 12 to 18 weeks of age- early intervention trial; and from 18 to 24 weeks of age- late intervention trial. These time points were chosen in order to simulate an early and late detection, respectively, of the disease in humans. Therefore TRAMP mice and TRAMP mice administered with the anti-Jagged1/2 antibody (TRAMP Anti-Jag1/2) were sacrificed at 18 and 24 weeks of age, and the prostates collected for analysis. Blocking Jagged1/2 leads to decreased total prostate weights, relative to respective controls (TRAMP), in both early and late trials (Figure IV.1A and B). Noticeably, the prostate weights of TRAMP Anti-Jag1/2 did not differ significantly from those of WT animals.

The prostates were also classified regarding the type and evolution of tumor lesions. Histopathological analysis was carried out blindly and the tumors scored according to the following categories: Normal (0), prostatic intraepithelial neoplasia [PIN (1)], well differentiated adenocarcinoma [WDA (2)], moderately differentiated adenocarcinoma [MDA (3)], poorly differentiated adenocarcinoma [PDA (4)], or phylloides-like cancer [PHY (5)] (Kaplan-Lefko et al., 2003). The prostatic lesions evolve in a progressive manner, with different lobes of the prostate presenting different stages of tumor development. Therefore a score was attributed to each animal according to the most common and most severe lesion present, in order to statistically measure the effect of treatment on prostate tumor progression and its evolution over time.

TRAMP mice treated with Anti-Jagged1/2 presented a statistically significant inhibition of prostate tumor progression (Figure IV.1C-F). The evaluation of the most common lesion (Figure IV.1C) revealed a significant different score between treated and non-treated TRAMP mice. At the early intervention trial (18wks), the respective control group (TRAMP) presented a mean score of the most common lesion of 1.63 (Figure IV.1C) with the majority of animals (88%) classified with lesions of WDA (Figure IV.1E and F) while the TRAMP Anti-Jag1/2 mouse group presented a mean score of 0.62 (Figure IV.1C), with 22% of animals still showing no lesions (Normal), and the majority (100%) progressing to lesions of PIN (Figure IV.1E and F). At the late intervention trial (24 wks), the same kind of response was observed with the TRAMP group presenting a mean score of the most common lesion of 2.00 and 70% of animals with WDA while treated TRAMP mice (TRAMP Anti-Jag1/2) presented a mean score of 0.77 and 88% classified with lesions of PIN (Figure IV.1E and F). The evaluation of the most severe lesion also revealed a significant difference between the mouse groups. In the early

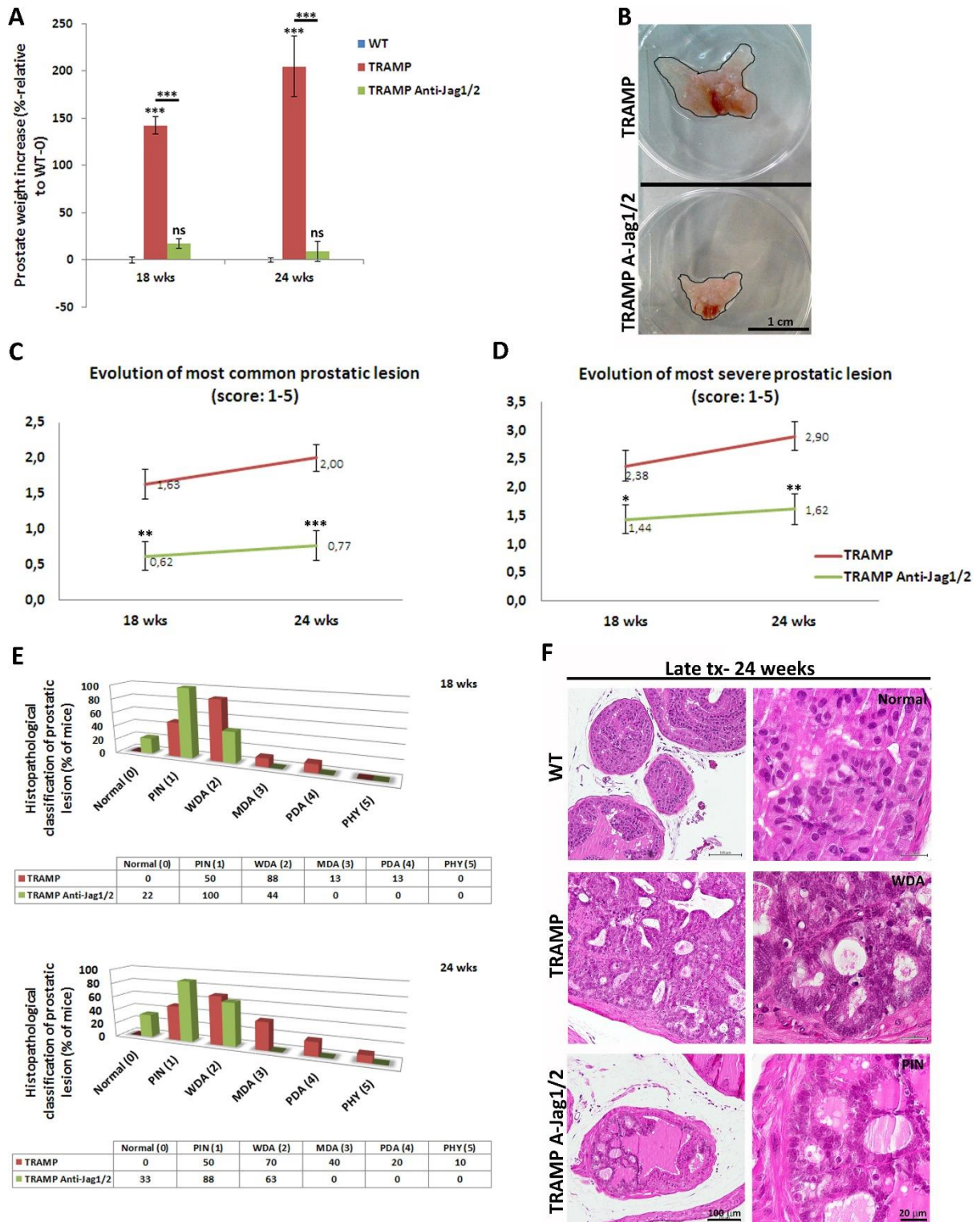
intervention trial (18 wks) non-treated mice (TRAMP) presented a mean score of the most severe lesion of 2.38 (Figure IV.1D) with 13% of these animals classified with more advanced stages of prostatic cancer (MDA and PDA) (Figure IV.1E), while the treated group (TRAMP Anti-Jag1/2) presented a mean score of 1.44 and only 44% of the animals evolved to lesions of WDA (Figure IV.1E). In the late intervention trials (24 wks) TRAMP mice presented a mean score of the most severe lesion of 2.90 (Figure IV.1D) with 70% of animals presenting advanced stages of disease (40%-MDA; 20%-PDA; 10%-PHY) (Figure IV.1E), while TRAMP Anti-Jag1/2 group presented a mean score of 1.62 with 63% classified with lesions of WDA and none of the treated mice presented (0%) more advanced stages of disease (Figure IV.1E). From the analysis of the most common and most severe lesion per animal it was also clear that there was no statistical interaction between the mouse groups throughout the evolution of the lesions (Figure IV.1C and D). This means that the effect of blocking Jagged1/2 remained constant in time (evolution of tumor progression).

4.2 Blocking Jagged1/2 had an anti-angiogenic effect in tumor vasculature

Since we have previously shown that Jagged1 is also strongly expressed in the vasculature of prostatic tumors and demonstrated the ability of endothelial *Jag1* to regulate prostate tumor growth by its pro-angiogenic function (Pedrosa et al., 2015b) we wanted to address whether the treatment with blocking Anti-Jagged1/2 antibody would also cause alterations in tumor vasculature. The endothelium was visualized by immunostaining against PECAM-1, while α -SMA was used to reveal perivascular cell coverage and thereby analyze vessel maturation (Figure IV.2A-C). Not surprisingly, tumor vasculature of TRAMP Anti-Jag1/2 was less dense (Figure IV.2A and B), and with decreased number of perivascular SMA positive cells, as demonstrated by the white arrows (Figure IV.2A and C). From figure IV.2 it is also clear that there were no major differences in tumor vasculature between early (18 wks) and late (24 wks) intervention trials.

Tumor vessel functionality in terms of perfusion and leakage was also analyzed by biotinylated lectin and Evans' Blue dye perfusion, respectively (Suppl. figure IV.1). Treatment of TRAMP mice with Anti-Jagged1/2 antibody led to a significant decrease in vessel perfusion relative to the respective controls (TRAMP) (Suppl. Figure IV.1A and B). Moreover, Evans' Blue extravasation was significantly increased in treated animals, as demonstrated by suppl. figure IV.1C and D.

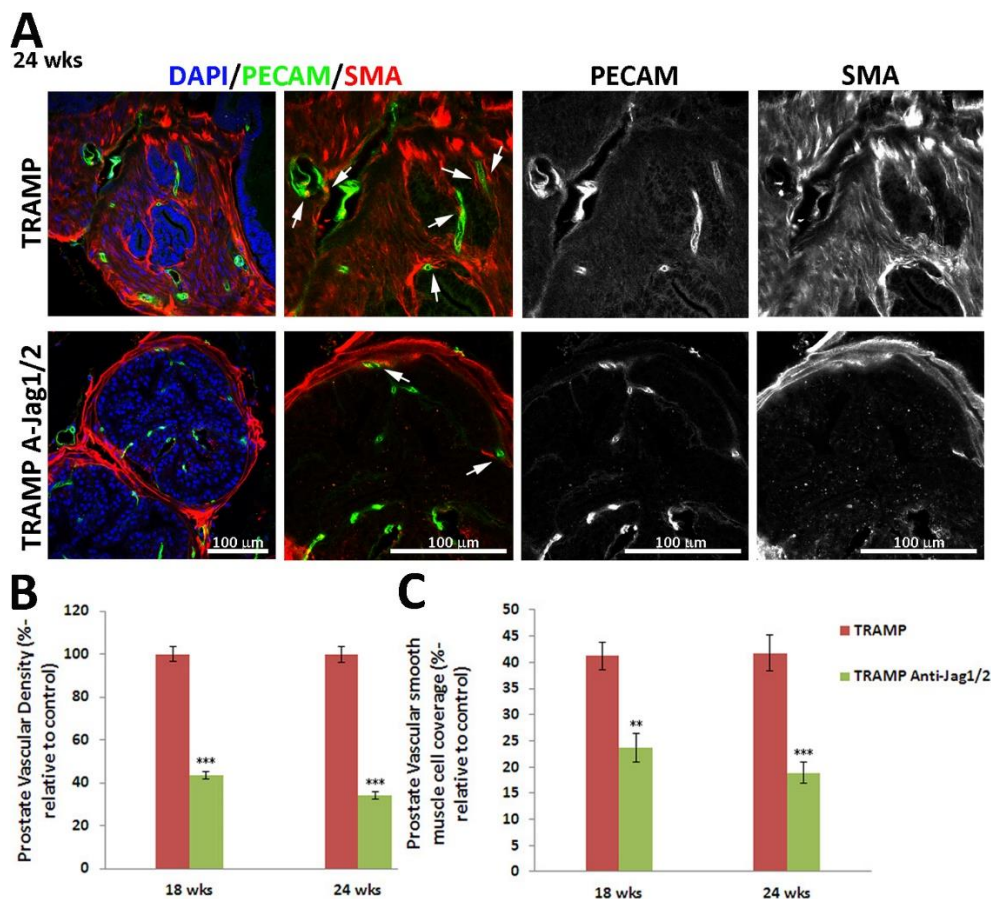
Figure IV.1- Administration of a blocking antibody against Jagged1 and Jagged2 inhibited prostate tumor development.



A. Prostate weight increase (in %, relative to WT-0%) in TRAMP (untreated) and TRAMP Anti-Jag1/2 (treated with the blocking antibody), in early (18 wks) and late (24 wks) intervention trials in prostate cancer treatment. In both trials, TRAMP Anti-Jag1/2 presented lower prostate weight increase than the TRAMP Ctrl group. **B.** Representative photographs of the prostates after dissection at 24 weeks of age. **C** and **D.** Evolution of most common and most severe prostatic lesions, respectively, of TRAMP vs TRAMP Anti-Jag1/2 groups based on histopathological classification of prostatic lesions according to

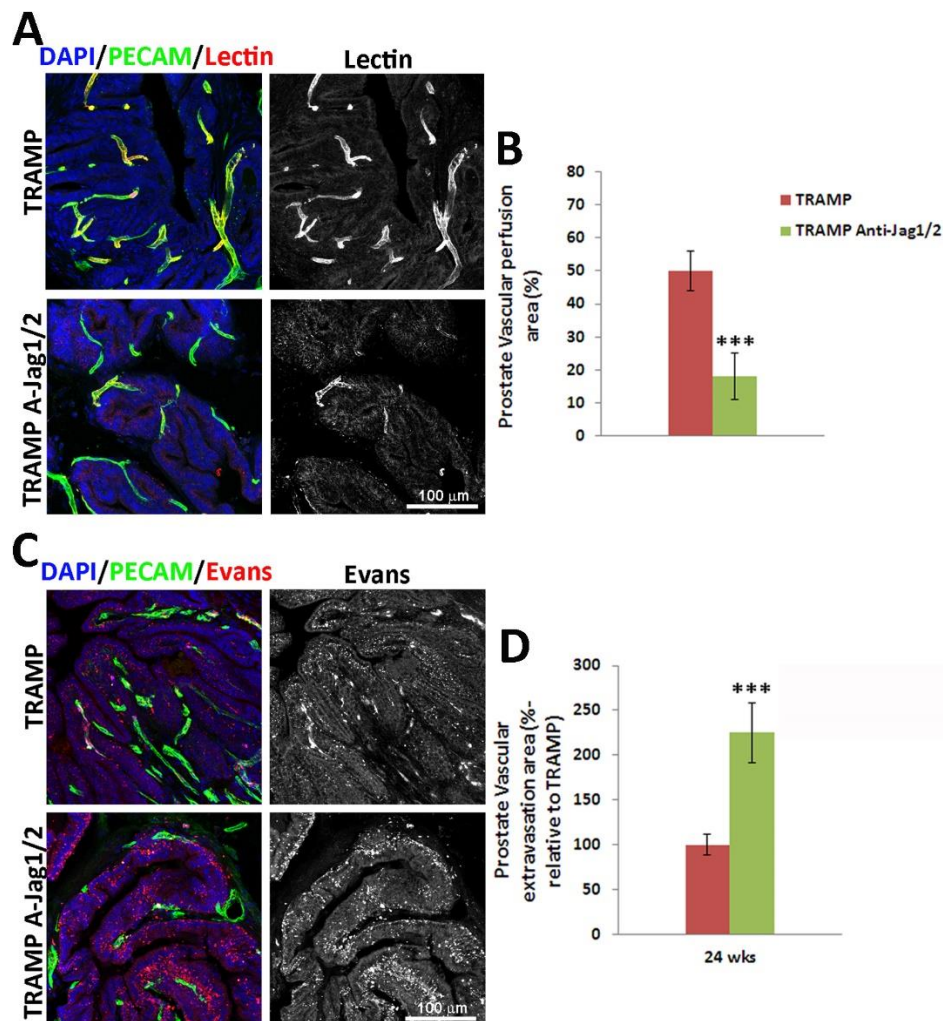
the following score (1-5): Normal (0); prostatic intraepithelial neoplasia [PIN (1)]; well differentiated adenocarcinoma [WDA (2)]; moderately differentiated adenocarcinoma [MDA (3)]; poorly differentiated adenocarcinoma [PDA (4)]; or phylloides-like cancer [PHY (5)]. TRAMP Anti-Jag1/2 mice presented a lower score evolution than controls (TRAMP). **E.** Frequency distribution (% of mice) of histopathological classification of prostatic lesions at 18 and 24 weeks, top and bottom respectively, in treated TRAMP mice (TRAMP Anti-Jag1/2) versus controls (TRAMP). **F.** H&E representative images of the histopathological classification in WT (no lesions), TRAMP (WDA), and TRAMP Anti-Jag1/2 (PIN) mice. Results are representative of n=6 (WT mice), n=13 (TRAMP) and n=12 (TRAMP Anti-Jag1/2) for each time point. Error bars represent SEM; ns represents non-significant; * represents p<0.05; ** represents p<0.01; *** represents p<0.001.

Figure IV.2- Prostate tumor vascular phenotype in TRAMP mice treated with Anti-Jagged1/2 antibody.



A. Representative confocal (one z layer) immunostaining images (40x amplification) marked for PECAM-1 (green) and SMA (red), to evaluate vascular density and vSMC of prostate samples. **B.** Percentage of vascular density (relative to control=100%) was decreased in TRAMP Anti-Jag1/2 mice relative to control group (TRAMP). **C.** Percentage of vascular smooth muscle coverage, showing decreased levels of SMA on TRAMP Anti-Jag1/2 vasculature, relative to controls. DAPI (blue) stains nuclei. White arrows indicate smooth muscle cells attached to the endothelial wall. Error bars represent SEM; ** represents p<0.01; *** represents p<0.001.

Supplemental Figure IV.1- Prostate tumor vascular perfusion and extravasation in Anti-Jagged1/2 treated samples.



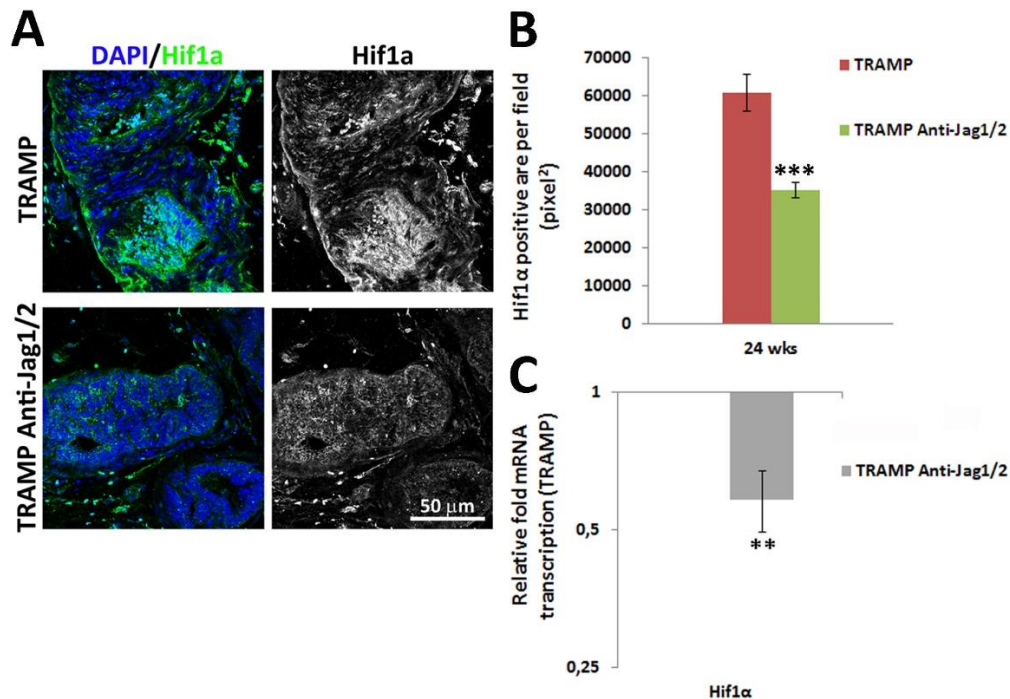
A. Representative images of Lectin (red) and PECAM-1 (green) immunostaining (20x amplification) (Maximum intensity projections) of treated (TRAMP Anti-Jag1/2) versus non-treated (TRAMP) prostate samples, to evaluate the co-localization of both signals, indicative of vessel perfusion. **B.** Percentage of perfused area in the total vascular area (given by vascular density measurements) showing decreased lectin labeling in the treated prostate samples. **C.** Representative images of Evans' Blue (red) and PECAM-1 (green) immunostaining (20x amplification) (Maximum intensity projections) images showing the extravasation areas. **D.** Percentage of vascular extravasation area, showing increased Evans' Blue staining in treated prostate samples relative to controls (TRAMP-100%). DAPI (blue) stains nuclei. Error bars represent SEM; *** represents $p < 0.001$.

4.3 Blocking Jagged1/2 led to alterations in local hypoxia levels

In order to evaluate tumor hypoxia, immunostaining for Hif1 α was performed in prostatic samples from TRAMP and TRAMP Anti-Jag1/2 treated mice at 24 weeks of age (Late intervention trial). As can be observed in Figure IV.3A and B, TRAMP Anti-Jag1/2 treated prostates showed decreased presence of Hif1 α , relative to the respective controls (TRAMP). Transcript levels of *Hif1 α* mRNA were also analyzed by qRT-PCR (Figure IV.3C). *Hif1 α* mRNA

levels varied in the same manner as the protein staining, with a down-regulation response in the prostates of treated mice. A similar response was observed in early intervention trial (data not shown).

Figure IV.3- Prostate tumor hypoxic levels in TRAMP mice treated with Anti-Jagged1/2 antibody.



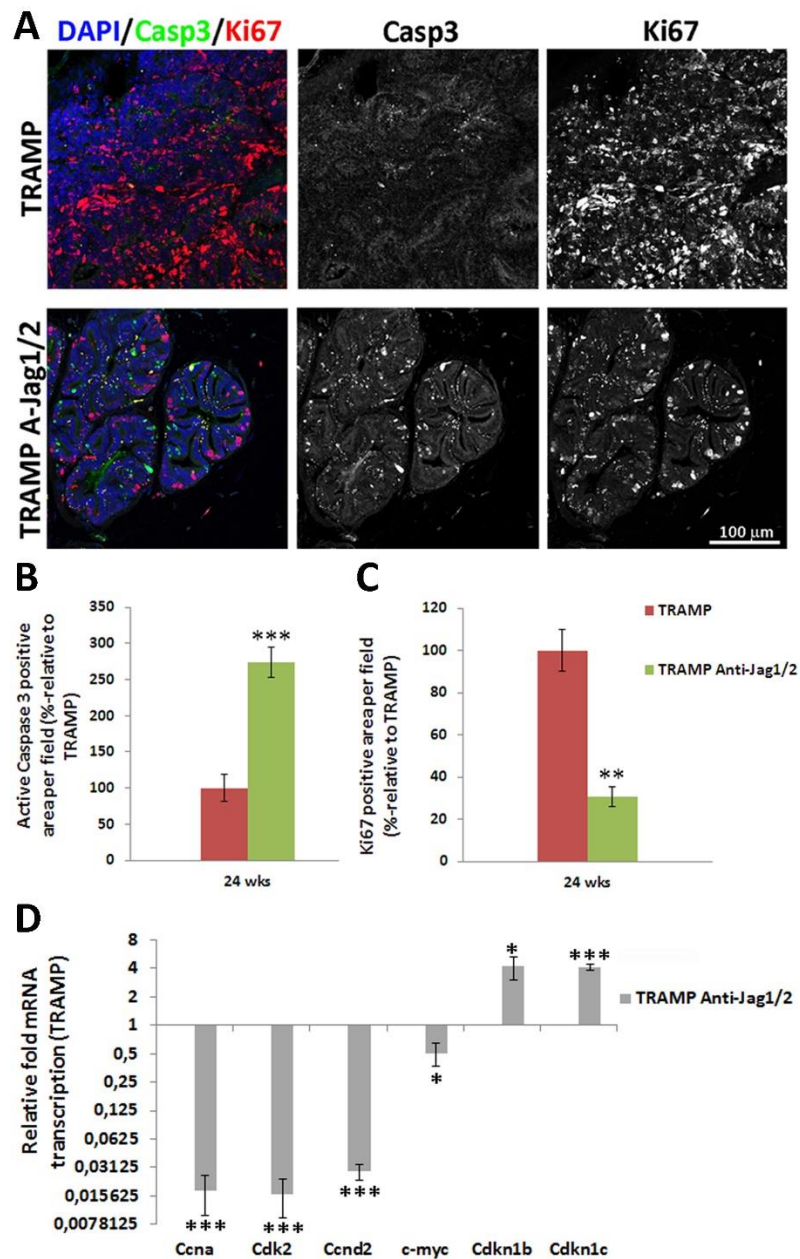
A. Representative images of Hif1α immunofluorescence (green) (20x amplification) (maximum intensity projections) in TRAMP Anti-Jag1/2 and respective control mice group (TRAMP). B. Quantification of Hif1α positive area per field (pixel²) demonstrating decreased staining in TRAMP Anti-Jag1/2 relative to control. C. Relative fold *Hif1α* mRNA expression showing decreased transcription in the TRAMP Anti-Jag1/2 group, at 24 weeks of age. DAPI (blue) stains nuclei. Error bars represent SEM; ** represents $p < 0.01$; *** represents $p < 0.001$.

4.4 Blocking Jagged1/2 promoted apoptosis and inhibited proliferation of prostatic tumor cells

To better understand the metabolic changes in prostatic tumor cells caused by the Anti-Jagged1/2 therapy, cellular apoptosis and proliferation were investigated by immunostaining for active caspase 3 and ki67, respectively, on prostate samples from non-treated (TRAMP) and treated (TRAMP Anti-Jag1/2) mice (Figure IV.4) in the late intervention trial. Treated mice presented increased cellular apoptosis (Figure IV.4A and B) and decreased proliferation (Figure IV.4A and C) relative to non-treated animals. Additionally, we evaluated the transcriptional changes, elicited by blocking Jagged1/2, of several cell-cycle regulatory genes (Figure IV.4D). We observed a down-regulation of the cell-cycle stimulating genes, *Ccna* (encoding for Cyclin A), *Cdk2* (encoding for cyclin dependent Kinase 2), *Ccnd2* (encoding for

CyclinD2), and *c-myc* in TRAMP Anti-Jag1/2 treated mice relative to controls (TRAMP). Conversely, the opposite response was observed in relation to the cell-cycle inhibitors, *Cdkn1b* (encoding for Cyclin-Dependent Kinase Inhibitor 1B or p27) and *Cdkn1c* (encoding for Cyclin-Dependent Kinase Inhibitor 1C or p57) in treated prostate samples. Similar cell cycle changes were found in the early intervention trial (data not shown).

Figure IV.4- Prostate cellular apoptosis and proliferation in TRAMP mice administered with blocking Jagged1/2 antibody.



A. Representative images of active Caspase3 (green) and Ki67 (red) immunofluorescence staining (20x amplification) (maximum intensity projections) in TRAMP mice treated with Anti-Jagged1/2 antibody relative to the respective controls (TRAMP). **B.** Prostatic lesions of TRAMP Anti-Jag1/2 mice presenting increased percentage of active caspase3 positive area per field, relative to control (100%), at 24 weeks of age. **C.** Prostate samples from treated TRAMP mice (TRAMP Anti-Jag1/2) presenting decreased

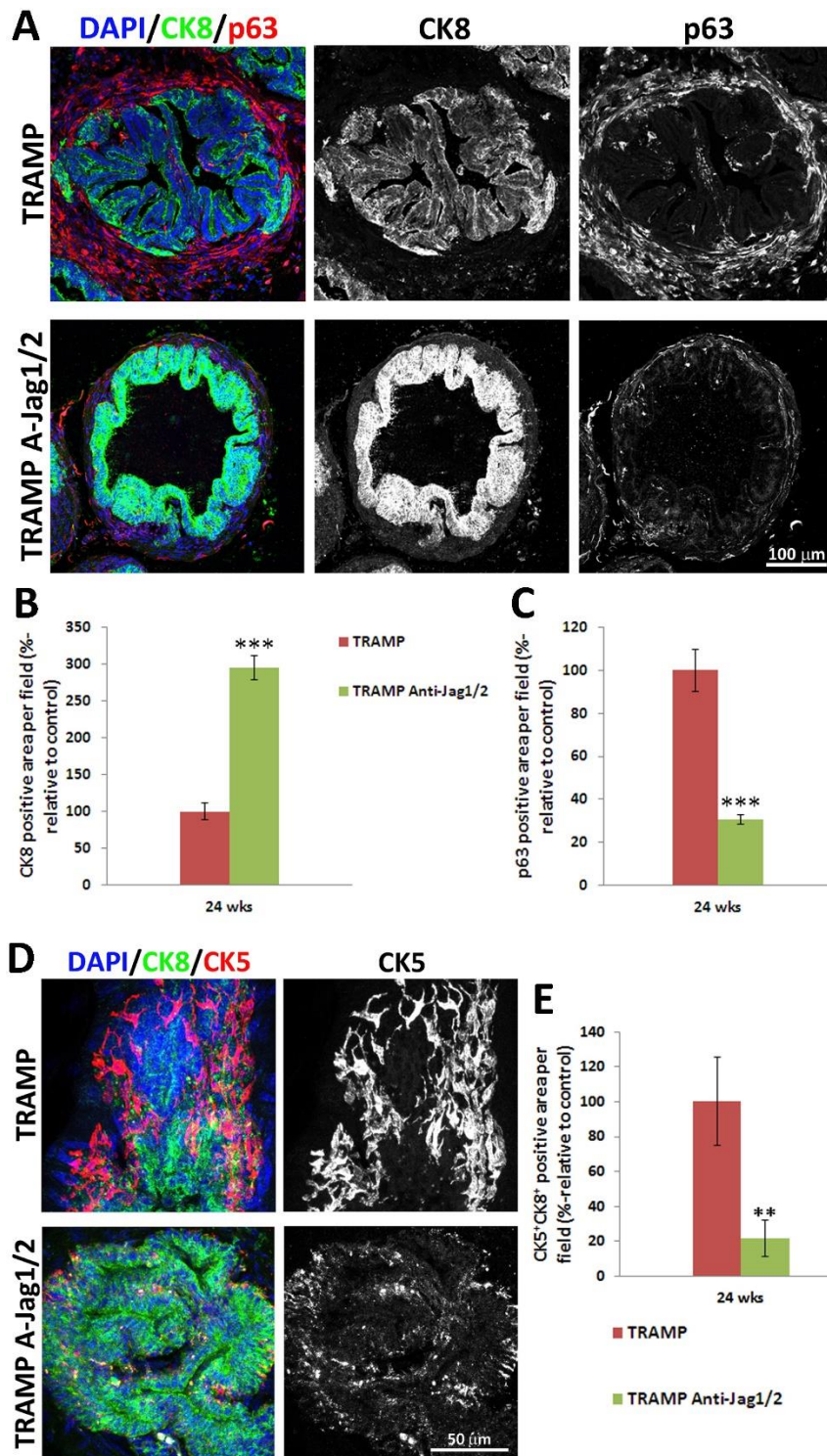
percentage of Ki67 positive area per field, relative to control (100%), at 24 weeks. **D.** Relative fold mRNA expression of cell cycle regulatory genes in TRAMP Anti-Jag1/2 prostate relative to TRAMP prostates, at 24 weeks of age. DAPI (blue) stains nuclei. Error bars represent SEM; * represents $p < 0.05$; ** represents $p < 0.01$; *** represents $p < 0.001$.

4.5 Treatment of prostatic tumor lesions with Anti-Jagged1/2 antibody inhibited the loss of the luminal identity and the proliferation of the basal compartment

Notch signaling has been described as important for the correct homeostasis of the prostate, inducing proliferation of luminal cells, while having the opposite effect on basal cells (Valdez et al., 2012). Consequently, we questioned if blocking Jagged1/2 would lead to changes in the proportions of prostatic cell populations. To investigate this, we performed immunostaining for CK8 and p63, luminal and basal cell specific markers, respectively (Wang et al., 2001). As demonstrated in figure IV.5, we observed that the treated mice (TRAMP Anti-Jag1/2) presented increased luminal staining (Figure IV.5A and B), accompanied by decreased basal staining (Figure IV.5A and C).

This effect on the prostate cell compartments could be a consequence of inhibition of basal cell proliferation and/or inhibition of de-differentiation of luminal cells into a more basal cell phenotype. Therefore, to test the first hypothesis we quantified the percentage of basal cells that were proliferating with co-staining for p63 and Ki67 (Suppl. Figure IV.2). Non-treated mice (TRAMP) presented many basal cells that were proliferating, while the treated mice displayed less co-stained cells. To test the second hypothesis we quantified the percentage of tumor cells that present double positive staining for CK8 and CK5, indicative of an intermediate phenotype between the fully differentiated luminal cells and the more progenitor basal-like cells (Wang et al., 2001). Figure IV.5D and E demonstrates that in the non-treated mice (TRAMP) as luminal cells loose CK8 marker, they concomitantly start to express CK5, suggestive of a de-differentiation process (Long, Morrissey, Fitzpatrick, & Watson, 2005). Moreover, in the treated mice (TRAMP Anti-Jag1/2) one can observe that this process was inhibited with these mice presenting decreased double staining, and with the CK5+ cells restricted to a basal-cell position. Similar cell population changes were found in the early intervention trial (data not shown).

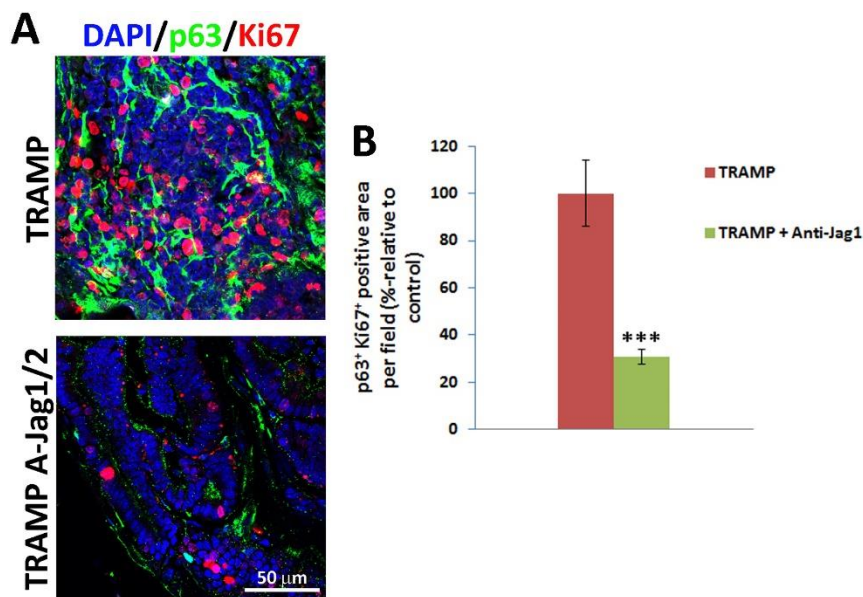
Figure IV.5- Treatment of TRAMP mice with Anti-Jagged1/2 antibody inhibited the loss of the luminal identity and the proliferation of the basal cell compartment of the prostate.



A. Representative immunofluorescence images (20x amplification) (maximum intensity projections) of Cytokeratin 8- CK8 (green), a luminal cell marker, and p63 (red), a basal cell marker, in TRAMP mice treated with Anti-Jagged1/2 antibody relative to the respective controls (TRAMP). **B.** Prostatic lesions of TRAMP Anti-Jag1/2 mice presenting increased percentage of CK8 positive area per field, relative to control-TRAMP (100%), at 24 weeks of age. **C.** Prostate samples from treated TRAMP mice (TRAMP

Anti-Jag1/2) presenting decreased percentage of p63 positive area per field, relative to control (100%), at 24 weeks. **D.** Representative immunofluorescence images (20x amplification) (maximum intensity projections) of double positive staining for the intermediate cell phenotype, consisting of CK8+ (green)/CK5+ (red) cells, in TRAMP mice treated with Anti-Jagged1/2 antibody relative to the untreated control (TRAMP). **E.** Prostatic lesion of treated TRAMP mice (TRAMP Anti-Jag1/2) presenting decreased percentage of double CK8/CK5 positive area per field, relative to control-TRAMP (100%), at 24 weeks. DAPI (blue) stains nuclei. Error bars represent SEM; ** represents $p < 0.01$; *** represents $p < 0.001$.

Supplemental Figure IV.2- Basal cell proliferation in Anti-Jagged1/2 treated samples.



A. Representative images of p63, basal cell marker (green) and Ki67 (red) immunostaining (20x amplification) of treated (TRAMP Anti-Jag1/2) versus non-treated (TRAMP) prostate samples, to evaluate the co-localization of both signals, indicative of basal cell proliferation. **B.** Percentage of double p63/Ki67 positive area per field showing decreased labeling in the treated prostate samples relative to controls (TRAMP-100%). DAPI (blue) stains nuclei. Error bars represent SEM; *** represents $p < 0.001$.

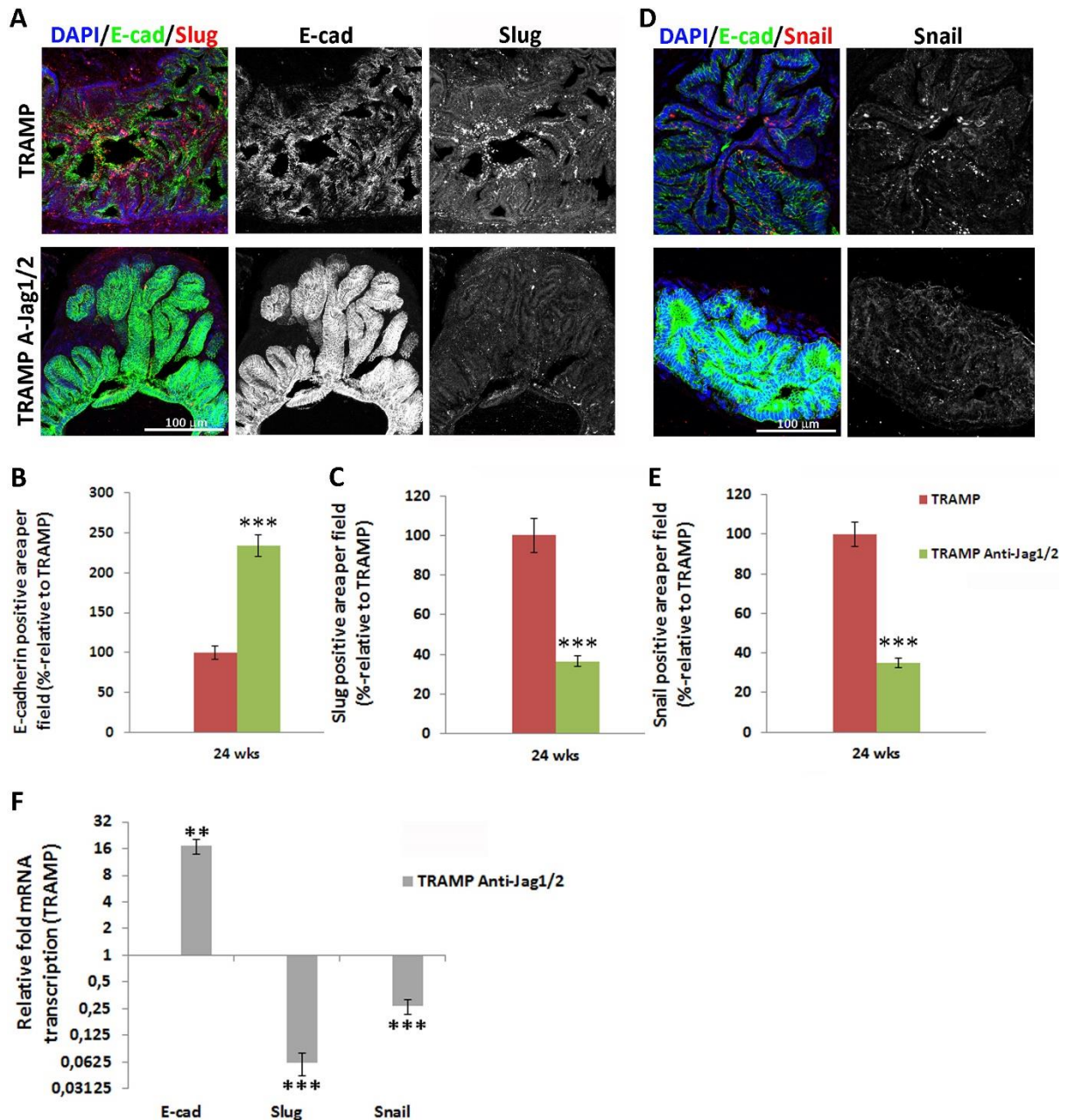
4.6 Anti-Jagged1/2 antibody inhibited epithelial-to-mesenchymal transition (EMT) in prostatic tumor lesions

Furthermore, we aimed to investigate if the alterations in cell proliferation/ apoptosis and in the cell compartments of the prostate caused by anti-Jagged1/2 therapy would contribute to increased and/or decreased pressure for the acquisition of an invasive phenotype and to epithelial-to-mesenchymal transition. To this purpose, we performed immunostaining for the epithelial adhesion marker, E-cadherin, and for Slug and Snail, transcription factors known for the induction of EMT (Thiery, 2002), in the prostatic lesions of TRAMP mice.

Blocking Jagged1/2 had a strong inhibitory effect on EMT, since TRAMP Anti-Jag1/2 treated prostates were associated with increased E-cadherin expression (Figure IV.6A and B) and

decreased Slug and Snail expression (figure IV.6A-E), relative to the respective untreated controls (TRAMP). Accordingly, in the treated prostates the mRNA expression levels of *E-cadherin* were increased, while both *Snail* and *Slug* were decreased (Figure IV.6F). A similar phenotype on EMT was found in the early intervention trial (data not shown).

Figure IV.6- Epithelial-to-mesenchymal transition in prostate lesions of TRAMP mice treated with Anti-Jagged1/2 antibody.



A. Representative images of E-cadherin (green) and Slug (red) immunofluorescence staining (20x amplification) (maximum intensity projections) in TRAMP Anti-Jag1/2 relative to the control (TRAMP). **B.** Increased percentage of E-cadherin per field in TRAMP Anti-Jag1/2, relative to control- TRAMP (100%), at 24 weeks of age **C.** Decreased Slug positive area per field in treated animals (TRAMP Anti-Jag1/2), relative to control – TRAMP(100%). **D.** Representative images of E-cadherin (green) and Snail (red)

immunofluorescence staining (20x amplification) (maximum intensity projections) in TRAMP Anti-Jag1/2 relative to the control (TRAMP). **E.** Decreased Snail positive area per field in treated animals (TRAMP Anti-Jag1/2), relative to control – TRAMP (100%). **F.** Relative fold of *E-cadherin*, *Slug* and *Snail* transcription at 24 weeks of age. DAPI (blue) stains nuclei. Error bars represent SEM; ** represents $p < 0.01$; *** represents $p < 0.001$.

4.7 Jagged1 and Jagged2 signal through Notch3/Hey1

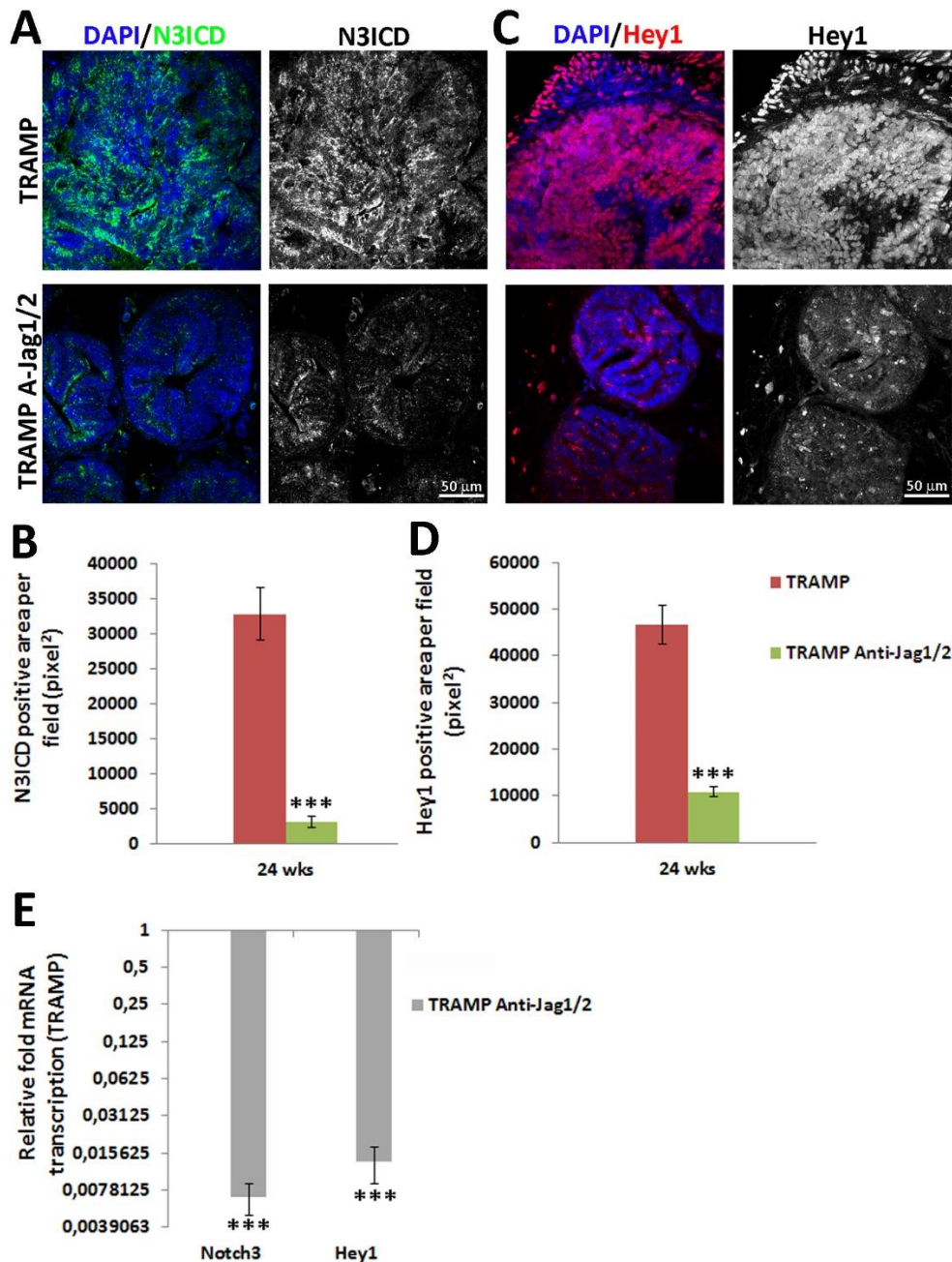
We have previously demonstrated that endothelial Jagged1 exerts an angiocrine function in prostate tumor growth by activating Notch3/Hey1, thus regulating tumor cell proliferation and de-differentiation (Pedrosa et al., 2015b). Moreover, we have also previously demonstrated that Notch3 and Hey1 are the main Notch receptor and effector to be ectopically expressed in TRAMP prostates relative to non-cancerous prostates (Pedrosa et al., 2016). Additionally, high levels of Notch3 have been described in prostate cancer cells with high metastatic potential (Ross et al., 2011), and expression of Notch3 positively correlated with Gleason score in human prostate cancer biopsies (Danza et al., 2013).

Therefore, we hypothesized that the therapeutic effects of Anti-Jagged1/2 could be a consequence of decreased activation of Notch3 and Hey1 transcription in prostatic tumor cells. To test this hypothesis we immunostained tumor samples for activated Notch3 (N3ICD) and for Hey1. As demonstrated in figure IV.7, blocking Anti-Jagged1/2 in TRAMP prostates led to decreased N3ICD (figure IV.7A and B), and Hey1 expression (figure IV.7C and D) relative to non-treated samples (TRAMP). Furthermore, at the transcript level, we observed a very strong down-regulation of both *Notch3* and *Hey1* in consequence of antibody administration (Figure IV.7E). The same response in Notch3 activation and Hey1 expression was found in the early intervention trial (data not shown).

4.8 Blocking Jagged1/2 rescued the loss of Androgen receptor expression in TRAMP prostates

The Notch effector Hey1 has been shown to be able to interact directly with Androgen receptor (AR), specifically repressing transcription from AR-dependent promoters (Belandia et al., 2005), and thereby its exclusion from the nucleus being associated with the development of hormone refractory disease. Since Anti-Jagged1/2 administration inhibited Hey1 expression in prostate samples from TRAMP mice, we aimed to investigate whether its administration was able to rescue AR expression. By performing immunostaining for AR, we were able to demonstrate that blocking Jagged1/2 increased AR expression in prostatic lesions of TRAMP mice (Suppl. Figure IV.3). The AR rescue phenotype was also confirmed in the early intervention trial (data not shown).

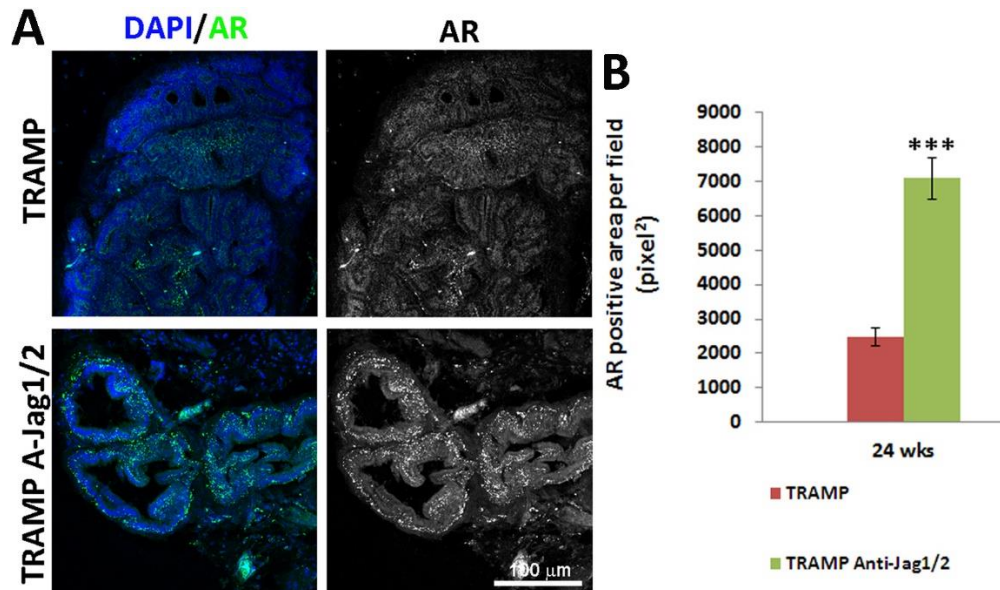
Figure IV.7- Notch3 intracellular domain (N3ICD) expression and Hey1 transcription and expression in prostate lesions of TRAMP mice treated with Anti-Jagged1/2 antibody.



A. Representative images of active Notch3 (N3ICD) (green) immunofluorescence staining (40x amplification) (maximum intensity projections) in TRAMP mice administered with Anti-Jagged1/2 antibody. **B.** Quantification of N3ICD positive area per field (pixel²) demonstrating decreased positive staining in treated animals (TRAMP Ani-Jag1/2) relative to control (TRAMP). **C.** Representative images of Hey1 (red) immunofluorescence staining (40x amplification) (maximum intensity projections) in TRAMP mice treated with Anti-Jagged1/2 versus untreated mice (TRAMP). **D.** Quantification of Hey1 positive area per field (pixel²), demonstrating decreased areas, relative to control, of treated samples (TRAMP Anti-Jag1/2). **E.** Relative fold mRNA transcription of *Notch3* and *Hey1* in prostate samples from

treated mice (TRAMP Anti-Jag1/2) relative to untreated prostate samples (TRAMP-1). DAPI (blue) stains nuclei. Error bars represent SEM; *** represents $p < 0.001$.

Supplemental Figure IV.3- Androgen receptor (AR) expression in prostate samples from Anti-Jagged1/2 treated TRAMP mice.



A. Representative images of AR (green) immunostaining (20x amplification) (Maximum intensity projections) of treated (TRAMP Anti-Jag1/2) versus non-treated (TRAMP) prostate samples. **B.** Percentage of AR positive area per field (pixel²) showing increased labeling in the treated prostate samples relative to controls (TRAMP). DAPI (blue) stains nuclei. Error bars represent SEM; *** represents $p < 0.001$.

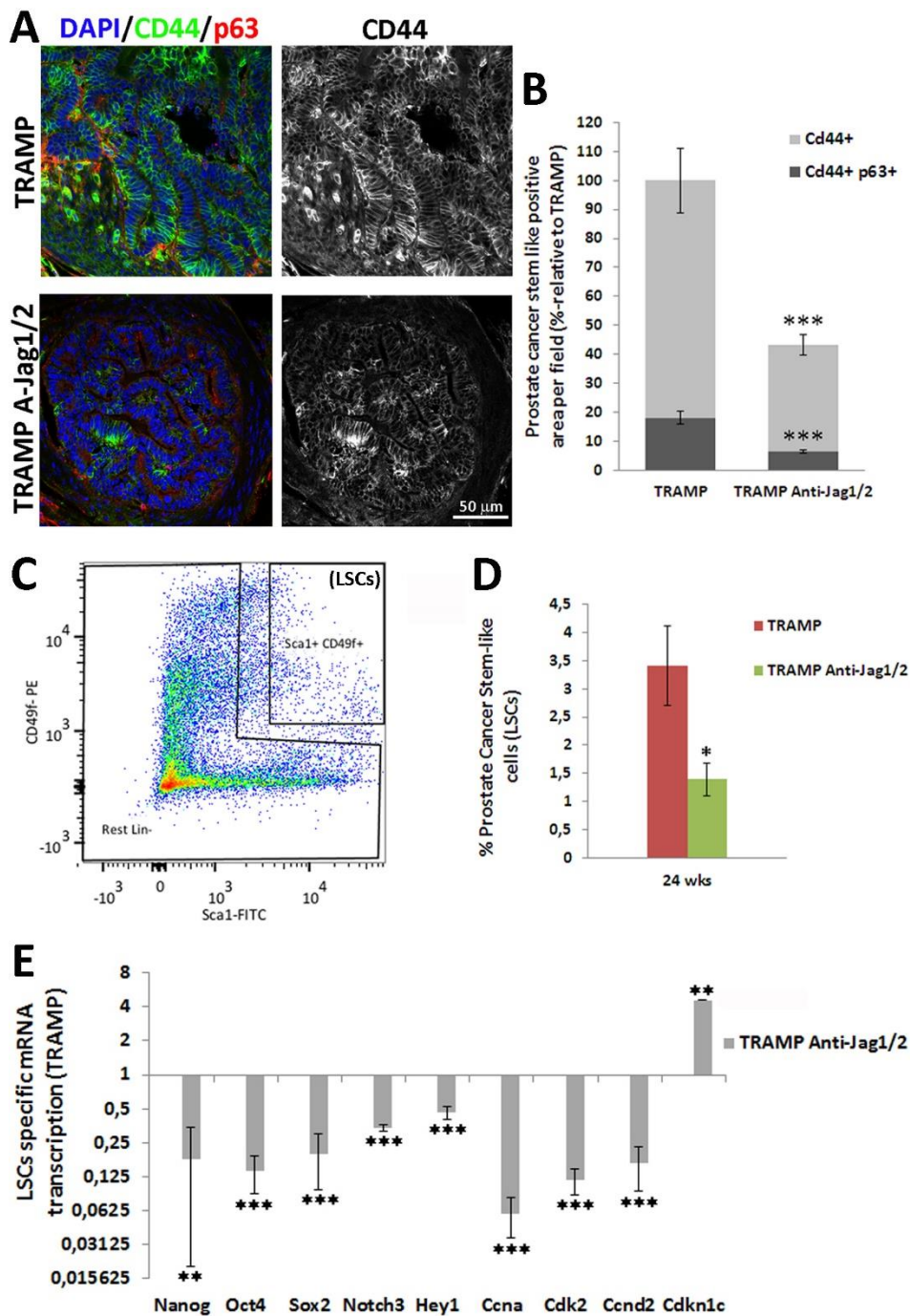
4.9 Jagged1/2 also regulated the proliferation of prostate cancer stem-like cells

Numerous studies have functionally associated Jagged1 to cancer “stemness” (Wang et al., 2006; Xu et al., 2012; Cao et al., 2014). Moreover cancer cells with high metastatic potential have increased expression of Jagged2 and Notch3 (Ross et al., 2011). Consequently, we wanted to understand if blocking Jagged1/2 had an effect on the pool of prostatic cancer-stem like cells. Due to the difficulty of defining this subpopulation of cells, as several markers have been associated with CSCs, we used two distinct approaches. Firstly, we quantified the percentage of basal cells that co-expressed CD44, as basal cells were described as the cell-of-origin of prostate cancer (Goldstein, Huang, Guo, Garraway, & Witte, 2010; Stoyanova et al., 2013). In figure IV.8A and B it can be observed that Anti-Jagged1/2 treated TRAMP mice not only had decreased CD44 expression but also presented decreased CD44⁺p63⁺ area relative to non-treated animals (TRAMP).

For the second approach, we isolated LSCs ($\text{Lin}^{-}(\text{cd45}^{-}, \text{cd31}^{-}, \text{ter119}^{-}) \text{Sca1}^{+}\text{Cd49f}^{+}$) by FACS (figure IV.8C). LSCs were demonstrated to be able of self-renewal and give rise to both basal and luminal populations (Lawson et al., 2007) and to be tumor initiating cells in a murine prostate

cancer model (Mulholland et al., 2009). As demonstrated in figure IV.8D, Anti-Jagged1/2 treated mice presented a lower number of LSCs relative to control mice (TRAMP). We have also analyzed the transcription profile of the isolated LSCs from both mouse groups (figure IV.8E) and observed that the LSCs from TRAMP Anti-Jag1/2 presented down-regulation of the embryonic and cancer stem-like cell markers, *Nanog*, *Oct4* and *Sox2* (Ben-Porath et al., 2008). The LSCs from treated mice also presented down-regulation of *Notch3* and *Hey1* and of the cell-cycle stimulating genes, *Ccna*, *Cdk2* and *Ccnd2*. Conversely, the opposite response was observed in relation to the cell-cycle inhibitor, *Cdkn1c*. Therefore, blocking anti-Jagged1/2 restricted the number of cancer stem-like cells by inhibiting their proliferation.

Figure IV.8- Cancer-stem like phenotype in prostatic lesions from TRAMP mice treated with Anti-Jagged1/2 antibody.



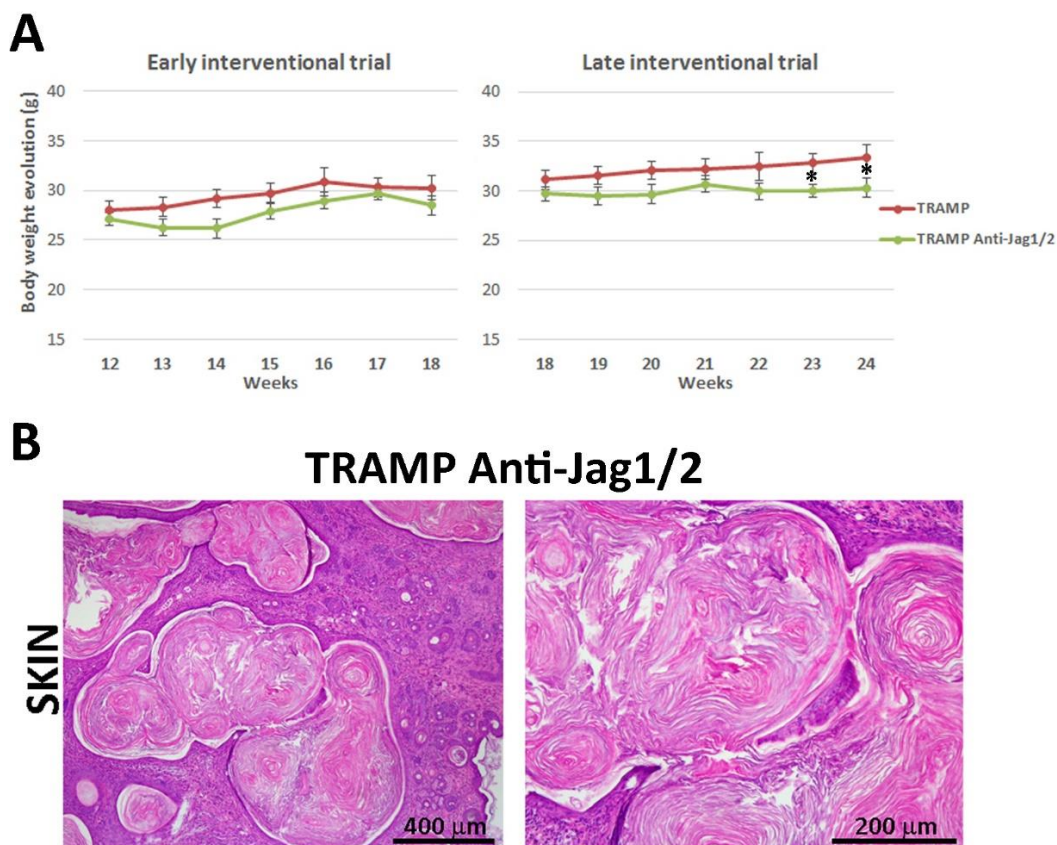
A. Representative images of CD44 (green) and p63 (red) immunofluorescence staining (40x amplification) (maximum intensity projections) in TRAMP mice administered with Anti-Jagged1/2 antibody. **B.** Quantification of CD44 and CD44/p63 double positive area per field (relative to control-TRAMP-100%) demonstrating decreased CD44 and CD44+p63+ staining in treated animals (TRAMP Anti-Jag1/2). **C.** LSCs (Lin⁻ (cd45⁻ ter119⁻) cd49f^{hi} Sca1^{hi}) sorted population. **D.** Decreased percentage of prostate cancer stem-like cells (LSCs) isolated from TRAMP prostates treated with Anti-Jag1/2 relative to untreated prostates (TRAMP) at 24 weeks of age. **E.** RNA was isolated from prostates collected at the end-point, and specific LSCs gene transcript analysis was performed by quantitative real-time RT-PCR for several genes: *Nanog*, *Oct4*, *Sox2*, *Notch3*, *Hey1*, *Ccna*, *Cdk2*, *Ccnd2* and

Cdkn1c. DAPI (blue) stains nuclei. Error bars represent SEM; * represents $p < 0.05$; ** represents $p < 0.01$; *** represents $p < 0.001$.

4.10 Therapeutic intervention trials using Anti-Jagged1/2 antibody had no toxic side effects other than in the skin

Generally, targeting the Notch pathway by pan-Notch inhibitors results in gastrointestinal and liver toxicity (Wong et al., 2004; van Es et al., 2005). Therefore, to evaluate possible side toxic effects of the systemic administration of Anti-Jagged1/2 antibody we have measured mice body weight once a week and collected all the vital organs (heart, liver, intestine, spleen, kidneys and skin) at the end-point of each intervention trial and processed the samples for histopathological analysis. As can be observed in suppl. figure IV.4A, treated mice presented a slightly slower weight gain tendency along the treatment, but this was only significantly different from non-treated mice in the final weeks of late intervention trials. Regarding the collected organs, no treatment associated signs of toxicity were found (data not shown), with the exception of the skin. From the third week of treatment the animals started to lose the fur especially in the areas of the abdomen, neck and muzzle, and developing small pustules, with the extension of the lesions varying from animal to animal. At a microscopic level (Suppl. figure IV.4B) these lesions were identified as lesions of follicular hyperkeratosis.

Supplemental Figure IV.4- Side effects of Anti-Jagged1/2 administration to TRAMP mice.



A. Body weight evolution (g) in early intervention trials (12-18 weeks of age) (right) and in late intervention trials (18-24 weeks of age) (left) in non-treated (TRAMP) and treated (TRAMP Anti-Jag1/2) mice groups. **B.** H&E representative images of skin lesions (4X amplification- right and 10X amplification- left) demonstrating hyperkeratotic lesions in treated TRAMP mice. Error bars represent SEM; * represents $p < 0.05$.

5. Discussion

In recent years, several therapeutic approaches for Notch signaling inhibition have been tested and used in cancer therapy. The compounds most widely used to inhibit Notch pathway activity are gamma-secretase inhibitors (GSIs), which were initially tested in T-ALL lines and later in prostate, breast, and lung cell lines and xenografts (Carvalho et al., 2014). Additionally, α -Secretase inhibitors (ASIs) against the ADAM10/17 metalloproteases that mediate receptor S2 cleavage, have also been tested (Zhou et al., 2006). However, it quickly became evident that these drugs caused toxicity in Notch-dependent tissues, particularly the gastrointestinal tract, liver and thymus (Wong et al., 2004; van Es et al., 2005). Moreover, antibodies binding the receptors Notch1 and Notch2 (Wu et al., 2010), and the ligand Delta-like 4 (Noguera-Troise et al., 2006), have been used experimentally and shown to inhibit cancer cell proliferation with minimal intestinal toxicity. Nonetheless, of the 28 clinical trials registered at the NIH to study the effects of Notch inhibitors, there is only one specific for prostate cancer: it combines the

anti-androgen bicalutamide with a GSI in patients with recurrent prostate cancer after prostatectomy or prostate radiation therapy. However, so far no benefits have been reported for these patients (Carvalho et al., 2014).

Facing these facts, and considering the consistent implication of both Jagged ligands in prostate cancer progression (Santagata et al., 2004; Ross et al., 2011), in this report we have investigated the therapeutic potential of targeting Jagged1/2 in an autochthonous murine model of prostate adenocarcinoma (TRAMP). We observed that blocking Jagged1/2 inhibited the development of prostatic lesions in TRAMP mice, at both intervention windows tested (early and late intervention trials), with a significant inhibitory effect both in tumor growth as in the degree of the lesion.

Unsurprisingly, we have also observed that blocking Jagged1/2 inhibited the neo-vascularization process, producing a vasculature that is less dense, immature and consequently less functional and leakier. Accordingly, a recent report using a Notch decoy that specifically blocks Jagged ligands mediated interaction with Notch1 receptor has shown the same anti-angiogenic effect on a xenograft model (Kangsamaksin et al., 2014). Moreover, we have also previously demonstrated that endothelial Jagged1 acts as a pro-angiogenic ligand in the same model of murine prostatic cancer (Pedrosa et al., 2015b): by specifically knocking-out endothelial *Jag1* we were able to inhibit prostate tumor growth by inhibiting angiogenesis and maturation processes, leading to a non-functional vasculature. Therefore, even though Jagged2 has been described to be expressed in the endothelium (Tsai et al., 2000), we believe that the anti-angiogenic phenotype we demonstrated for the antibody used against Jagged1/2 is most probably a consequence of blocking Jagged1 ligand.

We have also demonstrated that despite inhibiting tumor vascularization, thereby inhibiting the supply of nutrients and oxygen to the surrounding tumor tissues, prostate samples from Anti-Jagged1/2 treated TRAMP mice presented decreased levels of Hif1 α . We believe this overall effect on tumor hypoxia to be a consequence of an overlapping effect of the antibody in restricting tumor cell proliferation and de-differentiation process, while increasing apoptosis, thus leading to decreased consumption of local oxygen, when compared to untreated tumors, with consequently less acidotic microenvironment conditions and decreased hypoxia. Supporting this notion is the fact that Hif1 α is up-regulated in most prostate tumor tissues, compared with normal and benign prostate tissues (Zhong et al., 2004). Therefore, in the treated mice the progression of the lesions is strongly inhibited leading to a lower degree of dysplasia, and consequently to less hypoxia. Moreover, in our previous study with specific endothelial *Jag1* knock-out mutants, we have also observed that despite these mutant's vasculature being less mature and functional, the prostate samples of these mice also presented less hypoxic areas, due to the overall effect on tumor growth (Pedrosa et al., 2015b).

Administration of Anti-Jagged1/2 to TRAMP mice reduced proliferation of tumor cells and increased apoptosis. This effect was achieved by down-regulation of cell-cycle inducers *CyclinA*, *Cdk2* Kinase activity, *CyclinD2* and *c-myc* and by up-regulating the cell cycle suppressors, *Cdkn1b* (p27) and *Cdkn1c* (p57). Accordingly, a previous study has demonstrated that down-regulation of *Jag1* induces cell growth inhibition and S phase cell cycle arrest, by promoting *CyclinA* and *CDK2* activity while repressing p27 cell cycle suppressor, in prostate cancer cells (Zhang et al., 2006). Additionally, knockdown of *Notch1* and *Jagged1* reduced cell viability and induced apoptosis in the PC3 prostate cancer cell line (Wang et al., 2010).

Treatment of tumor prostatic lesions with Anti-Jagged1/2 antibody caused significant changes in the prostate cell populations. We have observed that in non-treated TRAMP mice, as the lesions progressed there was loss of the luminal identity, given by loss of epithelial CK8 staining, while there was abundant p63+ cells, indicative of a basal phenotype and a de-differentiation process, characteristic of cancer progression (Long et al., 2005). However, blocking Jagged1/2 led to significant inhibition of luminal cell identity loss, basal cell proliferation, and to inhibition of de-differentiation given by the decreased double positive staining for CK8/CK5, suggestive of inhibition of an intermediate/transient phenotype between basal and luminal (Wang et al., 2001). Accordingly, Wu et al. showed that gain of Notch function promoted proliferation and increased p63+ progenitor cell numbers in embryonic prostate as well as in postnatal prostate, and conversely, knockout of RBPJ, a transcriptional co-factor necessary for Notch signaling activation cascade, in mice decreased progenitor cell proliferation and survival (Wu et al., 2011). Moreover, work by Kwon et al., suggested that Notch signaling activation in luminal cells is able to preserve the transit amplifying luminal progenitor population in the prostate (Kwon et al., 2014). Controversially, Wang et al. showed that Notch inhibition, by Knocking-out *Notch1*, caused a significant proliferation of intermediate/transient epithelial cells in postnatal prostate (Wang et al., 2006). Additionally, another study demonstrated that knockout of RBPJ led to enhanced proliferation and suppression of differentiation in prostate basal cells (Valdez et al., 2012). Nevertheless, these studies were performed in normal prostates, suggesting that the tumorigenic process may itself alter Notch functions in both prostate cell compartments. Moreover, we have previously observed that *Jagged2* is normally expressed in the basal and stromal compartments of a healthy adult mouse prostate, while *Jagged1* seems to be non-expressed (Pedrosa et al., 2016). And even though stromal–epithelial interactions are poorly understood, it has been suggested that stromal cells may play an important role in prostate cancer (Lawson & Witte, 2007). Moreover, we have also shown that in TRAMP prostates, both Jagged ligands have increased expression and transcription (Pedrosa et al., 2016). Therefore, ectopic expression of Jagged ligands, in the tumorigenic prostate, as well as the basal and stromal expression of

Jagged2 may play a role in the de-differentiation process that we observed in dysplastic lesions of TRAMP mice.

The ability of tumor cells to invade the surrounding tissues and colonize distant organs, i.e. to metastasize, requires the process of epithelial-to-mesenchymal transition (EMT)(Hanahan & Weinberg, 2011). In this report we have demonstrated that Anti-Jagged1/2 antibody also inhibited EMT in prostatic tumor lesions, since antibody administration caused an increase in the cell-to-cell adhesion marker, E-cadherin, expression and transcription and a concomitant decrease in mesenchymal markers, Slug and Snail, expression and transcription. Accordingly, Jagged1-mediated Notch activation has been shown to induce epithelial-to-mesenchymal transition through Slug-induced repression of E-cadherin (Leong et al., 2007). Most specifically in prostate cancer, high JAG1 expression levels have been associated with metastasis development and regulation of migration and invasion (Santagata et al., 2004; Wang et al., 2010). Furthermore, in a previous study we have observed expression of Jagged2 and Notch3 in the stromal compartment of the healthy prostate, which was strongly up-regulated in the stroma TRAMP prostates (Pedrosa et al., 2016). We believe that this could be crucial for the invasion process that takes place in advanced lesions of prostate cancer as similarly demonstrated in prostate cancer cells with high metastatic potential (Ross et al., 2011).

In this report we have demonstrated that Jagged1/2 function in prostatic tumor lesions of TRAMP mice may exert its effects on Notch signaling through mediated activation of Notch3/Hey1. We have observed that blocking both ligands with the antibody lead to significant decreased levels of active Notch3 (N3ICD) and Hey1 expression in prostate tumor samples. Conversely, we have previously shown that endothelial Jagged1 up-regulated N3ICD and Hey1 transcription and expression in adjacent tumor cells by its angiocrine function (Pedrosa et al., 2015b). Moreover, Notch3 was shown to be activated by hypoxia and to sustain cell proliferation and colony formation in the prostatic cancer cell line LNCaP (Danza et al., 2013). Furthermore, along with Jagged2 as mentioned previously, high expression of Notch3 has been described in prostate cancer cells with high metastatic potential (Ross et al., 2011). We have also previously demonstrated that Notch3 and Hey1 were the most consistently and strongly upregulated and expressed Notch receptor and effector in prostate tumor lesions compared with healthy prostates (WT), and that the dysplastic areas presented active Notch3 and increased Hey1 nuclear expression (Pedrosa et al., 2016). Accordingly, amplification of the chromosome region comprising *Hey1* gene has been described in a large fraction of prostate cancers and correlated with aggressiveness of tumors (DeMarzo et al., 2003). Controversially, Belandia *et al.* have demonstrated that Hey1 is excluded from the nucleus in some human prostate cancers, while it co-localizes with androgen receptor in the epithelia of patients with benign prostatic hyperplasia, where it is found in both the cytoplasm and the nucleus (Belandia et al., 2005). In the same study they also demonstrated that Hey1 directly repressed AR activation and AR-dependent gene expression. This observation raised the


possibility that an abnormal Hey1 subcellular distribution may have a role in the aberrant hormonal responses observed in advanced forms of prostate cancer (Belandia et al., 2005). Consequently, we also investigated the effects on AR expression in our treated and non-treated samples and found that the prostates from Anti-Jagged1/2 treated TRAMP mice presented increased AR expression. It is known that prostate cancer, like healthy prostate, is dependent on androgen for its development. AR is expressed in cancer cells, and disruption of the downstream control signaling plays a significant role in tumorigenesis and metastasis of prostate cancer (Chang, Lee, Yeh, & Chang, 2014). Therefore, inhibiting AR is a therapeutic approach to treating primary prostate cancer to prevent tumor progression, however, prostate cancer may become resistant to androgen deprivation and may initiate metastasis (Karantanos, Corn, & Thompson, 2013). Taken together, AR expression rescue by Anti-Jagged1/2 administration to TRAMP mice may constitute an improved result for prostate cancer therapy, raising the possibility of adjuvant cancer therapy in androgen resistance tumors.

Notch signaling plays an important role in cancer stem cell (CSC) maintenance and self-renewal (Espinoza et al., 2013). Furthermore, the presence of prostate cancer stem cells has been associated with chemotherapy resistance, tumor aggressiveness and poor prognosis (Domingo-Domenech et al., 2012). Therefore we investigated the effect of blocking Jagged1/2 in cancer-stem like phenotype and found an inhibitory effect on prostate cancer stem-like cells proliferation and survival. We have found decreased numbers of both double positive CD44/p63 cells (Goldstein et al., 2010; Stoyanova et al., 2013) and LSCs (Mulholland et al., 2009) in Anti-Jagged1/2 treated TRAMP mice in relation to non-treated prostates. Moreover, LSCs from prostates treated with the anti-Jagged1/2 antibody presented down-regulation of embryonic and cancer stem-like cell markers (*Nanog*, *Oct4* and *Sox2*) (Ben-Porath et al., 2008), suggesting that blocking Jagged1/2 exerts an inhibitory effect on the stemness of this cell population. The LSCs from treated mice also presented down-regulation of *Notch3* and *Hey1* and of the cell-cycle stimulating genes, *Ccna*, *Cdk2*, and *Ccnd2* and up-regulation of the cell-cycle inhibitor, *Cdkn1c*, suggesting that the same effect observed on prostate tumor cells proliferation and survival also affected prostate cancer stem-like cells. Conversely, in other tumor settings, Jagged1 has been implicated in CSC regulation: Jagged1 expressing EC-tumor cell signaling has been described in the regulation of colorectal cancer stem cell phenotype (Lu et al., 2013); and in the ability of providing chemo resistance and aggressiveness to lymphoma cells by activating Notch2 and consequently Hey1 in these adjacent cells (Cao et al., 2014). Furthermore, Notch3 was demonstrated to control self-renewal of human stem/progenitor cells of the mammary gland by inducing Jagged1 (Sansone et al., 2007). More specifically, in a gene profiling study of prostate cancer cells, a subpopulation of CD133^{high}/CD44^{high} was isolated and found to express high levels of Notch1, Jagged1, Dll1 and Dll3 (Oktem et al., 2014). Additionally, in human prostate cancer

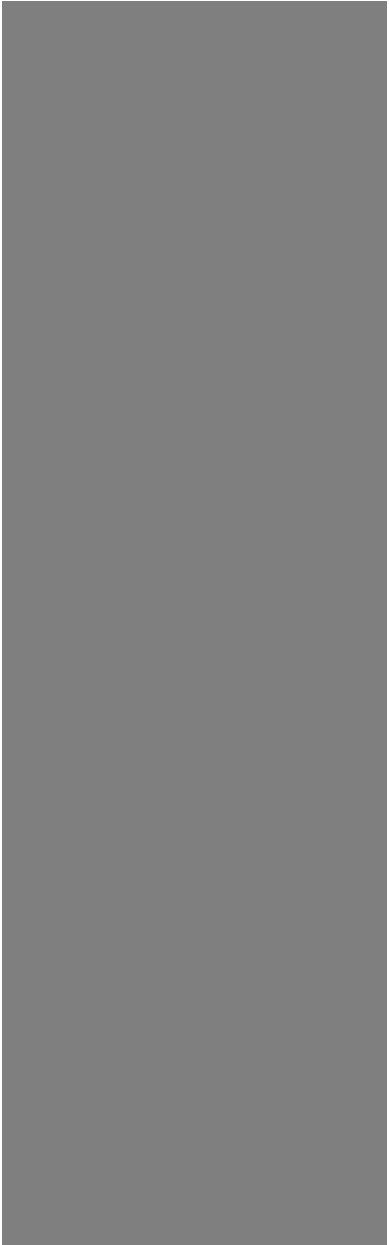
tissue samples, a docetaxel-resistant subpopulation that exhibited tumor-initiating capacity and was more abundantly observed in metastatic tumors, presented up-regulation of Notch and Hedgehog signaling (Domingo-Domenech et al., 2012). Taken together, our results suggest that targeting Jagged ligands may have an important effect on limiting prostate cancer stem-like cells survival and proliferation.

6. Conclusions

Collectively, this study demonstrates the potential therapeutic effect of blocking Jagged ligands in prostate cancer management. Anti-Jagged1/2 antibody strongly inhibited prostate tumor development and progression by several functions: inhibition of the neo-angiogenic and maturation processes; restriction of tumor cell proliferation and promotion of apoptosis; inhibition of the de-differentiation process by preventing loss of luminal identity and proliferation of basal cells as well as inhibiting EMT; rescuing of AR expression; and finally restricting CSC proliferation and survival. Overall these effects were achieved mainly by decreasing Notch3 activation and Hey1 expression. Therefore, this report provides substantial data for the introduction of Anti-Jagged1/2 antibodies in therapeutic strategies for prostate cancer.



**GENERAL
DISCUSSION,
CONCLUSIONS
AND FUTURE
DIRECTIONS**



GENERAL DISCUSSION

The objective of the experimental work included in this thesis was the characterization of Jagged1 (*Jag1*) function in adult angiogenesis, in physiological and pathological conditions, and in solid tumor development. Chapter I addressed the role of endothelial Jagged1 and the interaction with the Dll4 ligand in the regulation of physiological angiogenesis, by evaluating skin wound healing dynamics and angiogenic phenotypes in endothelial-specific *Jag1* mutants, and in endothelial-specific *Dll4OE* in combination with blocking antibodies for Dll4 and Jagged1, respectively. Chapter II addressed the role of endothelial *Jag1* in tumor angiogenesis evaluating the effect of its transcription modulation in both LLC transplants and autochthonous mouse prostate tumor growth and associated angiogenic phenotype. Chapter III provided an extensive transcription and expression analysis of members of the Notch signaling pathway in the tumorigenic mouse prostate when compared with a healthy mouse prostate revealing a specific Notch signaling axis to be ectopically expressed in the tumorigenic process. Finally, chapter IV addressed the use of an antibody directed against both Jagged ligands and its therapeutic potential in a murine model of prostate cancer.

In particular, the results presented in this thesis established that the Notch ligand, Jagged1, has a pro-angiogenic role in adult settings, such as regenerative and tumoral angiogenesis. Endothelial Jagged1 has been previously described as a pro-angiogenic ligand, opposing the function of the Dll4 ligand, in developmental settings, such as in the post-natal vascularization of the retina (Benedito et al., 2009). Moreover, administration of a soluble Jagged1 peptide to mice had been shown to significantly enhance wound healing *in vivo*, and promote vascular endothelial cell proliferation, migration and tube formation *in vitro* (Chigurupati et al., 2007). Nevertheless, in the studies described in chapter I we have specifically modulated *Jag1* in the endothelium, addressing for the first time the transcription modulation effects of this ligand in the wound vasculature *in vivo*.

Furthermore, during the time course of the experimental work related with the results presented in chapter II, a report was published in which Jagged-mediated Notch signaling in tumor transplants was disrupted by using a specific Notch1 decoy (Kangsamaksin et al., 2014). This report established that specifically blocking Jagged ligands-mediated Notch1 interactions, tumor growth was inhibited by an anti-angiogenic effect and by destabilizing pericyte-ECs interactions, thus affecting vessel functionality. However, the direct role of endothelial *Jag1* remained to be clearly characterized, and particularly taking in to consideration the possible downstream specific effects of different Notch receptors activation. Therefore, in this thesis we have also demonstrated that the pro-angiogenic role of endothelial *Jag1* is achieved through complex interactions with different Notch receptors. Using a skin wound healing model we have demonstrated that endothelial Jagged1 negatively regulates the transcription and activation of Notch1 (Benedito et al., 2009; Yoon et al., 2013), by, blocking Dll4 mediated Notch1 activation, and consequently positively regulating *Vegfr-2* and *Vegfr-3* transcription, as

previously described in the retina (Benedito et al., 2009). Additionally, in mice solid tumor models we have further validated and complemented the mechanistic process by which endothelial Jagged1 exerts this function, by showing that it not only positively regulates *Vegfr-2* transcription and expression, but that it also negatively regulates *Vegfr-1* transcription, specifically in ECs, as previously described in other experimental settings (Benedito et al., 2009; Kangsamaksin et al., 2014).

Bringing a novel perspective into the complex mechanism of Jagged1/Notch signaling we have also demonstrated that this endothelial ligand positively controls the transcription and activation of Notch4 (Uyttendaele et al., 2000; Emuss et al., 2009). This was shown both in physiological and tumoral angiogenesis. Moreover, we have implicated EC Jagged1/Notch4 signaling in vascular maturation, since both wounds and tumors from *eJag1OE* mutants and wounds from mice administered with a Notch 4 agonist exhibited increased vessel maturation, independently of *Dll4* levels.

Notch4 is a structurally divergent member of the Notch family of receptors, and little is known about the role of this receptor in the vasculature and how it functions, even though it is primarily expressed in the vasculature. Studies using the same null homozygous Notch4 allele mice (Notch4d1), that were first used to characterize the contribution of this receptor in development (Krebs et al., 2000), demonstrated that adult mice exhibited slightly elevated blood pressure (Takeshita et al., 2007), delayed tumor onset and reduced tumor perfusion (Costa et al., 2013). Recently, it was shown that this null allelic form (Notch4d1) is not null as it expresses a truncated transcript encoding most of the NOTCH4 extracellular domain (James et al., 2014). Therefore, James and colleagues generated a new Notch4 null mouse in which the entire coding region was deleted. These new null mice survived birth and exhibited a mild angiogenic phenotype in the post-natal retina, with a slightly delayed vessel growth, suggesting that Notch4 does not play a major role in developmental angiogenesis (James et al., 2014). Moreover, they have shown that Notch4 binds and sequesters full-length Notch1 thus inhibiting ligand-induced Notch1 signal transduction if expressed in the same cells. Therefore, they suggested that Notch4 may serve to attenuate Notch1 signaling in a negative feed-back loop (James et al., 2014). Moreover, it is known that the NOTCH4 promoter contains CSL binding sites (Li et al., 1998) and that expression of the activated form of NOTCH4 (NOTCH4ICD) induced transcription of Notch4 itself (Uyttendaele et al., 2000; Carlson et al., 2005) and of *Jag1* (Uyttendaele et al., 2000; Carlson et al., 2005). Even though, it has been shown *in vitro* and in developmental angiogenesis that a constitutively active version of Notch4 is a poor activator of transcription compared with Notch1 (James et al., 2014), in our models of adult angiogenesis Jagged1 seems to be able to substantially activate Notch4 and generate a significant phenotype. Consequently, endothelial Jagged1/Notch4 signaling may also contribute to the inhibition of Notch1 mediated signaling, downstream of Dll4/Notch1, further supporting the results presented here.

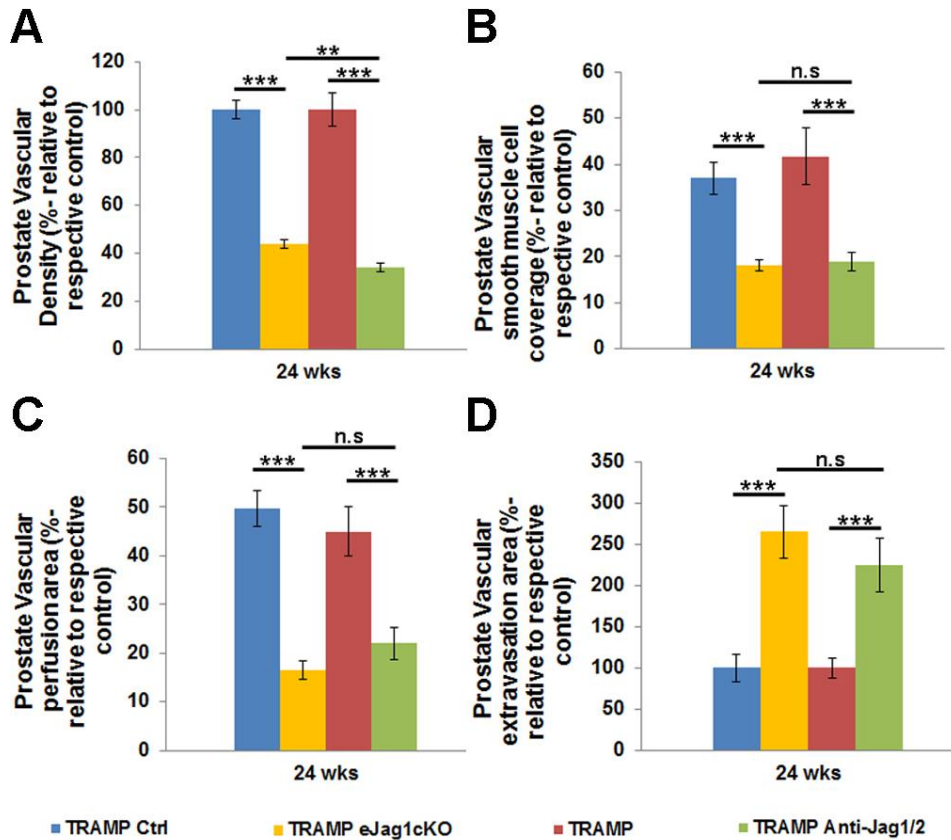
Furthermore, there is also evidence supporting a role for Notch4 in mediating smooth muscle cell recruitment. Endothelial specific expression of constitutively active NOTCH4 (encoded by the *int3* allele) in the adult mature vessel endothelium caused increased smooth muscle layers, resulting in arterialization of venous vessels (Carlson et al., 2005).

Collectively, it can be argued that endothelial Jagged1 mediated Notch4 signaling can contribute to the ability of the ligand in antagonizing Dll4/Notch1 derived effects, and to vessel maturation. The regulation of vessel maturation can be either by direct regulation of transcriptional cues, like the Ang1/Tie2 pathway, essential for this process, as demonstrated in chapter I and II, or by up-regulating and propagating the transcription and expression of endothelial Jagged1, which has been previously studied in its ability to regulate vSMC recruitment (High et al., 2007, 2008; Liu et al., 2009). Therefore, Jagged1/Notch4 not only counteracts Dll4/Notch1 in the endothelium but is also responsible for maintaining the fine balance between angiogenic growth and maturation processes.

The maturation process is also known to be regulated by the ability of endothelial Jagged1 to engage perivascular Notch3, directing the expression of *HeyL* and other signals laterally into the vessel wall (Liu et al., 2009). In the results presented in this thesis we have also validated this mechanistic regulation in both physiological and tumoral angiogenesis. However, this raises a new question, which involves the distinction between the highly intertwined roles of EC-Jagged1/Notch4 signaling and of EC-Jagged1/perivascular-Notch3 signaling. Therefore, further studies are required to dissect these different ligand/receptor coupled signaling mechanisms.

The work presented here also demonstrated that the pro-angiogenic and pro-maturation function of endothelial Jagged1 can be effectively targeted to inhibit tumor development and progression. Interestingly, blocking Jagged1/2 mimicked the vascular phenotype observed with endothelial-specific *Jag1* loss-of-function, producing a vasculature less dense, immature and consequently less functional and more leakier, therefore inhibiting the neo-vascularization process. When directly compared (Figure 21) one can observe that the vascular phenotype of *eJag1cKO* and of Anti-Jagged1/2 prostate tumor samples is basically equivalent. Even though the anti-Jagged1/2 treated prostate samples present a further decrease in vascular density relative to *eJag1cKO* (Fig. 21A), the recruitment of vSMCs (Fig.21B), vascular perfusion (Fig.21C) and vascular leakage (Fig.21C) do not significantly differ, suggesting that the overall functionality of the neo-vascular must be similar. These observations suggest that the angiogenic effect obtained with anti-Jagged1/2 treatment is most probably a consequence of blocking endothelial Jagged1.

Figure 21- Vascular phenotype comparison between *eJag1cKO* and anti-Jagged1/2 treated prostate samples.



A. Percentage of vascular density (relative to control=100%) demonstrating decreased density in both *eJag1cKO* and Anti-Jagged1/2 treated mice relative to respective control groups and a significant further decrease in treated samples compared with *eJag1cKO*. **B.** Percentage of vascular smooth muscle coverage, showing decreased levels of SMA on TRAMP *eJag1cKO* and Anti-Jag1/2 vasculature, relative to respective controls. **C.** Percentage of perfused area in the total vascular area (given by vascular density measurements) showing decreased lectin labeling in *eJag1cKO* and treated prostate samples. **D.** Percentage of vascular extravasation area, showing increased Evans' Blue staining in *eJag1cKO* and treated prostate samples relative to controls (TRAMP-100%). Error bars represent SEM; ** represents $p < 0.01$; *** represents $p < 0.001$; n.s represents non-significant.

Furthermore, we have also demonstrated that both prostate samples from Anti-Jagged1/2 treated TRAMP mice and TRAMP.*eJag1cKO* mutants presented decreased levels of Hif1 α , therefore decreased overall hypoxia, even though in both cases, there was limited vascular perfusion. Since hypoxia is a common feature of prostate tumors and has been associated with disease progression, metastatic spread, selection of cells with more aggressive phenotypes and treatment resistance (Chaudary & Hill, 2007; Marignol, Rivera-Figueroa, Lynch, & Hollywood, 2013), this may constitute an improved secondary effect of blocking Jagged1.

Additionally, it was demonstrated that endothelial Jagged1 contributes to tumor dysplasia not only by a pro-angiogenic effect, limiting the nutrient and oxygen delivery to tumor cells but also

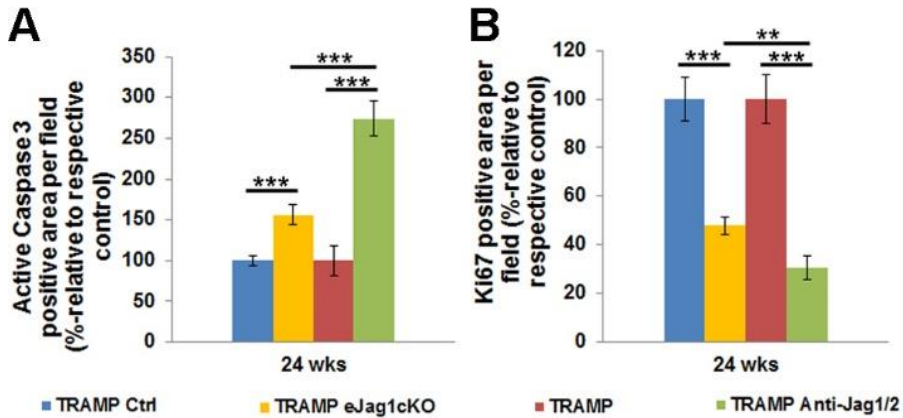
by an angiocrine effect mediated through activation of Notch3 and Hey1 expression in adjacent tumor cells. The ability of a soluble extracellular domain of JAGGED1 to mediate paracrine and juxtacrine Notch signaling between endothelial cells and tumor cells, has also been described (Lu et al., 2013; Cao et al., 2014). Interestingly, paracrine signaling from tumor cells expressing Jagged1 to endothelial cells has also been described in the stimulation of neo-angiogenesis (Zeng et al., 2005; Funahashi et al., 2008). Therefore, soluble Jagged1 seems to be able to function as a bridge in long-distance or paracrine Notch signaling between ECs and tumor cells. In fact, in the extensive Notch expression study that was presented in chapter III, a specific Notch signaling axis, Jagged1-2/Notch3/Hey1, was found to be ectopically expressed in the prostate tumorigenic tissue. Which suggests that for this process, not only endothelial Jagged1 is essential in its pro-angiogenic and pro-angiocrine functions, but also that the direct role of tumor epithelial expressed Jagged1 may exert relevant functions. This observation also leads to the speculation that in whole tumor microenvironment, Jagged1/Notch signaling acts in a similar manner to the lateral induction model proposed by Liu and colleagues, in the regulation of vascular maturation (Liu et al., 2009). Meaning that it is able to propagate a Notch signaling cascade from ECs to tumor cells and vice versa, and from tumor cell to adjacent ones, and so on, contributing to tumor cells dysplastic transformations.

In support of this speculation lies the fact that some of the effects observed on tumor cells proliferation/apoptosis, derived either from angiogenic or angiocrine functions in *eJag1cKO* mutants as in treated prostate samples, were very similar, despite being more pronounced in treated prostates. In both cases (*eJag1cKO* and treated samples) inhibition of Jagged1 was shown to inhibit prostatic cell growth, restricting tumor cell proliferation, and promoting cell cycle arrest and apoptosis, by regulating the transcription profile of several cell cycle regulatory genes (Zhang et al., 2006; Wang et al., 2010). However, if we directly compare the phenotypes described previously from both *eJag1cKO* and treated prostatic tumors samples it is clear that blocking Jagged1/2 had a more pronounced effect (Figure 22). Anti-Jagged1/2 treated prostate samples exhibited significantly increased apoptosis (Fig. 22A), and a further decreased proliferation (Fig. 22B), relative to *eJag1cKO* mutants prostates.

Blocking Jagged1, either by knocking-out endothelial *Jag1* or by targeting Jagged1/2 with the antibody, was also shown to inhibit epithelial-to-mesenchymal transition by regulating expression and transcription of E-cadherin and of the mesenchymal markers, Snail and Slug (Leong et al., 2007). However, treated samples also presented significantly higher E-cadherin (Fig. 23A) and lower Snail (Fig. 23B) stainings, than *eJag1cKO* samples, suggesting a stronger ability of the antibody in restricting EMT, and thus less susceptibility to the development of metastasis (Hanahan & Weinberg, 2011). Moreover, in chapter III it was shown expression of Jagged2 and Notch3 in the stromal compartment of the healthy prostate, which was strongly up-regulated in TRAMP prostates stroma, suggesting that stromal expression of Jagged2 and

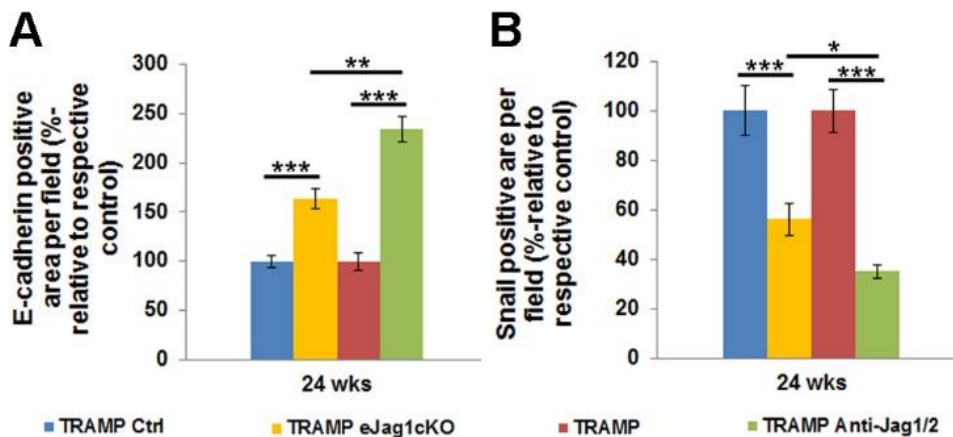
Notch3 could also contribute to the invasion process that takes place in advanced lesions (Ross et al., 2011). Therefore, blocking Jagged1/2 may potentially inhibit metastasis formation in a more effective way than targeting endothelial *Jag1* specifically (Santagata et al., 2004; Leong et al., 2007; Sethi et al., 2011; Xing et al., 2011, 2013).

Figure 22- Prostate cell proliferation and apoptosis comparison between eJag1cKO and anti-Jagged1/2 treated prostate tumor samples.



A. Prostatic lesions of TRAMP.eJag1cKO and TRAMP Anti-Jag1/2 mice presenting increased percentage of active caspase3 positive area per field, relative to respective controls (100%), at 24 weeks of age. **B.** Prostate samples from TRAMP.eJag1cKO and treated TRAMP mice (TRAMP Anti-Jag1/2) presenting decreased percentage of Ki67 positive area per field, relative to respective control groups (100%), at 24 weeks. Error bars represent SEM; ** represents p<0.01; *** represents p<0.001.

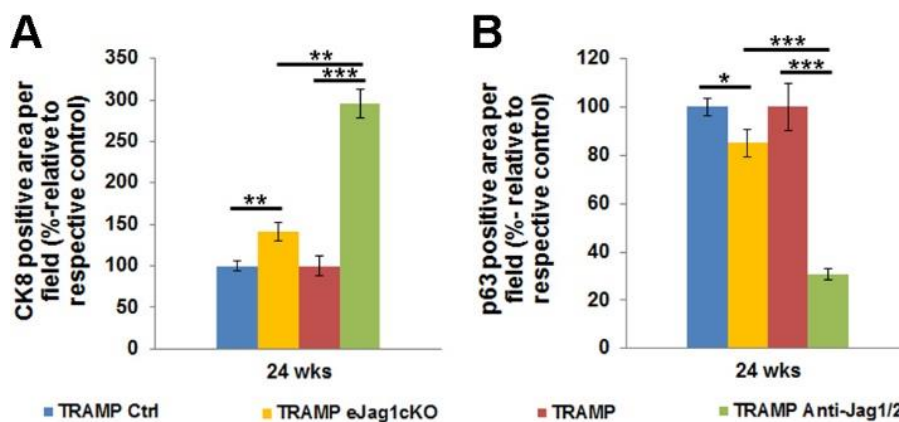
Figure 23- EMT phenotype comparison between eJag1cKO and anti-Jagged1/2 treated prostate tumor samples.



A. Increased percentage of E-cadherin per field in TRAMP.eJag1cKO and TRAMP Anti-Jag1/2, relative to respective control groups- (100%), at 24 weeks of age. **B.** Decreased Snail positive area per field in eJag1cKO mutants and treated animals prostate samples (TRAMP Anti-Jag1/2), relative to respective controls –100%). Error bars represent SEM; * represent p<0.05; ** represents p<0.01; *** represents p<0.001.

Treatment of tumor prostatic lesions with Anti-Jagged1/2 antibody also counteracted the cell population changes that accompany the evolution of prostatic tumors (Long et al., 2005). Thus, treatment significantly restricted the loss of luminal cell identity, inhibited basal cell proliferation and de-differentiation from luminal to a more basal-like cell phenotype. However, when analyzing the same cell population changes in *eJag1*cKO prostate tumor samples (data not included in the results presented in chapter II) we found a similar phenotype as in treated samples (Fig. 24). Although *eJag1*cKO prostate samples also presented increased staining for CK8, a luminal cell marker, indicative of an ability in restricting luminal cell loss, this increased staining was very mild when compared with treated samples (Fig. 24A). Very similarly, *eJag1*cKO prostate tumor samples also exhibited decreased p63 staining, indicative of an ability in restricting basal cell proliferation, but again this was still much more pronounced in treated samples (Fig. 24B). In this matter, it seems that the ectopic expression of Jagged ligands, in the tumorigenic prostate, and probably more importantly the basal expression of Jagged2, described in chapter III, may play a significant key role in the regulation of the de-differentiation process that is observed in dysplastic lesions of TRAMP mice, justifying the differences in cell populations changes between *eJag1*cKO and treated samples.

Figure 24- Cell population changes comparison between *eJag1*cKO and anti-Jagged1/2 treated prostate tumor samples.



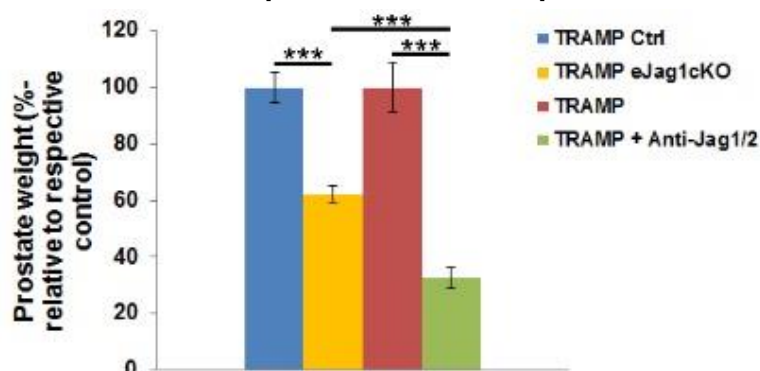
A. Prostatic lesions of TRAMP.*eJag1*cKO and TRAMP Anti-Jag1/2 mice presenting increased percentage of CK8 positive area per field, relative to respective control mice groups- (100%), at 24 weeks of age. **B.** Prostate samples from *eJag1*cKO mutants and treated TRAMP mice (TRAMP Anti-Jag1/2) presenting decreased percentage of p63 positive area per field, relative to respective controls (100%), at 24 weeks. Error bars represent SEM; ** represents $p < 0.01$; *** represents $p < 0.001$.

Blocking Jagged1/2 also had an inhibitory effect on prostate cancer stem-like cells proliferation and survival. Even though CSCs were not quantified in *eJag1*cKO prostates, one can speculate that endothelial-specific *Jag1* would also have some effect on this population of cells, either by the fact that CSCs are known to reside in niches near blood vessels (Borovski,

De Sousa E Melo, Vermeulen, & Medema, 2011) as by the angiocrine function in tumor cells. In fact, in glioma tumors, CSCs reside near endothelial cells, which are proposed to stimulate stemness through Notch and diffusible factors (Calabrese et al., 2007; Borovski et al., 2009). Furthermore, a soluble form of JAGGED1 secreted by the tumor associated endothelium was shown to promote the CSC phenotype in human colorectal cancer (Lu et al., 2013). Moreover, in lymphoma cells, endothelial Jagged1, through activation of Notch2/Hey1, was shown to regulate the ability of these cells to acquire chemoresistance and metastization, both characteristics of CSCs (Cao et al., 2014). Additionally, the anti-Jagged1/2 treated samples, presented a significant down-regulation of Notch3 and Hey1 in this specific tumor cell population. This suggests that in the case of prostate cancer, CSCs regulation is achieved through the axis Jagged/Notch3/Hey1 (Sansone et al., 2007; Domingo-Domenech et al., 2012; Oktem et al., 2014).

Altogether, it seems that the inhibitory effects of knocking-out endothelial-specific *Jag1* and of blocking Jagged1/2 are in some extent very similar, with an overall stronger effect on tumor growth achieved by the antibody administration, as observed by prostate weight measurements (Figure 25).

Figure 25- Prostate weights comparison between *eJag1* cKO and anti-Jagged1/2 treated prostate tumor samples.



Prostate weight at 24 wks of age in TRAMP.*eJag1*cKO and TRAMP Anti-Jag1/2 (treated with the blocking antibody) mice groups (% relative to respective controls-100%). Results are representative of n=12 in TRAMP Ctrl, TRAMP *eJag1*cKO and TRAMP Anti-Jag1/2 groups and n=13 in TRAMP mouse group. Error bars represent SEM; *** represents p<0.001.

The previous observations lead to the speculation that the stronger phenotypes observed in treated samples compared to *eJag1*cKO may be a simple consequence of different levels of functional Jagged1 present, which have also been demonstrated to be further decreased in treated samples endothelium as in whole prostate treated tissues. Therefore, this leads to another relevant question as to what is the real contribution of ectopically expressed Jagged2 that was found in prostatic lesions of TRAMP mice? To answer this question specific Jagged1 and Jagged2 blocking approaches have to be used and the respective phenotypes compared.

Noteworthy, Jagged2 was also present in the basal layer of a healthy prostate, and appeared in a luminal position in prostatic tumor tissues from the early beginning of the lesions. On the contrary, Jagged1 was only strongly expressed in more advanced lesions. Furthermore, the prostate cell population changes was the phenotype that presented a stronger discrepancy between *eJag1cKO* and treated samples, suggesting that Jagged2, as previously mentioned, may exert a relevant role in the regulation of basal cell proliferation and differentiation. Collectively, all the data presented here seems to support a model where Jagged2 may be involved in prostate cancer initiation and progression, given that deregulation of the basal cell lineage is a critical biological event for that process, while Jagged1 may be the ligand that propagates Notch signaling throughout the evolution of the tumorigenic prostatic process. And then both ligands exert their tumor biological effects through Notch3 activation and Hey1 expression, contributing to the dysplastic tumoral transformations.

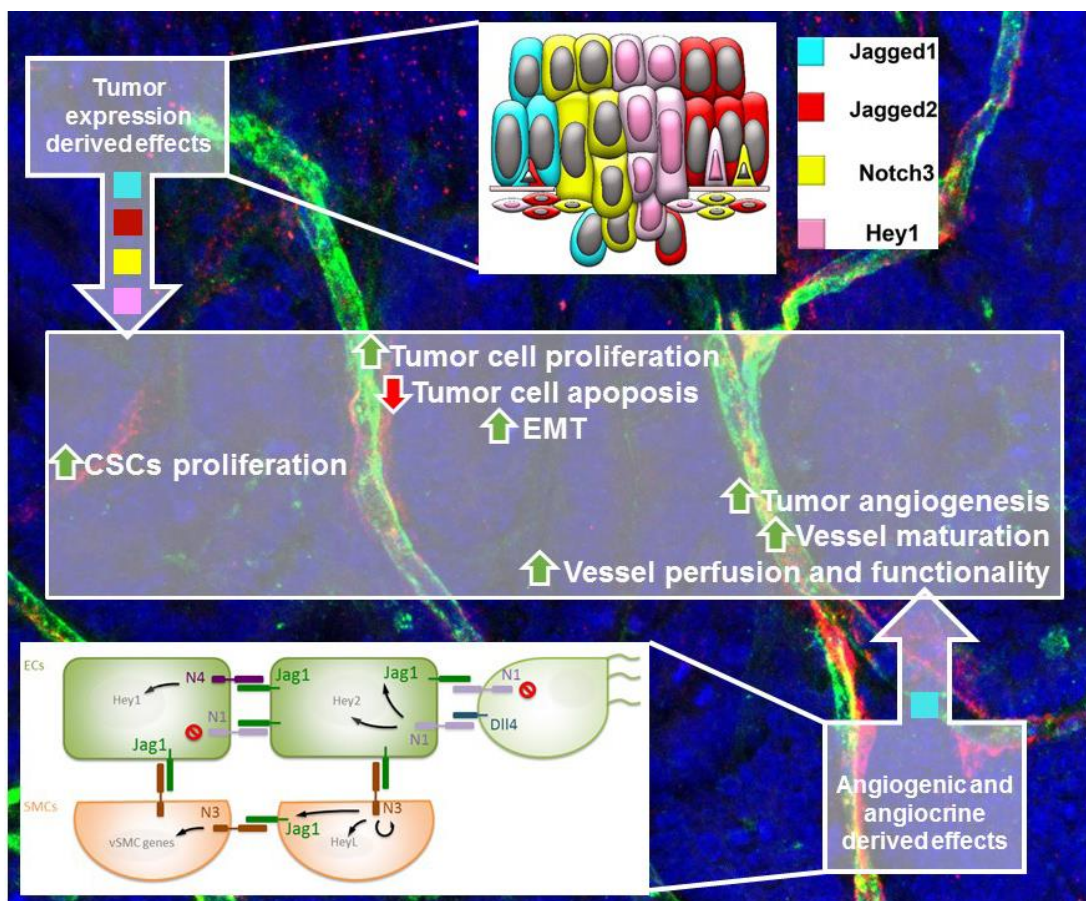
CONCLUSIONS

The results presented here contributed to a more comprehensive understanding of the role of Jagged1 in the adult organism and outside of the central nervous system, inclusively in tumor settings, such as prostate cancer.

More specifically, Jagged1 mediated Notch signaling has proven to be a complex network comprising multiple aspects in different cell types and dependent on the specific Notch receptor involved (Fig. 26). In the endothelium Jagged1 functions as a pro-angiogenic ligand through mediated Dll4/Notch1 antagonistic effect and as a pro-maturation ligand through both mediated EC-Notch4/Hey1 activation and EC-Notch3/HeyL expressing SMCs. Noteworthy, it was demonstrated that both these functions of Jagged1/Notch signaling are highly conserved in the adult organism, and more specifically that Jagged1 mediated Notch4 activation is also conserved in adult settings, including in physiological and pathological driven angiogenesis.

Endothelial Jagged1 also exerts an angiocrine function through mediated activation of Notch3 and Hey1 expression in the regulation of prostatic tumor development. This angiocrine function of endothelial Jagged1 as well as the ectopic expression of both Jagged ligands in prostate tumor tissues are critical regulators of prostatic tumor cells pathophysiology including proliferation, apoptosis, de-differentiation, EMT and CSC proliferation and survival (Fig. 26).

Figure 26- Jagged1 functions in the regulation of prostatic tumor growth.



Schematic representation of the findings presented in this thesis. On the bottom is represented the role of endothelial Jagged1 in the endothelium, contributing to angiogenesis, vascular maturation and increased vessel perfusion and functionality. Endothelial Jagged1 was also shown to exert an angiocrine effect directly on tumor cells through mediated activation of Notch3 and Hey1. On the top is represented the ectopic expression of the axis Jag1-2/Notch3/Hey1 found on prostate tumorigenic lesions. The pro-angiogenic and pro-angiocrine functions of *eJag1* together with the tumor expression derived effects contribute to prostate tumor cell proliferation, inhibition of apoptosis and to EMT induction. Moreover, CSCs proliferation was also presumably regulated by the Notch axis ectopically expressed in the tumor tissue.

Altogether, results presented here provide substantial mechanistic and functional data regarding the role of Jagged1 ligand in solid tumor development, providing a pre-clinical mouse study in which targeting this ligand with an Anti-Jagged1/2 antibody proved to be a potential therapeutic strategy for prostate cancer.

However, several questions remain to be answered given the complexity of Notch signaling network and the specificity and different expression patterns of the several components of the pathway in different tissues and/or pathological conditions. Nonetheless, this signaling pathway continues to intrigue and motivate scientists around the world, and even after a centennial of its discovery remains to be one the most studied and therapeutically promising signaling pathways in the biomedical field.

FUTURE DIRECTIONS

Results presented in this thesis provide relevant data for the potential future application therapies directed against Notch signaling. For instance, results presented in chapter I established that increased endothelial expression of Jagged1 has a profound pro-angiogenic effect that promotes healing processes. Therefore, activation of Jagged1 expression may prove to be potentially useful in situations where vascular function is a limiting factor, such as in ischemia, wound healing or diabetic retinopathy. More importantly, chapter I also demonstrates that crucial downstream effects of Dll4 and Jagged1 in endothelial cells are mediated by distinct Notch receptors which allows the uncoupling of different Notch responses in the angiogenic vasculature, and therefore may optimize the design of future therapeutic strategies.

On the contrary, blocking Jagged1 is useful in cases where limiting vascular growth and maturation is desirable such as in antiangiogenic therapies. Moreover, results presented in chapters II-IV not only demonstrate this potential anti-angiogenic effect in tumor development but they also demonstrate a direct effect on tumor cells. Furthermore, we suggest that targeting the axis Jagged1-2/Notch3/Hey1 may prove to be an attractive therapeutic option for prostate cancer patients, as we have demonstrated in a pre-clinical model of mouse prostate cancer. Given the high similarity between endocrine tumors, it can also be speculated that this therapeutic strategy would also be highly effective in treating breast cancer. In fact, it would not constitute a total surprise if the mechanisms regarding Notch signaling regulation, presented here, were to be validated in breast cancer, particularly since Jagged1 has also been implied in breast tumor regulation (Reedijk et al., 2005, 2008; Dickson et al., 2007; Cohen et al., 2010). The Notch ligand Jagged1 has also been broadly associated with many other solid tumor types, including cervical (Pang et al., 2010), colon (Rodilla et al., 2009; Pannequin et al., 2009; Lu et al., 2013; Kim et al., 2013; Dai et al., 2014), gastric (Sun, Wu, Tan, & Wang, 2012), head and neck (Lin et al., 2010), hepatic (Tschaharganeh et al., 2013), ovarian (Choi et al., 2008; Chen et al., 2010; Steg et al., 2011) and renal (Wu, Xu, Zhang, Lin, & Hou, 2011), which clearly provides enough supporting data to potentially test an Anti-Jagged1 approach in these solid tumors.

In conclusion, targeting Jagged1 can provide a new approach able to act on multiple aspects of tumor biology and on several types of cancer, possibly representing a promising tool in cancer treatment, applied alone or in combination with existing anti-cancer drugs.



REFERENCES



- Abramsson, A. (2002). Analysis of Mural Cell Recruitment to Tumor Vessels. *Circulation*, 105(1), 112–117.
- Achen, M. G., Jeltsch, M., Kukk, E., Mäkinen, T., Vitali, a, Wilks, a F., Alitalo, K., & Stacker, S. a. (1998). Vascular endothelial growth factor D (VEGF-D) is a ligand for the tyrosine kinases VEGF receptor 2 (Flk1) and VEGF receptor 3 (Flt4). *Proceedings of the National Academy of Sciences of the United States of America*, 95(2), 548–53.
- Aho, S. (2004). Soluble form of Jagged1: Unique product of epithelial keratinocytes and a regulator of keratinocyte differentiation. *Journal of Cellular Biochemistry*, 92(6), 1271–1281.
- Akazawa, C., Sasai, Y., Nakanishi, S., & Kageyama, R. (1992). Molecular characterization of a rat negative regulator with a basic helix-loop-helix structure predominantly expressed in the developing nervous system. *The Journal of biological chemistry*, 267(30), 21879–21885.
- Algire, G. (1943). Microscopic studies of the early growth of a transplantable melanoma of the mouse, using the transparent chamber technique. *J Natl Cancer Inst*, 4(1).
- Ali, S. H., & DeCaprio, J. A. (2001). Cellular transformation by SV40 large T antigen: interaction with host proteins. *Seminars in cancer biology*, 11(1), 15–23.
- Alitalo, K., & Carmeliet, P. (2002). Molecular mechanisms of lymphangiogenesis in health and disease. *Cancer cell*, 1(3), 219–27.
- Alva, J. a, Zovein, A. C., Monvoisin, A., Murphy, T., Salazar, A., Harvey, N. L., Carmeliet, P., & Iruela-Arispe, M. L. (2006). VE-Cadherin-Cre-recombinase transgenic mouse: a tool for lineage analysis and gene deletion in endothelial cells. *Developmental dynamics: an official publication of the American Association of Anatomists*, 235(3), 759–67.
- Anderson, L. M., & Gibbons, G. H. (2007). Notch : a mastermind of vascular morphogenesis, 117(2), 299–302.
- Arbiser, J. L. (1996). Angiogenesis and the skin: a primer. *Journal of the American Academy of Dermatology*, 34(3), 486–97.
- Armulik, A., Abramsson, A., & Betsholtz, C. (2005). Endothelial/pericyte interactions. *Circulation research*, 97(6), 512–523.
- Armulik, A., Genové, G., & Betsholtz, C. (2011). Pericytes: developmental, physiological, and pathological perspectives, problems, and promises. *Developmental cell*, 21(2), 193–215.
- Artavanis-Tsakonas, S., Rand, M. D., & Lake, R. J. (1999). Notch signaling: cell fate control and signal integration in development. *Science*, 284(5415), 770–776.
- Aster, J. C., Simms, W. B., Zavala-Ruiz, Z., Patriub, V., North, C. L., & Blacklow, S. C. (1999). The folding and structural integrity of the first LIN-12 module of human Notch1 are calcium-dependent. *Biochemistry*, 38(15), 4736–42.
- Bae, S., Bessho, Y., Hojo, M., & Kageyama, R. (2000). The bHLH gene Hes6, an inhibitor of Hes1, promotes neuronal differentiation. *Development (Cambridge, England)*, 127(13), 2933–43.
- Balasubramanian, R., Rashied, S., Filipovic, A., Slade, M., Yague, E., & Coombes, C. (2008). Gammasecretase is a potential therapeutic target in Breast cancer. *European Journal of Surgical Oncology (EJSO)*, 34(10), 1188. Elsevier.
- Becker, K.-F., Rosivatz, E., Blechschmidt, K., Kremmer, E., Sarbia, M., & Höfler, H. (2007). Analysis of the E-cadherin repressor Snail in primary human cancers. *Cells, tissues, organs*, 185(1-3), 204–12. Karger Publishers.
- Beckers, J., Clark, a, Wünsch, K., Hrabé De Angelis, M., & Gossler, a. (1999). Expression of the mouse Delta1 gene during organogenesis and fetal development. *Mechanisms of development*, 84(1-2), 165–8.
- Belandia, B., Powell, S. M., García-Pedrero, J. M., Walker, M. M., Bevan, C. L., & Parker, M. G. (2005). Hey1, a mediator of notch signaling, is an androgen receptor corepressor.

- Molecular and cellular biology*, 25(4), 1425–36.
- Benedito, R., & Duarte, A. (2005). Expression of Dll4 during mouse embryogenesis suggests multiple developmental roles. *Gene expression patterns : GEP*, 5(6), 750–755.
- Benedito, R., Roca, C., Sörensen, I., Adams, S., Gossler, A., Fruttiger, M., & Adams, R. H. (2009). The notch ligands Dll4 and Jagged1 have opposing effects on angiogenesis. *Cell*, 137(6), 1124–35.
- Benedito, R., Rocha, S. F., Woeste, M., Zamykal, M., Radtke, F., Casanovas, O., Duarte, A., Pytowski, B., & Adams, R. H. (2012). Notch-dependent VEGFR3 upregulation allows angiogenesis without VEGF-VEGFR2 signalling. *Nature*, 484(7392), 110–4. Nature Publishing Group.
- Benedito, R., Trindade, A., Hirashima, M., Henrique, D., da Costa, L. L., Rossant, J., Gill, P. S., & Duarte, A. (2008). Loss of Notch signalling induced by Dll4 causes arterial calibre reduction by increasing endothelial cell response to angiogenic stimuli. *BMC developmental biology*, 8, 117.
- Ben-Porath, I., Thomson, M. W., Carey, V. J., Ge, R., Bell, G. W., Regev, A., & Weinberg, R. A. (2008). An embryonic stem cell-like gene expression signature in poorly differentiated aggressive human tumors. *Nature genetics*, 40(5), 499–507.
- Bergers, G., & Song, S. (2005). The role of pericytes in blood-vessel formation and maintenance. *Neuro-oncology*, 7(4), 452–64.
- Berquin, I. M., Min, Y., Wu, R., Wu, H., & Chen, Y. Q. (2005). Expression signature of the mouse prostate. *The Journal of biological chemistry*, 280(43), 36442–51.
- Bertram, J. S., & Janik, P. (1980). Establishment of a cloned line of Lewis Lung Carcinoma cells adapted to cell culture. *Cancer letters*, 11(1), 63–73.
- Bessho, Y., Miyoshi, G., Sakata, R., & Kageyama, R. (2001). Hes7: A bHLH-type repressor gene regulated by Notch and expressed in the presomitic mesoderm. *Genes to Cells*, 6(2), 175–185.
- Betsholtz, C. (2004). Insight into the physiological functions of PDGF through genetic studies in mice. *Cytokine & Growth Factor Reviews*, 15(4), 215–228. Elsevier.
- Bettenhausen, B., Hrabě de Angelis, M., Simon, D., Guénet, J. L., & Gossler, a. (1995). Transient and restricted expression during mouse embryogenesis of Dll1, a murine gene closely related to Drosophila Delta. *Development (Cambridge, England)*, 121(8), 2407–18.
- Beverly, L. J., Ascano, J. M., & Capobianco, A. J. (2006). Expression of JAGGED1 in T-lymphocytes results in thymic involution by inducing apoptosis of thymic stromal epithelial cells. *Genes and immunity*, 7(6), 476–486.
- Blaumueller, C. M., Qi, H., Zagouras, P., & Artavanis-Tsakonas, S. (1997). Intracellular cleavage of Notch leads to a heterodimeric receptor on the plasma membrane. *Cell*, 90(2), 281–291.
- Borovski, T., De Sousa E Melo, F., Vermeulen, L., & Medema, J. P. (2011). Cancer Stem Cell Niche: The Place to Be. *Cancer Research*, 71(3), 634–639.
- Borovski, T., Verhoeff, J. J. C., ten Cate, R., Cameron, K., de Vries, N. A., van Tellingen, O., Richel, D. J., van Furth, W. R., Medema, J. P., & Sprick, M. R. (2009). Tumor microvasculature supports proliferation and expansion of glioma-propagating cells. *International journal of cancer. Journal international du cancer*, 125(5), 1222–30.
- Boucher, J. M., Peterson, S. M., Urs, S., Zhang, C., & Liaw, L. (2011). The miR-143/145 cluster is a novel transcriptional target of Jagged-1/Notch signaling in vascular smooth muscle cells. *The Journal of biological chemistry*, 286(32), 28312–21.
- Bouras, T., Pal, B., Vaillant, F., Harburg, G., Asselin-Labat, M.-L., Oakes, S. R., Lindeman, G. J., & Visvader, J. E. (2008). Notch signaling regulates mammary stem cell function and luminal cell-fate commitment. *Cell stem cell*, 3(4), 429–41.

- Bray, S. J. (2006). Notch signalling: a simple pathway becomes complex. *Nature reviews. Molecular cell biology*, 7(9), 678–689.
- Brou, C., Logeat, F., Gupta, N., Bessia, C., LeBail, O., Doedens, J. R., Cumano, a, Roux, P., Black, R. a, & Israël, a. (2000). A novel proteolytic cleavage involved in Notch signaling: the role of the disintegrin-metalloprotease TACE. *Molecular cell*, 5(2), 207–16.
- Byrne, A. M., Bouchier-Hayes, D. J., & Harmey, J. H. (2005). Angiogenic and cell survival functions of vascular endothelial growth factor (VEGF). *Journal of cellular and molecular medicine*, 9(4), 777–94.
- Calabrese, C., Poppleton, H., Kocak, M., Hogg, T. L., Fuller, C., Hamner, B., Oh, E. Y., Gaber, M. W., Finklestein, D., Allen, M., Frank, A., Bayazitov, I. T., Zakharenko, S. S., Gajjar, A., Davidoff, A., & Gilbertson, R. J. (2007). A perivascular niche for brain tumor stem cells. *Cancer cell*, 11(1), 69–82. Elsevier.
- Campos, a. H. (2002). Determinants of Notch-3 Receptor Expression and Signaling in Vascular Smooth Muscle Cells: Implications in Cell-Cycle Regulation. *Circulation Research*, 91(11), 999–1006.
- Cao, Z., Ding, B.-S., Guo, P., Lee, S. B., Butler, J. M., Casey, S. C., Simons, M., Tam, W., Felsher, D. W., Shido, K., Rafii, A., Scandura, J. M., & Rafii, S. (2014). Angiocrine factors deployed by tumor vascular niche induce B cell lymphoma invasiveness and chemoresistance. *Cancer cell*, 25(3), 350–65.
- Caolo, V., Schulten, H. M., Zhuang, Z. W., Murakami, M., Wagenaar, A., Verbruggen, S., Molin, D. G. M., & Post, M. J. (2011). Soluble jagged-1 inhibits neointima formation by attenuating notch-herp2 signaling. *Arteriosclerosis, Thrombosis, and Vascular Biology*, 31(5), 1059–1065.
- Cappellari, O., Benedetti, S., Innocenzi, A., Tedesco, F. S., Moreno-Fortuny, A., Ugarte, G., Lampugnani, M. G., Messina, G., & Cossu, G. (2013). DII4 and PDGF-BB Convert Committed Skeletal Myoblasts to Pericytes without Erasing Their Myogenic Memory. *Developmental Cell*, 1–14. Elsevier Inc.
- Carlson, T. R., Yan, Y., Wu, X., Lam, M. T., Tang, G. L., Beverly, L. J., Messina, L. M., Capobianco, A. J., Werb, Z., & Wang, R. (2005). Endothelial expression of constitutively active Notch4 elicits reversible arteriovenous malformations in adult mice. *Proceedings of the National Academy of Sciences of the United States of America*, 102(28), 9884–9.
- Carmeliet, P. (2000). Mechanisms of angiogenesis and arteriogenesis. *Nature medicine*, 6(4), 389–95.
- Carmeliet, P. (2003). Angiogenesis in health and disease. *Nature medicine*, 9(6), 653–60.
- Carmeliet, P. (2005). Angiogenesis in life, disease and medicine. *Nature*, 438(7070), 932–6.
- Carmeliet, P., Ferreira, V., Breier, G., Pollefeyt, S., Kieckens, L., Gertsenstein, M., Fahrig, M., Vandenhoek, A., Harpal, K., Eberhardt, C., Declercq, C., Pawling, J., Moons, L., Collen, D., Risau, W., & Nagy, A. (1996). Abnormal blood vessel development and lethality in embryos lacking a single VEGF allele. *Nature*, 380(6573), 435–9.
- Carmeliet, P., & Jain, R. K. (2011). Molecular mechanisms and clinical applications of angiogenesis. *Nature*, 473(7347), 298–307.
- Carmeliet, P., De Smet, F., Loges, S., & Mazzone, M. (2009). Branching morphogenesis and antiangiogenesis candidates: tip cells lead the way. *Nature reviews. Clinical oncology*, 6(6), 315–26. Nature Publishing Group.
- Carvalho, F. L. F., Simons, B. W., Eberhart, C. G., & Berman, D. M. (2014). Notch signaling in prostate cancer: A moving target. *The Prostate*, 74(9), 933–45.
- Chang, C., Lee, S. O., Yeh, S., & Chang, T. M. (2014). Androgen receptor (AR) differential roles in hormone-related tumors including prostate, bladder, kidney, lung, breast and liver. *Oncogene*, 33(25), 3225–34. Macmillan Publishers Limited.
- Chaudary, N., & Hill, R. P. (2007). Hypoxia and Metastasis. *Behind, The Biology*, 13(7), 1947–

1950.

- Chen, W., Possemato, R., Campbell, K. T., Plattner, C. A., Pallas, D. C., & Hahn, W. C. (2004). Identification of specific PP2A complexes involved in human cell transformation. *Cancer cell*, *5*(2), 127–136.
- Chen, X., Stoeck, A., Lee, S. J., Shih, I.-M., Wang, M. M., & Wang, T.-L. (2010). Jagged1 expression regulated by Notch3 and Wnt/ β -catenin signaling pathways in ovarian cancer. *Oncotarget*, *1*(3), 210–218.
- Chigurupati, S., Arumugam, T. V., Son, T. G., Lathia, J. D., Jameel, S., Mughal, M. R., Tang, S.-C., Jo, D.-G., Camandola, S., Giunta, M., Rakova, I., McDonnell, N., Miele, L., Mattson, M. P., & Poosala, S. (2007). Involvement of notch signaling in wound healing. *PLoS one*, *2*(11), e1167.
- Chin, M. T., Maemura, K., Fukumoto, S., Jain, M. K., Layne, M. D., Watanabe, M., Hsieh, C. M., & Lee, M. E. (2000). Cardiovascular basic helix loop helix factor 1, a novel transcriptional repressor expressed preferentially in the developing and adult cardiovascular system. *The Journal of biological chemistry*, *275*(9), 6381–7.
- Choi, J.-H., Park, J. T., Davidson, B., Morin, P. J., Shih, I.-M., & Wang, T.-L. (2008). Jagged-1 and Notch3 juxtacrine loop regulates ovarian tumor growth and adhesion. *Cancer research*, *68*(14), 5716–23.
- Claxton, S., & Fruttiger, M. (2004). Periodic Delta-like 4 expression in developing retinal arteries. *Gene expression patterns: GEP*, *5*(1), 123–7.
- Cohen, B., Shimizu, M., Izrailit, J., Ng, N. F. L., Buchman, Y., Pan, J. G., Dering, J., & Reedijk, M. (2010). Cyclin D1 is a direct target of JAG1-mediated Notch signaling in breast cancer. *Breast cancer research and treatment*, *123*(1), 113–24.
- Conlon, R. a, Reaume, a G., & Rossant, J. (1995). Notch1 is required for the coordinate segmentation of somites. *Development (Cambridge, England)*, *121*(5), 1533–45.
- Costa, M. J., Wu, X., Cuervo, H., Srinivasan, R., Bechis, S. K., Cheang, E., Marjanovic, O., Gridley, T., Cvetic, C. A., & Wang, R. A. (2013). Notch4 is required for tumor onset and perfusion. *Vascular cell*, *5*(1), 7. BioMed Central Ltd.
- Costello, L. C., & Franklin, R. B. (2005). “Why do tumour cells glycolyse?”: from glycolysis through citrate to lipogenesis. *Molecular and cellular biochemistry*, *280*(1-2), 1–8.
- Crisan, M., Corselli, M., Chen, W. C. W., & Péault, B. (2012). Perivascular cells for regenerative medicine. *Journal of cellular and molecular medicine*, *16*(12), 2851–60.
- Cunha, G. R., Donjacour, A. A., Cooke, P. S., Mee, S., Bigsby, R. M., Higgins, S. J., & Sugimura, Y. (1987). The endocrinology and developmental biology of the prostate. *Endocrine reviews*, *8*(3), 338–62.
- D'Souza, B., Miyamoto, a, & Weinmaster, G. (2008). The many facets of Notch ligands. *Oncogene*, *27*(38), 5148–67.
- Dai, Y., Wilson, G., Huang, B., Peng, M., Teng, G., Zhang, D., Zhang, R., Ebert, M. P. A., Chen, J., Wong, B. C. Y., Chan, K. W., George, J., & Qiao, L. (2014). Silencing of Jagged1 inhibits cell growth and invasion in colorectal cancer. *Cell death & disease*, *5*, e1170. Macmillan Publishers Limited.
- Daly, C., Eichten, A., Castanaro, C., Pasnikowski, E., Adler, A., Lalani, A. S., Papadopoulos, N., Kyle, A. H., Minchinton, A. I., Yancopoulos, G. D., & Thurston, G. (2012). Angiopoietin-2 Functions as a Tie2 Agonist in Tumor Models, Where It Limits the Effects of VEGF Inhibition. *Cancer Research*, *73*(1), 108–118.
- Dang, T., Kawaguchi, K., Carbone, D., & Hue, H. (2005). P-027 Targeting Notch3 pathway in lung cancer using gamma-secretaseinhibitors. *Lung Cancer*, *49*, S122. Elsevier.
- Danza, G., Di Serio, C., Ambrosio, M. R., Sturli, N., Lonetto, G., Rosati, F., Rocca, B. J., Ventimiglia, G., del Vecchio, M. T., Prudovsky, I., Marchionni, N., & Tarantini, F. (2013). Notch3 is activated by chronic hypoxia and contributes to the progression of human

- prostate cancer. *International journal of cancer. Journal international du cancer*, 133(11), 2577–86.
- Davis, S., Aldrich, T. H., Jones, P. F., Acheson, A., Compton, D. L., Jain, V., Ryan, T. E., Bruno, J., Radziejewski, C., Maisonpierre, P. C., & Yancopoulos, G. D. (1996). Isolation of Angiopoietin-1, a Ligand for the TIE2 Receptor, by Secretion-Trap Expression Cloning. *Cell*, 87(7), 1161–1169. Elsevier.
- DeMarzo, A. M., Nelson, W. G., Isaacs, W. B., & Epstein, J. I. (2003). Pathological and molecular aspects of prostate cancer. *The Lancet*, 361(9361), 955–964.
- Deng, G., Ma, L., Meng, Q., Ju, X., Jiang, K., Jiang, P., & Yu, Z. (2015). Notch signaling in the prostate: critical roles during development and in the hallmarks of prostate cancer biology. *Journal of cancer research and clinical oncology*.
- Dexter, J. S. (1914). The Analysis of a Case of Continuous Variation in *Drosophila* by a Study of Its Linkage Relations. *The American Naturalist*.
- Dickson, B. C., Mulligan, A. M., Zhang, H., Lockwood, G., O'Malley, F. P., Egan, S. E., & Reedijk, M. (2007). High-level JAG1 mRNA and protein predict poor outcome in breast cancer. *Modern pathology : an official journal of the United States and Canadian Academy of Pathology, Inc*, 20(6), 685–93.
- Diez, H., Fischer, A., Winkler, A., Hu, C.-J., Hatzopoulos, A. K., Breier, G., & Gessler, M. (2007). Hypoxia-mediated activation of Dll4-Notch-Hey2 signaling in endothelial progenitor cells and adoption of arterial cell fate. *Experimental cell research*, 313(1), 1–9.
- Ding, X.-Y., Ding, J., Wu, K., Wen, W., Liu, C., Yan, H.-X., Chen, C., Wang, S., Tang, H., Gao, C.-K., Guo, L.-N., Cao, D., Li, Z., Feng, G.-S., Wang, H.-Y., & Xu, Z.-F. (2012). Cross-talk between endothelial cells and tumor via delta-like ligand4/Notch/PTEN signaling inhibits lung cancer growth. *Oncogene*, 31(225), 2899–2906.
- Doi, H., Iso, T., Sato, H., Yamazaki, M., Matsui, H., Tanaka, T., Manabe, I., Arai, M., Nagai, R., & Kurabayashi, M. (2006). Jagged1-selective notch signaling induces smooth muscle differentiation via a RBP-Jkappa-dependent pathway. *The Journal of biological chemistry*, 281(39), 28555–28564.
- Domenga, V., Fardoux, P., Lacombe, P., Monet, M., Maciazek, J., Krebs, L. T., Klonjowski, B., Berrou, E., Mericskay, M., Li, Z., Tournier-Lasserre, E., Gridley, T., & Joutel, A. (2004). Notch3 is required for arterial identity and maturation of vascular smooth muscle cells. *Genes & development*, 18(22), 2730–2735.
- Domingo-Domenech, J., Vidal, S. J., Rodriguez-Bravo, V., Castillo-Martin, M., Quinn, S. A., Rodriguez-Barrueco, R., Bonal, D. M., Charytonowicz, E., Gladoun, N., de la Iglesia-Vicente, J., Petrylak, D. P., Benson, M. C., Silva, J. M., & Cordon-Cardo, C. (2012). Suppression of acquired docetaxel resistance in prostate cancer through depletion of notch- and hedgehog-dependent tumor-initiating cells. *Cancer cell*, 22(3), 373–88. Elsevier.
- Donovan, J., Kordylewska, A., Jan, Y. N., & Utset, M. F. (2002). Tetralogy of fallot and other congenital heart defects in Hey2 mutant mice. *Current biology : CB*, 12(18), 1605–10.
- Dor, Y., & Keshet, E. (1997). Ischemia-driven angiogenesis. *Trends in cardiovascular medicine*, 7(8), 289–94. Elsevier.
- Duarte, A., Hirashima, M., Bedito, R., Trindade, A., Diniz, P., Bekman, E., Costa, L., Henrique, D., & Rossant, J. (2004). Dosage-sensitive requirement for mouse Dll4 in artery development. *Genes & development*, 18(20), 2474–2478.
- Duhagon, M. A., Hurt, E. M., Sotelo-Silveira, J. R., Zhang, X., & Farrar, W. L. (2010). Genomic profiling of tumor initiating prostatospheres. *BMC genomics*, 11, 324.
- Dumont, D. J., Gradwohl, G., Fong, G. H., Puri, M. C., Gertsenstein, M., Auerbach, A., & Breitman, M. L. (1994). Dominant-negative and targeted null mutations in the endothelial receptor tyrosine kinase, tek, reveal a critical role in vasculogenesis of the embryo. *Genes and Development*, 8(16), 1897–1909.

- Dumont, D. J., Jussila, L., Taipale, J., Lymboussaki, A., Mustonen, T., Pajusola, K., Breitman, M., & Alitalo, K. (1998). Cardiovascular failure in mouse embryos deficient in VEGF receptor-3. *Science (New York, N.Y.)*, *282*(5390), 946–9.
- Dunwoodie, S. L., Henrique, D., Harrison, S. M., & Beddington, R. S. (1997). Mouse Dll3: a novel divergent Delta gene which may complement the function of other Delta homologues during early pattern formation in the mouse embryo. *Development (Cambridge, England)*, *124*(16), 3065–76.
- Elyaman, W., Bradshaw, E. M., Wang, Y., Oukka, M., Kivisakk, P., Chiba, S., Yagita, H., & Khoury, S. J. (2007). Jagged1 and Delta1 Differentially Regulate the Outcome of Experimental Autoimmune Encephalomyelitis. *The Journal of Immunology*, *179*(9), 5990–5998. American Association of Immunologists.
- Eming, S. a., Brachvogel, B., Odorisio, T., & Koch, M. (2007). Regulation of angiogenesis: Wound healing as a model. *Progress in Histochemistry and Cytochemistry*, *42*(3), 115–170.
- Emuss, V., Lagos, D., Pizzey, A., Gratrix, F., Henderson, S. R., & Boshoff, C. (2009). KSHV manipulates Notch signaling by DLL4 and JAG1 to alter cell cycle genes in lymphatic endothelia. *PLoS pathogens*, *5*(10), e1000616.
- van Es, J. H., van Gijn, M. E., Riccio, O., van den Born, M., Vooijs, M., Begthel, H., Cozijnsen, M., Robine, S., Winton, D. J., Radtke, F., & Clevers, H. (2005). Notch/gamma-secretase inhibition turns proliferative cells in intestinal crypts and adenomas into goblet cells. *Nature*, *435*(7044), 959–63.
- Espinoza, I., Pochampally, R., Xing, F., Watabe, K., & Miele, L. (2013). Notch signaling: targeting cancer stem cells and epithelial-to-mesenchymal transition. *OncoTargets and therapy*, *6*, 1249–1259.
- Ferrara, N., Carver-Moore, K., Chen, H., Dowd, M., Lu, L., O’Shea, K. S., Powell-Braxton, L., Hillan, K. J., & Moore, M. W. (1996). Heterozygous embryonic lethality induced by targeted inactivation of the VEGF gene. *Nature*, *380*(6573), 439–42.
- Ferrara, N., & Davis-Smyth, T. (1997). The biology of vascular endothelial growth factor. *Endocrine reviews*, *18*(1), 4–25.
- Ferrara, N., & Henzel, W. J. (1989). Pituitary follicular cells secrete a novel heparin-binding growth factor specific for vascular endothelial cells. *Biochemical and biophysical research communications*, *161*(2), 851–858.
- Fischer, A., Schumacher, N., Maier, M., Sendtner, M., & Gessler, M. (2004). The Notch target genes Hey1 and Hey2 are required for embryonic vascular development. *Genes and Development*, *18*(8), 901–911.
- Folkman, J. (1971). Tumor angiogenesis: therapeutic implications. *The New England journal of medicine*, *285*(21), 1182–1186.
- Fong, G. H., Rossant, J., Gertsenstein, M., & Breitman, M. L. (1995). Role of the Flt-1 receptor tyrosine kinase in regulating the assembly of vascular endothelium. *Nature*, *376*(6535), 66–70.
- Fortini, M. E., Rebay, I., Caron, L. A., & Artavanis-Tsakonas, S. (1993). An activated Notch receptor blocks cell-fate commitment in the developing Drosophila eye. *Nature*, *365*(6446), 555–7.
- Fraser, H. M., & Lunn, S. F. (2000). Angiogenesis and its control in the female reproductive system. *British medical bulletin*, *56*(3), 787–97.
- Fredriksson, L., Li, H., & Eriksson, U. (2004). The PDGF family: four gene products form five dimeric isoforms. *Cytokine & Growth Factor Reviews*, *15*(4), 197–204. Elsevier.
- Funahashi, Y., Hernandez, S. L., Das, I., Ahn, A., Huang, J., Vorontchikhina, M., Sharma, A., Kanamaru, E., Borisenko, V., Desilva, D. M., Suzuki, A., Wang, X., Shawber, C. J., Kandel, J. J., Yamashiro, D. J., & Kitajewski, J. (2008). A notch1 ectodomain construct

- inhibits endothelial notch signaling, tumor growth, and angiogenesis. *Cancer research*, 68(12), 4727–35.
- Gale, N. W., Dominguez, M. G., Noguera, I., Pan, L., Hughes, V., Valenzuela, D. M., Murphy, A. J., Adams, N. C., Lin, H. C., Holash, J., Thurston, G., & Yancopoulos, G. D. (2004). Haploinsufficiency of delta-like 4 ligand results in embryonic lethality due to major defects in arterial and vascular development. *Proceedings of the National Academy of Sciences of the United States of America*, 101(45), 15949–54.
- Gallahan, D., & Callahan, R. (1997). The mouse mammary tumor associated gene INT3 is a unique member of the NOTCH gene family (NOTCH4). *Oncogene*, 14(16), 1883–90.
- Georgiou, H. D., Namdarian, B., Corcoran, N. M., Costello, A. J., & Hovens, C. M. (2008). Circulating endothelial cells as biomarkers of prostate cancer. *Nature clinical practice. Urology*, 5(8), 445–54. Nature Publishing Group.
- Gerhardt, H., Golding, M., Fruttiger, M., Ruhrberg, C., Lundkvist, A., Abramsson, A., Jeltsch, M., Mitchell, C., Alitalo, K., Shima, D., & Betsholtz, C. (2003). VEGF guides angiogenic sprouting utilizing endothelial tip cell filopodia. *The Journal of cell biology*, 161(6), 1163–77.
- Gessler, M., Knobloch, K.-P., Helisch, A., Amann, K., Schumacher, N., Rohde, E., Fischer, A., & Leimeister, C. (2002). Mouse gridlock: no aortic coarctation or deficiency, but fatal cardiac defects in Hey2 *-/-* mice. *Current biology: CB*, 12(18), 1601–4.
- Gingrich, J. R., Barrios, R. J., Foster, B. A., & Greenberg, N. M. (1999). Pathologic progression of autochthonous prostate cancer in the TRAMP model. *Prostate cancer and prostatic diseases*, 2(2), 70–75.
- Gingrich, J. R., Barrios, R. J., Morton, R. A., Boyce, B. F., DeMayo, F. J., Finegold, M. J., Angelopoulou, R., Rosen, J. M., & Greenberg, N. M. (1996). Metastatic prostate cancer in a transgenic mouse. *Cancer research*, 56(18), 4096–4102.
- Gingrich, J. R., & Greenberg, N. M. (1996). A transgenic mouse prostate cancer model. *Toxicol Pathol*, 24(4), 502–504.
- Goldstein, A. S., Huang, J., Guo, C., Garraway, I. P., & Witte, O. N. (2010). Identification of a cell of origin for human prostate cancer. *Science (New York, N.Y.)*, 329(5991), 568–71.
- Gratton, J. P., Lin, M. I., Yu, J., Weiss, E. D., Jiang, Z. L., Fairchild, T. a, Iwakiri, Y., Groszmann, R., Claffey, K. P., Cheng, Y. C., & Sessa, W. C. (2003). Selective inhibition of tumor microvascular permeability by cavtratin blocks tumor progression in mice. *Cancer cell*, 4(1), 31–9.
- Greenberg, N. M., DeMayo, F., Finegold, M. J., Medina, D., Tilley, W. D., Aspinall, J. O., Cunha, G. R., Donjacour, A. A., Matusik, R. J., & Rosen, J. M. (1995). Prostate cancer in a transgenic mouse. *Proceedings of the National Academy of Sciences of the United States of America*, 92(8), 3439–3443.
- Gridley, T. (2001). Notch signaling during vascular development. *Proceedings of the National Academy of Sciences of the United States of America*, 98(10), 5377–8.
- Gurtner, G. C., Werner, S., Barrandon, Y., & Longaker, M. T. (2008). Wound repair and regeneration. *Nature*, 453(7193), 314–21.
- Gustafsson, M. V., Zheng, X., Pereira, T., Gradin, K., Jin, S., Lundkvist, J., Ruas, J. L., Poellinger, L., Lendahl, U., & Bondesson, M. (2005). Hypoxia requires notch signaling to maintain the undifferentiated cell state. *Developmental cell*, 9(5), 617–28. Elsevier.
- Bin Hafeez, B., Adhami, V. M., Asim, M., Siddiqui, I. A., Bhat, K. M., Zhong, W., Saleem, M., Din, M., Setaluri, V., & Mukhtar, H. (2009). Targeted knockdown of Notch1 inhibits invasion of human prostate cancer cells concomitant with inhibition of matrix metalloproteinase-9 and urokinase plasminogen activator. *Clinical cancer research: an official journal of the American Association for Cancer Research*, 15(2), 452–9.
- Hamada, Y., Kadokawa, Y., Okabe, M., Ikawa, M., Coleman, J. R., & Tsujimoto, Y. (1999).

- Mutation in ankyrin repeats of the mouse Notch2 gene induces early embryonic lethality. *Development (Cambridge, England)*, 126(15), 3415–3424.
- Han, G., Foster, B. A., Mistry, S., Buchanan, G., Harris, J. M., Tilley, W. D., & Greenberg, N. M. (2001). Hormone status selects for spontaneous somatic androgen receptor variants that demonstrate specific ligand and cofactor dependent activities in autochthonous prostate cancer. *The Journal of biological chemistry*, 276(14), 11204–13.
- Hanahan, D., & Folkman, J. (1996). Patterns and emerging mechanisms of the angiogenic switch during tumorigenesis. *Cell*, 86(3), 353–364.
- Hanahan, D., & Weinberg, R. A. (2011). Hallmarks of cancer: the next generation. *Cell*, 144(5), 646–674.
- Hanahan, D., Weinberg, R. A., & Francisco, S. (2000). The Hallmarks of Cancer Review University of California at San Francisco, 100, 57–70.
- Harrington, L. S., Sainson, R. C. a, Williams, C. K., Taylor, J. M., Shi, W., Li, J.-L., & Harris, A. L. (2008). Regulation of multiple angiogenic pathways by Dll4 and Notch in human umbilical vein endothelial cells. *Microvascular research*, 75(2), 144–54.
- Harrison, H., Farnie, G., Howell, S. J., Rock, R. E., Stylianou, S., Brennan, K. R., Bundred, N. J., & Clarke, R. B. (2010). Regulation of breast cancer stem cell activity by signaling through the Notch4 receptor. *Cancer research*, 70(2), 709–18.
- Hayward, S. W., Rosen, M. A., & Cunha, G. R. (1997). Stromal-epithelial interactions in the normal and neoplastic prostate. *British Journal of Urology*, 79(S2), 18–26.
- Heer, R., Robson, C. N., Shenton, B. K., & Leung, H. Y. (2007). The role of androgen in determining differentiation and regulation of androgen receptor expression in the human prostatic epithelium transient amplifying population. *Journal of cellular physiology*, 212(3), 572–8.
- Hellström, M., Phng, L.-K., Hofmann, J. J., Wallgard, E., Coultas, L., Lindblom, P., Alva, J., Nilsson, A.-K., Karlsson, L., Gaiano, N., Yoon, K., Rossant, J., Iruela-Arispe, M. L., Kalén, M., Gerhardt, H., & Betsholtz, C. (2007). Dll4 signalling through Notch1 regulates formation of tip cells during angiogenesis. *Nature*, 445(7129), 776–80.
- Hicklin, D. J., & Ellis, L. M. (2005). Role of the vascular endothelial growth factor pathway in tumor growth and angiogenesis. *Journal of clinical oncology: official journal of the American Society of Clinical Oncology*, 23(5), 1011–27.
- Higgins, L. H., Withers, H. G., Garbens, A., Love, H. D., Magnoni, L., Hayward, S. W., & Moyes, C. D. (2009). Hypoxia and the metabolic phenotype of prostate cancer cells. *Biochimica et biophysica acta*, 1787(12), 1433–43.
- High, F. a, Lu, M. M., Pear, W. S., Loomes, K. M., Kaestner, K. H., & Epstein, J. a. (2008). Endothelial expression of the Notch ligand Jagged1 is required for vascular smooth muscle development. *Proceedings of the National Academy of Sciences of the United States of America*, 105(6), 1955–9.
- High, F. A., Zhang, M., Proweller, A., Tu, L., Parmacek, M. S., Pear, W. S., & Epstein, J. A. (2007). An essential role for Notch in neural crest during cardiovascular development and smooth muscle differentiation. *The Journal of clinical investigation*, 117(2), 353–363.
- Hirata, H., Ohtsuka, T., Bessho, Y., & Kageyama, R. (2000). Generation of structurally and functionally distinct factors from the basic helix-loop-helix gene Hes3 by alternative first exons. *Journal of Biological Chemistry*, 275(25), 19083–19089.
- Hiratsuka, S., Minowa, O., Kuno, J., Noda, T., & Shibuya, M. (1998). Flt-1 lacking the tyrosine kinase domain is sufficient for normal development and angiogenesis in mice. *Proceedings of the National Academy of Sciences of the United States of America*, 95(16), 9349–54.
- Hiratsuka, S., Nakao, K., Nakamura, K., Katsuki, M., & Maru, Y. (2005). Membrane Fixation of Vascular Endothelial Growth Factor Receptor 1 Ligand-Binding Domain Is Important for

- Vasculogenesis and Angiogenesis in Mice, 25(1), 346–354.
- Hirschi, K. K., Rohovsky, S. A., Beck, L. H., Smith, S. R., & D'Amore, P. A. (1999). Endothelial Cells Modulate the Proliferation of Mural Cell Precursors via Platelet-Derived Growth Factor-BB and Heterotypic Cell Contact. *Circulation Research*, 84(3), 298–305.
- Hoch, R. V., & Soriano, P. (2003). Roles of PDGF in animal development. *Development (Cambridge, England)*, 130(20), 4769–84.
- Van Hoof, C., & Goris, J. (2004). PP2A fulfills its promises as tumor suppressor: which subunits are important? *Cancer cell*, 5(2), 105–106.
- Hori, K., Sen, A., & Artavanis-Tsakonas, S. (2013). Notch signaling at a glance. *Journal of cell science*, 126(Pt 10), 2135–40.
- Hrabě de Angelis, M., McIntyre, J., & Gossler, A. (1997). Maintenance of somite borders in mice requires the Delta homologue Dll1. *Nature*, 386(6626), 717–21.
- Hu, C., Diévar, A., Lupien, M., Calvo, E., Tremblay, G., & Jolicoeur, P. (2006). Overexpression of activated murine Notch1 and Notch3 in transgenic mice blocks mammary gland development and induces mammary tumors. *The American journal of pathology*, 168(3), 973–90.
- Hudson, D. L. (2004). Epithelial stem cells in human prostate growth and disease. *Prostate cancer and prostatic diseases*, 7(3), 188–94.
- Hunter, J. (1794). A treatise on the blood, inflammation and gunshot wounds. *Palmer JF (Ed)*, 195.
- Hurwitz, H., Fehrenbacher, L., Novotny, W., Cartwright, T., Hainsworth, J., Heim, W., Berlin, J., Baron, A., Griffing, S., Holmgren, E., Ferrara, N., Fyfe, G., Rogers, B., Ross, R., & Kabbinavar, F. (2004). Bevacizumab plus irinotecan, fluorouracil, and leucovorin for metastatic colorectal cancer. *The New England journal of medicine*, 350(23), 2335–2342.
- Huss, W. J., Hanrahan, C. F., Barrios, R. J., Simons, J. W., & Greenberg, N. M. (2001). Angiogenesis and prostate cancer: identification of a molecular progression switch. *Cancer research*, 61(6), 2736–43.
- Ide AG, Warren SL., B. N. H. (1939). Vascularization of the Brown-Pearce rabbit epithelioma transplant as seen in the transparent ear chamber. *Am J Roentgenol*, (42), 891.
- Ishibashi, M., Sasai, Y., Nakanishi, S., & Kageyama, R. (1993). Molecular characterization of HES-2, a mammalian helix-loop-helix factor structurally related to Drosophila hairy and Enhancer of split. *European journal of biochemistry / FEBS*, 215(3), 645–652.
- Iso, T., Kedes, L., & Hamamori, Y. (2003). HES and HERP families: multiple effectors of the Notch signaling pathway. *Journal of cellular physiology*, 194(3), 237–55.
- Iso, T., Sartorelli, V., Chung, G., Shichinohe, T., Kedes, L., & Hamamori, Y. (2001). HERP, a new primary target of Notch regulated by ligand binding. *Molecular and cellular biology*, 21(17), 6071–6079.
- Jain, R. K. (2003). Molecular regulation of vessel maturation. *Nature medicine*, 9(6), 685–93.
- James, A. C., Szot, J. O., Iyer, K., Major, J. A., Pursglove, S. E., Chapman, G., & Dunwoodie, S. L. (2014). Notch4 reveals a novel mechanism regulating Notch signal transduction. *Biochimica et biophysica acta*.
- Jemal, A., Bray, F., Center, M. M., Ferlay, J., Ward, E., & Forman, D. (2011). Global cancer statistics. *CA: a cancer journal for clinicians*, 61(2), 69–90.
- Jeon, H.-M., Kim, S.-H., Jin, X., Park, J. B., Kim, S. H., Joshi, K., Nakano, I., & Kim, H. (2014). Crosstalk between glioma-initiating cells and endothelial cells drives tumor progression. *Cancer research*, 74(16), 4482–92.
- Jiang, R., Lan, Y., Chapman, H. D., Shawber, C., Norton, C. R., Serreze, D. V., Weinmaster, G., & Gridley, T. (1998). Defects in limb, craniofacial, and thymic development in Jagged2 mutant mice. *Genes and Development*, 12(7), 1046–1057.

- Jiang, X., Zhou, J. H., Deng, Z. H., Qu, X. H., Jiang, H. Y., & Liu, Y. (2007). [Expression and significance of Notch1, Jagged1 and VEGF in human non-small cell lung cancer]. *Zhong Nan Da Xue Xue Bao Yi Xue Ban*, 32(6), 1031–1036.
- Jin, S., Hansson, E. M., Tikka, S., Lanner, F., Sahlgren, C., Farnebo, F., Baumann, M., Kalimo, H., & Lendahl, U. (2008). Notch signaling regulates platelet-derived growth factor receptor-beta expression in vascular smooth muscle cells. *Circulation research*, 102(12), 1483–1491.
- Joutel, a, Andreux, F., Gaulis, S., Domenga, V., Cecillon, M., Battail, N., Piga, N., Chapon, F., Godfrain, C., & Tournier-Lasserre, E. (2000). The ectodomain of the Notch3 receptor accumulates within the cerebrovasculature of CADASIL patients. *The Journal of clinical investigation*, 105(5), 597–605.
- Joutel, A., Corpechot, C., Ducros, A., Vahedi, K., Chabriat, H., Mouton, P., Alamowitch, S., Domenga, V., Cécillion, M., Marechal, E., Maciazek, J., Vayssiere, C., Cruaud, C., Cabanis, E. A., Ruchoux, M. M., Weissenbach, J., Bach, J. F., Bousser, M. G., & Tournier-Lasserre, E. (1996). Notch3 mutations in CADASIL, a hereditary adult-onset condition causing stroke and dementia. *Nature*, 383(6602), 707–710.
- Kaipainen, A., Korhonen, J., Mustonen, T., van Hinsbergh, V. W., Fang, G. H., Dumont, D., Breitman, M., & Alitalo, K. (1995). Expression of the fms-like tyrosine kinase 4 gene becomes restricted to lymphatic endothelium during development. *Proceedings of the National Academy of Sciences of the United States of America*, 92(8), 3566–70.
- Kangsamaksin, T., Murtomaki, A., Kofler, N. M., Cuervo, H., Chaudhri, R. A., Tattersall, I. W., Rosenstiel, P. E., Shawber, C. J., & Kitajewski, J. (2014). NOTCH Decoys That Selectively Block DLL/NOTCH or JAG/NOTCH Disrupt Angiogenesis by Unique Mechanisms to Inhibit Tumor Growth. *Cancer discovery*, 5(2), 182–97.
- Kao, H. Y., Ordentlich, P., Koyano-Nakagawa, N., Tang, Z., Downes, M., Kintner, C. R., Evans, R. M., & Kadesch, T. (1998). A histone deacetylase corepressor complex regulates the Notch signal transduction pathway. *Genes and Development*, 12(15), 2269–2277.
- Kaplan-Lefko, P. J., Chen, T.-M. M. T., Ittmann, M. M., Barrios, R. J., Ayala, G. E., Huss, W. J., Maddison, L. a, Foster, B. a, Greenberg, N. M., Kaplan- Lefko, P., & Chen, T.-M. M. T. (2003). Pathobiology of autochthonous prostate cancer in a pre-clinical transgenic mouse model. *The Prostate*, 55(3), 219–237.
- Karamysheva, A. F. (2008). Mechanisms of angiogenesis. *Biochemistry. Biokhimiia*, 73(7), 751–762.
- Karantanos, T., Corn, P. G., & Thompson, T. C. (2013). Prostate cancer progression after androgen deprivation therapy: mechanisms of castrate resistance and novel therapeutic approaches. *Oncogene*, 32(49), 5501–11.
- Kerbel, R. S. (2006). Antiangiogenic therapy: a universal chemosensitization strategy for cancer? *Science*, 312(5777), 1171–1175.
- Kidd, S., Kelley, M. R., & Young, M. W. (1986). Sequence of the notch locus of *Drosophila melanogaster*: relationship of the encoded protein to mammalian clotting and growth factors. *Molecular and cellular biology*, 6(9), 3094–108.
- Kiernan, A. E., Xu, J., & Gridley, T. (2006). The Notch ligand JAG1 is required for sensory progenitor development in the mammalian inner ear. *PLoS genetics*, 2(1), e4.
- Kim, M.-H., Kim, H.-B., Yoon, S. P., Lim, S.-C., Cha, M. J., Jeon, Y. J., Park, S. G., Chang, I.-Y., & You, H. J. (2013). Colon cancer progression is driven by APEX1-mediated upregulation of Jagged. *The Journal of clinical investigation*.
- Kokubo, H., Lun, Y., & Johnson, R. L. (1999). Identification and expression of a novel family of bHLH cDNAs related to *Drosophila* hairy and enhancer of split. *Biochemical and biophysical research communications*, 260(2), 459–465.
- Kong, D., Banerjee, S., Ahmad, A., Li, Y., Wang, Z., Sethi, S., & Sarkar, F. H. (2010). Epithelial to mesenchymal transition is mechanistically linked with stem cell signatures in prostate

- cancer cells. *PLoS one*, 5(8), e12445.
- Kong, D., Li, Y., Wang, Z., & Sarkar, F. H. (2011). Cancer Stem Cells and Epithelial-to-Mesenchymal Transition (EMT)-Phenotypic Cells: Are They Cousins or Twins? *Cancers*, 3(1), 716–29.
- Korkaya, H., & Wicha, M. S. (2007). Selective targeting of cancer stem cells: a new concept in cancer therapeutics. *BioDrugs: clinical immunotherapeutics, biopharmaceuticals and gene therapy*, 21(5), 299–310.
- Koyano-Nakagawa, N., Kim, J., Anderson, D., & Kintner, C. (2000). Hes6 acts in a positive feedback loop with the neurogenins to promote neuronal differentiation. *Development (Cambridge, England)*, 127(19), 4203–16.
- Krebs, L. T., Deftos, M. L., Bevan, M. J., & Gridley, T. (2001). The Nrarp gene encodes an ankyrin-repeat protein that is transcriptionally regulated by the notch signaling pathway. *Developmental biology*, 238(1), 110–119.
- Krebs, L. T., Shutter, J. R., Tanigaki, K., Honjo, T., Stark, K. L., & Gridley, T. (2004). Haploinsufficient lethality and formation of arteriovenous malformations in Notch pathway mutants. *Genes & development*, 18(20), 2469–2473.
- Krebs, L. T., Xue, Y., Norton, C. R., Shutter, J. R., Maguire, M., Sundberg, J. P., Gallahan, D., Closson, V., Kitajewski, J., Callahan, R., Smith, G. H., Stark, K. L., & Gridley, T. (2000). Notch signaling is essential for vascular morphogenesis in mice. *Genes & development*, 14(11), 1343–52.
- Krebs, L. T., Xue, Y., Norton, C. R., Sundberg, J. P., Beatus, P., Lendahl, U., Joutel, A., & Gridley, T. (2003). Characterization of Notch3-deficient mice: normal embryonic development and absence of genetic interactions with a Notch1 mutation. *Genesis (New York, N.Y. : 2000)*, 37(3), 139–43.
- Krop, I., Demuth, T., Guthrie, T., Wen, P. Y., Mason, W. P., Chinnaiyan, P., Butowski, N., Groves, M. D., Kesari, S., Freedman, S. J., Blackman, S., Watters, J., Loboda, A., Podtelezhnikov, A., Lunceford, J., Chen, C., Giannotti, M., Hing, J., Beckman, R., & Lorusso, P. (2012). Phase I pharmacologic and pharmacodynamic study of the gamma secretase (Notch) inhibitor MK-0752 in adult patients with advanced solid tumors. *Journal of clinical oncology: official journal of the American Society of Clinical Oncology*, 30(19), 2307–13.
- Kubo, H., Fujiwara, T., Jussila, L., Hashi, H., Ogawa, M., Shimizu, K., Awane, M., Sakai, Y., Takabayashi, A., Alitalo, K., Yamaoka, Y., & Nishikawa, S. I. (2000). Involvement of vascular endothelial growth factor receptor-3 in maintenance of integrity of endothelial cell lining during tumor angiogenesis. *Blood*, 96(2), 546–53. American Society of Hematology.
- Kurita, T., Medina, R. T., Mills, A. A., & Cunha, G. R. (2004). Role of p63 and basal cells in the prostate. *Development (Cambridge, England)*, 131(20), 4955–64.
- Kwon, O.-J., Valdez, J. M., Zhang, L., Zhang, B., Wei, X., Su, Q., Ittmann, M. M., Creighton, C. J., & Xin, L. (2014). Increased Notch signalling inhibits anoikis and stimulates proliferation of prostate luminal epithelial cells. *Nature communications*, 5, 4416. Nature Publishing Group.
- Ladi, E., Nichols, J. T., Ge, W., Miyamoto, A., Yao, C., Yang, L.-T., Boulter, J., Sun, Y. E., Kintner, C., & Weinmaster, G. (2005). The divergent DSL ligand Dll3 does not activate Notch signaling but cell autonomously attenuates signaling induced by other DSL ligands. *The Journal of cell biology*, 170(6), 983–92.
- Lamar, E., Deblandre, G., Wettstein, D., Gawantka, V., Pollet, N., Niehrs, C., & Kintner, C. (2001). Nrarp is a novel intracellular component of the Notch signaling pathway. *Genes and Development*, 15(15), 1885–1899.
- Lamouille, S., Xu, J., & Derynck, R. (2014). Molecular mechanisms of epithelial-mesenchymal transition. *Nature reviews. Molecular cell biology*, 15(3), 178–96.

- Lardelli, M., Dahlstrand, J., & Lendahl, U. (1994). The novel Notch homologue mouse Notch 3 lacks specific epidermal growth factor-repeats and is expressed in proliferating neuroepithelium. *Mechanisms of development*, 46(2), 123–36.
- Lawson, D. A., & Witte, O. N. (2007). Stem cells in prostate cancer initiation and progression. *The Journal of clinical investigation*, 117(8), 2044–50.
- Lawson, D. A., Xin, L., Lukacs, R. U., Cheng, D., & Witte, O. N. (2007). Isolation and functional characterization of murine prostate stem cells. *Proceedings of the National Academy of Sciences of the United States of America*, 104(1), 181–6.
- Lee, J., Gray, A., Yuan, J., Luoh, S. M., Avraham, H., & Wood, W. I. (1996). Vascular endothelial growth factor-related protein: a ligand and specific activator of the tyrosine kinase receptor Flt4. *Proceedings of the National Academy of Sciences of the United States of America*, 93(5), 1988–1992.
- Leimeister, C., Externbrink, a, Klamt, B., & Gessler, M. (1999). Hey genes: a novel subfamily of hairy- and Enhancer of split related genes specifically expressed during mouse embryogenesis. *Mechanisms of development*, 85(1-2), 173–7.
- Leimeister, C., Schumacher, N., Steidl, C., & Gessler, M. (2000). Analysis of HeyL expression in wild-type and Notch pathway mutant mouse embryos. *Mechanisms of development*, 98(1-2), 175–8.
- Leong, K. G., & Gao, W.-Q. (2008). The Notch pathway in prostate development and cancer. *Differentiation; research in biological diversity*, 76(6), 699–716.
- Leong, K. G., Niessen, K., Kulic, I., Raouf, A., Eaves, C., Pollet, I., & Karsan, A. (2007). Jagged1-mediated Notch activation induces epithelial-to-mesenchymal transition through Slug-induced repression of E-cadherin. *The Journal of experimental medicine*, 204(12), 2935–48.
- Leung, D. W., Cachianes, G., Kuang, W. J., Goeddel, D. V., & Ferrara, N. (1989). Vascular endothelial growth factor is a secreted angiogenic mitogen. *Science (New York, N.Y.)*, 246(4935), 1306–9.
- Li, D., Masiero, M., Banham, A. H., & Harris, A. L. (2014). The notch ligand JAGGED1 as a target for anti-tumor therapy. *Frontiers in oncology*, 4(September), 1–13.
- Li, L., Huang, G. M., Banta, A. B., Deng, Y., Smith, T., Dong, P., Friedman, C., Chen, L., Trask, B. J., Spies, T., Rowen, L., & Hood, L. (1998). Cloning, characterization, and the complete 56.8-kilobase DNA sequence of the human NOTCH4 gene. *Genomics*, 51(1), 45–58.
- Li, L., Miano, J. M., Cserjesi, P., & Olson, E. N. (1996). SM22 alpha, a marker of adult smooth muscle, is expressed in multiple myogenic lineages during embryogenesis. *Circulation research*, 78(2), 188–195.
- Limbourg, A., Ploom, M., Elligsen, D., Sørensen, I., Ziegelhoeffer, T., Gossler, A., Drexler, H., & Limbourg, F. P. (2007). Notch ligand Delta-like 1 is essential for postnatal arteriogenesis. *Circulation research*, 100(3), 363–71.
- Lin, J.-T., Chen, M.-K., Yeh, K.-T., Chang, C.-S., Chang, T.-H., Lin, C.-Y., Wu, Y.-C., Su, B.-W., Lee, K.-D., & Chang, P.-J. (2010). Association of high levels of Jagged-1 and Notch-1 expression with poor prognosis in head and neck cancer. *Annals of surgical oncology*, 17(11), 2976–83.
- Lindhahl, P. (1997). Pericyte Loss and Microaneurysm Formation in PDGF-B-Deficient Mice. *Science*, 277(5323), 242–245.
- Liu, H., Kennard, S., & Lilly, B. (2009). NOTCH3 expression is induced in mural cells through an autoregulatory loop that requires endothelial-expressed JAGGED1. *Circulation research*, 104(4), 466–475.
- Liu, Z., Shirakawa, T., Li, Y., Soma, A., Oka, M., Dotto, G. P., Fairman, R. M., Velazquez, O. C., & Herlyn, M. (2003). Regulation of Notch1 and Dll4 by Vascular Endothelial Growth Factor in Arterial Endothelial Cells: Implications for Modulating Arteriogenesis and

- Angiogenesis, 23(1), 14–25.
- Lobov, I. B., Renard, R. A., Papadopoulos, N., Gale, N. W., Thurston, G., Yancopoulos, G. D., & Wiegand, S. J. (2007). Delta-like ligand 4 (Dll4) is induced by VEGF as a negative regulator of angiogenic sprouting. *Proceedings of the National Academy of Sciences of the United States of America*, 104(9), 3219–3224.
- Logeat, F., Bessia, C., Brou, C., LeBail, O., Jarriault, S., Seidah, N. G., & Israël, a. (1998). The Notch1 receptor is cleaved constitutively by a furin-like convertase. *Proceedings of the National Academy of Sciences of the United States of America*, 95(14), 8108–12.
- Long, R. M., Morrissey, C., Fitzpatrick, J. M., & Watson, R. W. G. (2005). Prostate epithelial cell differentiation and its relevance to the understanding of prostate cancer therapies. *Clinical science (London, England : 1979)*, 108(1), 1–11.
- Louis, A. A., Van Eyken, P., Haber, B. A., Hicks, C., Weinmaster, G., Taub, R., & Rand, E. B. (1999). Hepatic Jagged1 expression studies. *Hepatology*, 30(5), 1269–1275.
- Lu, J., Ye, X., Fan, F., Xia, L., Bhattacharya, R., Bellister, S., Tozzi, F., Sceusi, E., Zhou, Y., Tachibana, I., Maru, D. M., Hawke, D. H., Rak, J., Mani, S. a, Zweidler-McKay, P., & Ellis, L. M. (2013). Endothelial Cells Promote the Colorectal Cancer Stem Cell Phenotype through a Soluble Form of Jagged-1. *Cancer cell*, 23(2), 171–85. Elsevier Inc.
- Ludlow, J. W. (1993). Interactions between SV40 large-tumor antigen and the growth suppressor proteins pRB and p53. *FASEB journal : official publication of the Federation of American Societies for Experimental Biology*, 7(10), 866–871.
- Maisonpierre, P. C., Suri, C., Jones, P. F., Bartunkova, S., Wiegand, S. J., Radziejewski, C., Compton, D., McClain, J., Aldrich, T. H., Papadopoulos, N., Daly, T. J., Davis, S., Sato, T. N., & Yancopoulos, G. D. (1997). Angiopoietin-2, a natural antagonist for Tie2 that disrupts in vivo angiogenesis. *Science*, 277(5322), 55–60.
- Manderfield, L. J., High, F. A., Engleka, K. A., Liu, F., Li, L., Rentschler, S., & Epstein, J. A. (2012). Notch activation of Jagged1 contributes to the assembly of the arterial wall. *Circulation*, 125(2), 314–323.
- Marignol, L., Rivera-Figueroa, K., Lynch, T., & Hollywood, D. (2013). Hypoxia, notch signalling, and prostate cancer. *Nature reviews. Urology*, 10(7), 405–13. Nature Publishing Group.
- Martin, D. B. (2004). Quantitative Proteomic Analysis of Proteins Released by Neoplastic Prostate Epithelium. *Cancer Research*, 64(1), 347–355.
- McCright, B., Gao, X., Shen, L., Lozier, J., Lan, Y., Maguire, M., Herzlinger, D., Weinmaster, G., Jiang, R., & Gridley, T. (2001). Defects in development of the kidney, heart and eye vasculature in mice homozygous for a hypomorphic Notch2 mutation. *Development (Cambridge, England)*, 128(4), 491–502.
- McNeal, J. E. (1969). Origin and development of carcinoma in the prostate. *Cancer*, 23(1), 24–34. Wiley Subscription Services, Inc., A Wiley Company.
- Meadows, K. L., & Hurwitz, H. I. (2012). Anti-VEGF therapies in the clinic. *Cold Spring Harbor perspectives in medicine*, 2(10).
- Medema, J. P. (2013). Cancer stem cells: the challenges ahead. *Nature cell biology*, 15(4), 338–44. Nature Publishing Group.
- Moellering, R. E., Cornejo, M., Davis, T. N., Del Bianco, C., Aster, J. C., Blacklow, S. C., Kung, A. L., Gilliland, D. G., Verdine, G. L., & Bradner, J. E. (2009). Direct inhibition of the NOTCH transcription factor complex. *Nature*, 462(7270), 182–8. Macmillan Publishers Limited. All rights reserved.
- Monvoisin, A., Alva, J. A., Hofmann, J. J., Zovein, A. C., Lane, T. F., & Iruela-Arispe, M. L. (2006). VE-cadherin-CreERT2 transgenic mouse: a model for inducible recombination in the endothelium. *Developmental dynamics : an official publication of the American Association of Anatomists*, 235(12), 3413–3422.
- Morgan, T. H. (1917). The Theory of the Gene. *Am Nat*, (51), 513–544.

- Moses, M. A. (1997). The regulation of neovascularization of matrix metalloproteinases and their inhibitors. *Stem cells*, 15(3), 180–189.
- Mulholland, D. J., Xin, L., Morim, A., Lawson, D., Witte, O., & Wu, H. (2009). Lin-Sca-1+CD49^{high} stem/progenitors are tumor-initiating cells in the Pten-null prostate cancer model. *Cancer research*, 69(22), 8555–62.
- Murre, C., Bain, G., van Dijk, M. A., Engel, I., Furnari, B. A., Massari, M. E., Matthews, J. R., Quong, M. W., Rivera, R. R., & Stuiver, M. H. (1994). Structure and function of helix-loop-helix proteins. *Biochimica et Biophysica Acta (BBA) - Gene Structure and Expression*, 1218(2), 129–135.
- Murta, D., Batista, M., Silva, E., Trindade, A., Henrique, D., Duarte, A., & Lopes-da-Costa, L. (2013). Dynamics of Notch pathway expression during mouse testis post-natal development and along the spermatogenic cycle. *PLoS one*, 8(8), e72767.
- Murta, D., Batista, M., Silva, E., Trindade, A., Mateus, L., Duarte, A., & Lopes-da-Costa, L. (2014). Differential expression of Notch component and effector genes during ovarian follicle and corpus luteum development during the oestrous cycle. *Reproduction, fertility, and development*.
- Murta, D., Batista, M., Trindade, A., Silva, E., Henrique, D., Duarte, A., & Lopes-da-Costa, L. (2014). In vivo notch signaling blockade induces abnormal spermatogenesis in the mouse. *PLoS one*, 9(11), e113365.
- Murta, D., Batista, M., Trindade, A., Silva, E., Mateus, L., Duarte, A., & Lopes-da-Costa, L. (2015). Dynamics of Notch signalling in the mouse oviduct and uterus during the oestrous cycle. *Reproduction, fertility, and development*. CSIRO PUBLISHING.
- Nakagawa, O., Nakagawa, M., Richardson, J. a, Olson, E. N., & Srivastava, D. (1999). HRT1, HRT2, and HRT3: a new subclass of bHLH transcription factors marking specific cardiac, somitic, and pharyngeal arch segments. *Developmental biology*, 216(1), 72–84.
- Nam, Y., Sliz, P., Song, L., Aster, J. C., & Blacklow, S. C. (2006). Structural basis for cooperativity in recruitment of MAML coactivators to Notch transcription complexes. *Cell*, 124(5), 973–83.
- Neufeld, G., Cohen, T., Gengrinovitch, S., & Poltorak, Z. (1999). Vascular endothelial growth factor (VEGF) and its receptors. *The FASEB journal : official publication of the Federation of American Societies for Experimental Biology*, 13(1), 9–22.
- Neufeld, G., Kessler, O., & Herzog, Y. (2002). The interaction of Neuropilin-1 and Neuropilin-2 with tyrosine-kinase receptors for VEGF. *Advances in experimental medicine and biology*, 515, 81–90.
- Niessen, K., Fu, Y., Chang, L., Hoodless, P. A., McFadden, D., & Karsan, A. (2008). Slug is a direct Notch target required for initiation of cardiac cushion cellularization. *The Journal of cell biology*, 182(2), 315–25.
- Niimi, H., Pardali, K., Vanlandewijck, M., Heldin, C.-H., & Moustakas, A. (2007). Notch signaling is necessary for epithelial growth arrest by TGF-beta. *The Journal of cell biology*, 176(5), 695–707.
- Noguera-Troise, I., Daly, C., Papadopoulos, N. J., Coetzee, S., Boland, P., Gale, N. W., Lin, H. C., Yancopoulos, G. D., & Thurston, G. (2006). Blockade of Dll4 inhibits tumour growth by promoting non-productive angiogenesis. *Nature*, 444(7122), 1032–1037.
- Ntziachristos, P., Lim, J. S., Sage, J., & Aifantis, I. (2014). From Fly Wings to Targeted Cancer Therapies: A Centennial for Notch Signaling. *Cancer Cell*, 25(3), 318–334. Elsevier Inc.
- Nyfeler, Y., Kirch, R. D., Mantei, N., Leone, D. P., Radtke, F., Suter, U., & Taylor, V. (2005). Jagged1 signals in the postnatal subventricular zone are required for neural stem cell self-renewal. *The EMBO journal*, 24(19), 3504–3515.
- Oktem, G., Bilir, A., Uslu, R., Inan, S. V., Demiray, S. B., Atmaca, H., Ayla, S., Sercan, O., & Uysal, A. (2014). Expression profiling of stem cell signaling alters with spheroid formation

- in CD133high/CD44high prostate cancer stem cells. *Oncology Letters*, 7(6), 2103–2109. Spandidos Publications.
- Osborne, B. A., & Minter, L. M. (2007). Notch signalling during peripheral T-cell activation and differentiation. *Nature reviews. Immunology*, 7(1), 64–75.
- Outtz, H. H., Wu, J. K., Wang, X., & Kitajewski, J. (2010). Notch1 deficiency results in decreased inflammation during wound healing and regulates vascular endothelial growth factor receptor-1 and inflammatory cytokine expression in macrophages. *Journal of immunology (Baltimore, Md. : 1950)*, 185(7), 4363–73.
- Pang, R. T. K., Leung, C. O. N., Ye, T.-M., Liu, W., Chiu, P. C. N., Lam, K. K. W., Lee, K.-F., & Yeung, W. S. B. (2010). MicroRNA-34a suppresses invasion through downregulation of Notch1 and Jagged1 in cervical carcinoma and choriocarcinoma cells. *Carcinogenesis*, 31(6), 1037–44.
- Pannequin, J., Bonnans, C., Delaunay, N., Ryan, J., Bourgaux, J.-F., Joubert, D., & Hollande, F. (2009). The wnt target jagged-1 mediates the activation of notch signaling by progastrin in human colorectal cancer cells. *Cancer research*, 69(15), 6065–73.
- Papetti, M., & Herman, I. M. (2002). Mechanisms of normal and tumor-derived angiogenesis. *American journal of physiology. Cell physiology*, 282(5), C947–70.
- Park, J. E., Keller, G. A., & Ferrara, N. (1993). The vascular endothelial growth factor (VEGF) isoforms: differential deposition into the subepithelial extracellular matrix and bioactivity of extracellular matrix-bound VEGF. *Molecular biology of the cell*, 4(12), 1317–26.
- Park, J. T., Li, M., Nakayama, K., Mao, T.-L., Davidson, B., Zhang, Z., Kurman, R. J., Eberhart, C. G., Shih, I.-M., & Wang, T.-L. (2006). Notch3 gene amplification in ovarian cancer. *Cancer research*, 66(12), 6312–8.
- Partanen, T. a, Arola, J., Saaristo, a, Jussila, L., Ora, a, Miettinen, M., Stacker, S. a, Achen, M. G., & Alitalo, K. (2000). VEGF-C and VEGF-D expression in neuroendocrine cells and their receptor, VEGFR-3, in fenestrated blood vessels in human tissues. *The FASEB journal: official publication of the Federation of American Societies for Experimental Biology*, 14(13), 2087–2096.
- Patrawala, L., Calhoun, T., Schneider-Broussard, R., Zhou, J., Claypool, K., & Tang, D. G. (2005). Side population is enriched in tumorigenic, stem-like cancer cells, whereas ABCG2+ and ABCG2- cancer cells are similarly tumorigenic. *Cancer research*, 65(14), 6207–19.
- Pear, W. S., & Simon, M. C. (2005). Lasting longer without oxygen: The influence of hypoxia on Notch signaling. *Cancer cell*, 8(6), 435–7. Elsevier.
- Pedrosa, A.-R., Graça, J. L., Carvalho, S., Peleteiro, M. C., Duarte, A., & Trindade, A. (2016). Notch signaling dynamics in the adult healthy prostate and in prostatic tumor development. *The Prostate*, 76(1), 80–96.
- Pedrosa, A.-R., Trindade, A., Carvalho, C., Graça, J., Carvalho, S., Peleteiro, M. C., Adams, R. H., & Duarte, A. (2015b). Endothelial Jagged1 promotes solid tumor growth through both pro-angiogenic and angiocrine functions. *Oncotarget*.
- Pedrosa, A.-R., Trindade, A., Fernandes, A.-C., Carvalho, C., Gigante, J., Tavares, A. T., Dieguez-Hurtado, R., Yagita, H., Adams, R. H., & Duarte, A. (2015a). Endothelial Jagged1 Antagonizes Dll4 Regulation of Endothelial Branching and Promotes Vascular Maturation Downstream of Dll4/Notch1. *Arteriosclerosis, Thrombosis, and Vascular Biology*, 35(5), 1134–1146.
- Pissarra, L., Henrique, D., & Duarte, a. (2000). Expression of hes6, a new member of the Hairy/Enhancer-of-split family, in mouse development. *Mechanisms of development*, 95(1-2), 275–8.
- Poltorak, Z., Cohen, T., Sivan, R., Kandelis, Y., Spira, G., Vlodavsky, I., Keshet, E., & Neufeld, G. (1997). VEGF145, a Secreted Vascular Endothelial Growth Factor Isoform That Binds to Extracellular Matrix. *Journal of Biological Chemistry*, 272(11), 7151–7158.

- Previs, R. A., Coleman, R. L., Harris, A. L., & Sood, A. K. (2015). Molecular pathways: translational and therapeutic implications of the notch signaling pathway in cancer. *Clinical cancer research: an official journal of the American Association for Cancer Research*, 21(5), 955–61.
- Purow, B. (2012). Notch inhibition as a promising new approach to cancer therapy. *Advances in experimental medicine and biology*, 727, 305–19.
- Purow, B. W., Haque, R. M., Noel, M. W., Su, Q., Burdick, M. J., Lee, J., Sundaresan, T., Pastorino, S., Park, J. K., Mikolaenko, I., Maric, D., Eberhart, C. G., & Fine, H. A. (2005). Expression of Notch-1 and its ligands, Delta-like-1 and Jagged-1, is critical for glioma cell survival and proliferation. *Cancer research*, 65(6), 2353–63.
- Ramsauer, M., & D'Amore, P. A. (2002). Getting Tie(2)d up in angiogenesis. *Journal of Clinical Investigation*, 110(11), 1615–1617. American Society for Clinical Investigation.
- Rana, N. A., & Haltiwanger, R. S. (2011). Fringe benefits: functional and structural impacts of O-glycosylation on the extracellular domain of Notch receptors. *Current opinion in structural biology*, 21(5), 583–9.
- Raza, A., Franklin, M. J., & Dudek, A. Z. (2010). Pericytes and vessel maturation during tumor angiogenesis and metastasis. *American journal of hematology*, 85(8), 593–8.
- Reedijk, M., Odorcic, S., Chang, L., Zhang, H., Miller, N., McCready, D. R., Lockwood, G., & Egan, S. E. (2005). High-level coexpression of JAG1 and NOTCH1 is observed in human breast cancer and is associated with poor overall survival. *Cancer research*, 65(18), 8530–7.
- Reedijk, M., Pinnaduwege, D., Dickson, B. C., Mulligan, A. M., Zhang, H., Bull, S. B., O'Malley, F. P., Egan, S. E., & Andrulis, I. L. (2008). JAG1 expression is associated with a basal phenotype and recurrence in lymph node-negative breast cancer. *Breast cancer research and treatment*, 111(3), 439–48.
- Ribatti, D., Vacca, A., Nico, B., Roncali, L., & Dammacco, F. (2001). Postnatal vasculogenesis. *Mechanisms of Development*, 100(2), 157–163.
- Ridgway, J., Zhang, G., Wu, Y., Stawicki, S., Liang, W. C., Chanthery, Y., Kowalski, J., Watts, R. J., Callahan, C., Kasman, I., Singh, M., Chien, M., Tan, C., Hongo, J. A., de Sauvage, F., Plowman, G., & Yan, M. (2006). Inhibition of Dll4 signalling inhibits tumour growth by deregulating angiogenesis. *Nature*, 444(7122), 1083–1087.
- Risau, W. (1997). Mechanisms of angiogenesis. *Nature*, 386(6626), 671–674.
- Risbridger, G. P., Davis, I. D., Birrell, S. N., & Tilley, W. D. (2010). Breast and prostate cancer: more similar than different. *Nature reviews. Cancer*, 10(3), 205–12. Nature Publishing Group.
- Rizzo, P., Miao, H., D'Souza, G., Osipo, C., Song, L. L., Yun, J., Zhao, H., Mascarenhas, J., Wyatt, D., Antico, G., Hao, L., Yao, K., Rajan, P., Hicks, C., Siziopikou, K., Selvaggi, S., Bashir, A., Bhandari, D., Marchese, A., Lendahl, U., Qin, J.-Z., Tonetti, D. a, Albain, K., Nickoloff, B. J., & Miele, L. (2008). Cross-talk between notch and the estrogen receptor in breast cancer suggests novel therapeutic approaches. *Cancer research*, 68(13), 5226–35.
- Robinson, D. R., Kalyana-Sundaram, S., Wu, Y.-M., Shankar, S., Cao, X., Ateeq, B., Asangani, I. A., Iyer, M., Maher, C. A., Grasso, C. S., Lonigro, R. J., Quist, M., Siddiqui, J., Mehra, R., Jing, X., Giordano, T. J., Sabel, M. S., Kleer, C. G., Palanisamy, N., Natrajan, R., Lambros, M. B., Reis-Filho, J. S., Kumar-Sinha, C., & Chinnaiyan, A. M. (2011). Functionally recurrent rearrangements of the MAST kinase and Notch gene families in breast cancer. *Nature medicine*, 17(12), 1646–51.
- Roca, C., & Adams, R. H. (2007). Regulation of vascular morphogenesis by Notch signaling. *Genes & development*, 21(20), 2511–24.
- Rodilla, V., Villanueva, A., Obrador-Hevia, A., Robert-Moreno, A., Fernández-Majada, V., Grilli, A., López-Bigas, N., Bellora, N., Albà, M. M., Torres, F., Duñach, M., Sanjuan, X.,

- Gonzalez, S., Gridley, T., Capella, G., Bigas, A., & Espinosa, L. (2009). Jagged1 is the pathological link between Wnt and Notch pathways in colorectal cancer. *Proceedings of the National Academy of Sciences of the United States of America*, 106(15), 6315–20.
- Ross, A. E., Marchionni, L., Vuica-Ross, M., Cheadle, C., Fan, J., Berman, D. M., & Schaeffer, E. M. (2011). Gene expression pathways of high grade localized prostate cancer. *The Prostate*, 71(14), 1568–77.
- Rossant, J., & Howard, L. (2002). Signaling pathways in vascular development. *Annual review of cell and developmental biology*, 18, 541–573.
- Sahlgren, C., Gustafsson, M. V., Jin, S., Poellinger, L., & Lendahl, U. (2008). Notch signaling mediates hypoxia-induced tumor cell migration and invasion. *Proceedings of the National Academy of Sciences*, 105(17), 6392–6397.
- Sainson, R. C. a, Aoto, J., Nakatsu, M. N., Holderfield, M., Conn, E., Koller, E., & Hughes, C. C. W. (2005). Cell-autonomous notch signaling regulates endothelial cell branching and proliferation during vascular tubulogenesis. *FASEB journal: official publication of the Federation of American Societies for Experimental Biology*, 19(8), 1027–9.
- Sainson, R. C. A., & Harris, A. L. (2007). Anti-Dll4 therapy: can we block tumour growth by increasing angiogenesis? *Trends in molecular medicine*, 13(9), 389–95. Elsevier.
- Sansone, P., Storci, G., Giovannini, C., Pandolfi, S., Pianetti, S., Taffurelli, M., Santini, D., Ceccarelli, C., Chieco, P., & Bonafé, M. (2007). p66Shc/Notch-3 interplay controls self-renewal and hypoxia survival in human stem/progenitor cells of the mammary gland expanded in vitro as mammospheres. *Stem cells (Dayton, Ohio)*, 25(3), 807–15.
- Sansone, P., Storci, G., Tavolari, S., Guarnieri, T., Giovannini, C., Taffurelli, M., Ceccarelli, C., Santini, D., Paterini, P., Marcu, K. B., Chieco, P., & Bonafè, M. (2007). IL-6 triggers malignant features in mammospheres from human ductal breast carcinoma and normal mammary gland. *The Journal of clinical investigation*, 117(12), 3988–4002.
- Santagata, S., Demichelis, F., Riva, A., Varambally, S., Hofer, M. D., Kutok, J. L., Kim, R., Tang, J., Montie, J. E., Chinnaiyan, A. M., Rubin, M. A., & Aster, J. C. (2004). JAGGED1 expression is associated with prostate cancer metastasis and recurrence. *Cancer research*, 64(19), 6854–7.
- Sasai, Y., Kageyama, R., Tagawa, Y., Shigemoto, R., & Nakanishi, S. (1992). Two mammalian helix-loop-helix factors structurally related to Drosophila hairy and Enhancer of split. *Genes and Development*, 6(12 PART B), 2620–2634.
- Sato, T. N., Tozawa, Y., Deutsch, U., Wolburg-Buchholz, K., Fujiwara, Y., Gendron-Maguire, M., Gridley, T., Wolburg, H., Risau, W., & Qin, Y. (1995). Distinct roles of the receptor tyrosine kinases Tie-1 and Tie-2 in blood vessel formation. *Nature*, 376(6535), 70–4.
- Scehnet, J. S., Jiang, W., Kumar, S. R., Krasnoperov, V., Trindade, A., Benedito, R., Djokovic, D., Borges, C., Ley, E. J., Duarte, A., & Gill, P. S. (2007). Inhibition of Dll4-mediated signaling induces proliferation of immature vessels and results in poor tissue perfusion. *Blood*, 109(11), 4753–60.
- Scheppeke, L., Murphy, E. a, Zarpellon, A., Hofmann, J. J., Merkulova, A., Shields, D. J., Weis, S. M., Byzova, T. V, Ruggeri, Z. M., Iruela-Arispe, M. L., & Cheresh, D. a. (2012). Notch promotes vascular maturation by inducing integrin-mediated smooth muscle cell adhesion to the endothelial basement membrane. *Blood*, 119(9), 2149–58.
- Schweisguth, F. (2004). Regulation of Notch Signaling Activity. *Current Biology*, 14(3), R129–R138.
- Scorey, N., Fraser, S. P., Patel, P., Pridgeon, C., Dallman, M. J., & Djamgoz, M. B. A. (2006). Notch signalling and voltage-gated Na⁺ channel activity in human prostate cancer cells: independent modulation of in vitro motility. *Prostate Cancer and Prostatic Diseases*, 9(4), 399–406.
- Sekine, C., Koyanagi, A., Koyama, N., Hozumi, K., Chiba, S., & Yagita, H. (2012). Differential regulation of osteoclastogenesis by Notch2/Delta-like 1 and Notch1/Jagged1 axes.

- Arthritis research & therapy*, 14(2), R45.
- Senger, D. R., Galli, S. J., Dvorak, A. M., Perruzzi, C. A., Harvey, V. S., & Dvorak, H. F. (1983). Tumor cells secrete a vascular permeability factor that promotes accumulation of ascites fluid. *Science (New York, N.Y.)*, 219(4587), 983–985.
- Sethi, N., Dai, X., Winter, C. G., & Kang, Y. (2011). Tumor-Derived Jagged1 Promotes Osteolytic Bone Metastasis of Breast Cancer by Engaging Notch Signaling in Bone Cells. *Cancer Cell*, 19(2), 192–205.
- Sethi, S., Macoska, J., Chen, W., & Sarkar, F. H. (2010). Molecular signature of epithelial-mesenchymal transition (EMT) in human prostate cancer bone metastasis. *American journal of translational research*, 3(1), 90–9.
- Shahi, P., Seethammagari, M. R., Valdez, J. M., Xin, L., & Spencer, D. M. (2011). Wnt and Notch pathways have interrelated opposing roles on prostate progenitor cell proliferation and differentiation. *Stem cells (Dayton, Ohio)*, 29(4), 678–88.
- Shalaby, F., Rossant, J., Yamaguchi, T. P., Gertsenstein, M., Wu, X. F., Breitman, M. L., & Schuh, a C. (1995). Failure of blood-island formation and vasculogenesis in Flk-1-deficient mice. *Nature*, 376(6535), 62–6.
- Shawber, C., Boulter, J., Lindsell, C. E., & Weinmaster, G. (1996). Jagged2: a serrate-like gene expressed during rat embryogenesis. *Developmental biology*, 180(1), 370–6.
- Sheldon, H., Heikamp, E., Turley, H., Dragovic, R., Thomas, P., Oon, C. E., Leek, R., Edelmann, M., Kessler, B., Sainson, R. C. a, Sargent, I., Li, J.-L., & Harris, A. L. (2010). New mechanism for Notch signaling to endothelium at a distance by Delta-like 4 incorporation into exosomes. *Blood*, 116(13), 2385–94.
- Shen, M. M., & Abate-Shen, C. (2010). Molecular genetics of prostate cancer: new prospects for old challenges. *Genes & Development*, 24(18), 1967–2000.
- Shibuya, M., Yamaguchi, S., Yamane, A., Ikeda, T., Tojo, A., Matsushime, H., & Sato, M. (1990). Nucleotide sequence and expression of a novel human receptor-type tyrosine kinase gene (flt) closely related to the fms family. *Oncogene*, 5(4), 519–524.
- Shimizu, M., Cohen, B., Goldvasser, P., Berman, H., Virtanen, C., & Reedijk, M. (2011). Plasminogen activator uPA is a direct transcriptional target of the JAG1-Notch receptor signaling pathway in breast cancer. *Cancer research*, 71(1), 277–86.
- Shirayoshi, Y., Yuasa, Y., Suzuki, T., Sugaya, K., Kawase, E., Ikemura, T., & Nakatsuji, N. (1997). Proto-oncogene of int-3, a mouse Notch homologue, is expressed in endothelial cells during early embryogenesis. *Genes to cells: devoted to molecular & cellular mechanisms*, 2(3), 213–224.
- Shou, J., Ross, S., Koeppen, H., de Sauvage, F. J., & Gao, W.-Q. (2001). Dynamics of Notch Expression during Murine Prostate Development and Tumorigenesis. *Cancer Res.*, 61(19), 7291–7297.
- Shutter, J. R., Scully, S., Fan, W., Richards, W. G., Kitajewski, J., Deblandre, G. A., Kintner, C. R., & Stark, K. L. (2000). Dll4, a novel Notch ligand expressed in arterial endothelium. *Genes & development*, 14(11), 1313–1318.
- Shweiki, D., Itin, A., Soffer, D., & Keshet, E. (1992). Vascular endothelial growth factor induced by hypoxia may mediate hypoxia-initiated angiogenesis. *Nature*, 359(6398), 843–845.
- Siekmann, A. F., & Lawson, N. D. (2007). Notch signalling limits angiogenic cell behaviour in developing zebrafish arteries. *Nature*, 445(7129), 781–784.
- Sikandar, S. S., Pate, K. T., Anderson, S., Dizon, D., Edwards, R. A., Waterman, M. L., & Lipkin, S. M. (2010). NOTCH signaling is required for formation and self-renewal of tumor-initiating cells and for repression of secretory cell differentiation in colon cancer. *Cancer research*, 70(4), 1469–78.
- Smith D, Eisenberg P, Stagg R, Manikhas G, Pavlovskiy A, Sikic B, Kapoun A, Benner S. A
Smith D, Eisenberg P, Stagg R, Manikhas G, Pavlovskiy A, Sikic B, Kapoun A, Benner S.

- A First-In-human, phase I trial of the anti-DLL4 antibody (OMP-21M18) targeting c, G. 2010. (2010). First-In-human, phase I trial of the anti-DLL4 antibody (OMP-21M18) targeting cancer stem cells in patients with advanced solid tumors. *22nd EORTC-NCI-AACR symposium on Molecular Targets and Cancer Therapeutics*. Berlin, Germany.
- Sörensen, I., Adams, R. H., & Gossler, A. (2009). *DLL1-mediated Notch activation regulates endothelial identity in mouse fetal arteries*. *Blood* (Vol. 113).
- South, A. P., Cho, R. J., & Aster, J. C. (2012). The double-edged sword of Notch signaling in cancer. *Seminars in cell & developmental biology*, 23(4), 458–64.
- Spinner, N. B., Colliton, R. P., Crosnier, C., Krantz, I. D., Hadchouel, M., & Meunier-Rotival, M. (2001). Jagged1 mutations in alagille syndrome. *Human mutation*, 17(1), 18–33.
- Stadelmann, W. K., Digenis, A. G., & Tobin, G. R. (1998). Physiology and healing dynamics of chronic cutaneous wounds. *The American Journal of Surgery*, 176(2), 26S–38S.
- Steg, A. D., Katre, A. A., Goodman, B., Han, H.-D., Nick, A. M., Stone, R. L., Coleman, R. L., Alvarez, R. D., Lopez-Berestein, G., Sood, A. K., & Landen, C. N. (2011). Targeting the notch ligand JAGGED1 in both tumor cells and stroma in ovarian cancer. *Clinical cancer research: an official journal of the American Association for Cancer Research*, 17(17), 5674–85.
- Steinle, J. J., Meininger, C. J., Forough, R., Wu, G., Wu, M. H., & Granger, H. J. (2002). Eph B4 receptor signaling mediates endothelial cell migration and proliferation via the phosphatidylinositol 3-kinase pathway. *The Journal of biological chemistry*, 277(46), 43830–5.
- Stoyanova, T., Cooper, A. R., Drake, J. M., Liu, X., Armstrong, A. J., Pienta, K. J., Zhang, H., Kohn, D. B., Huang, J., Witte, O. N., & Goldstein, A. S. (2013). Prostate cancer originating in basal cells progresses to adenocarcinoma propagated by luminal-like cells. *Proceedings of the National Academy of Sciences of the United States of America*, 110(50), 20111–6.
- De Strooper, B., Annaert, W., Cupers, P., Saftig, P., Craessaerts, K., Mumm, J. S., Schroeter, E. H., Schrijvers, V., Wolfe, M. S., Ray, W. J., Goate, A., & Kopan, R. (1999). A presenilin-1-dependent gamma-secretase-like protease mediates release of Notch intracellular domain. *Nature*, 398(6727), 518–22.
- Su, S. L., Huang, I. P., Fair, W. R., Powell, C. T., & Heston, W. D. (1995). Alternatively spliced variants of prostate-specific membrane antigen RNA: ratio of expression as a potential measurement of progression. *Cancer research*, 55(7), 1441–3.
- Suchting, S., Freitas, C., le Noble, F., Benedito, R., Breant, C., Duarte, A., & Eichmann, A. (2007). The Notch ligand Delta-like 4 negatively regulates endothelial tip cell formation and vessel branching. *Proceedings of the National Academy of Sciences of the United States of America*, 104(9), 3225–3230.
- Sun, H.-W., Wu, C., Tan, H.-Y., & Wang, Q.-S. (2012). Combination DLL4 with Jagged1-siRNA can enhance inhibition of the proliferation and invasiveness activity of human gastric carcinoma by Notch1/VEGF pathway. *Hepato-gastroenterology*, 59(115), 924–9.
- Sun, Y., Niu, J., & Huang, J. (2009). Neuroendocrine differentiation in prostate cancer. *American journal of translational research*, 1(2), 148–62.
- Suri, C., Jones, P. F., Patan, S., Bartunkova, S., Maisonpierre, P. C., Davis, S., Sato, T. N., & Yancopoulos, G. D. (1996). Requisite role of angiopoietin-1, a ligand for the TIE2 receptor, during embryonic angiogenesis. *Cell*, 87(7), 1171–80.
- Swiatek, P. J., Lindsell, C. E., del Amo, F. F., Weinmaster, G., & Gridley, T. (1994). Notch1 is essential for postimplantation development in mice. *Genes & development*, 8(6), 707–719.
- Takeshita, K., Satoh, M., Ii, M., Silver, M., Limbourg, F. P., Mukai, Y., Rikitake, Y., Radtke, F., Gridley, T., Losordo, D. W., & Liao, J. K. (2007). Critical role of endothelial Notch1 signaling in postnatal angiogenesis. *Circulation research*, 100(1), 70–8.


- Tammela, T., Zarkada, G., Wallgard, E., Murtomäki, A., Suchting, S., Wirzenius, M., Waltari, M., Hellström, M., Schomber, T., Peltonen, R., Freitas, C., Duarte, A., Isoniemi, H., Laakkonen, P., Christofori, G., Ylä-Herttuala, S., Shibuya, M., Pytowski, B., Eichmann, A., Betsholtz, C., & Alitalo, K. (2008). Blocking VEGFR-3 suppresses angiogenic sprouting and vascular network formation. *Nature*, *454*(7204), 656–60.
- Tang, Y., Urs, S., & Liaw, L. (2008). Hairy-related transcription factors inhibit Notch-induced smooth muscle alpha-actin expression by interfering with Notch intracellular domain/CBF-1 complex interaction with the CBF-1-binding site. *Circulation research*, *102*(6), 661–668.
- Taylor, R. a., Toivanen, R., & Risbridger, G. P. (2010). Stem cells in prostate cancer: Treating the root of the problem. *Endocrine-Related Cancer*, *17*(4).
- The Cancer Genome Atlas Research Network. (2011). Integrated genomic analyses of ovarian carcinoma. *Nature*, *474*(7353), 609–15. Nature Publishing Group, a division of Macmillan Publishers Limited. All Rights Reserved.
- Thiery, J. P. (2002). Epithelial-mesenchymal transitions in tumour progression. *Nature reviews. Cancer*, *2*(6), 442–54.
- Thomas, M., & Augustin, H. G. (2009). The role of the Angiopoietins in vascular morphogenesis. *Angiogenesis*, *12*(2), 125–137.
- Thurston, G., Noguera-Troise, I., & Yancopoulos, G. D. (2007). The Delta paradox: DLL4 blockade leads to more tumour vessels but less tumour growth. *Nature reviews. Cancer*, *7*(5), 327–31. Nature Publishing Group.
- Timmerman, L. A., Raya, A., Bertra, E., Di, J., Aranda, S., Palomo, S., McCormick, F., & Izpisua, J. C. (2004). Notch promotes epithelial-mesenchymal transition during cardiac development and oncogenic transformation, *5*, 1–17.
- Tischer, E., Mitchell, R., Hartman, T., Silva, M., Gospodarowicz, D., Fiddes, J. C., & Abraham, J. A. (1991). The human gene for vascular endothelial growth factor. Multiple protein forms are encoded through alternative exon splicing. *The Journal of biological chemistry*, *266*(18), 11947–54.
- Tolcher, A. W., Messersmith, W. A., Mikulski, S. M., Papadopoulos, K. P., Kwak, E. L., Gibbon, D. G., Patnaik, A., Falchook, G. S., Dasari, A., Shapiro, G. I., Boylan, J. F., Xu, Z.-X., Wang, K., Koehler, A., Song, J., Middleton, S. A., Deutsch, J., DeMario, M., Kurzrock, R., & Wheler, J. J. (2012). Phase I Study of RO4929097, a Gamma Secretase Inhibitor of Notch Signaling, in Patients With Refractory Metastatic or Locally Advanced Solid Tumors. *Journal of Clinical Oncology*, *30*(19), 2348–2353.
- Tomlins, S. A., Mehra, R., Rhodes, D. R., Cao, X., Wang, L., Dhanasekaran, S. M., Kalyana-Sundaram, S., Wei, J. T., Rubin, M. A., Pienta, K. J., Shah, R. B., & Chinnaiyan, A. M. (2007). Integrative molecular concept modeling of prostate cancer progression. *Nature genetics*, *39*(1), 41–51. Nature Publishing Group.
- Trindade, A., Djokovic, D., Gigante, J., Badenes, M., Pedrosa, A.-R. R., Fernandes, A.-C. C., Lopes-da-Costa, L., Krasnoperov, V., Liu, R., Gill, P. S., & Duarte, A. (2012). Low-dosage inhibition of Dll4 signaling promotes wound healing by inducing functional neo-angiogenesis. (T. Kume, Ed.) *PLoS ONE*, *7*(1), e29863.
- Trindade, A., Kumar, S. R., Scehnet, J. S., Lopes-da-Costa, L., Becker, J., Jiang, W., Liu, R., Gill, P. S., & Duarte, A. (2008). Overexpression of delta-like 4 induces arterialization and attenuates vessel formation in developing mouse embryos. *Blood*, *112*(5), 1720–1729.
- True, L., Coleman, I., Hawley, S., Huang, C.-Y., Gifford, D., Coleman, R., Beer, T. M., Gelmann, E., Datta, M., Mostaghel, E., Knudsen, B., Lange, P., Vessella, R., Lin, D., Hood, L., & Nelson, P. S. (2006). A molecular correlate to the Gleason grading system for prostate adenocarcinoma. *Proceedings of the National Academy of Sciences of the United States of America*, *103*(29), 10991–6.
- Tsai, S., Fero, J., & Bartelmez, S. (2000). Mouse Jagged2 is differentially expressed in hematopoietic progenitors and endothelial cells and promotes the survival and

- proliferation of hematopoietic progenitors by direct cell-to-cell contact. *Blood*, 96(3), 950–7. American Society of Hematology.
- Tschaharganeh, D. F., Chen, X., Latzko, P., Malz, M., Gaida, M. M., Felix, K., Ladu, S., Singer, S., Pinna, F., Gretz, N., Sticht, C., Tomasi, M. L., Delogu, S., Evert, M., Fan, B., Ribback, S., Jiang, L., Brozzetti, S., Bergmann, F., Dombrowski, F., Schirmacher, P., Calvisi, D. F., & Breuhahn, K. (2013). Yes-Associated Protein Up-regulates Jagged-1 and Activates the NOTCH Pathway in Human Hepatocellular Carcinoma. *Gastroenterology*, 144(7), 1530–1542.e12.
- Uyttendaele, H., Closson, V., Wu, G., Roux, F., Weinmaster, G., & Kitajewski, J. (2000). Notch4 and Jagged-1 induce microvessel differentiation of rat brain endothelial cells. *Microvascular research*, 60(2), 91–103.
- Uyttendaele, H., Marazzi, G., Wu, G., Yan, Q., Sassoon, D., & Kitajewski, J. (1996). Notch4/int-3, a mammary proto-oncogene, is an endothelial cell-specific mammalian Notch gene. *Development*, 122(7), 2251–2259.
- Valdez, J. M., Zhang, L., Su, Q., Dakhova, O., Zhang, Y., Shahi, P., Spencer, D. M., Creighton, C. J., Ittmann, M. M., & Xin, L. (2012). Notch and TGF β form a reciprocal positive regulatory loop that suppresses murine prostate basal stem/progenitor cell activity. *Cell stem cell*, 11(5), 676–88.
- Varadkar, P., Kraman, M., Despres, D., Ma, G., Lozier, J., & McCright, B. (2008). Notch2 is required for the proliferation of cardiac neural crest-derived smooth muscle cells. *Developmental Dynamics*, 237(4), 1144–1152.
- Vashchenko, N., & Abrahamsson, P.-A. (2014). Neuroendocrine differentiation in prostate cancer: implications for new treatment modalities. *European urology*, 47(2), 147–55.
- Veikkola, T., Karkkainen, M., Claesson-Welsh, L., & Alitalo, K. (2000). Regulation of angiogenesis via vascular endothelial growth factor receptors. *Cancer research*, 60(2), 203–212.
- Vikkula, M., Boon, L. M., Iii, K. L. C., Calvert, J. T., Diamonti, A. J., Goumnerov, B., Pasyk, K. A., Marchuk, D. A., Warman, M. L., Cantley, L. C., Mulliken, J. B., & Olsen, B. R. (1996). Vascular Dismorphogenesis Caused by an Activating Mutation in the Receptor Tyrosine Kinase TIE2. *Cell*, 87(7), 1181–1190. Elsevier.
- Villa, N., Walker, L., Lindsell, C. E., Gasson, J., Iruela-Arispe, M. L., & Weinmaster, G. (2001). Vascular expression of Notch pathway receptors and ligands is restricted to arterial vessels. *Mechanisms of development*, 108(1-2), 161–164.
- Waltenberger, J., Claesson-Welsh, L., Siegbahn, A., Shibuya, M., & Heldin, C. H. (1994). Different signal transduction properties of KDR and Flt1, two receptors for vascular endothelial growth factor. *The Journal of biological chemistry*, 269(43), 26988–26995.
- Wang, Q., Zhao, N., Kennard, S., & Lilly, B. (2012). Notch2 and Notch3 function together to regulate vascular smooth muscle development. *PloS one*, 7(5), e37365.
- Wang, R., Chadalavada, K., Wilshire, J., Kowalik, U., Hovinga, K. E., Geber, A., Fligelman, B., Leversha, M., Brennan, C., & Tabar, V. (2010). Glioblastoma stem-like cells give rise to tumour endothelium. *Nature*, 468(7325), 829–33.
- Wang, X.-D., Leow, C. C., Zha, J., Tang, Z., Modrusan, Z., Radtke, F., Aguet, M., de Sauvage, F. J., & Gao, W.-Q. (2006). Notch signaling is required for normal prostatic epithelial cell proliferation and differentiation. *Developmental biology*, 290(1), 66–80.
- Wang, Y., Hayward, S., Cao, M., Thayer, K., & Cunha, G. (2001). Cell differentiation lineage in the prostate. *Differentiation; research in biological diversity*, 68(4-5), 270–9.
- Wang, Z., Li, Y., Banerjee, S., Kong, D., Ahmad, A., Nogueira, V., Hay, N., & Sarkar, F. H. (2010). Down-regulation of Notch-1 and Jagged-1 inhibits prostate cancer cell growth, migration and invasion, and induces apoptosis via inactivation of Akt, mTOR, and NF-kappaB signaling pathways. *Journal of cellular biochemistry*, 109(4), 726–36.


- Wang, Z., Li, Y., Banerjee, S., & Sarkar, F. H. (2009). Emerging role of Notch in stem cells and cancer. *Cancer letters*, 279(1), 8–12.
- Wang, Z., Li, Y., Kong, D., Banerjee, S., Ahmad, A., Azmi, A. S., Ali, S., Abbruzzese, J. L., Gallick, G. E., & Sarkar, F. H. (2009). Acquisition of epithelial-mesenchymal transition phenotype of gemcitabine-resistant pancreatic cancer cells is linked with activation of the notch signaling pathway. *Cancer research*, 69(6), 2400–7.
- Ward, N. L., & Dumont, D. J. (2002). The angiopoietins and Tie2/Tek: adding to the complexity of cardiovascular development. *Seminars in cell & developmental biology*, 13(1), 19–27.
- Weidner, N., Carroll, P. R., Flax, J., Blumenfeld, W., & Folkman, J. (1993). Tumor angiogenesis correlates with metastasis in invasive prostate carcinoma. *The American journal of pathology*, 143(2), 401–9.
- Weinmaster, G., Roberts, V. J., & Lemke, G. (1992). Notch2: a second mammalian Notch gene. *Development (Cambridge, England)*, 116(4), 931–41.
- Weng, A. P., Ferrando, A. A., Lee, W., Morris, J. P., Silverman, L. B., Sanchez-Irizarry, C., Blacklow, S. C., Look, A. T., & Aster, J. C. (2004). Activating mutations of NOTCH1 in human T cell acute lymphoblastic leukemia. *Science (New York, N.Y.)*, 306(5694), 269–71.
- Westermarck, B., & Heldin, C.-H. (2009). Platelet-Derived Growth Factor Structure, function and implications in normal and malignant cell growth. Informa UK Ltd UK.
- Wharton, K. A., Johansen, K. M., Xu, T., & Artavanis-Tsakonas, S. (1985). Nucleotide sequence from the neurogenic locus notch implies a gene product that shares homology with proteins containing EGF-like repeats. *Cell*, 43(3 Pt 2), 567–81.
- Whelan, J. T., Kellogg, A., Shewchuk, B. M., Hewan-Lowe, K., & Bertrand, F. E. (2009). Notch-1 signaling is lost in prostate adenocarcinoma and promotes PTEN gene expression. *Journal of cellular biochemistry*, 107(5), 992–1001.
- Williams, C. K., Li, J.-L. L., Murga, M., Harris, A. L., & Tosato, G. (2006). Up-regulation of the Notch ligand Delta-like 4 inhibits VEGF-induced endothelial cell function. *Blood*, 107(3), 931–939.
- Wilson, J. J., & Kovall, R. a. (2006). Crystal structure of the CSL-Notch-Mastermind ternary complex bound to DNA. *Cell*, 124(5), 985–96.
- Winkler, E. A., Bell, R. D., & Zlokovic, B. V. (2010). Pericyte-specific expression of PDGF beta receptor in mouse models with normal and deficient PDGF beta receptor signaling. *Molecular neurodegeneration*, 5, 32.
- Wong, G. T., Manfra, D., Poulet, F. M., Zhang, Q., Josien, H., Bara, T., Engstrom, L., Pinzon-Ortiz, M., Fine, J. S., Lee, H.-J. J., Zhang, L., Higgins, G. A., & Parker, E. M. (2004). Chronic treatment with the gamma-secretase inhibitor LY-411,575 inhibits beta-amyloid peptide production and alters lymphopoiesis and intestinal cell differentiation. *The Journal of biological chemistry*, 279(13), 12876–82.
- World Cancer Report 2014. (2014). Retrieved June 18, 2015, from <http://www.scribd.com/doc/249125578/World-Cancer-Report-2014#scribd>
- Wu, K., Xu, L., Zhang, L., Lin, Z., & Hou, J. (2011). High Jagged1 expression predicts poor outcome in clear cell renal cell carcinoma. *Japanese journal of clinical oncology*, 41(3), 411–6.
- Wu, X., Xu, K., Zhang, L., Deng, Y., Lee, P., Shapiro, E., Monaco, M., Makarenkova, H. P., Li, J., Lepor, H., & Grishina, I. (2011). Differentiation of the ductal epithelium and smooth muscle in the prostate gland are regulated by the Notch/PTEN-dependent mechanism. *Developmental biology*, 356(2), 337–49.
- Wu, Y., Cain-Hom, C., Choy, L., Hagenbeek, T. J., de Leon, G. P., Chen, Y., Finkle, D., Venook, R., Wu, X., Ridgway, J., Schahin-Reed, D., Dow, G. J., Shelton, A., Stawicki, S., Watts, R. J., Zhang, J., Choy, R., Howard, P., Kadyk, L., Yan, M., Zha, J., Callahan, C. a,

- Hymowitz, S. G., & Siebel, C. W. (2010). Therapeutic antibody targeting of individual Notch receptors. *Nature*, *464*(7291), 1052–7. Nature Publishing Group.
- Xing, F., Kobayashi, A., Okuda, H., Watabe, M., Pai, S. K., Pandey, P. R., Hirota, S., Wilber, A., Mo, Y.-Y., Moore, B. E., Liu, W., Fukuda, K., Iizumi, M., Sharma, S., Liu, Y., Wu, K., Peralta, E., & Watabe, K. (2013). Reactive astrocytes promote the metastatic growth of breast cancer stem-like cells by activating Notch signalling in brain. *EMBO molecular medicine*, *5*(3), 384–96. EMBO Press.
- Xing, F., Okuda, H., Watabe, M., Kobayashi, A., Pai, S. K., Liu, W., Pandey, P. R., Fukuda, K., Hirota, S., Sugai, T., Wakabayashi, G., Koeda, K., Kashiwaba, M., Suzuki, K., Chiba, T., Endo, M., Mo, Y.-Y., & Watabe, K. (2011). Hypoxia-induced Jagged2 promotes breast cancer metastasis and self-renewal of cancer stem-like cells. *Oncogene*, *30*(39), 4075–86.
- Xu, K., Usary, J., Kousis, P. C., Prat, A., Wang, D.-Y., Adams, J. R., Wang, W., Loch, A. J., Deng, T., Zhao, W., Cardiff, R. D., Yoon, K., Gaiano, N., Ling, V., Beyene, J., Zacksenhaus, E., Gridley, T., Leong, W. L., Guidos, C. J., Perou, C. M., & Egan, S. E. (2012). Lunatic fringe deficiency cooperates with the Met/Caveolin gene amplicon to induce basal-like breast cancer. *Cancer cell*, *21*(5), 626–41.
- Xue, Y., Gao, X., Lindsell, C. E., Norton, C. R., Chang, B., Hicks, C., Gendron-Maguire, M., Rand, E. B., Weinmaster, G., & Gridley, T. (1999). Embryonic lethality and vascular defects in mice lacking the Notch ligand Jagged1. *Human molecular genetics*, *8*(5), 723–730.
- Yamada, S., Ebihara, S., Asada, M., Okazaki, T., Niu, K., Ebihara, T., Koyanagi, A., Yamaguchi, N., Yagita, H., & Arai, H. (2009). Role of ephrinB2 in nonproductive angiogenesis induced by Delta-like 4 blockade. *Blood*, *113*(15), 3631–9.
- Yan, M., Callahan, C. A., Beyer, J. C., Allamneni, K. P., Zhang, G., Ridgway, J. B., Niessen, K., & Plowman, G. D. (2010). Chronic DLL4 blockade induces vascular neoplasms. *Nature*, *463*(7282), E6–7. Macmillan Publishers Limited. All rights reserved.
- Ye, Q.-F., Zhang, Y.-C., Peng, X.-Q., Long, Z., Ming, Y.-Z., & He, L.-Y. (2012). Silencing Notch-1 induces apoptosis and increases the chemosensitivity of prostate cancer cells to docetaxel through Bcl-2 and Bax. *Oncology Letters*, *3*(4), 879–884. Spandidos Publications.
- Yong, T., Sun, A., Henry, M. D., Meyers, S., & Davis, J. N. (2011). Down regulation of CSL activity inhibits cell proliferation in prostate and breast cancer cells. *Journal of cellular biochemistry*, *112*(9), 2340–51.
- Yoon, C.-H., Choi, Y.-E., Koh, S.-J., Choi, J., Park, Y.-B., & Kim, H.-S. (2013). High glucose-induced jagged 1 in endothelial cells disturbs notch signaling for angiogenesis: A novel mechanism of diabetic vasculopathy. *Journal of Molecular and Cellular Cardiology*.
- Yu, Y., Zhang, Y., Guan, W., Huang, T., Kang, J., Sheng, X., & Qi, J. (2014). Androgen receptor promotes the oncogenic function of overexpressed Jagged1 in prostate cancer by enhancing cyclin B1 expression via Akt phosphorylation. *Molecular cancer research: MCR*, *12*(6), 830–42.
- Zarkada, G., Heinolainen, K., Makinen, T., Kubota, Y., & Alitalo, K. (2015). VEGFR3 does not sustain retinal angiogenesis without VEGFR2. *Proceedings of the National Academy of Sciences of the United States of America*, *112*(3), 761–6.
- Zavadil, J., Cermak, L., Soto-Nieves, N., & Böttinger, E. P. (2004). Integration of TGF-beta/Smad and Jagged1/Notch signalling in epithelial-to-mesenchymal transition. *The EMBO journal*, *23*(5), 1155–65.
- Zeng, Q., Li, S., Chepeha, D. B., Giordano, T. J., Li, J., Zhang, H., Polverini, P. J., Nor, J., Kitajewski, J., & Wang, C.-Y. (2005). Crosstalk between tumor and endothelial cells promotes tumor angiogenesis by MAPK activation of Notch signaling. *Cancer cell*, *8*(1), 13–23. Elsevier.

- Zhang, H. T., Craft, P., Scott, P. A., Ziche, M., Weich, H. A., Harris, A. L., & Bicknell, R. (1995). Enhancement of tumor growth and vascular density by transfection of vascular endothelial cell growth factor into MCF-7 human breast carcinoma cells. *Journal of the National Cancer Institute*, 87(3), 213–9.
- Zhang, Y., Wang, Z., Ahmed, F., Banerjee, S., Li, Y., & Sarkar, F. H. (2006). Down-regulation of Jagged-1 induces cell growth inhibition and S phase arrest in prostate cancer cells. *International journal of cancer. Journal international du cancer*, 119(9), 2071–7.
- Zhong, H., Semenza, G. L., Simons, J. W., & De Marzo, A. M. (2004). Up-regulation of hypoxia-inducible factor 1alpha is an early event in prostate carcinogenesis. *Cancer detection and prevention*, 28(2), 88–93.
- Zhong, T. P., Rosenberg, M., Mohideen, M. a, Weinstein, B., & Fishman, M. C. (2000). gridlock, an HLH gene required for assembly of the aorta in zebrafish. *Science (New York, N.Y.)*, 287(5459), 1820–4.
- Zhou, B.-B. S., Peyton, M., He, B., Liu, C., Girard, L., Caudler, E., Lo, Y., Baribaud, F., Mikami, I., Reguart, N., Yang, G., Li, Y., Yao, W., Vaddi, K., Gazdar, A. F., Friedman, S. M., Jablons, D. M., Newton, R. C., Fridman, J. S., Minna, J. D., & Scherle, P. A. (2006). Targeting ADAM-mediated ligand cleavage to inhibit HER3 and EGFR pathways in non-small cell lung cancer. *Cancer cell*, 10(1), 39–50. Elsevier.
- Zhu, H., Zhou, X., Redfield, S., Lewin, J., & Miele, L. (2013). Elevated Jagged-1 and Notch-1 expression in high grade and metastatic prostate cancers. *American journal of translational research*, 5(3), 368–78.
- Zhu, T. S., Costello, M. A., Talsma, C. E., Flack, C. G., Crowley, J. G., Hamm, L. L., He, X., Hervey-Jumper, S. L., Heth, J. A., Muraszko, K. M., DiMeco, F., Vescovi, A. L., & Fan, X. (2011). Endothelial cells create a stem cell niche in glioblastoma by providing NOTCH ligands that nurture self-renewal of cancer stem-like cells. *Cancer research*, 71(18), 6061–72.



**ANNEX I -
Primers pair
sequence
list**



Gene	Forward Sequence (5' – 3')	Reverse Sequence (5' – 3')
Notch primers		
Jag1	CCAGCCAGTGAAGACCAAGT	CAATTCGCTGCAAATGTGTT
Jag2	AGTGCCATCTGGCTTTGAAT	CGCTGCACATGGGTTAGAG
Dll1	GTTGTCTCCATGGCACCTG	TGCACGGCTTATGGTGAGTA
Dll3	GCACATGGGAGTTGCACTTC	CGGCATTCATCAGGCTCTTC
Dll4	GGAACCTTCTCACTCAACATCC	CTCGTCTGTTCGCCAAATCT
Notch1	ACAGTAACCCCTGCATCCAC	GGTTGGACTCACACTCGTTG
Notch2	GACTGCACAGAAGACGTGGA	GCGTAGCCCTTCAGACACTC
Notch3	GTGTCAATGGTGGTGTCTGC	GCACACTCATCCACATCCAG
Notch4	GAGGGACACTCCACCTTTCA	CTGGTGCCTGACACAGTCAT
Hey1	GGTACCCAGTGCCTTTGAGA	GTGTGCAGCATTTCAGGTG
Hey2	CTGAATTGAGAAGACTAGTGCCA	AGCATCTTCAAATGATCCACTGT
HeyL	CCGCATCAACAGTAGCCTTT	ACGGTCATCTGCAAGACCTC
Hes1	GCGAAGGGCAAGAATAAATG	TGTCTGCCTTCTCTAGCTTGG
Hes2	CGGATCAACGAGAGCCTAAG	GTCTGCCTTCTCCAACCTCG
Hes5	GCACCAGCCCAACTCCAA	GGCGAAGGCTTTGCTGTGT
Nrarp	AGTCGCTGCTGCAGAACAT	AACAGCTTCACCAGCTCCAG
Vegf primers		
Vegf-a	GGAGAGCAGAAGTCCCATGA	ACACAGGACGGCTTGAAGAT
Vegf-r1	GACCCTCTTTTGGCTCCTTC	CAGTCTCTCCCGTGCAAACCT
Vegf-r2	GGACTCTCCCTGCCTACCTC	CGGCTCTTTCGCTTACTGTT
Vegf-r3	CGAAGCAGACGCTGATGATA	CCCAGGAAAGGACACACAGT
Angiocrine Primers		
Pdgfr- β	TGATGAAGGTCTCCCAGAGG	AGGAGATGGTGGAGGAAGTG

ANNEX I- Primers pair sequence list

Pdgf-b	CCTCGGCCTGTGACTAGAAG	TTTCGGTGCTTGCCTTTG
Tek	CCCCTGAACTGTGATGATGA	CTGGGCAAATGATGGTCTCT
Ang-1	CCATTTGAGACTGTGCAGAT	CCCATTACATCCATATTGC
Ang-2	CCTGGAGGTTGGACTGTCAT	CCCAGCCAGTACTCACCATC
Cell-cycle primers		
Ccna	GAAGACAAGCCAGTGAACGT	TCTTCTCCCACCTCAACCAG
Cdk2	AATGCAGAGGGGTCCATCAA	CTCCAGATATCCACGGCTGT
Ccnd2	CAGTCACCCCTCACGACTTC	ACAGAGCGATGAAGGTCTGC
c-myc	GCCCAGTGAGGATATCTGGA	GACCGCAACATAGGATGGAG
Cdkn1b	TCTGTTGGCCCTTTTGT	GTGGACCAAATGCCTGACTC
Cdkn1c	GTTCTCCTGCGCAGTTCTCT	CTGAAGGACCAGCCTCTCTC
EMT primers		
E-cad	CCAAAGTGACGCTGAAGTCC	TACACGCTGGGAAACATGAG
Snail	CTTGTGTCTGCACGACCTGT	GGAGAATGGCTTCTCACCAG
Slug	GGCTGCTTCAAGGACACATT	TGCCCTCAGGTTTGATCTGT
Hif1 α	GCCTTAACCTGTCTGCCACT	GGAGCCATCATGTTCCATTT
Tgf- β	TGGAGCAACATGTGGA ACTC	CGTCAA AAGACAGCCACTCA
Stem primers		
Nanog	ATGAAGTGCAAGCGGTGGCAGAAA	CCTGGTGGAGTCACAGAGTAGTT C
Oct4	CTGAGGGCCAGGCAGGAGCACGA G	CTGTAGGGAGGGCTTCGGGCACT T
Sox2	GCC CGA GGC TTA AGC CTT TC	GGC GGC TTC AGC TCC GTC TC
Control primers		
β -Actin	TGTTACCAACTGGGACGACA	GGGGTGTGAAGGTCTCAAA
Pecam	CAAGCAAAGCAGTGAAGCTG	TCTAACTTCGGCTTGGGAAA